博士論文

Formulation and characterization of micro/nano emulsion systems encapsulating vitamins and phytochemicals using conventional and microchannel emulsification

（機械的乳化及びマイクロチャネル乳化を利用したビタミン・ファイトケミカルを内包したマイクロ・ナノエマルションの作製及び特性評価）

NAUMAN KHALID

ナウマン カリド

Formulation and characterization of micro/nano emulsion systems encapsulating vitamins and phytochemicals using conventional and microchannel emulsification

（機械的乳化及びマイクロチャネル乳化を利用したビタミン・ファイトケミカルを内包したマイクロ・ナノエマルションの作製及び特性評価）

A Dissertation Presented

by

NAUMAN KHALID

ナウマン カリド

Submitted to the Graduate School of the Agricultural and Life Sciences
The University of Tokyo, Japan in partial fulfillment
of the requirements for the degree of

DOCTOR OF PHILOSOPHY

July 2015

"It is certified that the contents and form of the thesis entitled "Formulation and characterization of micro/nano emulsion systems encapsulating vitamins and phytochemicals using conventional and microchannel emulsification" submitted by Mr. Nauman Khalid, Registration No. 39-127410, have been found satisfactory for the award of degree of the Doctorate of Philosophy."

Thesis Evaluation Committee:

_____
Prof. Dr. Hiroshi NABETANI

_____
Prof. Dr. Kensuke OKADA

_____
Assoc. Prof. Dr. Yukie SAITO

_____
Assoc. Prof. Dr. Tetsuya ARAKI

_____
Dr. Isao KOBAYASHI (Senior Researcher, NFRI, NARO)

_____
Prof. Dr. Ken FURUYA, Dean, Graduate School
of Agricultural and Life Sciences

Dedication

To my parents.
*The reason of what I become today.
Thanks for your great support, prayers, continuous
care and motivation.*

*To my family, friends and teachers.
I am grateful to all of you.
You have been a source of inspiration and just like
a chocolate with sweet aroma and taste.*

ACKNOWLEDGMENT

In the name of Allah, the Most Gracious and the Most Merciful

Alhamdulillah. All praise and glory to **Almighty Allah (Subhanahu Wa Taalaa)** who gave me courage and patience to carry out this work. Peace and blessing of Allah be upon last Prophet **Muhammad (Peace Be upon Him)**.

I would like to express my deepest gratitude and very special appreciation to my supervisor, **Prof. Dr. Hiroshi Nabetani**, for his enthusiastic supervision of my thesis. His helpful guidance, constructive criticism, valuable suggestion, consistent supervision, and encouragement helped me getting through the journey of my PhD study. I also would like to express my gratitude to **Dr. Isao Kobayashi**, **Prof. Dr. Mitsutoshi Nakajima**, **Dr. Marcos A. Neves** and **Dr. Kunihiko Uemura** for their useful advices and providing all facilities for my research in National Food Research Institute, Tsukuba, University of Tsukuba and my peaceful stay at Tsukuba Guest House.

I would also like to thank the esteemed coordinators of the International Program in Agriculture Development Studies **Prof. Dr. Kensuke Okada** and **Dr. Taro Takahashi** for providing all facilities and valuable suggestions in the University of Tokyo. I would like to thank the members of the reading committee **Dr. Yukie Saito**, **Dr. Isao Kobayashi** and **Dr. Tetsuya Araki** for their important remarks about my thesis. I would like to thank **Dr. Goran T. Vladisavljević** Senior Lecturer, Loughborough University, UK, **Prof. Dr. Ching ping Tan** from Putra University, Malaysia and **Prof. Dr. Sosaku Ichikawa** from Tsukuba University for their positive comments and useful advices on my research.

I am grateful to my family for their love, support, perfect understanding, and encouragement that inspired me for the success of this study. I could never have completed this thesis and would never have got this far without them. It is enjoyable and exciting to have lab fellows like Dr. Wang Zheng, Dr. Safa Souilem, Dr. Dammak Ilyas, Dr. Hiroyuki Kozu, Dr. Nanik Purwanti and Dr. Yanru Zhang who helped me a lot in

getting used to many experimental techniques. I also have a good time with my Laboratory technicians Miss Hori and Miss Takahashi, who helped me consistently during my research. I also shared my feelings with other lab mates from Dr. Nakajima's Laboratory.

I am grateful to Pakistan Student Association, Tokyo University for their friendship and good company during my memorable years in the University of Tokyo. I appreciate the kind help and support from Mudassar Nawaz Khan in Tsukuba Guest House. I also appreciate the help and valuable comments of Dr. Asif Ahmad, Dr. Iftikhar Ahmed and Dr. Anwaar Ahmed, who solved all of my educational problems back in Pakistan. Special thanks to my friends back in Pakistan, specially Wahab Nazir, Waqas Sadiq and Zoq for sharing laughter and tears, and always being there whenever I needed.

Finally, I would like to acknowledge the **Ministry of Education, Culture, Sports, Science and Technology, Japan (MEXT)** for providing scholarship to pursue MSc in Japan and also acknowledges **The University of Tokyo** from giving me admission and **Tokyo University Fellowship** for PhD studies.

NAUMAN KHALID

論 文 の 内 容 の 要 旨

Thesis Summary

<div align="right">

農学国際専攻　国際農業開発学コース

平成 24 年度　　　博士課程 入学

氏　　名　　ナウマン カリド

指導教員名 教授 鍋谷　浩志

</div>

論文題目

Formulation and characterization of micro/nanoemulsion systems encapsulating vitamins and phytochemicals using conventional and microchannel emulsification

（機械的乳化及びマイクロチャネル乳化を利用したビタミン・ファイトケミカル
を内包したマイクロ・ナノエマルションの作製及び特性評価）

The deficiency of micronutrients regarded as "hidden hunger" affects more than one-third of the world's population, resulting devastating consequences for public health, social development and future of country. Vitamins and phytochemicals have a role in health beyond basic nutrition. These functional ingredients are very sensitive towards environmental stresses like heat, light and oxidation. Moreover, numerous physiological factors limit their usage in food and pharmaceutical products. The research focuses on the encapsulation of vitamins and phytochemicals in different emulsions and microspheres using microchannel and conventional emulsification systems. Moreover, the research also evaluates the physical and chemical stability of encapsulated vitamins and phytochemicals.

The first part of thesis deals with the encapsulation of L-ascorbic acid (L-AA) in different systems. The study in chapters 2 and 3 aimed to formulate monodisperse food-grade water-in-oil-in-water (W/O/W)

emulsions and aqueous microspheres containing a high concentration of L-AA. The W/O/W emulsions were prepared using homogenization and subsequent microchannel emulsification (MCE). The asymmetric straight-through microchannel (MC) array constitutes numerous 10×100 μm microslots with a 30 μm depth, each connected to a 10 μm-diameter circular MC with a 70 μm depth. Monodisperse W/O/W emulsions containing W/O droplets with average diameters (d_{av}) of 26.0 to 31.5 μm and coefficient of variations (CVs) below 10% were successfully formulated via an asymmetric straight-through MC array at a low hydrophobic emulsifier concentration, regardless of L-AA concentration. The d_{av} represents the average of the diameters of all the droplets in the emulsion sample. The W/O droplets dispersed in these monodisperse W/O/W emulsions were physically stable in variation of d_{av} and CV for more than 10 d of storage at 4 °C. The monodisperse W/O/W emulsions also exhibited L-AA encapsulation efficiency (EE$_{L-AA}$) exceeding 80% during storage. Stable monodisperse aqueous microspheres containing high concentrations of L-AA (up to 30% (w/w)) with different concentrations of sodium alginate and $MgSO_4$ were generated using MCE. The aqueous microspheres generated from the MCs under optimized conditions had a d_{av} of 14 to 16 μm and a CV of less than 8% at the disperse phase pressures of 5 to 15 kPa. The L-AA loaded microspheres were physically stable in terms of their d_{av} and CV for >10 d of storage at 40 °C. The aqueous microspheres exhibited EE$_{L-AA}$ exceeding 70% during the evaluated storage period.

Chapters 4 and 5 aimed to conduct comparative studies with conventional emulsification devices to encapsulate L-AA in the dispersed phase of W/O and W/O/W emulsions. W/O emulsions with EE$_{L-AA}$ greater than 95% were prepared using rotor-stator homogenizer at 7000 rpm for 5 min. The prepared W/O emulsions under this operating conditions had d_{av} of 2.0 to 3.0 μm and CV of 13% to 22%. All the W/O emulsions were stable for more than 30 d at 4 °C or 25 °C with slight increase in d_{av} and without phase separation. Their EE$_{L-AA}$ was 50% at 4 °C and 30% at 25 °C after 30 d of storage. Two-step homogenization was conducted to prepare W/O/W emulsions containing L-AA. First-step homogenization prepared W/O emulsions with a d_{av} of 2.0 to 3.0 μm. Second-step homogenization prepared W/O/W emulsions with an average W/O droplet diameter of 14 to 18 μm and CVs of 18% to 25%. The results indicated that stable W/O/W emulsions containing a high concentration of L-AA were obtained by adding gelatin and $MgSO_4$ in the inner aqueous phase and glucose in both aqueous phases. EE$_{L-AA}$ in the W/O/W emulsions was 40% on day 30 and followed first-order kinetics.

The second part of study encapsulates different forms of vitamin D. Chapter 6 deals with formulation of food grade O/W emulsions loaded with ergocalciferol (VD$_2$) by MCE. The primary characterization was performed with grooved type MCE, while storage stability and vitamin D encapsulation efficiency was performed with straight through MCE. The grooved type MC array plate used has channel depth of around 5 μm and channel width of about 18 μm, while asymmetric straight-through MC array consists of numerous 10×80 μm microslots each connected to a 10 μm diameter circular MC. Monodisperse O/W emulsions with Sauter mean diameter ($d_{3,2}$) of 33.9 μm with relative span (RSF) width less than 0.20 (CV in between 5-10%) were successfully formulated via an asymmetric straight-through MC array. The $d_{3,2}$ represents the diameter of a droplet having the same area per unit volume as that of the total collection of droplets in emulsions. The O/W droplets were physically stable for more than 15 d of storage at 4 °C without any significant increase in $d_{3,2}$. The monodisperse O/W emulsions also exhibited VD$_2$ encapsulation efficiency (EE$_{VD2}$) of more than 85% during storage period. Chapter 7 deals with encapsulation of both VD$_2$ and cholecalciferol (VD$_3$) in food-grade O/W emulsions using asymmetric straight-through MCE. 1% (w/w) sodium cholate or Tween 20 in water was used as the continuous phase, while 0.5% (w/w) of each VD$_2$ and VD$_3$ in different oils served as the dispersed phase. Monodisperse O/W emulsions with $d_{3,2}$ of 28 to 32 μm and RSF widths below 0.3 were formulated via an asymmetric straight-through MC array under appropriate operating conditions. The monodisperse O/W emulsions stabilized with Tween 20 remained stable for >30 d with EE$_{VD2}$ and EE$_{VD3}$ of above 70% at 4 and 25 °C. In contrast, those stabilized with sodium cholate had stability of >30 d with EE$_{VD2}$ and EE$_{VD3}$ of over 70% only at 25 °C.

Chapter 8 deals with cross comparative studies with conventional homogenization techniques to encapsulate vitamin D. Both VD$_2$ and VD$_3$ at 0.5% (w/w) was encapsulated in refined soybean oil, olive oil and MCT. The phosphate buffer (pH 7) containing 1% (w/w) Tween 20 served as a continuous phase. The two liquid phases were emulsified with a homogenizer at 5,000 to 20,000 rpm for 5 min or the homogenizer at 7,000 rpm for 5 min plus a microfluidizer in a single pass at 100 MPa. The microfluidization produced the O/W emulsions with a volume mean diameter ($d_{4,3}$) of 0.41 μm and a RSF width of about 1.9. The $d_{4,3}$ represents the diameter of a droplet having the same volume in total weight of emulsions. The emulsions prepared at the high homogenization speeds and by microfluidization maintain

liquid consistency and whitish color after 30 d of storage period. In contrast, those prepared at the low homogenization speeds were quickly destabilized after 1 d of storage. During the storage, there was no significant difference in $d_{4,3}$ of the O/W emulsions prepared with the microfluidizer in comparison to $d_{4,3}$ of the O/W emulsions prepared with the homogenizer. There was little effect of homogenization speed on release profile of the vitamin D-loaded O/W emulsions. The EE of both VD_2 and VD_3 became less than 70% after 10 d of storage and less than 10% after 30 d of storage at 4 $^{\circ}$C.

The third part of research is to encapsulate phytochemicals and include quercetin, γ-oryzanol and β-sitosterol. Chapter 9 encapsulates quercetin in different food-grade O/W emulsions stabilized by different emulsifiers. 1% (w/w) Tween 20, sodium cholate, decaglycerol monolaurate, polyglyerol-5-laurate or bovine serum albumin in Milli-Q water was used as the continuous phase, while 0.4 mg mL^{-1} in different oils served as dispersed phase. Successful emulsification was conducted with all emulsifiers. The produced monodisperse droplets have $d_{3,2}$ of 28 to 34 μm with span width below 0.25. The $d_{3,2}$ slightly decreased at 25 $^{\circ}$C, while increased $d_{3,2}$ was observed in emulsions stabilized by sodium cholate at 4 $^{\circ}$C. The emulsions stabilized with 1% Tween 20 have quercetin EE of 80% and 70% at 4 and 25 $^{\circ}$C respectively. Chapter 10 encapsulates a slight high concentration of β-sitosterol and γ-oryzanol in different food-grade oil O/W emulsions using MCE. A 24 × 24-mm MCE chip (WMS 1-4) containing 23,348 straight-through MCs was used for this study. 1% (w/w) Tween 20 or decaglycerol monolaurate (ML-750) in Milli-Q water was used as the continuous phase, while 0.5-4% (w/w) β-sitosterol and γ-oryzanol in MCT served as dispersed phase. Successful emulsification was conducted with different concentrations of β-sitosterol and γ-oryzanol. The $d_{3,2}$ of 1% (w/w) β-sitosterol and γ-oryzanol loaded emulsions ranged between 26 to 28 μm with span width below 0.21 at Q_d of 2 mL h^{-1} after 30 d of storage at 4 and 25°C. The O/W emulsions stabilized with Tween 20 have β-sitosterol and γ-oryzanol EEs above 80% at 4 and 25°C, in comparison to the emulsions stabilized with ML-750 have EE of β-sitosterol over 80% and γ-oryzanol EE above 50% at 4 and 25°C.

The research indicate that MCE is a promising technique for encapsulating vitamins and phytochemicals, with superior control of processing parameters and various other physical and chemical conditions. The forthcoming scaling up of MCE devices is expected to further improve the quality of different emulsions and make practical their production on industrial scales.

TABLE OF CONTENTS

Page

LIST OF TABLES

LIST OF FIGURES

Chapter 1

Introduction

Health and safety are considered to be the prime factors for food industries and worldwide the number of functional foods are increasing at rapid rate. The functional foods improves the health promoting properties of polyunsaturated lipids, omega-3 fatty acids, phytochemicals, vitamins etc. However, the major challenges in incorporating these compounds in food matrix are their susceptibility towards oxidative deterioration, unpleasant odour, hydrophobicity and many more. These factors affect the organoleptic and sensory properties of the foods in which they are incorporated.

1.1 Functional foods

The recent trends in food and nutritional science proves that diet plays a significant role in maintaining health and homeostasis of body. The term ''functional food'' itself was first used in Japan, in the 1980s, for food products fortified with special constituents that possess advantageous physiological effects [1]. Functional foods not only satisfy hunger but also provide vital nutrients for mitigation of many diseases. However, there is no clear definition of functional foods. Technically, these are defined as foods that have a potentially positive effect on health beyond basic nutrition [1]. In last decade (Fig. 1.1), there was more than 50,000 publications that describes functional attributes of these functional foods. The global market of functional food is estimated to at least 33 billion US$ [2]. Other experts like Sloan [3] has calculated the global functional food market to be 47.6 billion US$, being the United States the largest market segment, followed by Europe and Japan. Some estimations report even more global market value (nearly 61 billion US$) [4]. Functional foods include many nutritive compounds which offer some kind of health benefits to consumers. These vital ingredients includes antioxidants, vitamins, phytochemicals, fish oil for omega 3 and omega 6 fatty acids, soy isoflavones, probiotics, co-enzymes and many micro-minerals.
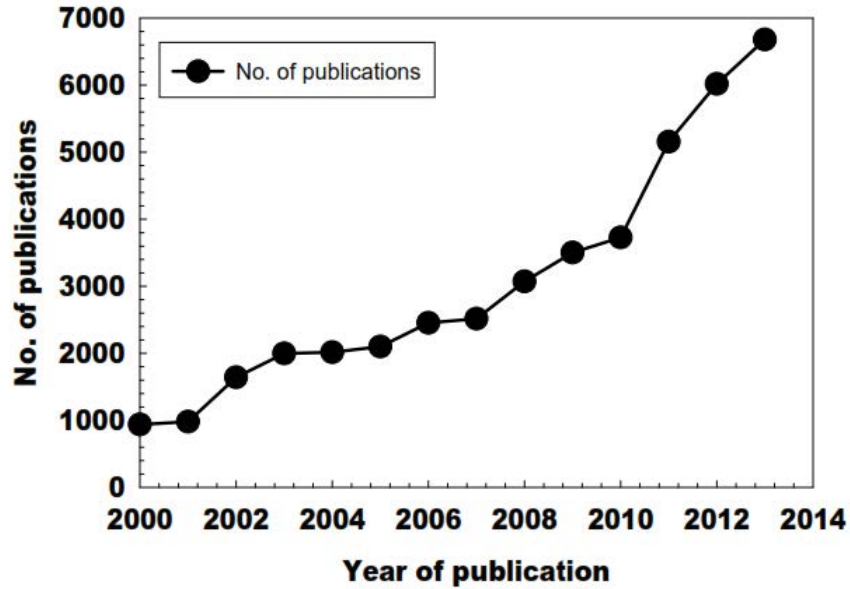
Figure 1.1: The functional foods development in terms of scientific publications from 2000-2013. The values are obtained from Thomson reuters "ISI Web of Knowledge" search engine.

1.2 Delivery systems for food ingredients

The incorporation of functional compounds into food matrix has many challenges. These functional food ingredients are susceptible to degradation due to environmental stress conditions like temperature, humidity, light, oxygen and its interaction with other food ingredients and therefore lose their bioactivity and nutritive value. Different nutrient delivery systems like emulsification and encapsulation are prime tools to deliver these important nutrients in different food and pharmaceutical systems with good efficiencies. These systems encapsulates vital nutrients in form of emulsions, microspheres, solid lipid nanoparticles (SLNs) and many more [5]. In recent decade numerous emulsification devices have been developed to encapsulate functional nutrients, each of these devices has numerous advantages and disadvantages [5]. The choice of particular device depends upon production method, volume of materials to be homogenized, droplet size distribution and required physicochemical properties of final products [6]. Recently, microfluidic devices have getting more popularity in comparison to conventional devices on the basis of energy and encapsulation efficiencies. Microfluidic devices produce monodisperse emulsions and limits the process of Ostward ripening and flocculation [7]. The better stability and physicochemical properties of monodisperse emulsions have attracted various industries to produce valuable emulsion products like functional microparticles, nanoparticles and multiple emulsions [8].

1.3 Emulsions

Emulsion is a two-phase system of two immiscible liquids, in which low mass fraction liquid is dispersed as small spherical droplets and scientifically called as dispersed phase and the phase present in large mass fraction called as continuous phase. The simplest example of emulsion is oil-in-water (O/W) emulsion like milk and water-in-oil (W/O) emulsion like margarine.

Emulsions are characterized on the basis of droplet sizes as micro or macro emulsions. The droplet sizes of emulsions generally range somewhere from 0.1 to 100 μm [9]. Emulsions are thermodynamically unstable and destabilization mechanisms can be observed as sedimentation and skimming due to density differences, droplet aggregation and coalescence [10]. The stability of emulsions are govern by various factors like emulsion composition, strength of emulsifiers, emulsification devices and other physicochemical parameters [10]. It is also possible to formulate multiple emulsions like water-in-oil-in-water (W/O/W) and oil-in-water-in-oil (O/W/O) emulsions [11]. Multiple emulsions are designed for controlled or sustained drug delivery, bioavailability enhancement, enzyme immobilization and taste masking [11-13].

1.4 Emulsification devices

The emulsification devices are characterized into mechanical and microfluidic devices. The most common mechanical devices include rotor-stator homogenizers, static mixers colloid mills, high-pressure homogenizers and ultrasonic homogenizers [6]. Laminar, turbulent and cavitational flows driven by shear forces are common mechanism in these conventional devices [14, 15]. The droplet distribution depends upon the amount of shear forces incorporated into emulsion fluids and further driven by interfacial forces and Laplace pressure [16]. The brief explanation of these mechanical devices are reviewed below.

1.4.1 Mechanical emulsification devices

Rotor-stator homogenizers (Fig. 1.4.1a) Rotor-stator (RS) homogenizers have practical applications in food, chemical, cosmetics and biochemical industries. RS homogenizers are used to produce dispersions like adhesives, pesticides, lattices, food ingredients and dairy products. RS are referred as high shear mixers with rotating blades and have capacity to generate shear value of 10^4-10^5 s^{-1}. RS homogenizers ranges from 1 to >1000 L in volume and usually operate from 50 to 20,000 rpm (rotation

per minute) depending upon unit operations in industries. Mixing in the RS is initiated when energy imparted by the rotating blades pushes the coarse emulsion up the mixing head and forces the emulsion through narrow clearances between the rotor blades and stator. The mixture is pushed axially from the rotating blades towards the gaps in the stator, where it is subjected to a chaotic environment and a number of stresses such as turbulence, cavitation, shear and elongational, causing droplet breakage [17]. Emulsification with the rotor stator requires constant recirculation in the high shearing zones and the efficiency of recirculation is a fundamental problem that has received plenty of attention. The emulsion droplets formulated through RS homogenizer typically have droplet diameters between 1.5 to 10 μm.

Static mixers (Fig. 1.4.1b) Static mixers (SM) are motionless elements inserted in tubes or pipes. SM induce flow in the radial direction creating plug flow conditions with very little back mixing. The elements are very compact and they range in size from a few millimeters up to meters in diameter depending on the application [18]. There are variety of SM available in industries and mostly differ in geometry, but operate in a relatively similar fashion. Mixing performance in SM is easily predicted based on flow rate, viscosity, density, percentage of mixture components and pipe dimensions [19]. Moreover, mixing effect depends on the continuous separation, distribution, and reunion of particles in the stream of material SM have the advantage over other mixers because they are cheaper for use (loss of energy expenses), and they are very easy to install and to clean [19]. The emulsion droplets formulated through SM typically have droplet diameters between 4 to 20 μm.

Colloid mills (Fig. 1.4.1c) are the devices used to reduce the particle size of a solid in suspension in a liquid. It basically work on the principle of RS homogenizer. Colloid mills (CM) are suitable for emulsification with fluids having velocities greater than 20 mPa s [14]. In CM the coarse emulsion is passed through a narrow gap between the rotor and the stator. A rotor turns at high speeds of 3000 – 20000 rpm. The high levels of hydraulic shear applied to the process disrupt structures in the fluid [15]. CM produces emulsions with droplet diameter in between 1 to 5 μm with throughput capacity up to 20,000 L h^{-1}.

High pressure homogenizers (Fig. 1.4.1d) are widely used in the dairy industry for the homogenisation of milk and milk products. In high pressure homogenizer (HPH), a coarse emulsion is forced through a narrow gap(s), resulting in velocities of up to hundreds of m s^{-1} at high pressure ratings (5 - 500 MPa) and flow rates (10-10000 L h^{-1}) [20]. Velocity is driven by a pressure gradient dependent on the gap size of the flow channel and the pump. Cavitation, turbulent and laminar shear cause droplet breakage in the

active region. However, a deeper understanding of the dominant mechanism(s) is difficult to ascertain with confidence due to the high flow velocities within the narrow gap, which makes accurate measurements and models which estimating the velocity flow fields very difficult [21].

Ultrasonic homogenizers (Fig. 1.4.1e) are devices well-suited for laboratory scale experiments due to its simplicity and ease of operation [22]. Ultrasonic homogenization (UH) is a fairly quick and simple technique but has significant drawbacks preventing commercialisation, such as large energy requirements per unit volume and tremendous heat loss[17]. The mechanism of droplet breakage during emulsification using ultrasonication is attributed to intensified mechanical vibrations in the probe which create pressure waves in the emulsion that leads to the formation of bubbles [23]. Commercial UH produces emulsions with throughput capacity up to 300,000 L h^{-1} with ultrasonic frequencies ranging between 20 to 50 kHz.

1.4.2 Microfluidic emulsification devices

Microfluidic devices produces energy efficient monodisperse emulsions. Various researchers investigated microstructured devices, like T or Y shaped junctions [24, 25], flow focusing devices [26], membrane emulsification devices [27] and microchannel emulsification devices [28]. The brief explanation of these microfluidic devices are reviewed below.

T or Y junctions (Fig. 1.4.2a) shows the simplest microfluidic structure for producing droplets and bubbles in T junctions [29-33]. In standard geometry, the main channel carries the continuous phase and the dispersed phase is injected through the inlet channel. The shear stress generated by the continuous phase causes the tip of the dispersed phase to distort in the downstream direction until the neck of the dispersed phase breaks up into a droplet [34-36]. It has been found that both monodispersed O/W and W/O emulsions can be prepared in the same T-junction device, by choosing appropriate surfactants in the oil or aqueous phase [37].
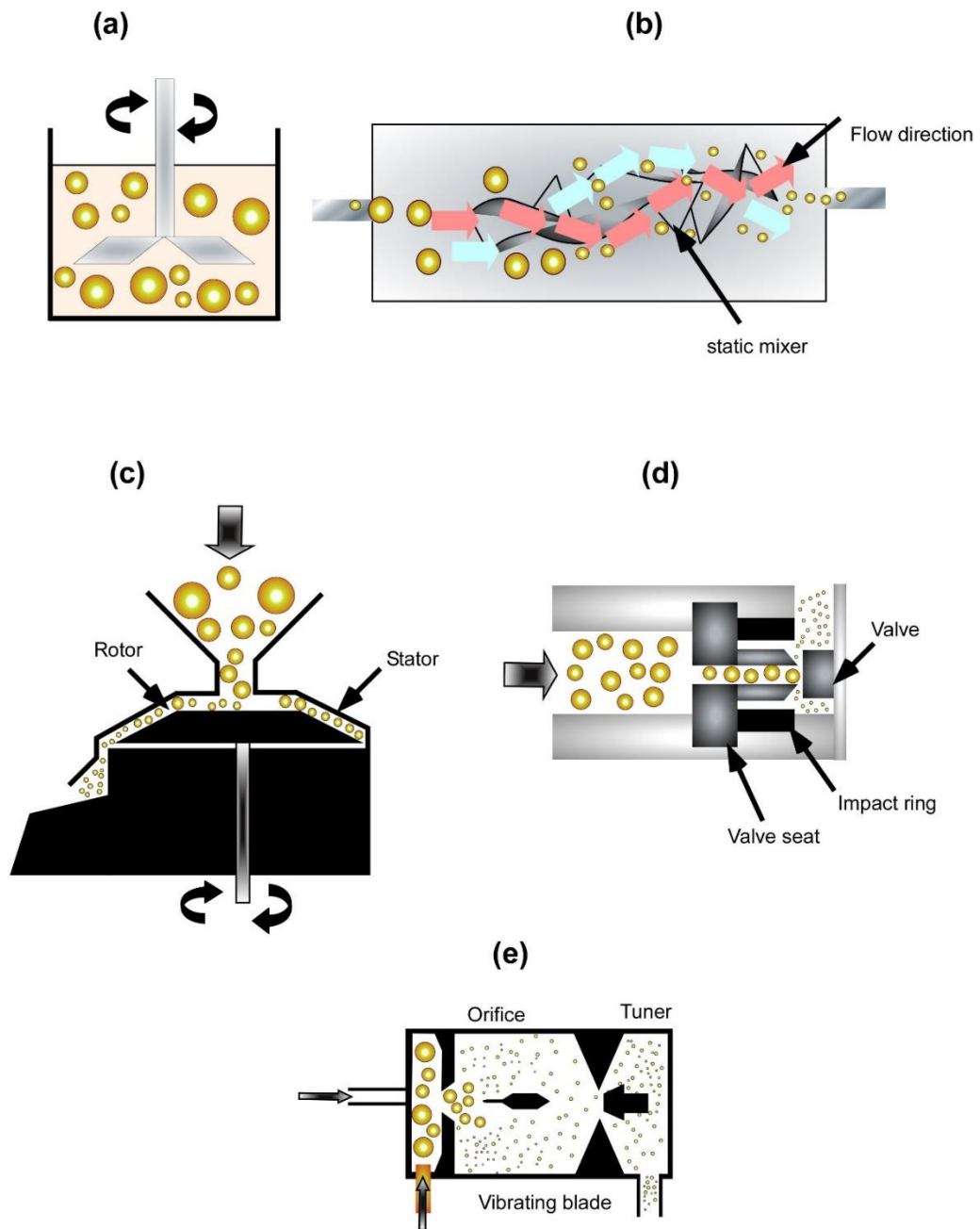
Figure 1.4.1: Schematic presentation of typical mechanical emulsification devices. (a) rotor-stator homogenizer, (b) static mixers, (c) colloid mill, (d) high pressure homogenizer and (e) ultrasonic homogenizer.

In a Y-junction, the dispersed and continuous phases are injected through two separate inlet channels and the emulsion is removed using a common outlet channel (Fig. 1.4.2b). The size of the droplets formed in Y-junction is independent on the flow rate and viscosity of the dispersed phase [38],

which is a behaviour different to that in a T-junction. The typical droplet size regime in T or Y junctions range between 5 to 30 μm.

Microfluidic flow focusing devices (Fig. 1.4.21c) shows the typical planar microfluidic flow focusing device (MFFD) developed by Anna *et al*. [39]. In MFFD devices, the droplets are generated in coflowing streams and forced through a small orifice which is known as hydrodynamic flow focusing [40-42]. Drop generation in MFFDs take place with four different flow regimes i.e. squeezing, dripping, jetting and tip-streaming [43].

Membrane emulsification Membrane emulsification (ME) is a process that forms emulsion by injecting a dispersed phase or premix through a microporous membrane into the continuous phase (Fig. 1.4.2d). In the former case, fine droplets are produced directly at the membrane/continuous phase interface, whereas in the latter case, pre-existing droplets are homogenised by passing premix through the membrane [27]. A microporous glass membrane called Shirasu porous glass (SPG) membrane was originally used as emulsification device[44]. The droplet size in ME largely depends upon membrane pore size [44]. Typical monodisperse droplets are produced with coefficient of variation (CV) less than 10% [27]. ME requires relative small shear stress and low energy input (10^4-10^6 J m^{-3}) to prepare emulsions than conventional emulsification devices (10^6-10^8 J m^{-3}) [45]. Variety of materials are used to conduct membrane emulsification for production of O/W or W/O emulsions. These includes uniform porous glass [44], polypropylene hollow fibres [27], ceramics [46], polytetrafloroethylene [47] and silicon nitride [48]. The surface of membrane must be completely wetted with continuous phase for production of monodisperse emulsions. Based upon geometry there are variety of membrane emulsification like dead end type [49], cross flow type [50], vibrating type [48] and rotating type membrane emulsification [51]. The most widespread application of ME is in synthesis of particles through solidification of droplets [50]. ME can be used to produce particles from a wide variety of organic and inorganic materials, including hydrogels, polymers, inorganic oxides, metals and solid lipids [27].

Microchannel emulsification The term MCE was coined by Kawakatsu *et al.* [52] and has capacity to form monodisperse emulsion droplets by using microchannel (MC) arrays precisely fabricated on single-crystal silicon microchip [52] or stainless steel microchips [53]. These MC arrays can be fabricated as microgrooves horizontally to the microchip surface (Fig. 1.4.2e (i))[52] or vertically as straight-through microholes (Fig. 1.4.2e (ii))[54]. The grooved microchips exhibits low droplet productivity due to limited number of MCs but extremely productive in elucidating droplet generation behavior in MCs.

The straight-thorough microchips consist of several hundreds of thousands of MCs and have monodisperse droplet productivity even at dripping regime of 50 mL h^{-1} [54].

Sugiura *et al.* [55] proposed interfacial tension-driven droplet formation mechanism form the channels with an elongated section. The model for predicting droplet diameter in MCE was also presented and is based on droplet formation mechanism and on experimental observation [56, 57]. Monodisperse emulsion droplets with diameters of 1 μm to 500 μm and coefficient of variation below 5% have been successfully formulated through MCE [27]. The MCE has been used to produce many encapsulated dispersions with improved properties such as β-carotene [58], oleuropein [59], γ-oryzanol [60], L-ascorbic acid [61] and ascorbic acid derivatives [62].

(e)

(i)   **(ii)**
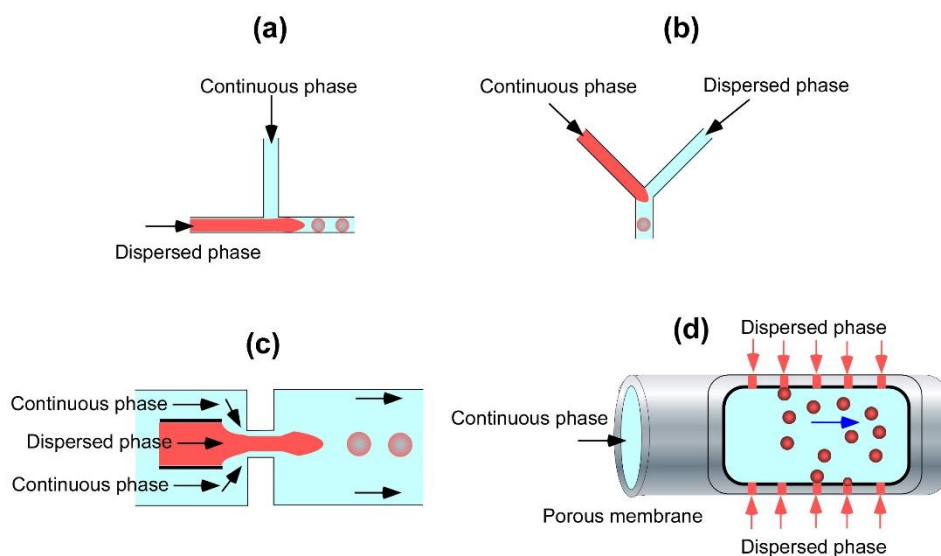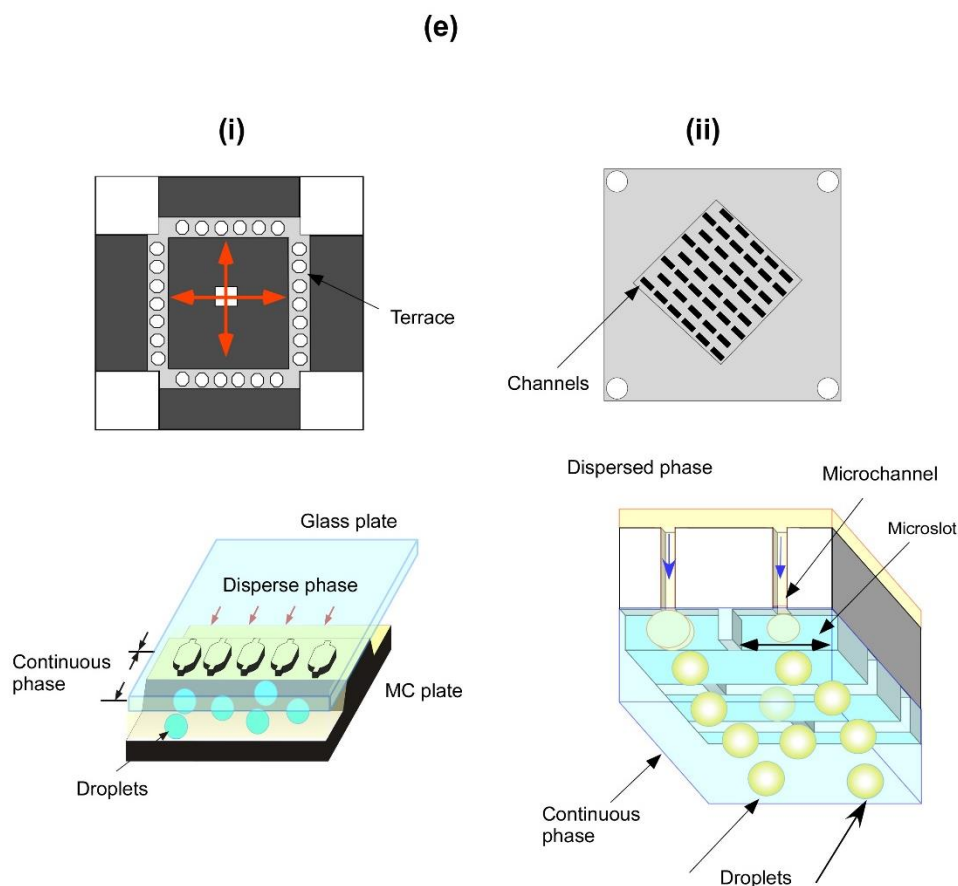
Figure 1.4.2: Schematic presentation of typical microfluidic emulsification devices. (a) T-junction, (b) Y-junction, (c) flow focusing device, (d) membrane emulsification and (e) microchannel emulsification (MCE), (i) grooved type MCE (ii) straight through MCE.

1.6 Micronutrient deficiencies

1.6.1 Vitamins

The deficiency of essential vitamins and minerals are regarded as "hidden hunger" and it affects more than one-third of the world's population, threaten women and children, resulting devastating consequences for public health, social development and future of country. These micronutrient deficiencies contribute significantly to the burden of disease and linked to adverse functional outcomes such as stunting, wasting, increased susceptibility to infections during pregnancy, decreased IQ level, cognitive losses, blindness, and premature mortality. The major micronutrient malnutrition issues affecting populations in developed and developing countries addressed in the WHO Guidelines are shown in Table 1.1. The thesis focuses on the encapsulation of vitamin C and D. The brief overview of these vital vitamins are highlighted below.

Vitamin C (Fig. 1.6.1a) shows the structural presentation of vitamin C, and this vitamin is also regarded as L-ascorbic acid. vitamin C market is segmented into dietary supplements, cosmetic formulations, animal feed fortification and food and beverage products. Vitamin C is also regarded as dietary intake of vitamin C [63]. It is present in many leafy vegetables and fruits, noticeably in guava, orange, apple, strawberry, kiwi, capsicum, pawpaw and cauliflower [64]. The importance of vitamin C is seen clearly in scurvy, a life-threatening vitamin C deficiency disease that results in loss of energy, depression, mood disorders, poor wound healing, and connective tissue disorders, culminating in death [65]. Vitamin C plays an important role in formation of collagen (in bones, teeth and cartilage) and activation of various enzymes related nervous system, and detoxification of drugs in liver. Similarly, this vitamin increase the bioavailability of iron, calcium and folic acid [66]. Vitamin C reduce aging process in human and brighten the skin by boasting immune system and stimulate the formation of bile in the gallbladder [67].

Table 1.1: Vitamin deficiency conditions and their worldwide prevalence. Adapted from Allen *et al.* [68]

Micronutrient	Deficiency Prevalence	Major Deficiency Disorders
Folate (Vitamin B_6)	Insufficient data	Megaloblastic anemia, neural tube and other birth defects, heart disease, stroke, impaired cognitive function, depression
Cobolamine (Vitamin B_{12})	Insufficient data	Megaloblastic anemia (associated with Helicobacter pylori induced gastric atrophy
Thiamine (Vitamin B_1)	Insufficient data, estimated as common in developing countries and in famines, displaced persons	Beriberi (cardiac and neurologic), Wernicke and Korsakov syndromes (alcoholic confusion and paralysis)
Riboflavin (Vitamin B_2)	Insufficient data, est. to be common in developing countries	Non-specific-fatigue, eye changes, dermatitis, brain dysfunction, impaired iron absorption
Niacin (Vitamins B_3)	Insufficient data, estimated as common in developing countries and in famines, displaced persons	Pellagra (dermatitis, diarrhea, dementia, death)
Vitamin B_6	Insufficient data, estimated as common in developing countries and in famines, displaced persons	Dermatitis, neurological disorders, convulsions, anemia, elevated plasma homocysteine
Vitamin C	Common in famines, displaced persons	Scurvy (fatigue, hemorrhages, low resistance to infection, anemia)
Vitamin D	Widespread in all age groups, low exposure to ultra violet rays of sun	Rickets, osteomalacia, osteoporosis, colo-rectal cancer

Vitamin D (Fig. 1.6.1b) shows different structural forms of vitamin D and this vitamin plays a vital role in maintaining and developing healthy skeletal system, since it maintains calcium level in the body. Deficiency of vitamin D results in increased risk of diabetes, hypertension, cancer and autoimmune diseases [69-72]. Broad spectrum deficiencies of vitamin D includes rickets in children, osteomalacia in adults and osteoporosis in women, all of these lead to softening and weakening of bones [73-75]. Vitamin D is synthesized in the skin and involves the phytochemical conversion of provitamin D by the action of ultra-violet (UV-B) rays [76, 77]. The terminology and classification related to vitamin D is confusing and can be classified into 5 different forms and metabolites, among these vitamin D_2 (ergocalciferol) and D_3 (cholecalciferol) are important (Fig. 1.6.1b (i, ii)) [78, 79]. Both forms of vitamin D are converted to 25-hydoxyvitamin [25-(OH)D] in the liver. The quantification of 25-(OH)D in blood gives the quantitation of vitamin D status. A cutoff value of 30 ng/mL is sometimes used for optimal vitamin status [79].

(a)
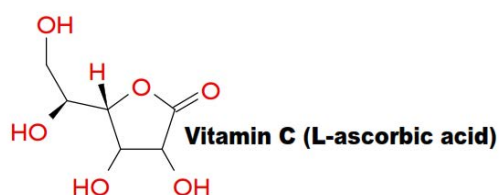
(b)
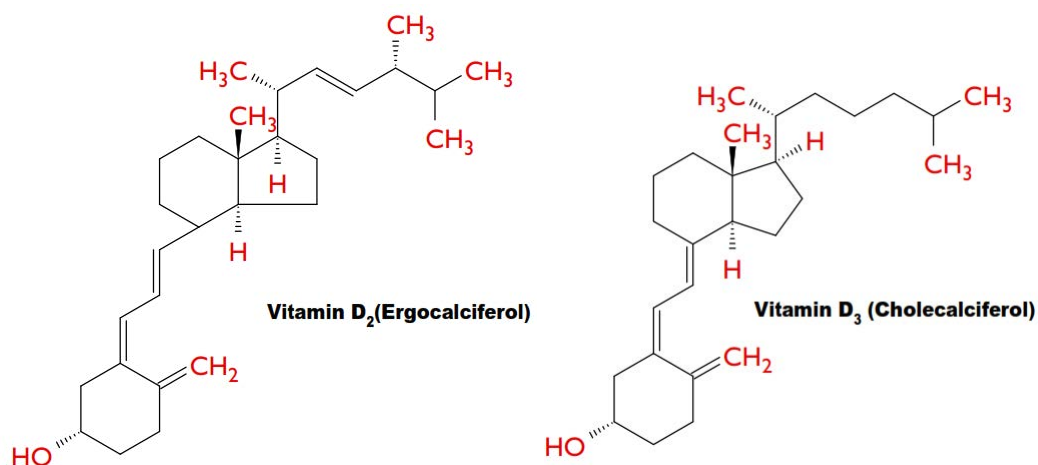
Figure 1.6.1: Structural illustration of vitamins used in research work.

1.6.2 Phytochemicals

Phytochemicals are a large group of plant-derived compounds responsible for disease protection. These compounds are present in diets high in fruits, vegetables, beans, cereals, and plant-based beverages such as tea and wine [80]. This diverse group comprises of phenolic acids, flavonoids, stilbenes, lignans and phytosterols [80]. Among these diverse groups, flavonoids are the most extensively studied group. Research suggest that this group contributes to the reduced mortality rate in people consuming high level of plant based foods [81]. Due to the lack of food composition data, the Standing Committee on the Scientific Evaluation of Dietary Reference Intakes and Its Panel on Dietary Antioxidants and Related Compounds of the Food and Nutrition Board at the Institute of Medicine chose not to create a Dietary Reference Intake (DRI) for these compounds and a recommended intake for phytochemicals does not currently exist [82]. Table 1.2 shows potential health benefits from some of the phytochemical compounds.

Table 1.2: Potential health benefits of some of the phytochemicals

Food	Phytochemical	Health benefit
Soybeans, soy milk, and tofu	Isoflavones	Reduction in blood pressure [83]
Strawberries, red wine, blueberries	Anthocyanins	Improve vision, decreased platelet aggregation and neuroprotective effects [83]
Red wine, grape juice, grape extracts, cocoa	Proanthocyanidins and favan-3-ols	Reduction in plasma cholesterol, inhibition of proinflammatory responses [83]
Garlic, onions, leeks, olives, scallions	Sulfides, thiols	Decrease in low density lipoproteins [84]
Carrots, tomatoes, and tomato products, and various types of fruits and vegetables	Carotenoids, lycopene, β-carotenes	Neutralization of free radicals [84]
Broccoli and other cruciferous vegetables such as kale, horseradish	Isothiocyanates	Neutralization of free radicals, protection against cancer [85]

This thesis focus on three important phytochemicals i.e. quercetin, γ-oryzanol and β-sitosterol. The detail functionality of these compounds are highlighted in chapter 8 and 9. The brief description regarding their health benefits are reviewed below.

Quercetin (Fig. 1.6.2a) shows the structural presentation of quercetin (3,3',4',5,7-pentahydroxyflavanone) and quercetin is categorized as a flavonol and belongs to the family of flavonoids [86]. Flavonols are present in variety of fruits, vegetables, seeds, flowers and nuts [87]. These are also abundant in variety of medicinal plants like *Ginko bioloba*, *Solanum trilobatum* and many others [88]. Most of the dietary intake is as flavonol glycosides of quercetin, kaempferol and myricetin [89]. Quercetin exhibit a wide range of biological activities, including anti-oxidant, anti-cancer, anti-toxic, anti-thrombotic, anti-aging, metal chelating and anti-microbial activities [88, 90-92]. Similarly, it has impact on obesity, sleep and mood disorders [88, 93]. Recently, quercetin is used in many sport supplements in order to reduce post-exercise immune system perturbations [94].

γ-oryzanol (Fig. 1.6.2b) is a naturally occurring component in rice bran and rice germ which consist of a mixture of ferulic acid esters of sterols and triterpene alcohols [95]. There are increasing number of reports indicating the benefits, efficacy and safety of γ-oryzanol. The antioxidant effect of γ-oryzanol was well documented and excellent in inhibiting lipid peroxidation. Kanno *et al.* [96] reported that γ-oryzanol (0.5% ~1%) inhibited thermal oxidative polymerization of soybean oil. Wilson *et al.* [97] reported that γ-oryzanol reduced plasma cholesterol in hypercholesterolemic hamsters. There are number of clinical studies reported that γ-oryzanol is beneficial in the treatment of relieving menopausal (climacteric) symptom [98].

β-sitosterol (Fig. 1.6.2c) is a predominant phytosterol found in higher plants and as well as in human foods [99]. β-sitosterol is the most extensive studied phytosterol due to its role in hypercholesterolemia [100], cardiovascular diseases [101] and benign prostatic hyperplasia [102]. β-sitosterol is used in a variety of enriched commercial foods such as fruits juice, milk, yoghurt and spreads. Safety concerns regarding the use of β-sitosterol have been well addressed in different *in vivo* and clinical studies [103, 104].

(a)
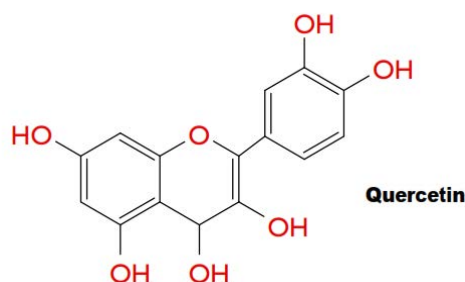
(b)
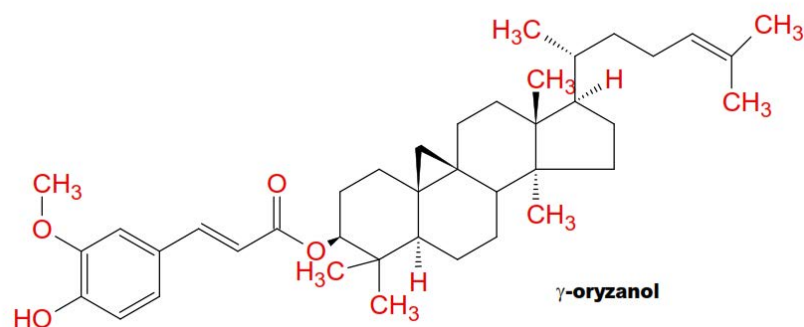
(c)
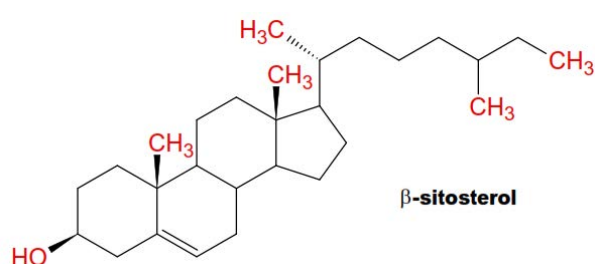
Figure 1.6.2: Structural illustration of phytochemicals used in research work.

1.7 Potential reasons for encapsulation of vitamins and phytochemicals

Vitamins and phytochemicals have a role in health beyond basic nutrition. These functional ingredients are very sensitive towards environmental stress like heat, light and oxidation. Moreover, numerous physiological factors limit their usage in food and pharmaceutical products. Vitamin C can undergo reversible oxidation reactions [105]. Moreover, the chemical properties of vitamin C allow it to react with a wide variety of potentially harmful reactive oxygen species. The environmental factors such as temperature, pH, oxygen, metal ion, UV and x-ray also affect the stability [106, 107]. Vitamin C is highly oxidative which can cause a problem in food systems. In the processing stage, it can change color from whitish to yellowish which in turns destabilized the system. The challenges associated with vitamin D fortification and encapsulation are: poor water solubility; chemical degradation when exposed to light, oxygen, or elevated temperatures; and variable oral bioavailability [108, 109]. The main disadvantages of using quercetin and phytosterols in therapeutics and functional foods are, poor solubility in aqueous and oil medium, crystallization behavior at ambient and body temperatures, poor permeability and low bioavailability [110-112], degradability at high temperatures [113] and and moisture contents [114].

Recent developments toward the encapsulation of functional ingredients have focused mostly on optimizing encapsulation techniques, coupled with the use of natural ingredients to improve the functionalities and applications [115]. In recent decade numerous delivery systems have developed to improve the stability and functionality of functional ingredients. These includes solid lipid nanoparticles, microspheres, gel microbeads, giant vesicles, and many others. All of these systems have its own advantages and disadvantages, but these technologies gave boom to market, in 2013 sales of vitamins and phytochemical encapsulated supplements in the United Kingdom totalled £ 674.6 million, a growth of about 16% over the previous five years [116].

1.8 Objective of thesis

The primary objective of this thesis was to formulate and characterize different dispersion systems encapsulating vitamins and phytochemicals using different homogenization techniques. One of the most important objective of emulsion science is to get extremely monodisperse emulsion droplets with minimum thermal impact on finished product. This monodispersity can be achieved using microfluidic devices that requires a low energy inputs ($< 10^5$ -10^6 J m^{-3}). MCE is a promising techniques to produce monodisperse emulsions just by spontaneous transformation of interfaces. Previous literature points out the droplet generation mechanism in different MCE devices in detail but there is gap in elucidating the physical and chemical stabilities of emulsion droplets encapsulating vital bioactives in these MCE devices. The thesis focuses on the optimization, generation characteristics, physical and chemical stabilities of various bioactives in MCE. The other objective of this thesis was to encapsulate a slightly high concentration of bioactives in MCE. The outcome of this objective will help in designing new products containing a slight high amount of functional compounds that could be the replacers of high energy drinks or chemical supplements. The secondary objective of this thesis was to conduct a comparative study for evaluating physical and chemical stability of emulsion droplets encapsulating bioactives formulated with conventional emulsification and MCE.

1.9 Structure of thesis

The thesis is structured as shown in Fig. 1.9. The introduction briefly explained the emulsion devices and important of various bioactives in human health. The introduction also highlights the importance of encapsulation for bioactives. The **chapter 2 to 5** deals with the encapsulation of vitamin C (L-ascorbic

acid) in different dispersion systems formulated either with conventional devices or MCE. The **chapter 6 to 8** shows the encapsulation of different forms of vitamin D in different dispersion systems formulated with MCE and high pressure homogenization. The **chapter 9 and 10** deals with encapsulation of quercetin, γ-oryzanol and β-sitosterol in O/W emulsions using MCE. The **last chapter** summarizes the conclusions and future perspectives of MCE.
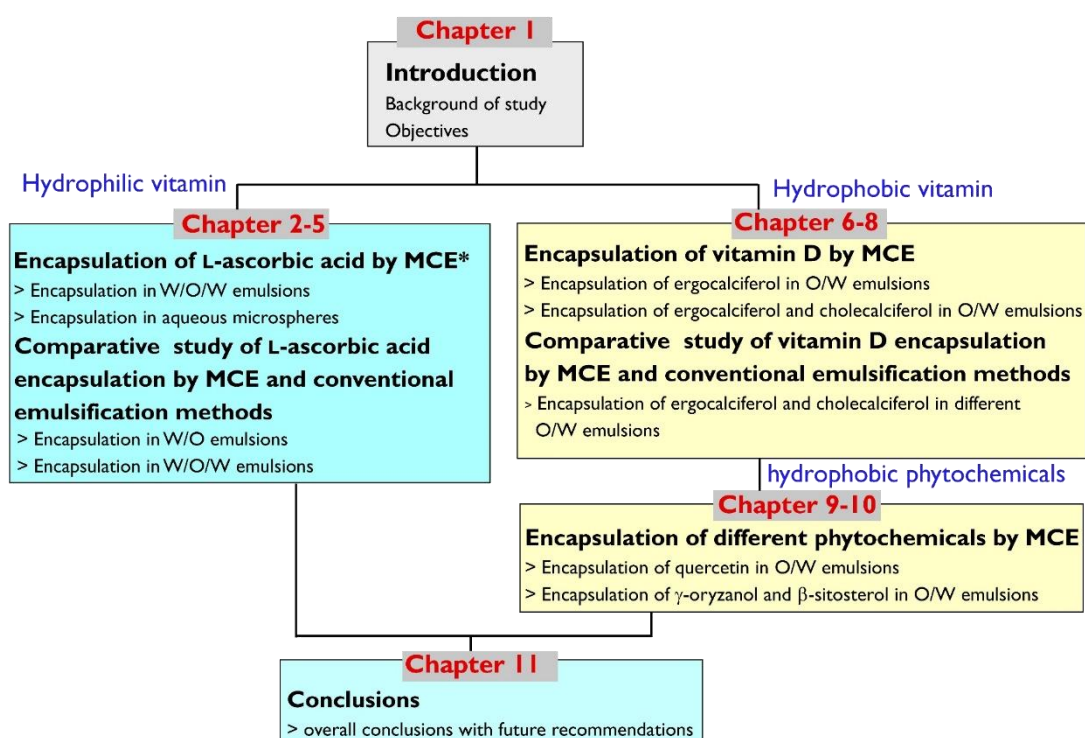
Figure 1.9: Structural presentation of thesis and bioactives used in research work.

References

[1] Siro I, Kapolna E, Kapolna B and Lugasi A, *Appetite*, **51,** 456-467 (2008).

[2] Hilliam M, *The World of Food Ingredients*, **12,** 50-52 (2000).

[3] Sloan E, *Food Technology*, **56,** 32-57 (2002).

[4] Benkouider C, *International Food Ingredients*, **5,** 66-68 (2004).

[5] McClements DJ, *Annual review of Food Science and Technology*, **1,** 241-269 (2010).

[6] Santana RC, Perrechil FA and Cunha RL, *Food Engineering Reviews*, **5,** 107-122 (2013).

[7] Taylor P, *Advances in Colloid and Interface Science*, **75,** 107-163 (1998).

[8] Shah RK, Shum HC, Rowat AC, Lee D, Agresti JJ, Utada AS, Chu L-Y, Kim J-W, Fernandez-Nieves A, Martinez CJ and Weitz DA, *Materials Today*, **11,** 18-27 (2008).

[9] Clausse D, Gomez F, Dalmazzone C and Noik C, *Journal of Colloid and Interface Science*, **287,** 694-703 (2005).

[10] Tadros TF, Emulsion Science and Technology: A General Introduction, in: Emulsion Science and Technology, Wiley-VCH Verlag GmbH & Co. KGaA, 2009, pp. 1-56.

[11] Khan AY, Talegaonkar S, Iqbal Z, Ahmed FJ and Khar RK, *Current Drug Delivery*, **3,** 429-443 (2006).

[12] Muschiolik G, *Current Opinion in Colloid & Interface Science*, **12,** 213-220 (2007).

[13] Lamba H, Sathish K and Sabikhi L, *Food Bioprocess Technology*, 1-20 (2015).

[14] McClements D, Food emulsions, principles, practices, and techniques, CRC Press, Washington DC, 2004.

[15] Walstra P, *Chemical Engineering Science*, **48,** 333-349 (1993).

[16] Dickinson E and Walstra P, Food colloids and polymers: stability and mechanical properties, Elsevier, 1993.

[17] Ouzineb K, Lord C, Lesauze N, Graillat C, Tanguy PA and McKenna T, *Chemical Engineering Science*, **61,** 2994-3000 (2006).

[18] Paul EL, Atiemo-Obeng V and Kresta SM, Handbook of industrial mixing: science and practice, John Wiley & Sons, 2004.

[19] Bauman I, *Chemical and Biochemical Engineering Quarterly*, **15,** 159-166 (2001).

[20] Innings F and Trägårdh C, *Experimental Thermal and Fluid Science*, **32,** 345-354 (2007).

[21] Håkansson A, Trägårdh C and Bergenståhl B, *Chemical Engineering Science*, **64,** 2915-2925 (2009).

[22] Landfester K, Eisenblätter J and Rothe R, *JCT research*, **1,** 65-68 (2004).

[23] Richardson ES, Pitt WG and Woodbury DJ, *Biophysical Journal*, **93,** 4100-4107 (2007).

[24] Garstecki P, Fuerstman MJ, Stone HA and Whitesides GM, *Lab on a Chip*, **6,** 437-446 (2006).

[25] Steegmans ML, Schroën KG and Boom RM, *Langmuir*, **25,** 3396-3401 (2009).

[26] Anna SL, Bontoux N and Stone HA, *Applied Physics Letters*, **82,** 364-366 (2003).

[27] Vladisavljevic GT, Kobayashi I and Nakajima M, *Microfluidics and Nanofluidics*, **13,** 151-178 (2012).

[28] Vladisavljevic GT, Khalid N, Neves MA, Kuroiwa T, Nakajima M, Uemura K, Ichikawa S and Kobayashi I, *Advanced Drug Delivery Reviews*, **65,** 1626-1663 (2013).

[29] Thorsen T, Roberts RW, Arnold FH and Quake SR, *Physics Review Letters*, **86,** 4163-4166 (2001).

[30] Yi GR, Thorsen T, Manoharan VN, Hwang MJ, Jeon SJ, Pine DJ, Quake SR and Yang SM, *Advance Materials*, **15,** 1300-1304 (2003).

[31] He M, Edgar JS, Jeffries GDM, Lorenz RM, Shelby JP and Chiu DT, *Anal. Chem.*, **77,** 1539-1544 (2005).

[32] van der Graaf S, Steegmans MLJ, van der Sman RGM, Schroën CGPH and Boom RM, *Colloids and Surface. A.*, **266,** 106-116 (2005).

[33] Dendukuri D, Tsoi K, Hatton TA and Doyle PS, *Langmuir*, **21,** 2113-2116 (2005).

[34] Zhao C-X and Middelberg APJ, *Chemical Engineering Science*, **66,** 1394-1411 (2011).

[35] Teh S-Y, Lin R, Hung L-H and Lee AP, *Lab on a Chip*, **8,** 198-220 (2008).

[36] Garstecki P, Fuerstman MJ, Stone HA and Whitesides GM, *Lab on a Chip*, **6,** 437-446 (2006).

[37] Xu JH, Li SW, Tan J, Wang YJ and Luo GS, *Langmuir*, **22,** 7943-7946 (2006).

[38] Steegmans MLJ, Schroë KGPH and Boom RM, *Langmuir*, **25,** 3396-3401 (2009).

[39] Anna SL, Bontoux N and Stone HA, *Applied Physics Letters*, **82,** 364-366 (2003).

[40] Garstecki P, Gañán-Calvo A and Whitesides G, *Bulletain of Polish Acad Sci., Tech. Sci.*, **53,** 361-372 (2005).

[41] Lewis P, Graham R, Nie Z, Xu S, Seo M and Kumacheva E, *Macromolecules* **38,** 4536-4538 (2005).

[42] Xu Q and Nakajima M, *Applied Physics Letters*, **85,** 3726-3728 (2004).

[43] Anna SL and Mayer HC, *Phyicss. Fluids.*, **18,** (2006).

[44] Nakashima T, Shimizu M and Kukizaki M, *Advanced Drug Delivery Reviews*, **45,** 47-56 (2000).

[45] Schröder V, Behrend O and Schubert H, *Journal of Colloid and Interface Science*, **202,** 334-340 (1998).

[46] Schröder V and Schubert H, *Colloids and Surfaces A*, **152,** 103-109 (1999).

[47] Yamazaki N, Naganuma K, Nagai M, Ma GH and Omi S, *Journal of Dispersion Science and Technology*, **24,** 249-257 (2003).

[48] Zhu J and Barrow D, *Journal of Membrane Science*, **261,** 136-144 (2005).

[49] Arnot T, Field R and Koltuniewicz A, *Journal of Membrane Science*, **169,** 1-15 (2000).

[50] Vladisavljević GT and Williams RA, *Advances in Colloid and Interface Science*, **113,** 1-20 (2005).

[51] Joscelyne SM and Trägårdh G, *Journal of Membrane Science*, **169,** 107-117 (2000).

[52] Kawakatsu T, Kikuchi Y and Nakajima M, *Journal of the American Oil Chemists Society*, **74,** 317-321 (1997).

[53] Kobayashi I, Wada Y, Hori Y, Neves MA, Uemura K and Nakajima M, *Chemical Engineering & Technology*, **35,** 1865-1871 (2012).

[54] Kobayashi I, Nakajima M, Chun K, Kikuchi Y and Fukita H, *AichE Journal*, **48,** 1639-1644 (2002).

[55] Sugiura S, Nakajima M, Iwamoto S and Seki M, *Langmuir*, **17,** 5562-5566 (2001).

[56] Sugiura S, Nakajima M and Seki M, *Langmuir*, **18,** 5708-5712 (2002).

[57] Sugiura S, Nakajima M and Seki M, *Langmuir*, **18,** 3854-3859 (2002).

[58] Neves MA, Ribeiro HS, Kobayashi I and Nakajima M, *Food Biophysics*, **3,** 126-131 (2008).

[59] Souilem S, Kobayashi I, Neves M, Sayadi S, Ichikawa S and Nakajima M, *Food Bioprocess Technology*, **7,** 2014-2027 (2014).

[60] Neves MA, Ribeiro HS, Fujiu KB, Kobayashi I and Nakajima M, *Industrial & Engineering Chemistry Research*, **47,** 6405-6411 (2008).

[61] Khalid N, Kobayashi I, Neves MA, Uemura K, Nakajima M and Nabetani H, *Colloids and Surfaces A*, **458,** 69-77 (2014).

[62] Khalid N, Kobayashi I, Neves MA, Uemura K, Nakajima M and Nabetani H, *Colloids and Surfaces A,* **459,** 247-253 (2014).

[63] Abbas S, Da Wei C, Hayat K and Xiaoming Z, *Food Reviews International*, **28,** 343-374 (2012).

[64] Carr AC and Vissers M, *Nutrients*, **5,** 4284-4304 (2013).

[65] Weinstein M, Babyn P and Zlotkin S, *Pediatrics*, **108,** e55-e55 (2001).

[66] Levine M, Wang Y, Padayatty SJ and Morrow J, *Proceedings of the National Academy of Sciences*, **98,** 9842-9846 (2001).

[67] Simon JA and Hudes ES, *Archives of Internal Medicine*, **160,** 931-936 (2000).

[68] Allen L, de Benoist B, Dary O and Hurrell R, Guidelines on food fortification with micronutrients, in, World Health Organization and Food and Agricultural Organization of the United Nations, Geneva, 2006, pp. 6-10.

[69] Cantorna MT and Mahon BD, *Experimental biology and medicine (Maywood, N.J.)*, **229,** 1136-1142 (2004).

[70] Hypponen E, Laara E, Reunanen A, Jarvelin MR and Virtanen SM, *Lancet*, **358,** 1500-1503 (2001).

[71] Kendrick J, Targher G, Smits G and Chonchol M, *Atherosclerosis*, **205,** 255-260 (2009).

[72] Lappe JM, Travers-Gustafson D, Davies KM, Recker RR and Heaney RP, *The American Journal of Clinical Nutrition*, **85,** 1586-1591 (2007).

[73] Bandeira F, Costa AG, Soares Filho MA, Pimentel L, Lima L and Bilezikian JP, *Arquivos brasileiros de endocrinologia e metabologia*, **58,** 504-513 (2014).

[74] Song IG and Park CJ, *Blood Research*, **49,** 84 (2014).

[75] Ward LM, Gaboury I, Ladhani M and Zlotkin S, *CMAJ : Canadian Medical Association journal = journal de l'Association medicale canadienne*, **177,** 161-166 (2007).

[76] Holick MF, *Journal of cellular biochemistry*, **88,** 296-307 (2003).

[77] Holick MF, *Journal of investigative medicine : the official publication of the American Federation for Clinical Research*, **59,** 872-880 (2011).

[78] Japelt RB and Jakobsen J, *Frontiers in Plant Science*, **4,** 136 (2013).

[79] Thacher TD and Clarke BL, *Mayo Clinic proceedings. Mayo Clinic*, **86,** 50-60 (2011).

[80] Arts IC and Hollman PC, *The American Journal of Clinical Nutrition*, **81,** 317S-325S (2005).

[81] Hertog MG, Feskens EJ, Kromhout D, Hertog M, Hollman P, Hertog M and Katan M, *The Lancet*, **342,** 1007-1011 (1993).

[82] Standing Committee on the Scientific Evaluation of Dietary Reference Intakes and Its Panel on Dietary Antioxidants and Related Compounds, Dietary Reference Intakes: Proposed Definition and Plan for Review of Dietary Antioxidants and Related Compounds, in Dietary Reference Intakes, in, Institute of Medicine, Washington, D.C, 1998, pp. 1-13.

[83] Erdman JW, Balentine D, Arab L, Beecher G, Dwyer JT, Folts J, Harnly J, Hollman P, Keen CL and Mazza G, *The Journal of Nutrition*, **137,** 718S-737S (2007).

[84] Dinkova-Kostova AT, *Planta medica*, **74,** 1548-1559 (2008).

[85] Juge N, Mithen R and Traka M, *Cellular and Molecular Life Sciences*, **64,** 1105-1127 (2007).

[86] Ross JA and Kasum CM, *Annual Review of Nutrition*, **22,** 19-34 (2002).

[87] Häkkinen SH, Kärenlampi SO, Heinonen IM, Mykkänen HM and Törrönen AR, *Journal of Agricultural and Food Chemistry*, **47,** 2274-2279 (1999).

[88] Kelly GS, *Monograph. Alternative Medicine Rev*iew **16,** 172-194 (2011).

[89] Cao J, Zhang Y, Chen W and Zhao X, *British Journal of nutrition*, **103,** 249-255 (2010).

[90] Meyers KJ, Rudolf JL and Mitchell AE, *Journal of Agricultural and Food Chemistry*, **56,** 830-836 (2008).

[91] Borska S, Drag-Zalesinska M, Wysocka T, Sopel M, Dumanska M, Zabel M and Dziegiel P, *Folia Histochemica et Cytobiologica*, **48,** 222-221 (2010).

[92] Das S, Mandal AK, Ghosh A, Panda S, Das N and Sarkar S, *Current Aging Science*, **1,** 169-174 (2008).

[93] Joshi D, Naidu P, Singh A and Kulkarni S, *Journal of Medicinal Food*, **8,** 392-396 (2005).

[94] Davis JM, Carlstedt CJ, Chen S, Carmichael MD and Murphy EA, *International Journal of Sport Nutrition and Exercise Metabolism*, **20,** 56-62 (2010).

[95] Patel M and Naik S, *Journal of Science and Industrial Research*, **63,** 569-578 (2004).

[96] Kanno H, Usuki R and Kaneds T, *Nippon Shokuhin Kogyo Gakkaishi (J. Jpn. Soc. Food Sci. Technol.)*, **32,** 170 (1985).

[97] Wilson TA, Nicolosi RJ, Woolfrey B and Kritchevsky D, *The Journal of Nutritional Biochemistry*, **18,** 105-112 (2007).

[98] Murase Y and Iishima H, *Obstetics and Gynecological Practices*, **12,** 147-149 (1963).

[99] Phillips KM, Ruggio DM and Ashraf-Khorassani M, *Journal of Agricultural and Food Chemistry*, **53,** 9436-9445 (2005).

[100] Scholle JM, Baker WL, Talati R and Coleman CI, *Journal of the American College of Nutrition*, **28,** 517-524 (2009).

[101] Genser B, Silbernagel G, De Backer G, Bruckert E, Carmena R, Chapman MJ, Deanfield J, Descamps OS, Rietzschel ER, Dias KC and Marz W, *European Heart Journal*, **33,** 444-451 (2012).

[102] Berges RR, Kassen A and Senge T, *BJU International*, **85,** 842-846 (2000).

[103] Katan MB, Grundy SM, Jones P, Law M, Miettinen T and Paoletti R, *Mayo Clinic proceedings*, **78,** 965-978 (2003).

[104] Hamedi A, Ghanbari A, Saeidi V, Razavipour R and Azari H, *Journal of Functional Foods*, **8,** 252-258 (2014).

[105] Yuan J-P and Chen F, *Journal of Agricultural and Food Chemistry*, **46,** 5078-5082 (1998).

[106] Munyaka AW, Makule EE, Oey I, Van Loey A and Hendrickx M, *Journal of Food Science*, **75,** C336-C340 (2010).

[107] Van den Broeck I, Ludikhuyze L, Weemaes C, Van Loey A and Hendrickx M, *Journal of Agricultural and Food Chemistry*, **46,** 2001-2006 (1998).

[108] Haham M, Ish-Shalom S, Nodelman M, Duek I, Segal E, Kustanovich M and Livney YD, *Food & Function*, **3,** 737-744 (2012).

[109] Guttoff M, Saberi AH and McClements DJ, *Food Chemistry*, **171,** 117-122 (2015).

[110] Ader P, Wessmann A and Wolffram S, *Free Radical Biology & Medicine*, **28,** 1056-1067 (2000).

[111] Borghetti GS, Lula IS, Sinisterra RD and Bassani VL, *AAPS Pharmaceutical Science and Tech*ology **10,** 235-242 (2009).

[112] Pouton CW, *European journal of pharmaceutical sciences : official Journal of the European Federation for Pharmaceutical Sciences*, **29,** 278-287 (2006).

[113] Khuwijitjaru P, Yuenyong T, Pongsawatmanit R and Adachi S, *Journal of oleo science*, **58,** 491-497 (2009).

[114] Gawrysiak-Witulska M, Rudzinska M, Wawrzyniak J and Siger A, *Journal of the American Oil Chemists' Society*, **89,** 1673-1679 (2012).

[115] Neves MA, Hashemi J and Prentice C, *Current Opinion in Food Science*, **1,** 7-12 (2015).

[116] Euromonitor International, Vitamins and Dietary Supplements- United Kingdom, 2010.

Chapter 2

Monodisperse W/O/W emulsions encapsulating ʟ-ascorbic acid: Insights on their formulation using microchannel emulsification and stability studies*

_____

2.1 Introduction

Double emulsions are complex polydisperse systems in which water-in-oil and oil-in-water emulsions, which are stabilized by lipophilic and hydrophilic emulsifiers respectively, simultaneously exists [1]. These emulsions can further be categorized as water-in-oil-in-water (W/O/W) and oil-in-water-in-oil (O/W/O). O/W/O emulsions have limited applications in food and bio-industries [2]. In contrast, W/O/W emulsions are useful for producing lower-calorie encapsulated products than traditional oil-in-water (O/W) emulsions because part of the oily dispersed phase is replaced by aqueous droplets [3]. W/O/W emulsions have interesting applications in numerous industries, especially pharmaceutical industries for developing targeted drug delivery systems [4] and cosmetics and food industries for encapsulating flavors, therapeutics, and nutritional compounds [1, 5].

To date, two-stage emulsification has been adopted to produce W/O/W emulsions using a variety of production techniques [6]. Traditional emulsification devices include rotor-stator homogenizers (e.g., colloid mills, toothed-disk dispersing machines, and stirred vessels) and ultrasonic and high-pressure homogenizers [7]. The formation of W/O/W emulsions by rotor-stator homogenizers incorporates intense energy in the system because of vigorous external forces, resulting in a broader droplet size distribution with polydispersity [8]. The resultant emulsions usually have a coefficient of variation (CV) exceeding 20%. The typical droplet diameters are 1 to 10 μm for rotor-stator blenders, 1 to 5 μm for colloid mills, and 0.1 to 1 μm for high-pressure homogenizers [7]. Membrane emulsification (ME) [9], microchannel emulsification (MCE) [10], and microfluidic emulsification (MFE) using different types of geometries [11] have been developed over the last two decades to produce monodisperse emulsions with narrow size distributions. All of these emulsification devices have their own benefits and limitations, as stated in a recent review [12]. Major advantages of these emulsification techniques include the generation of uniform droplets, the precise control of droplet size and shape, and *in situ* microscopic monitoring (unusual for ME) that allows fine tuning of the process parameters during droplet generation [12].

Kawakatsu *et al.* [13] introduced MCE, an advanced and promising technique that is capable of generating uniformly sized droplets with average diameters of 1 to 500 μm and CVs of <5%. MCE works on the droplet generation mechanism driven by spontaneous transformation of the liquid-liquid interface on the terrace that exploits interfacial tension dominant on a micron scale [14]. This droplet generation requires no external shear force and minimum energy input (typically 10^3 to 10^4 J m^{-3}) [14].

Microchannel (MC) arrays fabricated for MCE are classified as grooved MC arrays (each consisting of parallel MCs with slit-like terraces outside them) [13] and straight-through MC arrays (each consisting of two-dimensionally positioned through-holes) [15, 16]. The droplet generation via each grooved MC array can be easily judged with direct microscopic observation, whereas straight-through MC arrays are advantageous for producing monodisperse emulsions at higher droplet productivity. Kobayashi et al. recently produced monodisperse O/W emulsions at a maximum droplet productivity of 1.4 L h^{-1} [17].

Various food-grade materials (e.g., refined vegetable oils, a medium-chain triglyceride oil, hydrophilic and hydrophilic emulsifiers, proteins, and hydrocolloids) have been examined for producing monodisperse O/W, W/O, and W/O/W emulsions by MCE [18]. Monodisperse W/O/W emulsions can be produced by a two-step emulsification process: high-pressure homogenization followed by MCE [19, 20]. Similarly, MCE has also been used to produce monodisperse microdispersions (e.g., solid lipid microspheres [21], gel microbeads [22], and giant vesicles [23]). MCE has promising potential for producing uniformly sized oil droplets containing such functional lipids as β-carotene [24] and γ-oryzanol [25]. However, further investigation and optimization of the MCE process are needed in order to encapsulate hydrophilic compounds in aqueous droplets.

L-AA is a powerful antioxidant because of its capacity to neutralize free radicals [26]. The chemistry, functions, metabolism, bioavailability, and effect of processing have been comprehensively reviewed [27, 28]. L-AA (vitamin C) is also important in minimizing the risk of serious diseases (e.g., heart disease, cataracts, improving the immune system and cancer). The recommended intake of L-AA is 30 to 40 mg per day, but some studies extend this limit to 250 to 1000 mg per day. L-AA is naturally present in many fruits and vegetables; however, exposure to high temperature during cooking and processing, moisture, oxygen, pH, and light deteriorate its antioxidant activity and thus results in the formation of toxic compounds [29].

Encapsulation of bioactive compounds in W/O/W emulsions is an emerging technology that has undergone intensive research in recent years. Lack of stability of W/O/W emulsions is a major problem because of the presence of two thermodynamically unstable interfaces. Their stabilization requires two different emulsifiers: one with a low hydrophilic lipophilic balance (HLB) for stabilizing the water-oil interface and another with a high HLB for stabilizing the oil-water interface. A variety of processes can be utilized to encapsulate L-AA (e.g., spray drying [30], spray chilling [30], and extrusion [31]). L-AA can

also be encapsulated in different formulations (e.g., liposomes [31], W/O and W/O/W emulsions [32, 33], and nanoparticles). Despite the advantages of each of these techniques, no single stabilization method is available for different food-processing environments due to lack of long term storage stability and rapid decline in encapsulation efficiency.

The objective of this study was to develop a novel method for preparing monodisperse W/O/W emulsions that encapsulate a high concentration of hydrophilic bioactive compound by using a two-stage process including asymmetric straight-through MCE. We encapsulated L-AA, a model hydrophilic bioactive compound, in W/O/W emulsions at a high concentration up to 30% (w/v). We also analyzed the stability of the resultant W/O/W emulsions and the retention profile of L-AA encapsulated in them.

2.2 Materials and methods

Materials

Refined soybean oil was purchased from Wako Pure Chemical Industries, Ltd. (Osaka, Japan). Milli-Q water with a resistivity of 18MΩ cm was used to formulate all aqueous-phase solutions. L-AA (99.9% purity), D(+)-glucose, magnesium sulfate, gelatin, disodium hydrogen phosphate dodecahydrate (sodium phosphate, dibasic), sodium dihydrogen phosphate dehydrate, and HPLC grade methanol were purchased from Wako Pure Chemical Industries, Ltd. Tetraglycerin monolaurate condensed ricinoleic acid ester (CR-310, HLB: <1) was procured from Sakamoto Yakuhin Kogyo Co., Ltd. (Osaka, Japan). Decaglycerol monolaurate (Sunsoft A-12, HLB: 12) was supplied by Taiyo Kagaku Co., Ltd. (Yokkaichi, Japan). All the chemicals were of the highest grade available and were used without further purification.
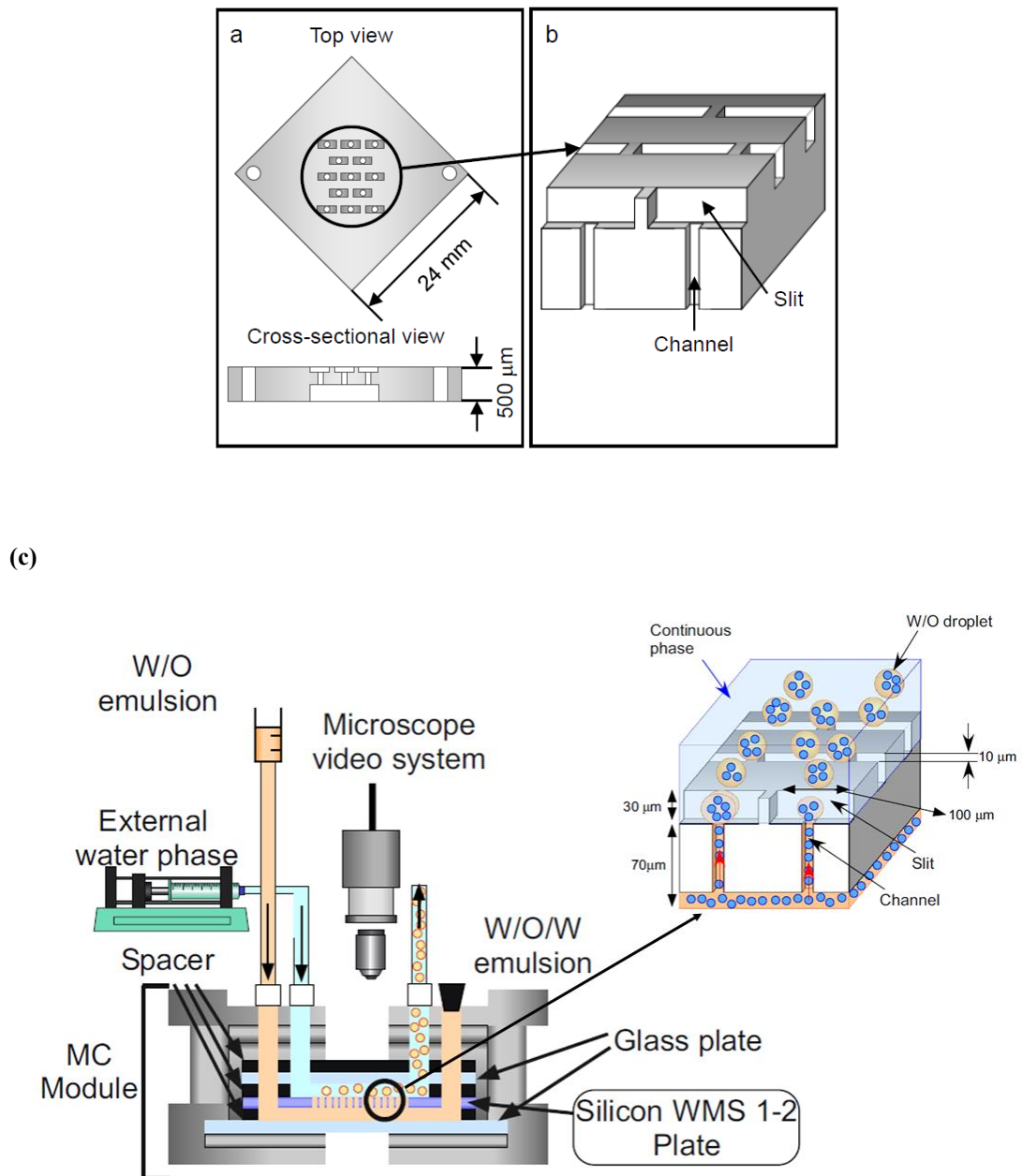
Figure 2.1: Schematic representations of (a) an asymmetric straight-through MC array (WMS-1-2) plate, (b) asymmetric straight-through MCs, and (c) MCE setup and generation of W/O/W emulsion droplets via asymmetric straight-through MCs.

Formulation of W/O emulsions through homogenization

Soybean oil solution containing 4 to 8% (w/w) CR-310 was used as the oil phase. Milli-Q water solution containing 10 to 30% (w/v) L-AA, 1% (w/w) magnesium sulfate, and 1% (w/v) gelatin was used as the inner aqueous phase. The L-AA has maximum solubility of 32% in water at 25 °C. A total of 100 mL of the water-oil mixture with a volume fraction (φ) of the inner aqueous phase of 30% was

emulsified with a rotor-stator homogenizer (Polytron PT-3000; Kinematica AG, Littau, Switzerland) at 10,000 rpm for 5 min to formulate a W/O emulsion. Homogenization at 10,000 rpm increased the system temperature to around 48 °C with L-AA retention to 90% in prepared W/O emulsions. The resultant W/O emulsions had a whitish color with smooth consistency.

Formulation of W/O/W emulsions through microchannel emulsification

W/O/W emulsions were formulated by MCE using an asymmetric straight-through MC array (Fig. 2.1). The MCE instrument consists of a silicon asymmetric straight-through MC array plate (WMS1-2, EP Tech Co., Ltd., Hitachi, Japan), a stainless-steel module, a liquid chamber to feed a dispersed phase (W/O emulsion), a syringe pump (Model 11; Harvard Apparatus. Inc., Holliston, USA) to feed a continuous phase (outer aqueous phase), and a microscope video system to monitor droplet generation [10, 19]. A 24 × 24 mm MC array plate fabricated using photolithography, deep reactive-ion etching, and thermal oxidation [19] was used in this study. An asymmetric straight-through MC array consisting of MCs lies within a 10×10 mm central region of the plate. Each asymmetric through-hole consisted of a 10×100 μm microslot with a 30 μm depth on the outlet side and a 10 μm-diameter circular MC with a 70 μm depth on the inlet side.

The module was initially filled with the outer aqueous phase (5 mM phosphate buffer (pH 7.0) with 1% (w/w) Sunsoft A-12, 1% (w/w) magnesium sulfate, and 10 to 30% (w/v) glucose). An MC array plate that was hydrophilically treated was degassed in the outer aqueous phase by ultrasonic vibration at 100 kHz (VS-100III, As One Co., Osaka, Japan) for 20 min. This plate was then mounted in the module. The W/O emulsion was fed into the module by lifting the dispersed phase reservoir, subsequently reaching the MC inlets. Further pressurization of the W/O emulsion initiated its passage through MCs at breakthrough pressure ($\Delta P_{d,BT}$), leading to the generation of W/O droplets (defined as oil droplets containing smaller inner aqueous droplets) in the outer aqueous phase. The pressure applied to the dispersed phase (ΔP_d) (kPa) was estimated by

$$\Delta P_d = \rho_d \Delta h_d g \qquad (2.1)$$

where ρ_d is the dispersed phase density (kg m^{-3}), Δh_d is the height of the dispersed phase reservoir (m), and g is acceleration due to gravity (m s^{-2}). To achieve stable W/O droplet generation, $\Delta P_{d,BT}$ ranged

from 5.1 to 6.0 kPa, depending on the L-AA concentration in the inner aqueous phase. The flow rate of the outer aqueous phase (Q_c) was controlled from 50 to 200 mL h^{-1} during droplet generation.

Osmotic pressure (Π_d) plays a key role in the stability of W/O/W emulsions. In the present study, the osmotic pressure was calculated by the Morse equation, which is a modified form of the van't Hoff equation:

$$\Pi_d = iMRT \qquad (2.2)$$

where i is the van't Hoff factor with a value of 2 for magnesium sulfate, M is the molar mass of solvents (kmol m^{-3}), R is the gas constant with a value of 8.31kPa m^3 (K mol)$^{-1}$, and T is the thermodynamic temperature (K). The Π_d for inner and outer aqueous phases was adjusted to 0.164 MPa to avoid droplet instability.

Measurement and analysis

The average droplet diameter (d_{av}) of the collected W/O and W/O/W emulsions were determined with image-analyzing software (WinROOF, Mitani Co. Ltd., Fukui, Japan) using images of 250 droplets taken with an optical microscope (DM IRM, Leica Microsystems, Wetzler, Germany). The coefficient of variation (CV) of these emulsions were expressed as

$$CV = \left(\frac{\sigma}{d_{av}}\right) \times 100 \qquad (2.3)$$

where σ is the standard deviation (µm) and d_{av} is the average droplet diameter (µm).

The densities of dispersed and continuous phases were measured using a density meter (DA-130 N, Kyoto Electronics Manufacturing Co., Ltd., Kyoto, Japan) at 25 °C. The viscosities of dispersed and continuous phases were measured with a vibro viscometer (SV-10, A&D Co., Ltd., Tokyo, Japan) at 25 °C by taking 35 mL of samples in a measuring vessel followed by immersion of sensor plates in that vessel. Viscosity was measured by detecting the electric current needed to resonate the sensor plates. The viscosity (η) was calculated by

$$\eta = \frac{\eta_{mea}}{\rho} \qquad (2.4)$$

where η_{mea} is the measured fluid viscosity and ρ is the fluid density. The static interfacial tension between the oil and the inner or outer aqueous phases was measured with a fully automatic interfacial tensiometer (PD-W, Kyowa Interface Sciences Co., Ltd., Saitama, Japan) using a pendant drop method.

Physical and chemical stability of L-AA loaded W/O/W emulsions

Physical stability of L-AA added W/O/W emulsions

The W/O/W emulsions loaded with L-AA formulated through MCE were observed under an optical microscope (DM IRM, Leica Microsystems, Wetzler, Germany) to evaluate consistency, homogeneity, and coalescence during 30d of refrigerated storage at 4 °C. The size and size distribution of the collected W/O droplets during storage time were determined using *WinROOF* software.

Chemical stability of L-AA in W/O/W emulsions

The amount of L-AA encapsulated in the W/O/W emulsions was determined by the spectrophotometric method reported by Zeng *et al.* [34] with slight modifications. All spectral measurements of methanolic extracts of W/O and W/O/W emulsions were carried out using a UV/VIS/NIR spectrophotometer (V-570, JASCO Co., Hachioji, Japan). First, 1 mL of the emulsion was extracted with 10 mL of methanol, followed by ultrasonication for 20 min. The methanolic extracts were then centrifuged (KN-70, KUBOTA Co., Tokyo, Japan) at 5,000 rpm for the first 60 min and at 2,000 rpm for another 15 min. A 1 mL aliquot of the subnatants was diluted twenty times with methanol and then injected into a quartz cell with a 10 mm pass length. The absorbance of L-AA in emulsion extract was measured at 247 nm using an appropriate blank. A representative standard curve of absorbance versus concentration gave linear least-squares regression with a coefficient of determination (r^2) of 0.9996. All experiments were repeated in triplicate and mean values were calculated. The retention ratio of L-AA (R_{AA}), defined as the ratio of the L-AA concentration measured at a given storage time (C_{AA}) to the initial L-AA concentration ($C_{AA,0}$), was calculated as follows:

$$R_{AA} = \left(\frac{c_{AA}}{c_{AA,0}}\right) \times 100 \qquad (2.5)$$

2.3 Results

Formulation of W/O and W/O/W emulsions loaded with L-AA

Fig. 2.2a presents a typical example of the droplet size distribution of W/O emulsion formulated at an L-AA concentration of 30% (w/v). Its $d_{av,W/O}$ was 2.9 μm, and its $CV_{W/O}$ was 15%. The $d_{av,W/O}$ values increased slightly with increasing L-AA concentrations in the range applied. W/O emulsion droplets must be smaller than the MC diameter to perform successful MCE. The inner aqueous droplets formulated in this study have diameters of less than 4 μm (Fig. 2.2a), indicating that they can easily pass through MCs with a diameter of 10 μm.

The freshly formulated W/O emulsions were used for MCE in order to produce W/O/W emulsions. After achieving $\Delta P_{d,BT}$, W/O droplets were generated via the asymmetric straight-through MC array. Figures 2.3a, b, and c depict the successful generation of uniformly sized W/O droplets from the slot outlets at the CR-310 concentration in the oil phase of 4% (w/w) and the L-AA concentration in the inner aqueous phase of 30% (w/v). The W/O/W emulsion formulated here had a $d_{av,w/o/w}$ of 30 μm and a $CV_{w/o/w}$ of 9.8%, demonstrating the formulation of a monodisperse W/O/W emulsion.

(a)
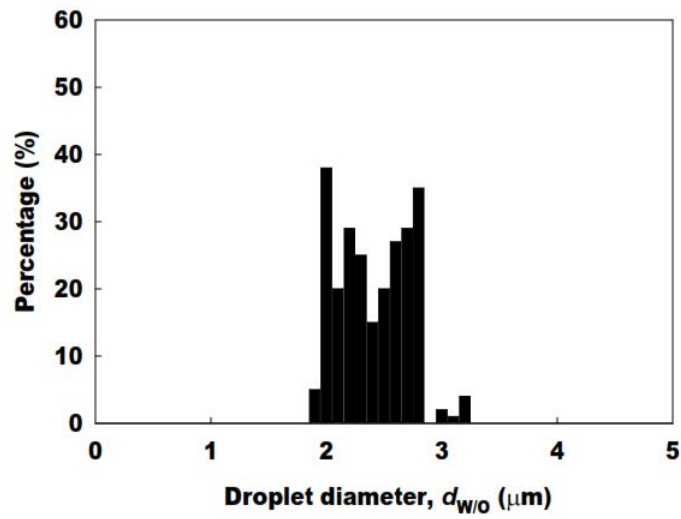
(b)
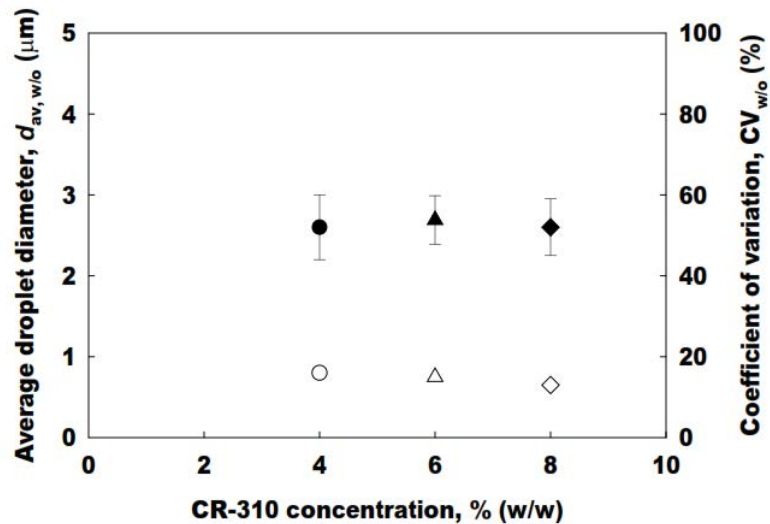
(c)
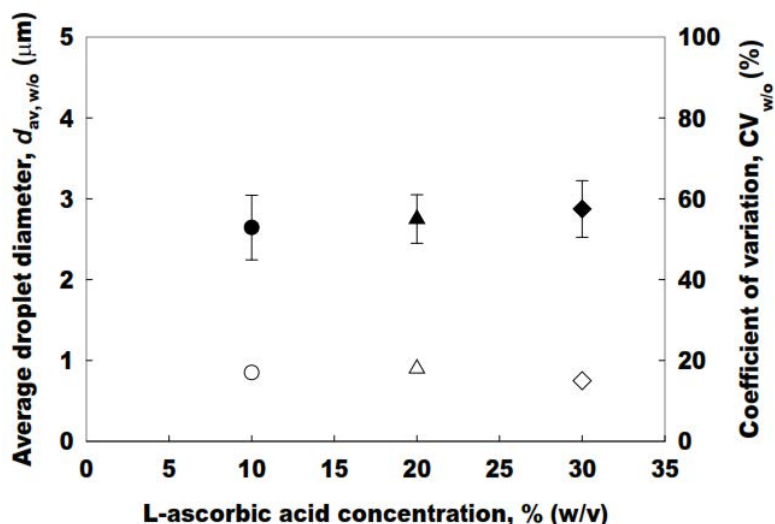
Figure 2.2: (a) Droplet size distribution of a W/O emulsion at 30% (w/v) L-AA. (b) Influence of CR-310 concentration on the average droplet diameter ($d_{av,W/O}$) and coefficient of variation ($CV_{W/O}$) of W/O emulsion formulated at 30% (w/v) L-AA. (c) d_{av} of W/O emulsions containing different concentrations of L-AA. In (b) and (c), solid keys denote $d_{av,W/O}$, and open keys denote $CV_{W/O}$.

Effect of CR-310 concentration in the oil phase

Fig. 2.3c, d, and e illustrate the effect of the CR-310 concentration on the formulation of W/O/W emulsions loaded with 30% L-AA in the inner aqueous phase when using the hydrophilic asymmetric straight-through MC array. W/O emulsions with $d_{av,W/O}$ of 2.6 μm and $CV_{W/O}$ of 13 to 16% were successfully formulated using different CR-310 concentrations (4 to 8% (w/w)) in the oil phase (Fig. 2.2b). Uniformly sized W/O droplets were stably generated from the slot outlets only for 4% (w/w) CR-310 (Fig. 2.3c). In contrast, for higher CR-310 concentrations of 6 and 8% (w/w), droplets were not stably generated (Figs. 2.3d, e), resulting in the formulation of unstable polydisperse W/O/W emulsions with large W/O droplets. At higher CR-310 concentrations, W/O droplets with increasing size and tail-like and oval shapes emerged from the slot outlets. These different geometrical shapes caused rough delayed detachment of W/O droplets from the slots (Figs. 2.3d, e). These results demonstrate that monodisperse W/O/W emulsions loaded with a high concentration of L-AA by MCE could be formulated only at a lower hydrophobic emulsifier in the outer aqueous phase.

56
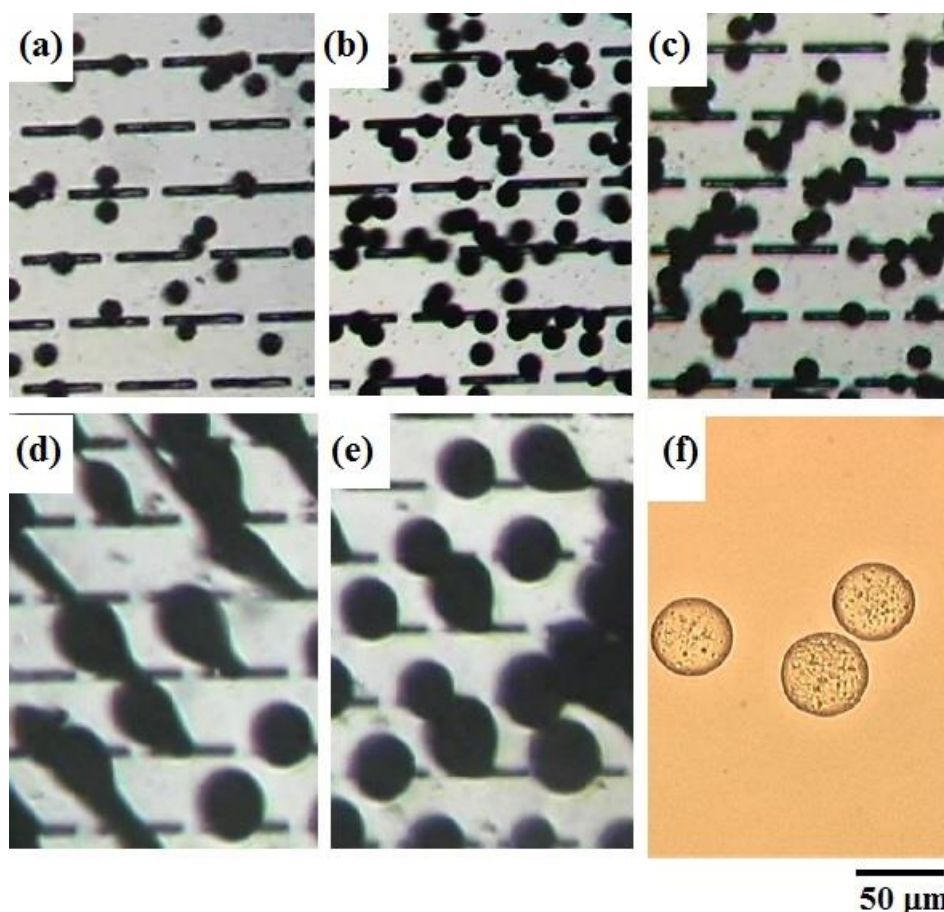
Figure 2.3: Effects of L-ascorbic acid and CR-310 concentrations on W/O droplet generation via an asymmetric straight-through MC. (a) 4% (w/w) CR-310 and 10% (w/v) L-AA. (b) 4% (w/w) CR-310 and 20% (w/v) L-AA. (c) 4% (w/w) CR-310 and 30% (w/v) L-AA. (d) 6% (w/w) CR-310 and 30% (w/v) L-AA. (e) 8% (w/w) CR-310 and 30% (w/v) L-ascorbic acid. (f) Optical micrograph of uniformly sized W/O droplets for 4% (w/w) CR-310 and 30% (w/v) L-AA.

Effect of L-AA concentration in the inner aqueous phase

The effect of L-AA concentration on the production of W/O/W emulsions by straight-through MCE was also investigated. L-AA content was varied from 10 to 30% (w/v) in the inner aqueous phase containing 1% (w/w) magnesium sulfate and 1% (w/v) gelatin, and glucose content was varied from 10 to 30% (w/v) in the outer aqueous phase containing 1% (w/w) Sunsoft A-12 and 1% (w/w) magnesium sulfate. The CR-310 concentration in the oil phase was kept at 4% (w/w). W/O emulsions with $d_{av,W/O}$ of 2.6 to 2.9 μm and $CV_{W/O}$ of 15 to 17% were successfully formulated using different L-AA concentrations in the inner aqueous phase (Fig. 2.2c). The d_{av} of the W/O emulsions is not significantly affected by L-AA concentration. The slight increase in droplet size may correspond toward increase in concentration of L-AA. The viscosity of dispersed phase increases with increasing the L-AA concentration (Table 2.1), providing small area for rotor-starter homogenizer to reduce the d_{av}. As a

result, a slight increase in d_{av} of W/O emulsions was obtained when using a high concentration of L-AA. On the other hand, the emulsifier concentration have no effect on the d_{av} of the W/O emulsions, which may be attributable to complete coverage of the emulsifier molecules at the interface, as clearly seen from the interfacial values. Successful MCE that means uniformly sized W/O droplets were generated regardless of L-AA concentration (Figs. 2.3a, b, and c). Smooth detachment of W/O droplets from the slot outlets was observed. The $d_{av,W/O/W}$ of the formulated W/O/W emulsions, which ranged from 26 to 33 μm, increased slightly with increasing L-AA concentration. Their $CV_{W/O/W}$ values were less than 10%, and the droplet size distribution data in Figs. 4a, b, and c demonstrate their monodispersity.

(a)
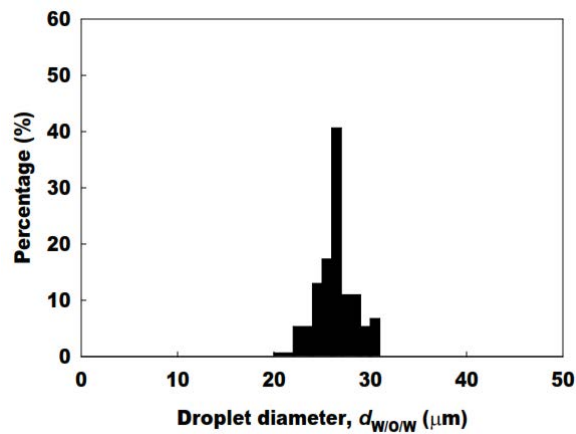
(b)
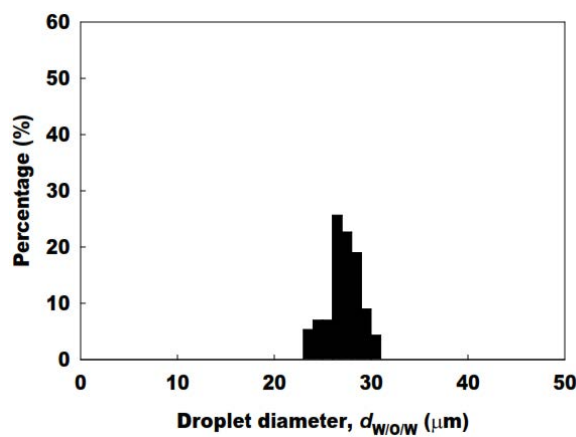
(c)
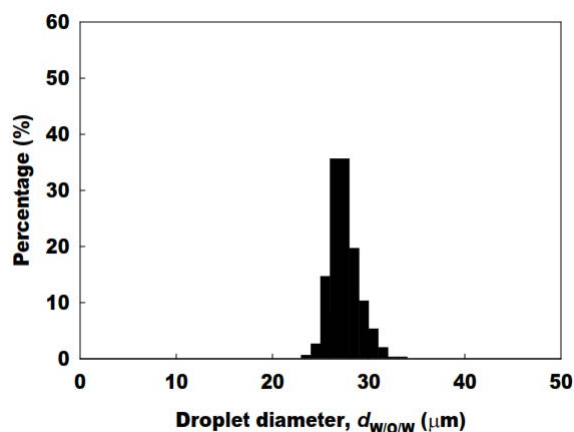
Figure 2.4: Size distributions of W/O droplets formulated using MCE. (a) 10% (w/v) L-AA. (b) 20% (w/v) L-ascorbic acid. (c) 30% (w/v) L-AA. The CR-310 concentration in the oil phase was 4% (w/w).

Physical and chemical stability of L-AA loaded W/O/W emulsions

The monodisperse W/O/W emulsions were stored at 4°C for 10 d. Immediately after formulation, emulsions with different L-AA concentrations had a whitish turbid appearance with good flowability. The appearance of the W/O/W emulsions did not change with time. Fig. 2.5a depicts time changes in the $d_{av,W/O/W}$ and $CV_{W/O/W}$ of the formulated W/O/W emulsions loaded with different L-AA concentrations. A slight increase in $d_{av,W/O/W}$ was observed, indicating that inner droplets might swell due to osmotic pressure difference and high concentration of L-AA. The initial solution preparation allows the penetration of oxygen into the system despite of osmotic pressure adjustment by Morse equation. The dissolved oxygen tends to increase the osmotic pressure over storage period, which slightly increases the d_{av} of W/O/W emulsions. There was an non-significant difference ($p > 0.05$) in $d_{av,W/O/W}$ and $CV_{W/O/W}$ during storage of the W/O/W emulsions containing 10% (w/w) L-AA. In contrast, $d_{av,W/O/W}$ and $CV_{W/O/W}$ of the W/O/W emulsions containing 30% (w/w) L-AA slowly increased from 30 μm to 31.5 μm with $CV_{W/O/W}$ around 10% during storage (Fig. 2.5a).

The freshly formulated W/O emulsions had an initial retention of more than 90% regardless of L-AA concentration. Figure 2.5b indicates L-AA retention in the W/O/W emulsions freshly formulated in section 3.3. Their initial retention of L-AA exceeded 85%. Their L-AA levels decreased slightly with time and exhibited 80% retention after 10 d.

59

(a)
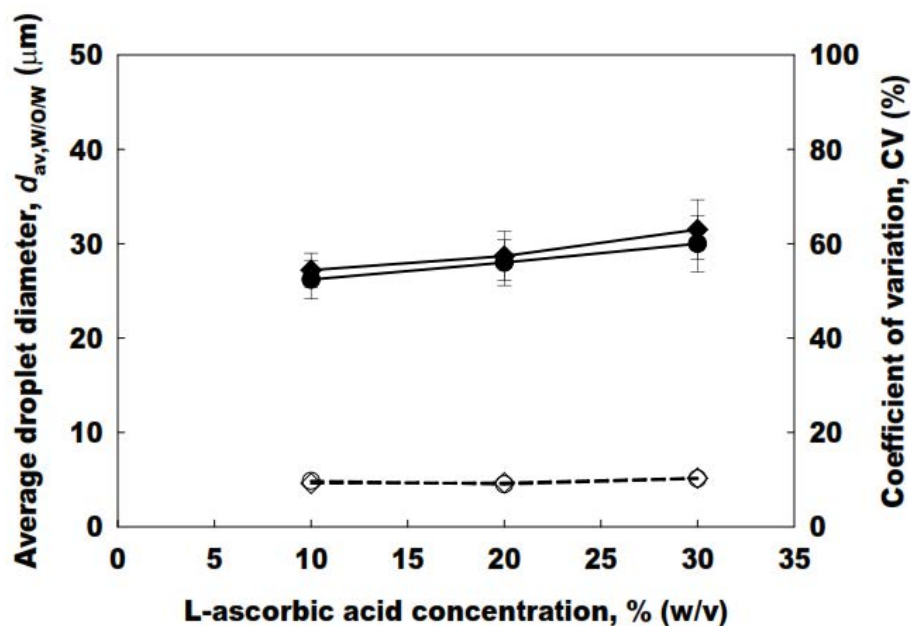
(b)
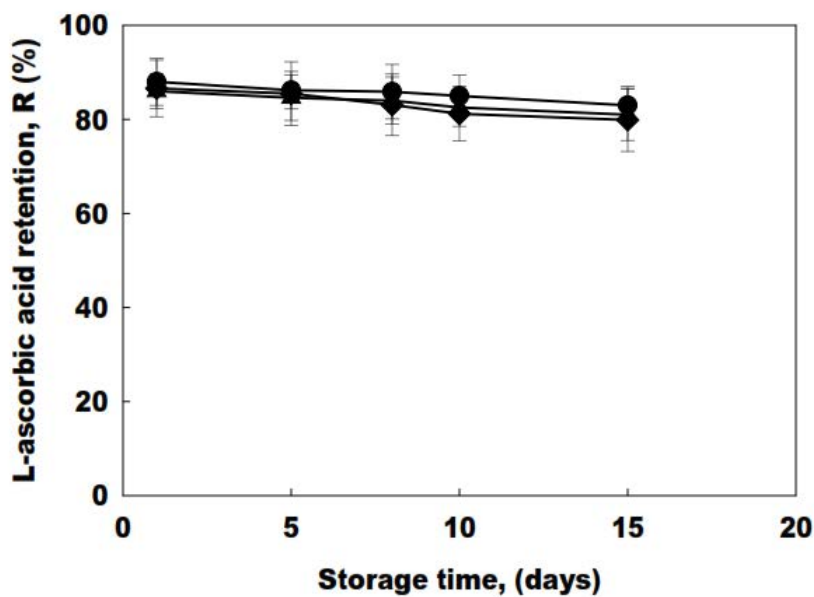
Figure 2.5: (a) Effect of L-ascorbic acid concentration on average droplet diameter ($d_{av,W/O/W}$) and coefficient of variation ($CV_{W/O/W}$) of the collected W/O/W emulsions. ●— denotes $d_{av,W/O/W}$ at day 1, and ◆— denotes $d_{av,W/O/W}$ at day 10. ⊖- denotes $CV_{W/O}$ at day 1, and ⋄- denotes $CV_{W/O}$ at day 10. **(b) L-AA retention (R) in the collected W/O/W emulsions at different concentrations.** ●— denotes 10% (w/v) L-AA, ▲ denotes 20% (w/v) L-AA and ◆— denotes 30% (w/v) L-AA.

2.4 Discussion

The present study was conducted to formulate stable monodisperse W/O/W emulsions loaded with a high concentration of L-AA. MCE was adopted to achieve this purpose, as MCE has the ability to formulate monodisperse emulsions under considerably mild processing conditions. In this study, some physicochemical parameters were also checked to clarify the processing conditions necessary to prepare monodisperse W/O/W emulsions.

Previous studies have encapsulated L-AA in W/O/W and O/W/O emulsions for topical creams and other pharmaceutical applications but seldom describe the retention and droplet size distribution of primary emulsions [35, 36]. The formulated double emulsions rapidly coalesce within a short time, resulting in increased polydispersity that limits their use in numerous applications. Moreover, only low concentrations of L-AA have been encapsulated in double emulsions including non-food-grade materials [27, 35-37]. Monodisperse W/O/W emulsions with $d_{av,W/O/W}$ of 40 μm were formulated by MCE using symmetric oblong straight-through MCs [19]. W/O/W emulsions for drug-delivery systems were also formulated by extruding a coarse W/O/W emulsion five times under pressures of 70 to 150 kPa through a Shirasu Porous Glass (SPG) membrane [2]. These studies focused on production characteristics but did not consider any encapsulated bioactive compound. Similarly, these MCE and ME studies did not evaluate the stability of formulated W/O/W emulsions. The present study obtained new findings regarding the formulation and storage stability of monodisperse W/O/W emulsions loaded with a high concentration of L-AA.

Emulsions prepared from the rotor-starter homogenizers always have border size distribution with CV more than 30%. In our study we prepared the W/O emulsions having CV more than 20% with boarder size distribution (Fig. 2.2a). The contact area of rotor-starter with emulsions is broader enough to generate polydisperse droplets. Moreover, the homogenization speed was mild enough to prepare W/O emulsions. The W/O emulsions prepared at this homogenization speed has d_{av} around 4 μm. Emulsifier concentration plays a significant role in stabilizing both W/O and W/O/W emulsions, and its optimization is very important for successful emulsification using MCs or membrane pores. Hasegawa *et al.* [38] stated that W/O/W emulsions can be formulated using low concentrations of emulsifiers in the oil and outer aqueous phases, and that emulsifier type influences the formulation of W/O/W emulsions. Kawakatsu *et al.* [39] stated that the tetraglyerol polyricinoleate (TGPR) concentration in the oil phase affects the stability of oil droplets, each containing inner aqueous droplets. At a high TGPR (5%

(w/w)) concentration, those containing stable inner aqueous droplets tended to coalesce, destabilizing W/O/W emulsions. In our study, stable W/O droplets were generated at a low CR-310 concentration (4% (w/w)) (Fig. 2.3c). However, higher CR-310 concentrations (6 and 8% (w/w)) resulted in unstable W/O droplet generation, during which the dispersed phase forms an elongated balloon-like shape over the slot outlets (Figs. 2.3d, e). Interfacial tension that exceeds other major forces on a micron scale plays an important role in droplet generation by MCE [14]. Interfacial tensions exceeding threshold level (c.a. ~1 mN m^{-1}) are needed to stably formulate monodisperse emulsions [40]. Karbstein and Schubert [3] demonstrated that dynamic interfacial tension between a vegetable oil and an aqueous solution containing an emulsifier is influenced by emulsifier concentration. During W/O droplet generation in our study, dynamic interfacial tension of a newly created interface is assumed to decrease more rapidly as the CR-310 concentration increases. At CR-310 concentrations exceeding a threshold level, a rapid decrease in dynamic interfacial tension may inhibit smooth pinch-off of the interface between the W/O emulsion and outer aqueous phases in the slot, resulting in generation of large W/O droplets. There is also a possibility that rapid adsorption of CR-310 molecules at the preceding interface has weak affinity interactions with the chip surfaces during W/O droplet generation, resulting in rough and irregular interfacial motion in the slot.

In our study, monodisperse W/O/W emulsions loaded with L-AA were successfully formulated using MCE, and their $d_{av,W/O/W}$ slightly depended on L-AA concentration. This dependence of $d_{av,W/O/W}$ on L-AA concentration is attributed to the variation in the viscosity of the outer aqueous phase, as the viscosity of the oil phase is much higher than the threshold level, below which droplet size becomes sensitive in MCE [41]. The viscosity of the outer aqueous phase ranged from 1.8 to 2.8 mPa s when the L-AA concentration varied (Table 2.1). This viscosity variation is attributed to the difference in the glucose concentration necessary to adjust the osmotic pressure in the outer aqueous phase. van Dijke, *et al.* [41] demonstrated that the droplet size of soybean O/W emulsions formulated by MCE increases with increasing viscosity of the continuous phase between 0.91 and 68.2 mPa s. The effect of viscosities on droplet generation behavior can be described in terms of viscosity ratio. At high viscosity ratios of the dispersed and continuous phases, the droplet size is not influenced, while at low viscosity ratios, the droplets become larger. There is a viscosity ratio below which successful MCE is not possible. In the present study the viscosity ratio was higher than a critical value, demonstrating that the continuous and disperse phases have not major effect upon d_{av}.

Table 2.1: Physicochemical properties of different phases used to formulate W/O/W emulsions.

Experimental system[a]	Emulsifier[b]	Viscosities[c, d, e] (mPa s)			Interfacial tension[f, g] (mN/m)	
	(%)	Oil phase	Inner aq. phase	Outer aq. Phase	Oil and Inner aq. Phases	Oil and outer aq. Phases
LAA- 10	CR-310- 4	64.8±0.26	1.9±0.01	1.8±0.05	6.2±0.30	1.8±0.40
LAA- 20	CR-310- 4	64.8±0.26	2.6±0.02	2.2±0.01	6.4±0.10	1.4±0.50
LAA- 30	CR-310- 4	64.8±0.26	3.0±0.01	2.8±0.01	6.2±0.30	1.6±0.20
LAA- 10	CR-310- 6	73.0±0.10	1.9±0.01	1.8±0.05	6.2±0.40	2.0±0.20
LAA- 20	CR-310- 6	73.0±0.10	2.6±0.02	2.2±0.01	6.4±0.20	2.0±0.20
LAA- 30	CR-310- 6	73.0±0.10	3.0±0.01	2.8±0.01	6.6±0.40	2.1±0.40
LAA- 10	CR-310- 8	77.4±0.21	1.9±0.01	1.8±0.05	6.6±0.90	1.5±0.40
LAA- 20	CR-310- 8	77.4±0.21	2.6±0.02	2.2±0.01	6.1±0.50	1.7±0.30
LAA- 30	CR-310- 8	77.4±0.21	3.0±0.01	2.8±0.01	6.0±0.40	1.6±0.40

[a]Internal aqueous phase containing 10 to 30% (w/v) L-ascorbic acid with 1% (w/w) $MgSO_4$ and 1% (w/v) gelatin, [b]4 to 8% (w/w) tetra glycerin condensed ricinoleic acid esters (CR-310) in soybean oil, [c]Viscosity of 4 to 8% (w/w) CR-310 in soybean oil, [d]Viscosity of 10 to 30% (w/v) water-in-oil emulsion having 1% (w/w) $MgSO_4$ and 1% (w/v) gelatin, [e]Viscosity of internal water phase having 1% (w/w) $MgSO_4$, 10 to 30% (w/v) glucose, and 1% (w/w) Sunsoft A-12, [f]Interfacial tension between internal aqueous phase and oil phase, [g]Interfacial tension between external aqueous phase and oil phase.

L-AA is readily and reversibly oxidized to dehydrascorbic acid, which is present in aqueous media as a hydrated hemiketal. The biological activity is lost when the dehydroascorbic acid lactone ring is irreversibly opened, giving rise to 2,3-diketogulonic acid. The oxidation of L-AA to dehydroascorbic acid and its further degradation products depends on several factors. Oxygen partial pressure, pH, temperature, light, and the presence of heavy metal ions are of great importance. The monodisperse W/O/W emulsions formulated in our study were stable for more than a week, maintaining whitish turbidity, consistency, and flowability. The presence of hypertonic inner aqueous phase causes water migration from an outer aqueous phase to an inner aqueous phase, resulting in slow swelling of the inner aqueous droplets that may be a possible reason for a slight increase in $d_{av,W/O/W}$ during storage. Similar inner aqueous droplet swelling in different food-grade W/O/W emulsions containing sodium chloride was reported by Sapei and Rousseau [30]. The physical stability of emulsions may also be affected by the acidic nature of L-AA. In this study, relatively high concentrations of L-AA are

encapsulated in inner aqueous droplets. At high concentrations of L-AA, the interfacial layer stabilizing inner aqueous droplets could be influenced by L-AA molecules, allowing slight swelling to take place with the passage of time. Hypertonic conditions promote such swelling, increasing the packing density of the inner aqueous droplets. The overall increase in this packaging density may enhance the stability and release profile of L-AA encapsulated in the monodisperse W/O/W emulsions. The beneficial effect of packaging density in W/O/W emulsions was previously reported by Sapei *et al.* [31].

The initial retention of L-AA in this study (Fig. 2.5b) was similar to our previous results for W/O/W emulsions loaded with L-AA formulated using conventional two-step emulsification [32]. Our previous studies on encapsulating L-AA in W/O and W/O/W emulsions demonstrated a decline rate of 10% with each week of storage time [32, 33]. In the present study, we achieve higher L-AA retentions of 81 to 83% after 15 days of storage. This higher retention can be ascribed to the narrow size distribution of the W/O droplets formulated by MCE, as well as very mild W/O droplet generation, since droplet generation in MCE was based upon difference in interfacial tension rather than high-energy second-step homogenization. This low-energy MCE process is considered to increase the retention of L-AA in W/O/W emulsions during storage. Previous studies confirmed that L-AA encapsulated in W/O/W emulsions is more stable and has good functionality in numerous pharmaceutical products [27, 35, 36, 42].

References

[1] Dickinson E, *Food Biophys*, **6,** 1-11 (2011).

[2] Vladisavljević GT, Shimizu M and Nakashima T, *J. Membrane Sci.*, **284,** 373-383 (2006).

[3] Karbstein H and Schubert H, *Chem. Eng. Proces.,* **34,** 205-211 (1995).

[4] Ferreira LAM, Seiller M, Grossiord JL, Marty JP and Wepierre J, *Int. J. Pharm.*, **109,** 251-259 (1994).

[5] Schmidts T, Dobler D, Nissing C and Runkel F, *J. Colloid Interface Sci*, **338,** 184-192 (2009).

[6] Jahanzad F, Crombie G, Innes R and Sajjadi S, *Chem. Eng. Res. Design.*, **87,** 492-498 (2009).

[7] McClements D, Food Emulsions: Principles, Practice and Techniques, CRC Press, Boca Raton, Florida, 2004, pp. 20-50.

[8] Matsumoto S, Kita Y and Yonezawa D, *J. Colloid Interface Sci.*, **57,** 353-361 (1976).

[9] Nakashima TS, M, *Ceramics Jpn*, **21,** 408 – 412 (1986).

[10] Kobayashi I and Nakajima M, *Eur. J. Lipid Sci. Technol.*, **104,** 720-727 (2002).

[11] Ralf S, Martin B, Thomas P and Stephan H, *Rep. Prog. Phys.*, **75,** 016601 (2012).

[12] Vladisavljevic' GT, Kobayashi I and Nakajima M, *Microfluid Nanofluid*, **13,** 151-178 (2012).

[13] Kawakatsu T, Kikuchi Y and Nakajima M, *J. Am. Oil Chem. Soc.*, **74,** 317-321 (1997).

[14] Sugiura S, Nakajima M, Iwamoto S and Seki M, *Langmuir*, **17,** 5562-5566 (2001).

[15] Kobayashi I, Nakajima M, Chun K, Kikuchi Y and Fukita H, *Aiche J.*, **48,** 1639-1644 (2002).

[16] Kobayashi I, Mukataka S and Nakajima M, *Langmuir*, **21,** 5722-5730 (2005).

[17] Kobayashi I, Neves MA, Wada Y, Uemura K and Nakajima M, *Green Process Synthesis.*, **1,** 353-362 (2012).

[18] Ribeiro HS, Janssen JJ, Kobayashi I and Nakajima M, Membrane emulsification for food applications, Wiley-VCH Verlag GmbH & Co, 2010.

[19] Kobayashi I, Lou XF, Mukataka S and Nakajima M, *J. Am. Oil Chem. Soc.*, **82,** 65-71 (2005).

[20] Souilem S, Kobayashi I, Neves M, Sayadi S, Ichikawa S and Nakajima M, *Food Bioprocess Technol.*, **7,** 2014-2027 (2014).

[21] Sugiura S, Nakajima M, Tong JH, Nabetani H and Seki M, *J. Colloid Interface Sci.*, **227,** 95-103 (2000).

[22] Iwamoto S, Nakagawa K, Sugiura S and Nakajima M, *AAPS Pharmscitech*, **3,** 72-76 (2002).

[23] Sugiura S, Kuroiwa T, Kagota T, Nakajima M, Sato S, Mukataka S, Walde P and Ichikawa S, *Langmuir*, **24,** 4581-4588 (2008).

[24] Neves MA, Ribeiro HS, Kobayashi I and Nakajima M, *Food Biophys*, **3,** 126-131 (2008).

[25] Neves MA, Ribeiro HS, Fujiu KB, Kobayashi I and Nakajima M, *Ind. Eng. Chem. Res.*, **47,** 6405-6411 (2008).

[26] Elmore AR, *Int. J. Toxicol.*, **24,** 51-111 (2005).

[27] Abbas S, Da Wei C, Hayat K and Xiaoming Z, *Food Rev. Int.*, **28,** 343-374 (2012).

[28] Bendich A, Antioxidant vitamins and human immune responses, New York Academy of Sciences, New York, 1996.

[29] Gallarate M, Carlotti M, Trotta M and Bovo S, *Int. J. Pharm.*, **188,** 233-241 (1999).

[30] Sapei L and Rousseau D, *Int. J. Food Nutr Public Health*, **5,** (2012).

[31] Sapei L, Naqvi MA and Rousseau D, *Food Hydrocolloid*, **27,** 316-323 (2012).

[32] Khalid N, Kobayashi I, Neves MA, Uemura K and Nakajima M, *Biosci. Biotechnol. Biochem*, **77,** 1171-1178 (2013).

[33] Khalid N, Kobayashi I, Neves MA, Uemura K and Nakajima M, *LWT - Food Sci. Technol.*, **51,** 448-454 (2013).

[34] Zeng W, Martinuzzi F and MacGregor A, *J. Pharm. Biomed. Anal.*, **36,** 1107-1111 (2005).

[35] Akhtar N, Ahmad M, Khan HA, J, Gulfishan, Mahmood A and Uzair M, *Bull. Chem. Soc. Ethiopia*, **24,** 1-10 (2010).

[36] Lee J, Kim J, Han S, Chang I, Kang H, Lee O, Oh S and Suh K, *J. Cosmet. Sci.*, **55,** 1-12 (2004).

[37] Farahmand S, Tajerzadeh H and Farboud ES, *Pharm. Develop. Technol.*, **11,** 255-261 (2006).

[38] Hasegawa Y, Imaoka H, Adachi S and Matsuno R, *Food Sci. Technol. Res.*, **7,** 300-302 (2001).

[39] Kawakatsu T, Tragardh G and Tragardh C, *Colloid Surface A*, **189,** 257-264 (2001).

[40] Kobayashi I, Zhang Y, Neves MA, Hori Y, Uemura K and Nakajima M, *Colloid Surface A*, **440,** 79-86 (2014).

[41] van Dijke K, Kobayashi I, Schroën K, Uemura K, Nakajima M and Boom R, *Microfluid Nanofluid*, **9,** 77-85 (2010).

[42] Ahmad I, Sheraz M, Ahmed S, Shaikh R, Vaid F, ur Rehman Khattak S and Ansari S, *AAPS PharmSciTech*, **12,** 917-923 (2011).

Chapter 3

Monodisperse aqueous microspheres encapsulating high concentration of L-ascorbic acid: Insights of preparation and stability evaluation from straight-through microchannel emulsification*

_____

3.1 Introduction

There are increasing demands for products which are expected to optimize health and target-delivery of supplements to the optimum absorption sites in the gastrointestinal tract. During last two decades, microspheres have been widely used in food, pharmaceutical and chemical industries[1-3]. Monodisperse microspheres have numerous advantages such as efficient drug delivery, higher bioavailability, high dispersibility and fast permeability[4-6]. Microspheres are generated by different methods including ionic gelation,[7] cross-linked emulsions,[8] sieve methods,[9] bio-electro spraying,[10] and numerous spray drying techniques[11]. All of these methods have potential advantages such as better particle size controllability, better particle morphology and better penetration at target areas.

Microparticle technology has potential applications in the controlled delivery of bioactives such as vitamins, probiotics, small bioactive peptides and antioxidants[12]. For instance, Ellis and Jacquier[13] formulated food-grade κ-carrageenan microspheres with a broad range of functionalities such as nutraceutical delivery systems or fat replacers. Prasertmanakit *et al.*[14] prepared ethyl cellulose microcapsules for protection and controlled release of folic acid in foods and supplements. Duclairoir *et al.*[15] formulated gliadin nanoparticles as efficient drug carriers for α-tocopherol or vitamin E.

Anionic polysaccharide gels like alginate (ALG) particles have numerous applications for encapsulation and delivery systems. Potential applications include encapsulation of drugs[16], probiotics[17], control flavor release[18], enzyme protection, and guided delivery of drugs to their target organs[19]. ALGs have an inert nature, high porosity, superior coverage, superior penetration rate, mild encapsulation temperature, and biocompatibility with numerous bioactive substances[20].

ALG is a natural, non-toxic, biodegradable, biocompatible, and inert polysaccharide found in all species of brown algae[21]. Chemically, ALG is composed of two types of uronic acids, guluronic (G) and mannuronic (M). Monomeric units consisting of G and M are arranged in three types of grouping: blocks of alternating M and G residues (MGMG-MGM...), blocks of G (GGGGGGG...), and blocks of M (MMM-MMM...)[22]. Sodium alginate (Na-ALG) is a water-soluble compound that gels in the presence of divalent cations[21]. Such gels can be heat-treated without melting, although they may eventually degrade. Gelling depends on ion binding ($Ca^{+2} < Zn^{+2} < Sr^{+2} < Ba^{+2}$), with the control of cation addition being important for producing homogeneous gels[22].

ALG composition is an important parameter in ALG particle formation. At a Na-ALG concentration below 1.0%, almost no spherical particles were formed, probably due to the lack of

enough carboxyl groups for gelation. Increasing Na-ALG concentration causes higher viscosity of an aqueous phase, resulting in larger droplets with a wide distribution[22,23]. Thus, for a given application, the Na-ALG concentration must be controlled in particle size, shape, and size distribution.

L-ascorbic acid (L-AA) is a water soluble vitamin and regarded as dietary intake of vitamin C[24]. L-AA is present in many leafy vegetables and fruits, noticeably in guava, orange, apple, strawberry, kiwi, capsicum, pawpaw and cauliflower[25]. The importance of vitamin C is seen clearly in scurvy, a life-threatening vitamin C deficiency disease that results in loss of energy, depression, mood disorders, poor wound healing, and connective tissue disorders, culminating in death[26]. Vitamin C plays an important role in formation of collagen (in bones, teeth and cartilage) and activation of various enzymes related to nervous system, and detoxification of drugs in liver. With a structure similar to carbohydrates, vitamin C can uniquely undergo reversible oxidation reactions[27]. Additionally, the chemical properties of vitamin C allow it to react with a wide variety of potentially harmful reactive oxygen species. Vitamin C is stable in powder form, while its stability decreases in aqueous formulations. Environmental factors that affect the stability include temperature, pH, oxygen, metal ion, UV and x-ray [28,29].

Microchannel emulsification (MCE) is a progressive method that enables preparing monodisperse droplets by spontaneous transformation of oil-water interface specifically driven by interfacial tension on a micron scale[30] and comprehensively reviewed by Vladisavljevic' et al.[31] Similarly, this emulsification technique allows integration of hundreds of thousands of droplet generation units on a single silicon and on the other hand stainless steel chips currently contain fewer number of droplet generating units[32,33]. Kawakatsu et al.[34] introduced MCE and this technology enables the production of different emulsions with diameter ranged from 1 μm to 500 μm. The fabricated microchannel (MC) arrays are classified as grooved MC arrays consisting of uniform microgrooves with slit-like terraces outside them and straight-through MC arrays having two-dimensionally positioned, symmetric or asymmetric micro-through-holes[31]. These straight-through MC arrays enable the mass production of monodisperse droplets, with precise control on processing parameters.

MCE has been used to produce monodisperse microdispersions including solid lipid microspheres,[35] gel microbeads[36] and giant vesicles[37]. Many dispersions encapsulating β-carotene,[38] oleuropein,[39] γ-oryzanol,[40] L-AA[41] and ascorbic acid derivatives [42] have been also prepared using MCE.

Several research groups have encapsulated L-AA at relatively low concentrations (up to 5%) in aqueous droplets using different homogenization techniques[43-46]. The main objective of this study is to formulate different pharmaceutical and food-based products such as energy drinks and fortified nutritional supplements containing high concentrations of bioactives. This model study was conducted with n-Decane as the continuous phase that can be replaced with appropriate viscosity oil such as, ethyl oleate, oleic acid or different types of medium chain triglyceride oils. Moreover, this study was conducted to optimize production method for obtaining monodisperse aqueous microspheres containing high concentration of L-AA using straight-through MCE. In this study L-AA was encapsulated at a concentration of 30% (w/w) in aqueous microspheres along with varying concentrations of Na-ALG. The study investigated the optimization of the formation conditions and effects of osmotic pressures and varying concentrations of L-AA on MCE. Moreover, the study also evaluate the stability of the prepared microspheres and the retention profile of the L-AA encapsulated in them.

3.2 Materials and Methods

Materials

L-AA (99.9% purity), anhydrous magnesium sulfate (MgSO$_4$) and sodium alginate (Na-ALG) were purchased from Wako Pure Chemical Ind. (Osaka, Japan). All of these chemicals were used for preparing a dispersed phase. Milli-Q water with a resistivity of 18 MΩ cm^{-1} was used to dissolve all the above-mentioned chemicals. *n*-Decane was procured from Wako Pure Chemical Ind. and tetraglycerol condensed ricinoleate (TGCR, CR-310) was supplied by Sakamoto Yakuhin Kogyo Co., Ltd. (Osaka, Japan). They were used for preparing a continuous phase. Hexamethyldisilazane (LS-7150), purchased from Shin-Etsu Chemical Co. Ltd. (Tokyo, Japan), was used for surface hydrophobization of a silicon MC array chip and a glass plate. HPLC grade methanol was used to extract L-AA from aqueous microspheres. All these chemicals were of analytical grade and used without further purification.

Emulsification Setup for microsphere characterization

Fig. 3.1a depicts a simplified schematic diagram of the experiment setup used for MCE. A hydrophobized silicon MC array plate is tightly attached to a hydrophobized glass plate in the emulsification module initially filled with the continuous phase. A syringe pump (Model 11, Harvard

Apparatus, Inc., Holliston, USA) was used to supply the continuous phase. The heating system provides temperature-controlled water circulation inside the module and outside the reservoir. A microscope video system was used to monitor and record droplet formation by MCE[47]. Fig. 3.1b and c depict a dead-end silicon MC array plate (Model MS407, EP Tech., Co. Ltd., Hitachi, Japan) consisting of 400 MCs fabricated on four MC arrays. Each channel has terraces outside its inlet and outlet, and wells are fabricated outside the terraces. Channel and terrace dimensions are presented in Fig. 3.1(d), except for channel and terrace depth (7 μm).

The glass and silicon MC array plates were treated with LS-7150 to make their surfaces hydrophobic, so that they became suitable for preparing aqueous liquid microspheres in the continuous oil phase. This hydrophobic treatment was performed using slight modification of the procedure by Kawakatsu et al.[48]. Briefly, these plates were surface-oxidized in a plasma reactor (PR500, Yamato Scientific Co., Ltd., Tokyo, Japan) for 15 min. The plates were then dipped in LS-7150 for the MC array plate or in a mixture of LS-7150 (20% (w/w)) and hexane (80% (w/w)) for the glass plate for two nights at room temperature. Finally, the unreacted materials were washed away.

Solutions preparation and emulsification procedure

Na-ALG solutions at different concentrations of 0.5 to 4.0% (w/w) were prepared by dissolving Na-ALG powder in Milli-Q water for at least 2 h with constant stirring using a magnetic stirrer at room temperature. The solutions at 4±1 °C were stored overnight to ensure complete hydration. They were then maintained at 45±1 °C prior to MCE. The disperse aqueous phase used for MCE contains 0.5 to 4.0% (w/w) Na-ALG, 0 to 2% (w/w) $MgSO_4$, and 5 to 30% (w/w) L-AA. The continuous phase is a solution of water-saturated decane containing 5% (w/w) Span 85 or TGCR. To prevent water diffusion from the surface of Na-ALG droplets, decane was pre-treated prior to preparing the continuous phase. Decane was saturated with water by mixing at a volume ratio of 9:1 (decane:water) for 30 min, after which they were separated by centrifugation at 1500 x *g* for 15 min using a table centrifuge (KN-70, Kubota Co., Tokyo, Japan). The decane supernatant part was used as the continuous phase[37].
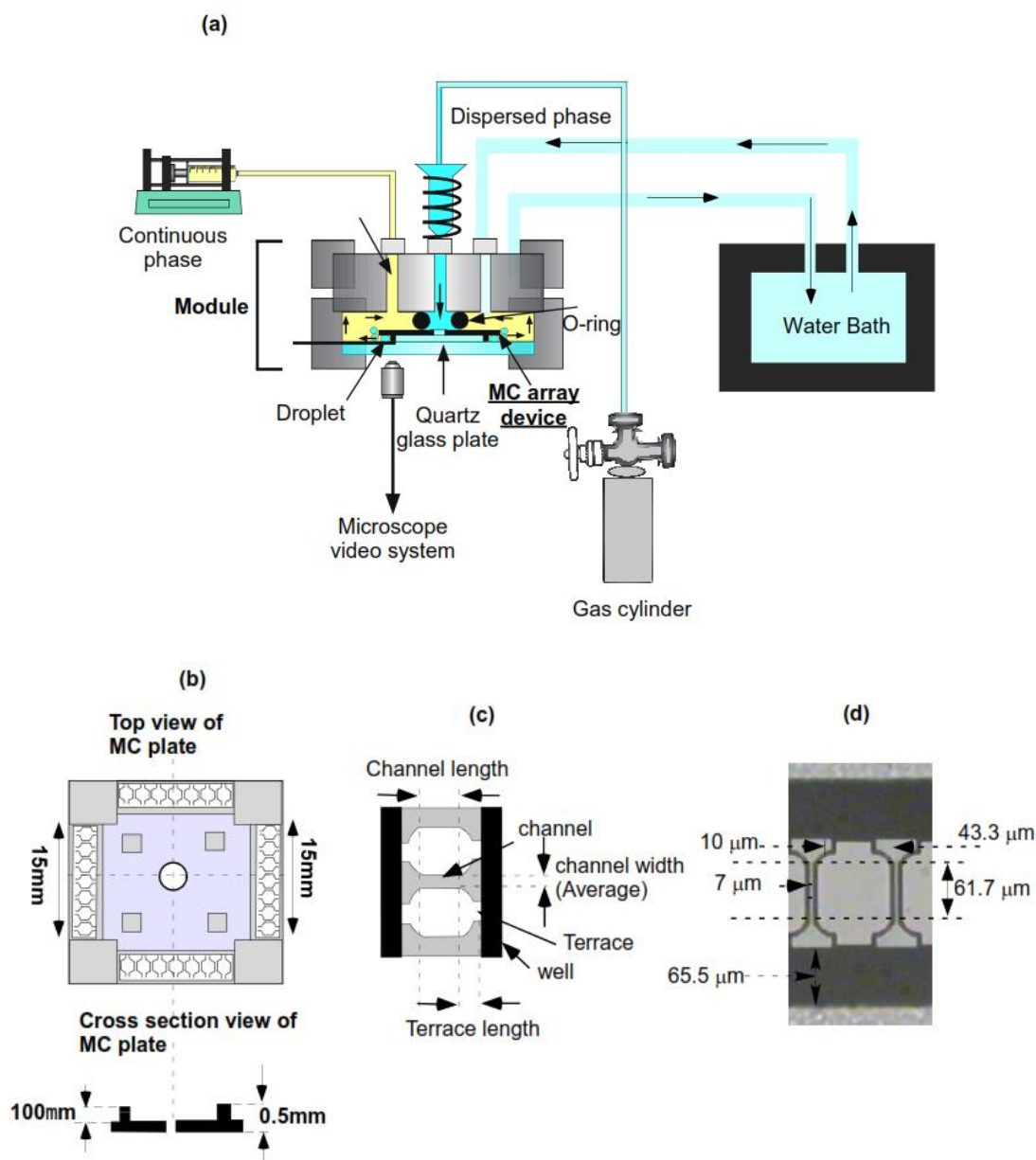
Figure 3.1: (a) Simplified schematic of MCE setup. (b) Top and cross-section views of the MC array plate (model MS407). (c) Schematic diagram of part of an MC array. (d) Optical micrograph and dimensions of part of an MC array.

The disperse phase in a reservoir was introduced into a module filled with the continuous phase by applying pressure using a pumping device (Fig. 3.1a). The module temperature was kept at 45 ± 1 ℃ during MCE. Liquid microsphere generation occurred when the disperse phase was forced through the MCs into the continuous phase. The resulting microspheres were then swept away by the cross-flow of the continuous phase, which was set at 10 to 15 mL h^{-1}. The flows of the disperse and

continuous phases were controlled in real time by monitoring liquid microsphere generation via MC arrays.

Straight-through MCE

Asymmetric microchannel array chip

In this study we used 24 × 24 mm MC array chip (Model WMS1-2) consisting of 10,313 MCs (Fig. 3.2) in a 10 × 10 mm in the center of the plate and four 1.5 mm diameter holes at the corners of the chip. This MC array was fabricated by repeated processes of photolithography and deep-reactive-ion etching (DRIE) on 5-inch silicon wafer [49]. Each asymmetric MC consisted of a circular microhole (10-μm diameter and 70-μm depth) located on the inlet side and a microslot (11×104-μm cross section and 21-μm depth) located on the outlet side. The slot aspect ratio of 9.5 was above the threshold value of 3 for stably generating monodisperse emulsion droplets [50]. The fabricated microholes and microslots were highly uniform, meeting the criterion for obtaining monodisperse microparticles. Oxygen plasma treatment was then performed to grow a hydrophilic silicon dioxide layer on the fabricated plate before carrying out hydrophobic treatment. Prior to the first use, the WMS1-2 chips as well as the glass plates were hydrophobilized by using LS-7150 (100% concentration for MC array chip, 20% (w/w) in hexane for glass plate) and left for two nights at room temperature. Afterwards, the unreacted material was washed away by using an ultrasonic bath (VS-100III, As One Co., Osaka, Japan) at a frequency of 100 kHz.

Preparation of aqueous dispersed phase

2.0% (w/w) Na-ALG aqueous solution was prepared by dissolving Na-ALG powder in Milli-Q water for at least 2 h under constant stirring at room temperature. The solution was stored at 4±1ºC overnight to ensure complete hydration. The dispersed phase used for straight-through MCE contains 2.0% (w/w) Na-ALG, 1% (w/w) MgSO$_4$ and 5-30% (w/w) L-AA. Na-ALG was chosen on the basis of its functionality in food systems, since it is a plant-based polysaccharide and easily to handle even at high concentration. Moreover, it is widely used for formulation of different types of microspheres. 2.0% (w/w) Na-ALG in the dispersed phase was used after optimization, since an optimized viscosity range was needed to conduct MCE. At higher viscosity it was difficult to pressurize the dispersed phase from the MCs. Moreover, MgSO$_4$ was added to increase the stability of L-AA in the dispersed phase. The

continuous phase contains water-saturated decane containing 5% (w/w) TGCR. Water saturation was carried out to prevent water diffusion from the surface of Na-ALG microspheres. Decane was water-saturated by mixing a volume ratio of 9:1 (decane:water) for 30 min, after which they were separated by centrifugation at 1500 g for 15 min using a table centrifuge (KN-70, Kubota Co., Tokyo, Japan). The decane supernatant part was used as the continuous phase[37]. All of the phases were maintained at 45±1°C prior to MCE.
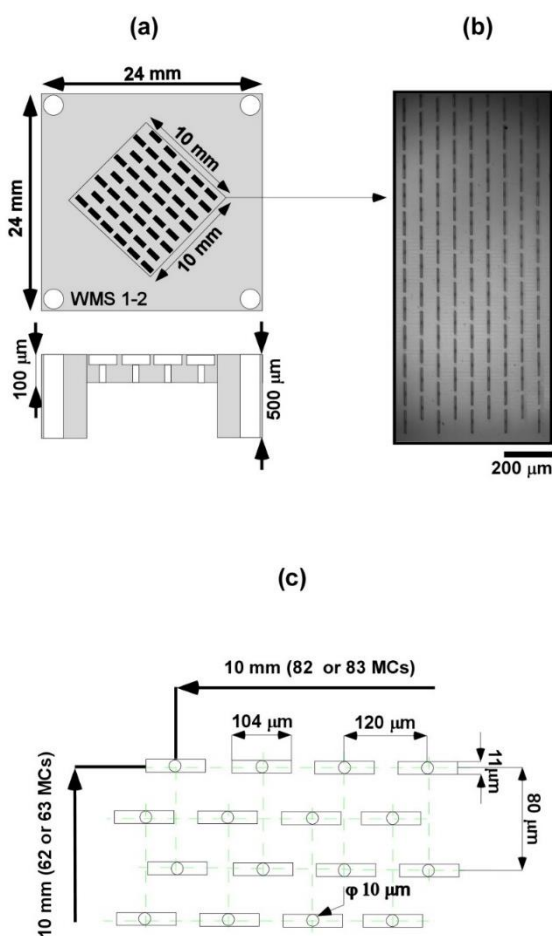
Figure 3.2: Schematic representation of asymmetric straight-through MC array chip used in microchannel emulsification. (a) WMS 1-2 silicon chip. (b) Optical micrograph of the bottom-illuminated chip surface. The circular micrchannels (MCs) are highlighted in dark black color in the center of light grey color microslot. (c) Arrangement of asymmetric MCs on the top side of a WMS 1-2 chip. Each horizontal row contains alternatively 82 or 83 MCs and vertical rows contain alternatively 62 or 63 MCs making the total number of MCs equal to 10,313 = 62 × 82 + 63 × 83.

Emulsification procedure

Each emulsification experiment was started with degassing of a WMS1-2 chip soaked in the continuous phase under ultrasonication at a 100 kHz for 20 min. During module assembly, the degassed hydrophobic WMS1-2 chip was mounted in a module compartment previously filled with

74

continuous phase (water saturated decane together with TGCR). Fig. 3.3a shows a simplified schematic diagram of the experimental setup used for MCE. A hydrophobized silicon MC array plate is tightly attached to hydrophobized glass plate in the emulsification module initially filled with the continuous phase.
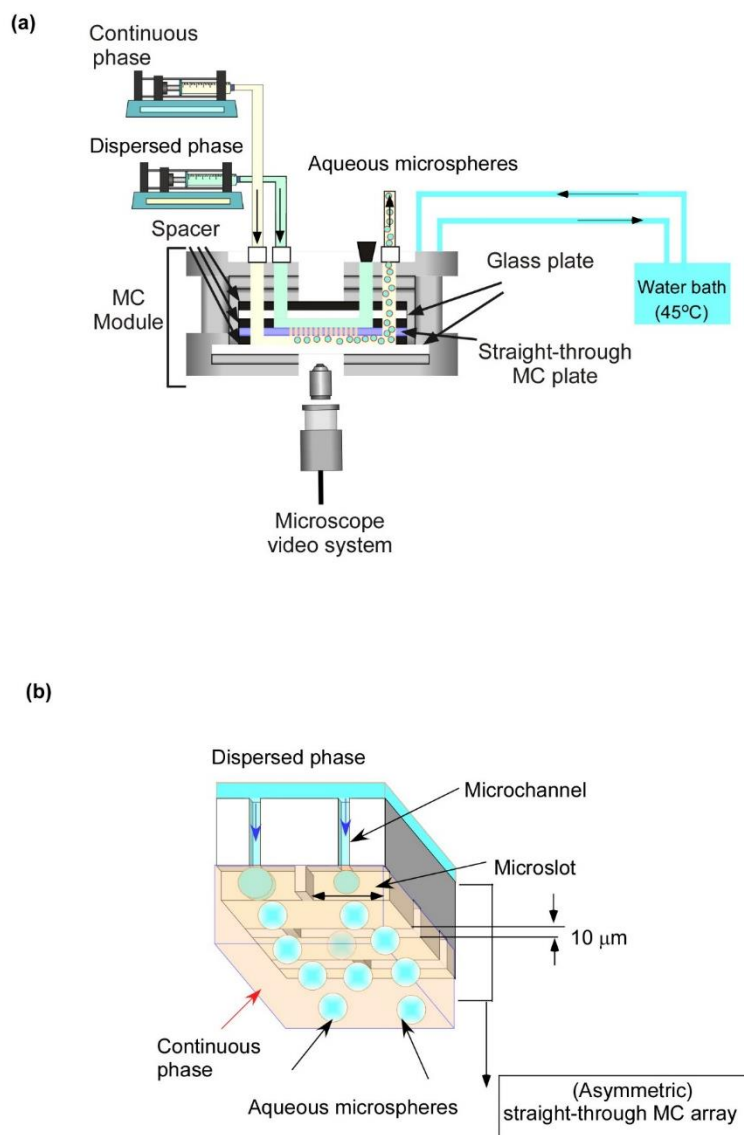
Figure 3.3: Simplified representation of microchannel emulsification. (a) Experimental set-up used in this work for straight-through MCE. (b) Generation process of aqueous microspheres in MCE.

A syringe pump (Model 11, Harvard Apparatus Inc., Holliston, USA) was used to supply both the continuous and dispersed phases. The heating system provides temperature controlled water circulation inside the module and outside the reservoir. The emulsification process was carried out for approximately 1 h and monitored through FASTCAM-1024 PCI high speed video system at 250 to 500

fps (Photron Ltd., Tokyo, Japan) attached to an inverted metallographic microscope (MS-511B, Seiwa Optical Co., Ltd., Tokyo, Japan).

The module temperature was kept at 45±1°C during MCE. Aqueous microsphere generation occurred when the dispersed phase occupies the active surface area of the WMS1-2 chip. The resulting microspheres were then swept away by the cross-flow of the continuous phase. The microsphere generation process is schematically illustrated in Fig. 3.3b. The dispersed phase flux (J_d) (L m^{-2} h^{-1}) was calculated using the following equation:

$$J_d = \frac{Q_d}{A_{MCA}} \qquad (3.1)$$

where Q_d is the dispersed phase flow rate (L h^{-1}) and A_{MCA} is the effective area of a straight-through MC array (1.0×10^{-4} m^2). The average flow velocity of the continuous phase over the plate surface (U_c) was calculated with the following equation:

$$U_c = \frac{Q_c}{A_{a,s}} \qquad (3.2)$$

where Q_c is the continuous phase flow rate (m h^{-1}), and $A_{a,s}$ (active surface area) is the flow area over the chip surface (m^2) and is calculated by measuring the dimensions of the spacer placed on the WMS1-2 chip:

$$A_{a,s} = W \times H \qquad (3.3)$$

where W is the spacer internal width (10^{-2} m), and H is the spacer thickness (10^{-3} m).

Measurement and analysis

The size and size distribution of the W/O aqueous microspheres obtained from straight-through MCE were determined as follows. The average droplet diameter (d_{av}) was defined by:

$$d_{av} = \sum_{i=1}^{n} d_i / n \qquad (3.4)$$

where d_i is the diameter of the ith microsphere measured using WinRoof software (Mitani Co., Ltd., Fukui, Japan) and n is the number of the microspheres measured ($n = 250$). The microsphere dispersity was expressed as CV, and is defined as:

$$CV = \frac{\sigma}{d_{av}} \times 100 \qquad (3.5)$$

where σ is the standard deviation and d_{av} is the average microsphere diameter (μm).

Measurement of fluid properties

The densities of dispersed and continuous phases were measured using a density meter (DA-130 N, Kyoto Electronics Manufacturing Co., Ltd., Kyoto, Japan) at 25 ± 2°C. The viscosities of dispersed and continuous phases were measured with a vibro viscometer (SV-10, A&D Co., Ltd., Tokyo, Japan) at 25 ± 2°C by taking either 10 or 35 mL of samples in a measuring vessel followed by immersion of sensor plates in that vessel. Viscosity was measured by detecting the electric current needed to resonate the sensor plates. The kinematic viscosity (υ) was calculated by following equation:

$$\upsilon = \frac{\eta_{mea}}{\rho} \qquad (3.6)$$

where η_{mea} is the measured viscosity and ρ is the fluid density. The static interfacial tension between the oil and aqueous phases was measured with a fully automatic interfacial tensiometer (PD-W, Kyowa Interface Sciences Co., Ltd., Saitama, Japan) using a pendant drop method. The key physical properties of dispersed and continuous phases are presented in Table 3.1.

Table 3.1: Viscosity and interfacial tension data for the liquid phases used for this study.

concentration % (w/w)	Viscosity, η^a (mPas)	Viscosity, η^b (mPas)	Interfacial tension, γ^c (mN/m)	Interfacial tension, γ^d (mN/m)
DP composition*				
0.5	1.67±0.02	4.11±0.01	6.5±0.1	6.9±0.2
1	3.75±0.05	8.85±0.05	6.7±0.5	6.6±0.4
2	34.9±3.51	59.4±1.80	6.9±0.1	6.7±0.1
3	112±2.11	334±3.51	7.0±0.5	6.8±0.3
4	731±6.50	777±8.50	6.2±0.7	6.4±0.6
DP with L-AA (5-30% (w/w))**				
10	40.2±0.40	62.50±1.50	6.9±0.3	6.7±0.3
20	45.7±0.88	69.21±4.01	7.0±0.2	6.9±0.1
30	50.6±3.06	73.72±6.32	7.0±0.4	6.8±0.3
CP composition***				
Decane+span 85	0.80±0.005	-	-	-
Decane+TGCR	0.84±0.004	-	-	-

*Dispersed phase composition, **L-AA, ***Continuous phase composition
[a] Viscosity of dispersed phase in presence of 1% (w/w) $MgSO_4$, [b] Viscosity of dispersed phase in presence of 0% (w/w) $MgSO_4$, [c] Interfacial tension in presence of 1% (w/w) $MgSO_4$, [d] Interfacial tension in presence of 0% (w/w) $MgSO_4$.

Physical and chemical stability

The liquid microspheres encapsulating L-AA formulated through straight-through MCE were observed with optical micrographs to evaluate d_{av}, CV, consistency, homogeneity, and coalescence during 10 d of storage at 4 °C.

The amount of L-AA encapsulated in the microspheres was determined spectrophotometrically. All spectral measurements of their methanolic extracts were carried out using a UV/VIS/NIR spectrophotometer (UV-1700, Shimadzu, Co., Kyoto, Japan). First, 1 mL of the sample containing aqueous microspheres was extracted with 9 mL of methanol, followed by ultrasonication for 20 min. The methanolic extracts were then centrifuged (Avanti, Beckman Coulter, Miami, USA) at 20,000 g for 30 min at 40 °C. A 1 mL aliquot of the supernatant was diluted 50 times with methanol and then injected into a quartz cell with a 10 mm pass length. The absorbance of L-AA in extract was measured at 245 nm using an appropriate blank. A representative standard curve of absorbance versus concentration gave linear least-squares regression with a coefficient of determination (r^2) of 0.9996. All experiments were repeated in triplicate and mean values were calculated. The encapsulation efficiency (EE) of L-AA in samples was calculated with the equation:

$$EE_{L-AA} = \frac{c_{L-AA}}{c_{L-AA,0}} \times 100 \qquad (3.7)$$

where C_{L-AA} is the concentration of L-AA at a given storage time and $C_{L-AA,0}$ is the concentration of L-AA initially encapsulated in the microspheres.

3.3 Results and Discussion

Effect of MgSO$_4$ concentration on preparation of liquid microspheres

Salt content is a key factor affecting the interfacial properties of emulsions and their stability [51,52], the study investigated the influence of salt content on the preparation of liquid microspheres using MCE and their stability. MCE experiments were conducted using varying concentrations of MgSO$_4$ (0 to 2% (w/w)) in the disperse phase containing 2% (w/w) Na-ALG and 5% (w/w) L-AA. The disperse phase was fed into the module at 15 kPa, while the flow rate of the continuous phase was set at 10 to 15 mL h^{-1}. Stable microspheres were generated using the MC array at a MgSO$_4$ concentration of 1% (w/w). The generated microspheres detached smoothly from the MC arrays and had a d_{av} of 15.5 μm and a CV of 5.0%, demonstrating their monodispersity (Figs. 3.4a and b). Higher MgSO$_4$ concentrations produced polydisperse microspheres, and at 2% (w/w) MgSO$_4$ the microspheres first exhibited a high

degree of coalescence and then disappeared (burst). This phenomenon leads to unstable microsphere generation. The microspheres obtained at 1% (w/w) $MgSO_4$ remained stable for more than 2 h inside the module without coalescence. In contrast, the microspheres generated without adding $MgSO_4$ (Fig. 3.4c) exhibited little coalescence after 30 min in the MC module, indicating that a certain osmotic pressure is needed to generate microspheres by MCE. The d_{av} of microspheres containing 2% (w/w) $MgSO_4$ increased to 21 μm with a CV of 16%.

The disperse phase osmotic pressure (Π_d) for the two-phase systems used in this section can be calculated using the van't Hoff equation [53]:

$$\Pi_d = iMRT \qquad (3.8)$$

where i is the van't Hoff factor with a value of 1.51 for $MgSO_4$ and 1 for L-ascorbic acid; M is the molar concentration of $MgSO_4$ (kmol m^{-3}), L-AA, and Na-ALG; R is a constant with a value of 8.31 kPa m^3 K^{-1} mol^{-1}; and T is the thermodynamic temperature (K). Π_d in the absence of $MgSO_4$ was 0.74 MPa, and Π_d in the presence of $MgSO_4$ ranged from 2.52 to 3.65 MPa. Shimizu et al. [54] and Cheng et al. [55] reported that the use of disperse phases with Π_d over a threshold value is needed to stably produce W/O emulsions with narrow droplet size distributions by ME using surface-modified Shirasu Porous Glass (SPG) membranes. Similar to ME, MCE also has a certain threshold Π_d necessary to generate droplets from MCs. Kobayashi, et al.[47] demonstrated that Π_d exceeding a certain threshold level stably produces monodisperse W/O emulsions with a CV of less than 3%. Similarly, at a higher Π_d, the transport of water molecules via the water–oil interface is suppressed because of weak interaction between charged hydrophilic groups and emulsifiers at the interface of W/O emulsions [56]. The generation stability of liquid microspheres via MC arrays in this study might correspond to this mechanism.

(a)
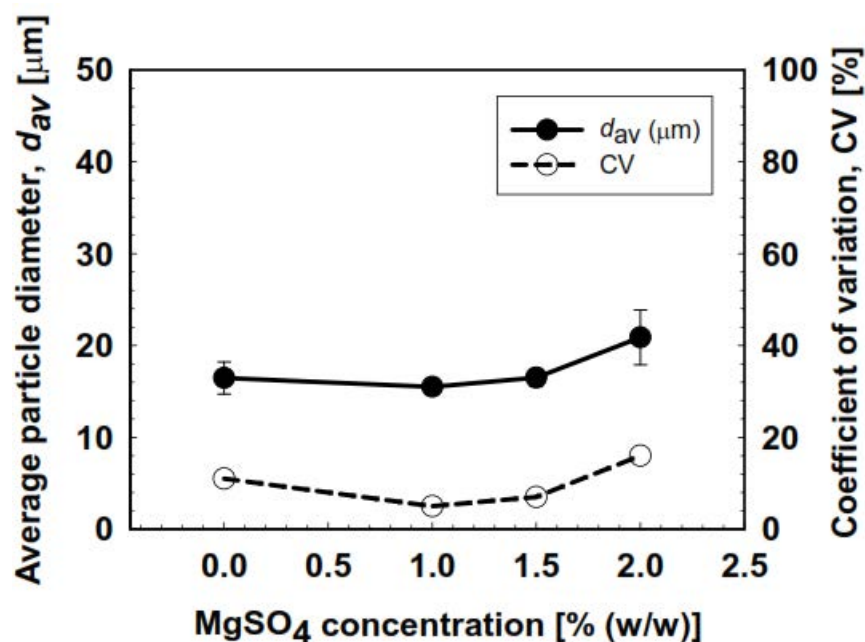
(b) 1% (w/w)   **(c) 0% (w/w)**
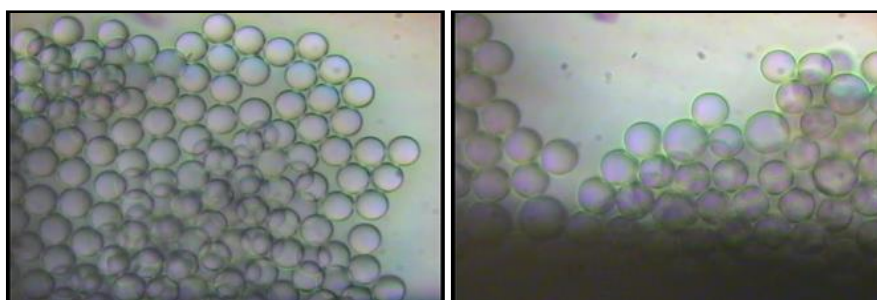
50 μm

Figure 3.4: (a) Effect of the MgSO₄ concentration on the average particle diameter (d_{av}) (━●━) and CV (-○-) of the resultant liquid microspheres. (b, c) Optical micrographs of monodisperse liquid microspheres of different MgSO₄ concentrations.

The aqueous microspheres generated without adding MgSO₄ exhibited coalescence just after formation, and their *in situ* stability was quite low. In contrast, the *in situ* stability of microspheres generated in the presence of 0.5 to 1% (w/w) MgSO₄ was very high. The generated microspheres remained stable for more than 2 h without any coalescence. It has been reported that microgel particles containing ionizable groups become deswollen in an aqueous phase containing salt because increased ionic strength decreases the Debye screening length on the particle surface and reduces the repulsive

electrostatic forces between charged groups on the neighboring particles[57,58]. In our study, the electrostatic interactions at low $MgSO_4$ concentrations between the charged groups ($MgSO_4$, water, and L-AA) in the liquid microspheres are in the stable range, leading to microsphere stability and monodispersity. In contrast, the electrostatic repulsive force in the liquid microspheres at high $MgSO_4$ concentrations increases due to higher osmotic pressure, which could burst the microspheres and result in less monodispersity.

Effect of Na-ALG Concentration on Preparation of Liquid Microspheres

Fig. 3.5a illustrates the effect of Na-ALG concentration on the preparation of liquid microspheres using MCE. The generated aqueous microspheres contained 0.5 to 4% (w/w) Na-ALG, 1% (w/w) $MgSO_4$, and 5% (w/w) L-AA. The disperse phase was supplied into the MC module at 15 kPa with the flow rate of the continuous phase was maintained at 10 mL h^{-1}. A decrease in d_{av} of microspheres was observed with increased concentration of Na-ALG up to a certain concentration (2% (w/w)), whereas further increase in the Na-ALG concentration increased the d_{av} of microspheres. Microspheres with the largest d_{av} of 24.6 μm and a CV of 10% were observed at a Na-ALG concentration of 4% (w/w). At a low Na-ALG concentration of 0.5% (w/w), a relatively broader particle size distribution occurred with a d_{av} of 20 μm and a CV of 12% (Fig. 3.5b). The optimum condition for successful microsphere production was 2% (w/w) Na-ALG, since a narrow size distribution was observed with a d_{av} of 15 μm and the smallest CV of 5% at this Na-ALG concentration (Fig. 3.5b). As presented in Table 3.1, the viscosity of the disperse phase increased sharply at Na-ALG concentrations exceeding 2% (w/w). Such high viscosities of the disperse phase (>100 mPa s) impeded crossing the narrow MCs, and only a few MCs made microspheres in the whole MC array plate. The viscosity of the disperse phase containing Na-ALG increased in the presence of $MgSO_4$ (Table 3.1), which plays a key role in the stability of microspheres as well as in microsphere generation.

ALG microspheres have traditionally been produced by extruding Na-ALG solution from a needle into a divalent cationic solution [59, 60]. These cationic solutions then induce gelation in microspheres. Gelling depends on ion binding ($Ca^{2+}< Zn^{2+}< Sr^{2+}< Ba^{2+}$). Mg^{2+} salt is also divalent but does not completely gelatinize the solution. This soft gel-like structure could modify the structure of ALG, as indicated by reduction of the viscosity of the disperse phase in the presence of $MgSO_4$ (Table 3.1). Furthermore, this soft gel-like structure creates weak linkage of Mg^{+2} ions with the ALG structure

(Fig. 3.6), giving microspheres better stability. Improved stability in the presence of $MgSO_4$ was observed in our study. Factors controlling microsphere production include the MC geometry, the composition of two liquid phases, and the type of emulsifiers[61,62]. The viscosity ratio of the dispersed phase to the continuous phase was indicated as an important factor affecting the size of emulsion droplets generated by MCE[63]. In our study, the viscosity of the disperse phase containing Na-ALG increased with increased Na-ALG concentration, while interfacial tension remained almost unchanged at the Na-ALG concentrations applied (Table 3.1). In our study, d_{av} decreased with increasing Na-ALG concentrations (0.5 to 2% (w/w)) and increased with increasing Na-ALG concentrations (2 to 5% (w/w)). These results at higher Na-ALG concentrations deviate from the previous study of Chuah *et al.*[64], who found size reduction in the resultant emulsion droplets with increasing Na-ALG concentration. However, these emulsion droplets do not contain any hydrophilic bioactive substance. The result presented in Fig. 3.5a correlated well with the previous MCE study of Kobayashi*, et al.*[49], who reported that a decrease in the d_{av} of oil-in-water (O/W) emulsion droplets stabilized using sodium dodecyl sulfate is influenced by increased viscosity of the disperse phase (silicone oil).

(a)
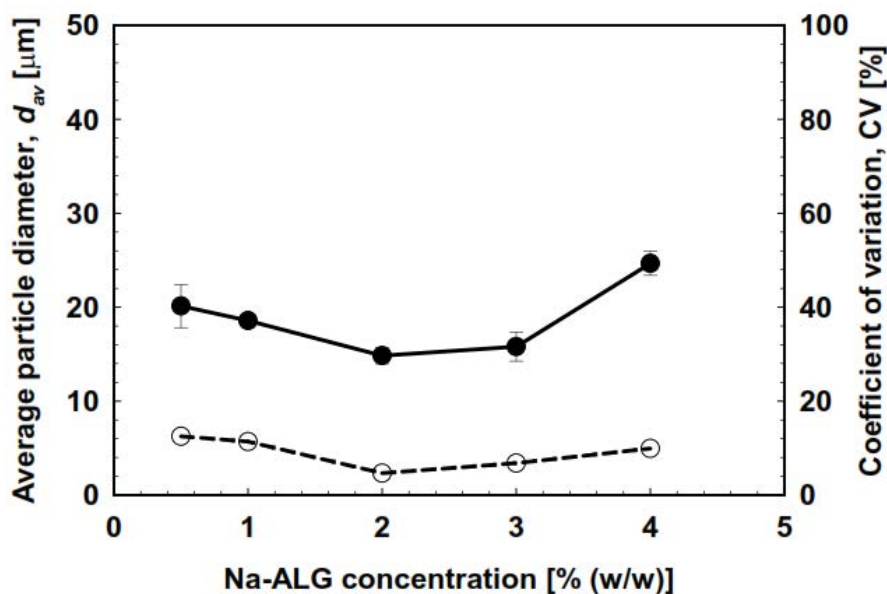
(b)
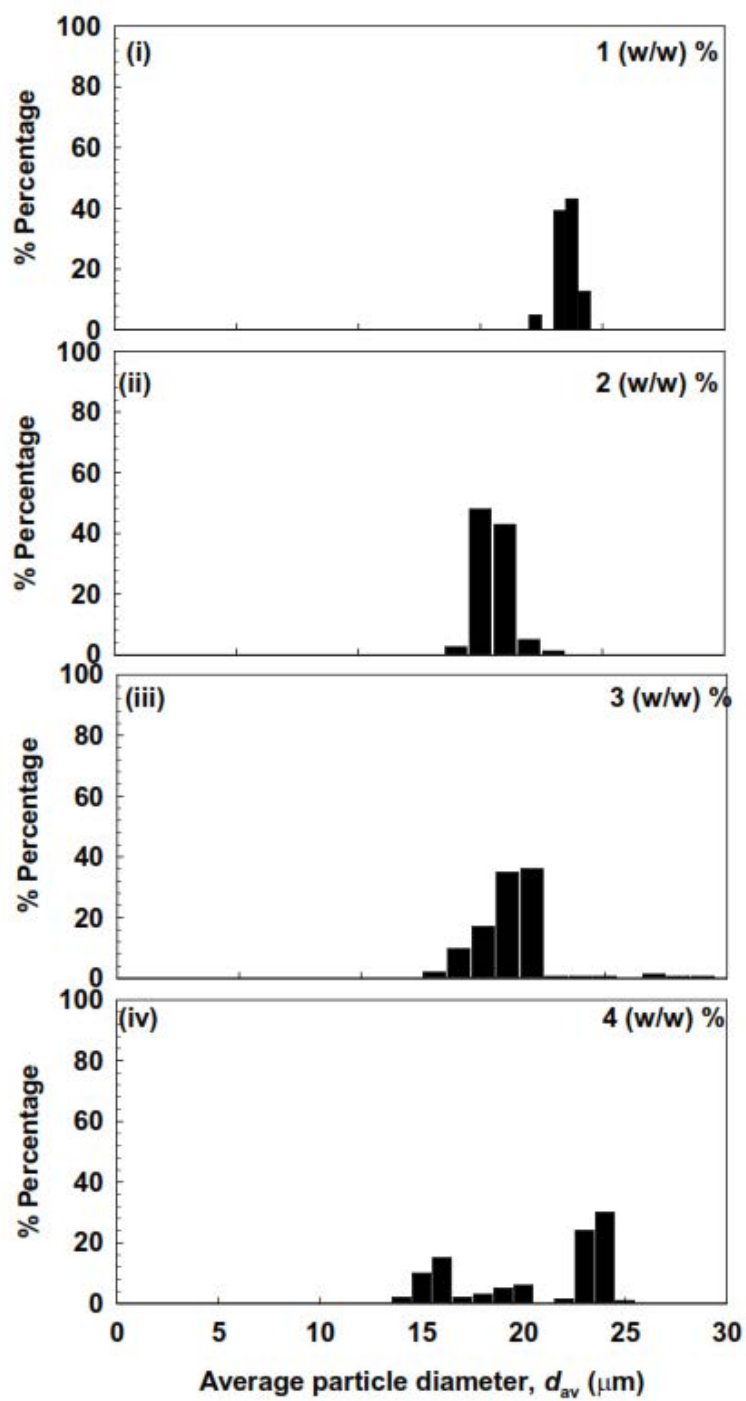
Figure 3.5: (a) Effect of Na-ALG concentration on d_{av} (—●—) and CV (—⊖—) of the resultant liquid microspheres. (b) Droplet size distributions of the liquid microspheres of different Na-ALG concentrations.
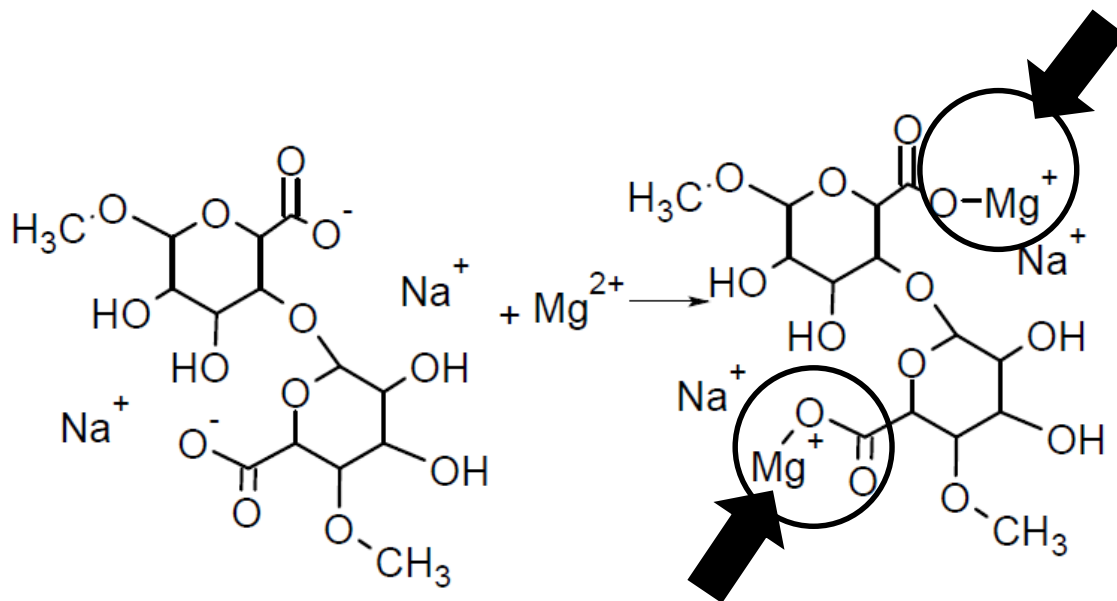
Figure 3.6: Potential mechanism representing the soft gel-like structure of Na-ALG in the presence of MgSO₄.

Effect of Pressure of the Dispersed Phase on Preparation of Liquid Microspheres

In order to investigate the effect of the hydraulic pressure of the disperse phase on the size and size distribution of the resultant microspheres, the disperse phase pressure was varied from 3 to 25 kPa at a fixed continuous flow rate of 10 mL h^{-1}. It should be noted that the flow rate of the continuous phase hardly affected the d_{av} and CV of the generated microspheres (Fig. 3.7a), which is advantageous for stable preparation of monodisperse liquid microspheres. The disperse phase used here contained 1 to 4% (w/w) Na-ALG, 1% (w/w) MgSO₄, and 5% (w/w) L-AA in Milli-Q water.

Fig. 3.7b illustrates the effect of the disperse phase pressure on the d_{av} and CV of the microspheres prepared at different Na-ALG concentrations. The breakthrough pressure ranged from 3 to 7 kPa with increasing concentration of Na-ALG. The d_{av} of the microsphere decreased with increasing disperse phase pressure. A higher disperse phase pressure produced more active MCs generating microspheres. Monodisperse liquid microspheres with d_{av} of 15 to 18 μm and CV of 4.5 to 9.5% were prepared at disperse phase pressures of 10 to 15 kPa, regardless of Na-ALG concentration. There was a slight effect on their d_{av} and CV at disperse phase pressures exceeding 15 kPa at Na-ALG concentrations of 2 and 3% (w/w). At a certain disperse phase pressure, d_{av} depended on the Na-ALG concentration. The d_{av} of microspheres increased with increasing concentration of Na-ALG. The

microspheres prepared with 4% (w/w) Na-ALG and generated at a disperse phase pressure of 25 kPa had a d_{av} of 26 μm and a CV of 10%. The results obtained from this part of the study confirmed the existence of a range of optimum disperse phase pressures for successfully preparing monodisperse liquid microspheres.

(a)
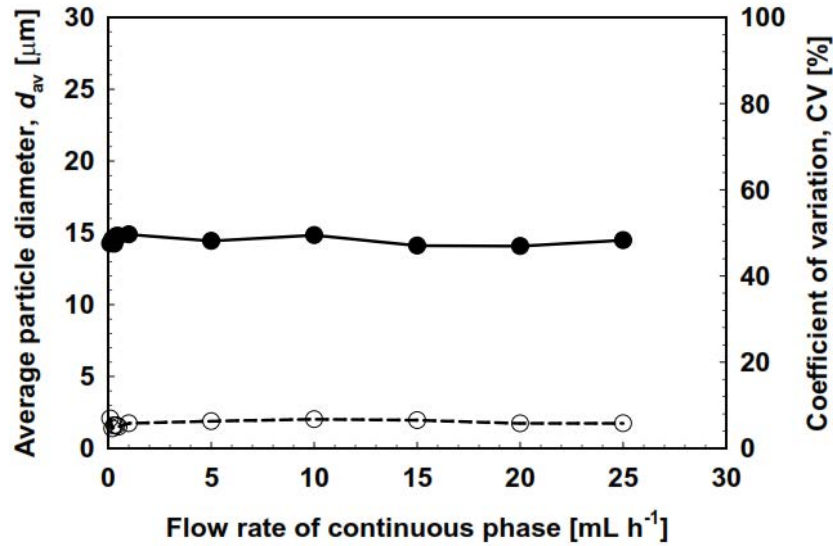
(b)
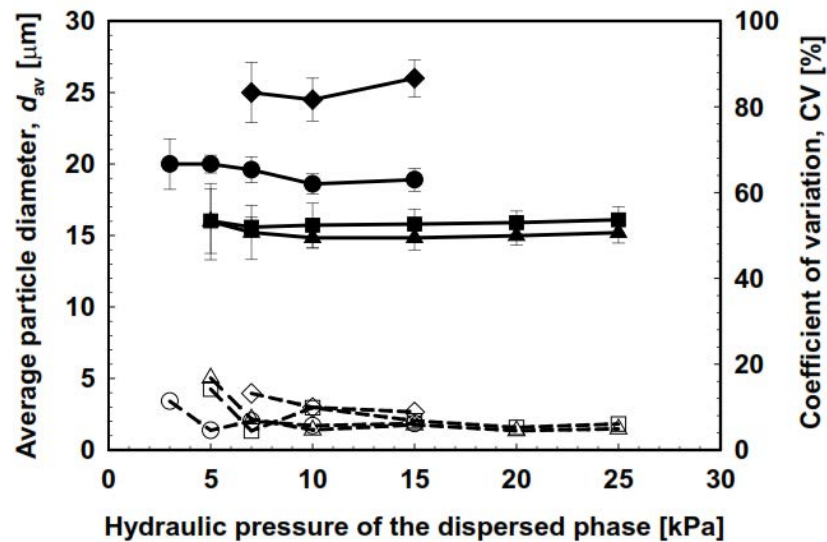
Figure 3.7: (a) Effect of the flow rate of the continuous phase (decane containing 5% (w/w) TCGR) on d_{av} (—●—) and (—○—) of the resultant liquid microspheres containing 2% (w/w) Na-ALG. (b) Effect of the hydraulic pressure of the disperse phase on the d_{av} and CV of the liquid microspheres of different Na-ALG concentrations. Na-ALG concentrations are denoted as (—●—) for 1% (w/w), (—▲—) for 2% (w/w), (—■—) for 3% (w/w), and (—◆—) for 4% (w/w), while similar open keys represents CVs of microspheres at different Na-ALG concentrations.

Effect of different operating conditions in straight-through MCE for encapsulation of L-AA in microspheres

The experiments were conducted using the dispersed phase containing 5% (w/w) L-AA together with 2% (w/w) Na-ALG and 1% (w/w) $MgSO_4$ in water. The continuous phase contains 5% (w/w) TGCR in water-saturated decane. The operating conditions and various physical properties of this two-phase system are summarized in Table 3.2. Uniformly sized W/O microspheres were generated from the asymmetric through holes with a d_{av} of 18.5 μm and a CV of 3.5% (Fig. 3.8). The generation of aqueous microspheres from asymmetric through-holes was clearly driven by spontaneous transformation of the oil-water interface in and over the microslot, following successful MCE process [65]. The generated microspheres detached smoothly without showing any coalescence. Neves *et al.* [40] successfully encapsulated β-carotene in monodisperse oil-in-water (O/W) emulsions with a d_{av} of 28.5 μm and a CV of 3.3% by straight-through MCE.

Table 3.2: Operating conditions and fluid properties of the continuous and dispersed phases.

System component	Operating conditions & physical properties
Continuous phase	
TGCR concentration % (w/w)	5
Density (kg m^{-3})	850
Viscosity (mPa s)	0.84
Flow velocity (mm s^{-1})	2.80
Dispersed phase	
Density (kg m^{-3})	1640
Viscosity (mPa s)	35.7
Encapsulated L-AA % (w/w)	5
L-AA retention (mg L^{-1})	0.51
Flux (L m^{-2} h^{-1})	5
Interfacial tension (mN m^{-1})	6.8

TGCR: Tetraglycerol condensed ricinoleate; L-AA: L-ascorbic acid
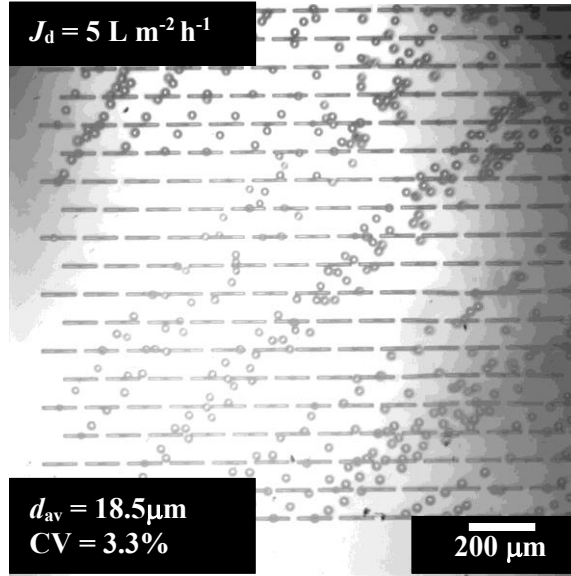
Figure 3.8: Optical micrograph of the experiment for evaluating preparation conditions of aqueous microspheres. The generated microspheres contain 5% (w/w) L-AA.

Dispersed phase flux is an important parameter in MCE that correlates with droplet productivity in the stable microsphere generation zone. Fig. 3.9a depicts the effect of J_d on the d_{av} and CV of the generated aqueous microspheres. The dispersed phase constitute 5% (w/w) L-AA, 2% (w/w) Na-ALG and 1% (w/w) $MgSO_4$ in water, while the continuous phase includes 5% (w/w) TGCR in water-saturated decane. The straight-through MCE was conducted by maintaining J_d between 5 and 20 L m^{-2} h^{-1}, while the continuous phase flow velocity was maintained constantly at 2.8 mm s^{-1}.

The d_{av} and CV quite slowly increased with increasing J_d until its critical value of 20 L m^{-2} h^{-1}. Outflow of the dispersed phase and unstable microsphere generation were observed after crossing the critical J_d of 15 L m^{-2} h^{-1} (Fig. 3.9b). The resultant microspheres had d_{av} of 18.7 to 20.7 μm and CV of 3.6 to 6.0%. The average generation frequency per active asymmetric MC ($f_{av,MC}$) was calculated from number of frames taken to generate 20 microspheres. As the number of frames per second for each video was already known from the high speed video system and could be used to calculate the frequency of microsphere generation:

$$f = \frac{n_f}{z} \times y \qquad (3.9)$$

where f is the frequency of microsphere generation (Hz), n_f is the number of microspheres counted, z is the number of frames taken to generate n_f droplets and y is the frame rate of the image sequence (Hz). The $f_{av,MC}$ increased with increasing J_d only in a narrow range. At J_d above 10 L m^{-2} h^{-1}, there was no further increase in $f_{av,MC}$ (Fig. 3.10). The influence of J_d on the microsphere generation

frequency per MC array chip (f_{MCA}) is also presented in Fig. 3.10. This microsphere generation frequency can be estimated by:

$$f_{MCA} = \frac{Q_d}{V_{av}} = \frac{6Q_d}{\pi d_{av}^3} \qquad (3.10)$$

where V_{av} is the average droplet volume. f_{MCA} increased linearly with increasing Q_d at J_d of 5 to 15 L m^{-2} h^{-1}. The monodisperse microspheres prepared at J_d of 15 L m^{-2} h^{-1} had a maximum productivity of 10.6×10^4 s^{-1}. In this case, we observed that 50% of asymmetric MCs generated uniformly sized microspheres at $f_{av,MC}$ of 16.2 s^{-1}. The maximum dispersed phase flux for preparing monodisperse emulsions usually increases with decreasing the dispersed phase viscosity [66].

(a)
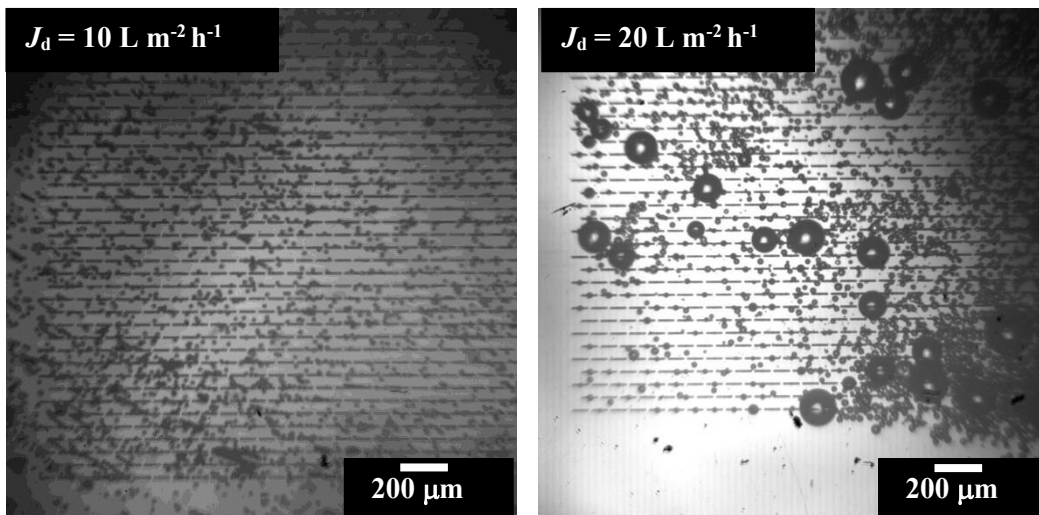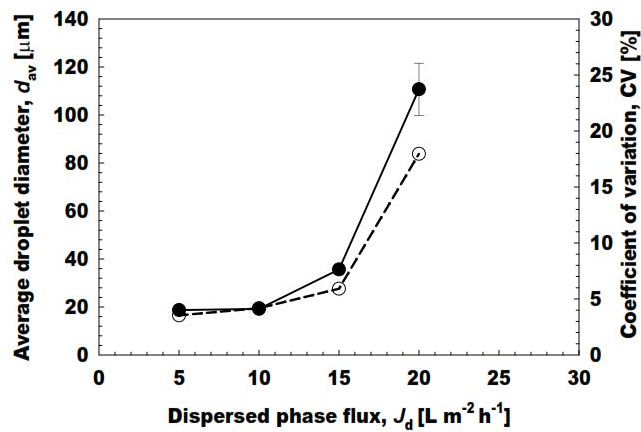
Figure 3.9: (a) The average diameter (d_{av}) and coefficient of variation (CV) of the microspheres with increasing dispersed phase flux (J_d). (–●–) denotes the d_{av} of the microspheres and (–⊖–) indicates their CV. (b) optical micrographs of microsphere generation at J_d of 10 and 20 L m^{-2} h^{-1}.
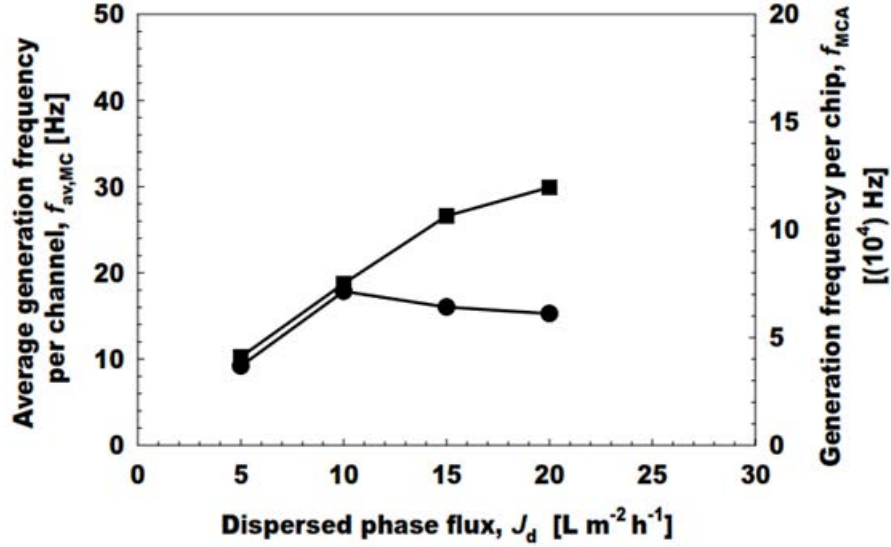
Figure 3.10: Effect of dispersed phase flux on microsphere generation Frequency and mean productivity containing L-AA. (—●—) denotes microsphere generation frequency per each active asymmetric microchannel (f_{MC}) and (—■—) denote microsphere Generation frequency per microchannel array chip (f_{MCA}).

Fig. 3.11a illustrates the effect of L-AA concentration on the d_{av} and CV of the aqueous microspheres prepared by straight-through MCE. The L-AA concentration in the dispersed phase varied from 5 to 30% (w/w) in the presence of 2% (w/w) Na-ALG solution and 1% (w/w) $MgSO_4$. Successful MCE was conducted with different concentrations of L-AA by keeping J_d at 5 L m^{-2} h^{-1} and U_c at 2.8 mm s^{-1} (Fig. 3.11b). The d_{av} and CV of the resultant microspheres hardly changed up to 20% (w/w) L-AA. Their CV was below 6%, demonstrating monodispersity of the aqueous microspheres obtained here. The d_{av} and CV of microspheres increased to 20.5 μm and 10.7% at the L-AA concentration of 30% (w/w) (Fig. 3.11b). The variation in monodispersity with increasing the L-AA concentration can be attributed to the interactions between the MC and terrace surfaces with the dispersed phase containing L-AA in the presence of a very thin layer of the continuous phase. Increase of the L-AA concentration in the dispersed phase is assumed to cause stronger interactions with MC and terrace surfaces, hence leading towards less monodispersity.

(a)
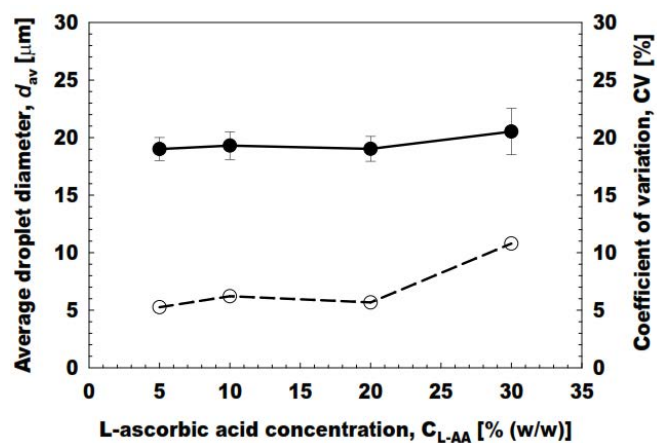
(b)
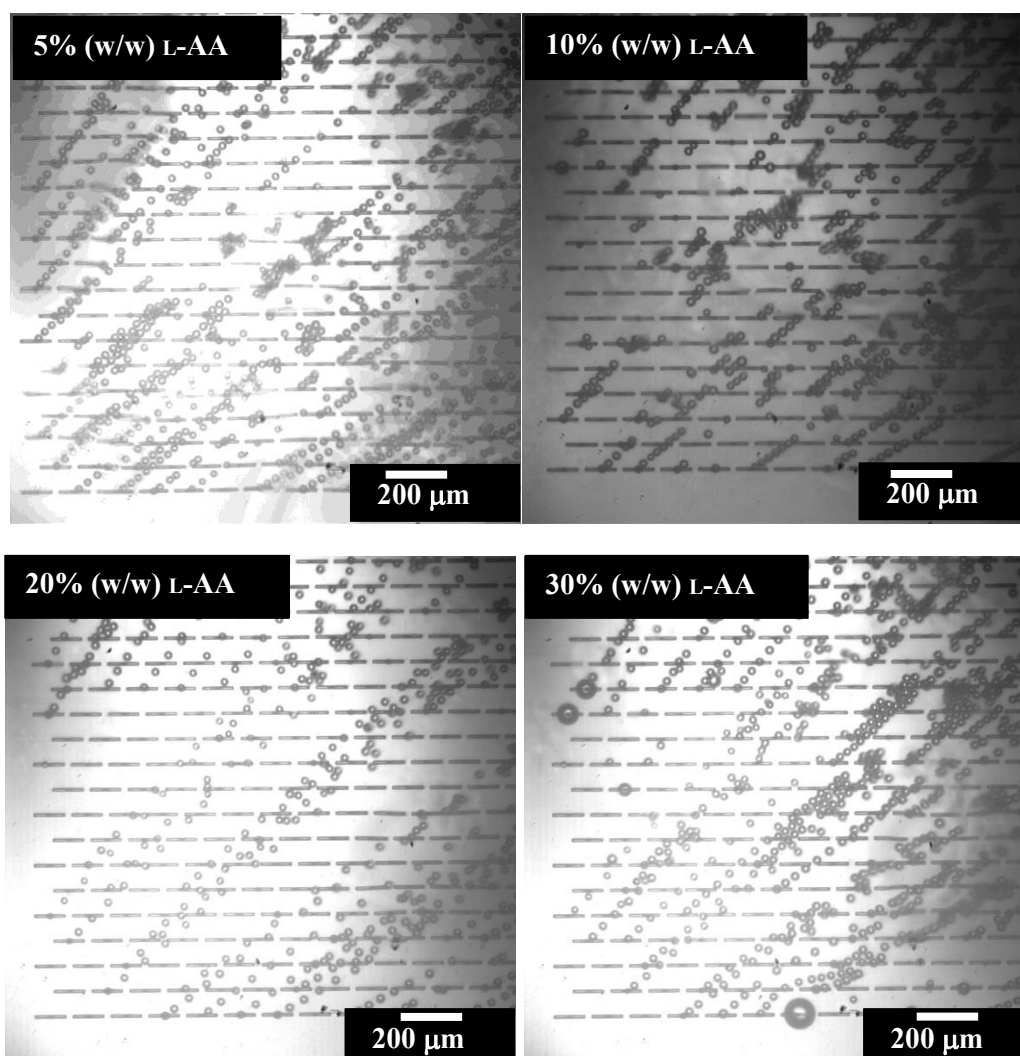
Figure 3.11: (a) Effect of L-AA concentration on the average diameter (d_{av}) and coefficient of variation (CV) of the microspheres. (b) Optical micrographs showing generation of aqueous microspheres with increasing L-AA concentration (5-30% (w/w)).

The results obtained here were comparable with our recent study using a grooved MC array. In that study the d_{av} of the aqueous microspheres increased with increasing the L-AA concentration. Our previous studies also encapsulated L-AA of high concentration up to 30% (w/w) in W/O and W/O/W emulsions with similar compositions in the absence of Na-ALG.[41,67,68] Viveros-Contreras et al.[69] encapsulated 1% (w/w) L-AA in calcium alginate matrix (2% (w/w)). The encapsulation in calcium alginate matrix improved the retention, microstructure and micropore volume of the resultant product. Devi and Kakati[70] also encapsulated L-AA in smart porous microparticles based on gelatin/Na-ALG polyelectrolyte complex. These smart microparticles have the potential to improve the stability and delivery of L-AA.

Stability evaluation of aqueous microspheres encapsulating L-AA

MCE using grooved MC arrays provides useful information regarding the basic behaviors of microsphere generation, whereas the drawback lies in low droplet productivity due to the low-density arrangement of microgrooves on a chip [71]. In contrast, straight-through MCE has much higher through-put capacity of monodisperse microspheres,[66] making it possible to collect microspheres sufficient for stability evaluation.

The monodisperse aqueous microspheres encapsulating 20% (w/w) L-AA were stored at 40±1 °C for 10 d. These microspheres were obtained by keeping J_d at 5 L m^{-2} h^{-1}. Immediately after collection, the microsphere-containing dispersion had a light yellowish turbid appearance with good flowability. Its appearance did not change with storage time. Fig. 3.12 depicts time changes in the d_{av} and CV of the resultant microspheres encapsulating L-AA. There was slight increase in their d_{av} and CV during evaluated storage period of 10 d. Their d_{av} and CV after 10 d of storage were 22.3 μm and 10%, respectively.

Khalid et al.[41] These authors pointed out the increased osmotic pressure as a key factor for increased in d_{av} of W/O/W emulsions. 2-20% (w/w) L-AA was encapsulated in solid lipid microcapsules using microfluidic approachComunian et al.[72] The average diameter of these particles varied from 170 to 342 μm during 30 d of storage period.

(a)
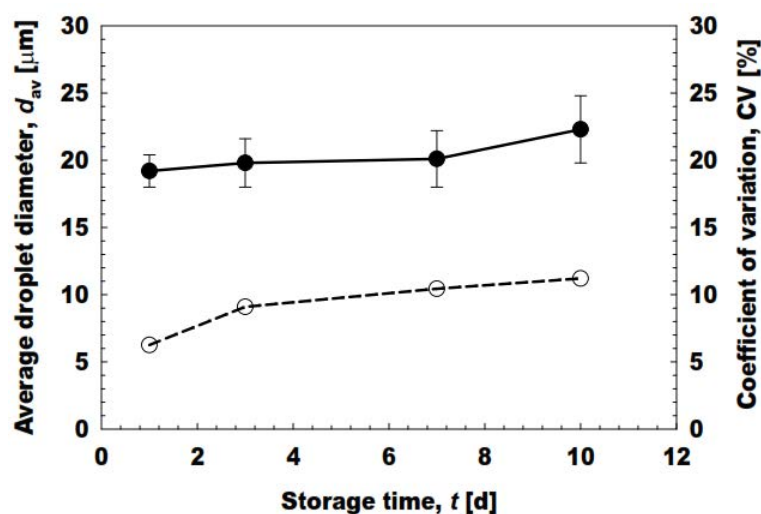
(b)
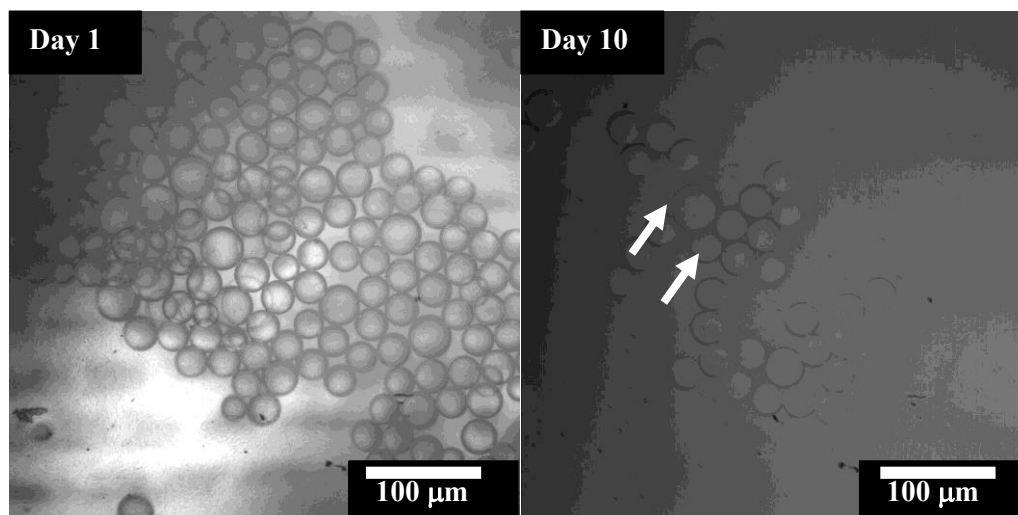
Figure 3.12: (a) Storage stability of the microspheres during 10 d of storage at 40 ºC. (━●━) denote their average diameter (d_{av}) and (-⊖-) denote their coefficient of variation (CV). (b) Optical micrographs at d 1 and 10. Arrows indicate bigger microspheres.

Encapsulation efficiency of L-AA in aqueous microspheres

The freshly prepared aqueous microspheres containing L-AA had an initial concentration of 2.7 mg mL^{-1} and regarded as 100% encapsulated efficiency (EE), since in MCE it was difficult to maintain the volume fraction of the microspheres (ϕ_{MS}) with passage of time in comparison to conventional emulsification techniques. The ϕ_{MS} during MCE corresponds to 0.62%. Fig. 3.13 indicates the retention and EE of aqueous microspheres. The EE gradually decreased with storage time and exhibited 71% EE of L-AA after 10 d of storage at 40ºC. This high EE at 40ºC can be ascribed to very mild generation

process of microspheres in straight-through MCE. Moreover, in MCE the generation was based upon difference in interfacial tension rather than high energy shear forces. In comparison the conventional emulsification methods produce emulsions with larger droplet sizes and have low energy and encapsulation efficiencies [73].

Our results can be considered well when compared to other L-AA encapsulation studies. Farhang *et al.*[74] encapsulated L-AA in liposomes and showed that liposomes have EE of 30% L-AA after 7 weeks at 25°C. Rozman and Gašperlin[75] encapsulated L-AA in W/O microemulsions and reported 60% EE in the samples stored at room temperature for 28 d. Khalid *et al.*[68] encapsulated high concentration of L-AA in food grade W/O emulsions prepared with either soybean or moringa oil and reported EE of 30% after 30 d of storage at 25°C. Comunian *et al.*[76] encapsulated L-AA by the double emulsion followed by complex coacervation and obtained EEs in the range of 15-40% for samples stored at 37°C for 60 d. Comunian *et al.*[72]   recently encapsulated L-AA in solid lipid microcapsules containing different coating agents by glass microfluidic device and obtained EE in the range of 46-96% when stored for 30 d at 20°C.
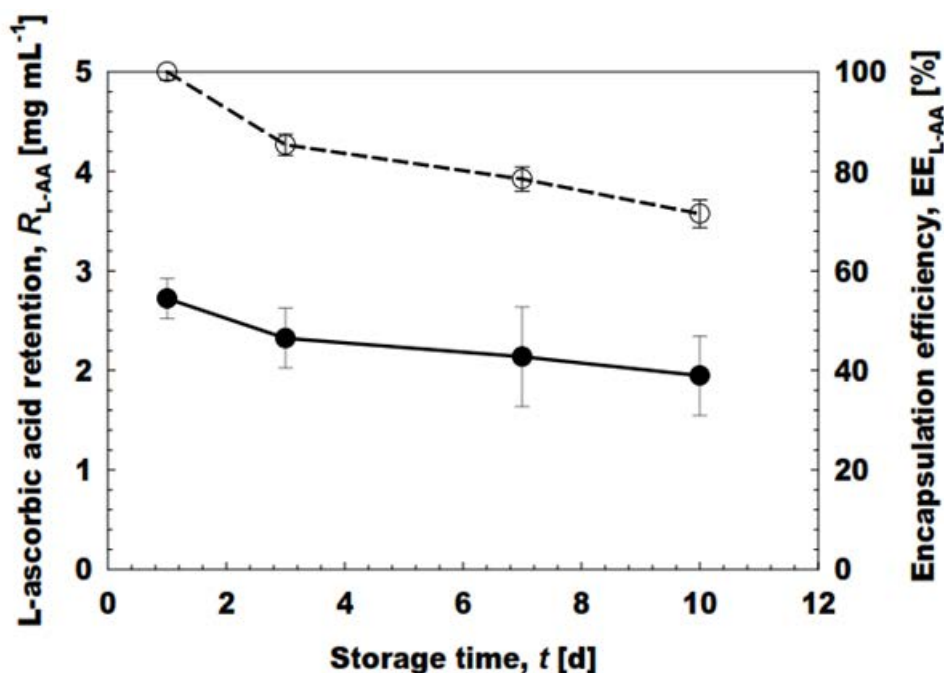
Figure 3.13: Encapsulation efficiency and retention of 20% (w/w) L-AA during 10 d of Storage. (▬●▬ **) denotes the L-AA retention in mg mL^{-1}, while (▬⊖▬) indicates the encapsulation efficiency of L-AA in the aqueous microspheres.**

References

[1] Shin J, Anisur RM, Ko MK, Im GH, Lee JH and Lee IS, *Ange. Chem. Int. Ed.*, **48,** 321-324 (2009).

[2] Yang S, Wang C, Chen L and Chen S, *Mat. Chem. Phys.*, **120,** 296-301 (2010).

[3] McQuade DT, Pullen AE and Swager TM, *Chem. Rev.*, **100,** 2537-2574 (2000).

[4] Freiberg S and Zhu X, *Int. J. Pharm.*, **282,** 1-18 (2004).

[5] Pekarek KJ, Jacob JS and Mathiowitz E, *Nature*, **367,** 258-260 (1994).

[6] Sinha V, Bansal K, Kaushik R, Kumria R and Trehan A, *Int. J. Pharm..*, **278,** 1-23 (2004).

[7] Dudhani AR and Kosaraju SL, *Carbohydr. Poly.*, **81,** 243-251 (2010).

[8] Qin R, Li F, Chen M and Jiang W, *Appl. Surface Sci.*, **256,** 27-32 (2009).

[9] Agnihotri SA and Aminabhavi TM, *J. Control Release.*, **96,** 245-259 (2004).

[10] Workman VL, Tezera LB, Elkington PT and Jayasinghe SN, *Adv. Functional Mat.*, **24,** 2648-2657 (2014).

[11] Ochiuz L and Peris J-E, *Med. Chem.*, **5,** 191-196 (2009).

[12] Li B-Z, Wang L-J, Li D, Bhandari B, Li S-J, Lan Y, Chen XD and Mao Z-H, *J. Food Eng.*, **92,** 250-254 (2009).

[13] Ellis A and Jacquier J, *J. Food Eng.*, **94,** 316-320 (2009).

[14] Prasertmanakit S, Praphairaksit N, Chiangthong W and Muangsin N, *AAPS PharmSciTech*, **10,** 1104-1112 (2009).

[15] Duclairoir C, Orecchioni A, Depraetere P and Nakache E, *J. Microencapsul.*, **19,** 53-60 (2002).

[16] Caballero F, Foradada M, Minarro M, Perez-Lozano P, Garcia-Montoya E, Tico JR and Sune-Negre JM, *Int. J. Pharm.*, (2013).

[17] Jiang T, Kim YK, Singh B, Kang SK, Choi YJ and Chol CS, *J. Nanosci. Nanotechnol.*, **13,** 5291-5295 (2013).

[18] King Alan H, Flavor Encapsulation with Alginates, in: Flavor Encapsulation, American Chemical Society, 1988, pp. 122-125.

[19] Anal AK, Bhopatkar D, Tokura S, Tamura H and Stevens WF, *Drug Develop Ind. Pharm.*, **29,** 713-724 (2003).

[20] Capone SH, Dufresne M, Rechel M, Fleury M-J, Salsac A-V, Paullier P, Daujat-Chavanieu M and Legallais C, *PLoS ONE*, **8,** e62032 (2013).

[21] Aslani P and Kennedy RA, *J. Control Release*, **42,** 75-82 (1996).

[22] Reis CP, Neufeld RJ, Vilela S, Ribeiro AJ and Veiga F, *J. Microencapsul.*, **23,** 245-257 (2006).

[23] Liu XD, Bao DC, Xue WM, Xiong Y, Yu WT, Yu XJ, Ma XJ and Yuan Q, *J. Appl. Polymer Sci.*, **87,** 848-852 (2003).

[24] Abbas S, Da Wei C, Hayat K and Xiaoming Z, *Food Rev. Int.*, **28,** 343-374 (2012).

[25] Carr AC and Vissers M, *Nutrients*, **5,** 4284-4304 (2013).

[26] Weinstein M, Babyn P and Zlotkin S, *Pediatrics*, **108,** e55-e55 (2001).

[27] Yuan J-P and Chen F, *J. Agric. Food Chem.*, **46,** 5078-5082 (1998).

[28] Munyaka AW, Makule EE, Oey I, Van Loey A and Hendrickx M, *J. Food Sci.*, **75,** C336-C340 (2010).

[29] Van den Broeck I, Ludikhuyze L, Weemaes C, Van Loey A and Hendrickx M, *J. Agric. Food Chem.*, **46,** 2001-2006 (1998).

[30] Sugiura S, Nakajima M, Kumazawa N, Iwamoto S and Seki M, *J. Phys. Chem. B*, **106,** 9405-9409 (2002).

[31] Vladisavljevic' GT, Kobayashi I and Nakajima M, *Microfluid Nanofluid.*, **13,** 151-178 (2012).

[32] Kobayashi I, Mukataka S and Nakajima M, *Ind. Eng. Chem. Res.*, **44,** 5852-5856 (2005).

[33] Kobayashi I, Wada Y, Hori Y, Neves MA, Uemura K and Nakajima M, *Chem. Eng. Technol.*, **35,** 1865-1871 (2012).

[34] Kawakatsu T, Kikuchi Y and Nakajima M, *J. Am. Oil Chem. Soc.*, **74,** 317-321 (1997).

[35] Sugiura S, Nakajima M, Tong JH, Nabetani H and Seki M, *J. Colloid Interface Sci.*, **227,** 95-103 (2000).

[36] Ikkai F, Iwamoto S, Adachi E and Nakajima M, *Colloid Polymer Sci.*, **283,** 1149-1153 (2005).

[37] Sugiura S, Kuroiwa T, Kagota T, Nakajima M, Sato S, Mukataka S, Walde P and Ichikawa S, *Langmuir*, **24,** 4581-4588 (2008).

[38] Neves MA, Ribeiro HS, Kobayashi I and Nakajima M, *Food Biophys.*, **3,** 126-131 (2008).

[39] Souilem S, Kobayashi I, Neves M, Sayadi S, Ichikawa S and Nakajima M, *Food Bioprocess Technol*, **7,** 2014-2027 (2014).

[40] Neves MA, Ribeiro HS, Fujiu KB, Kobayashi I and Nakajima M, *Ind. Eng. Chem. Res.*, **47,** 6405-6411 (2008).

[41] Khalid N, Kobayashi I, Neves MA, Uemura K, Nakajima M and Nabetani H, *Colloid Surface A.,* **458,** 69-77 (2014).

[42] Khalid N, Kobayashi I, Neves MA, Uemura K, Nakajima M and Nabetani H, *Colloid Surface A.,* **459,** 247-253 (2014).

[43] Desai KG and Park HJ, *J Microencapsul*, **22,** 179-192 (2005).

[44] Esposito E, Cervellati F, Menegatti E, Nastruzzi C and Cortesi R, *Int. J. Pharm.*, **242,** 329-334 (2002).

[45] Alishahi A, Mirvaghefi A, Tehrani MR, Farahmand H, Shojaosadati SA, Dorkoosh FA and Elsabee MZ, *Food Chem.*, **126,** 935-940 (2011).

[46] Goncalves GC, PM, *Revista de Ciências Farmacêuticas Básica e Aplicada* **30,** 217-224 (2009).

[47] Kobayashi I, Murayama Y, Kuroiwa T, Uemura K and Nakajima M, *Microfluid Nanofluid.*, **7,** 107-119 (2009).

[48] Kawakatsu T, Tragardh G and Tragardh C, *Colloid Surface A.,* **189,** 257-264 (2001).

[49] Kobayashi I, Mukataka S and Nakajima M, *Langmuir*, **21,** 7629-7632 (2005).

[50] Kobayashi I, Mukataka S and Nakajima M, *J. Colloid Interface Sci.*, **279,** 277-280 (2004).

[51] Binks BP and Rodrigues JA, *Ange. Chem. Int. Ed.*, **44,** 441-444 (2005).

[52] Binks BP, Murakami R, Armes SP and Fujii S, *Langmuir*, **22,** 2050-2057 (2006).

[53] Strathmann H, *Chemie Ingenieur Technik*, **62,** 261-261 (1990).

[54] Shimizu M, Nakashima T and Kukizaki M, *Kagaku Kogaku Ronbunshu*, **28,** 310-316 (2002).

[55] Cheng CJ, Chu LY and Xie R, *J. Colloid Interface Sci.*, **300,** 375-382 (2006).

[56] Opawale FO and Burgess DJ, *J. Colloid Interface Sci.*, **197,** 142-150 (1998).

[57] Kim K and Vincent B, *Korean Polymer J.*, **37,** 565-570 (2005).

[58] Kratz K, Hellweg T and Eimer W, *Colloid Surface A.*, **170,** 137-149 (2000).

[59] Poncelet D, Lencki R, Beaulieu C, Halle JP, Neufeld RJ and Fournier A, *Appl. Microbiol. Biotechnol.*, **38,** 39-45 (1992).

[60] Kuo CK and Ma PX, *Biomaterial*, **22,** 511-521 (2001).

[61] Tong JH, Nakajima M, Nabetani H and Kikuchi Y, *J. Surfactant Detergents.*, **3,** 285-293 (2000).

[62] Saito M, Yin LJ, Kobayashi I and Nakajima M, *Food Hydrocolloid*, **19,** 745-751 (2005).

[63] Kawakatsu T, Tragardh G, Tragardh C, Nakajima M, Oda N and Yonemoto T, *Colloid Surface A.*, **179,** 29-37 (2001).

[64] Chuah AM, Kuroiwa T, Kobayashi I, Zhang X and Nakajima M, *Colloid Surface A.*, **351,** 9-17 (2009).

[65] Kobayashi I, Vladisavljevic GT, Uemura K and Nakajima M, *Chem. Eng. Sci.*, **66,** 5556-5565 (2011).

[66] Vladisavljevic GT, Kobayashi I and Nakajima M, *Microfluid Nanofluid.*, **10,** 1199-1209 (2011).

[67] Khalid N, Kobayashi I, Neves MA, Uemura K and Nakajima M, *Biosci. Biotechnol. Biochem.*, **77,** 1171-1178 (2013).

[68] Khalid N, Kobayashi I, Neves MA, Uemura K and Nakajima M, *LWT - Food Sci. Technol.*, **51,** 448-454 (2013).

[69] Viveros-Contreras R, Téllez-Medina D, Perea-Flores M, Alamilla-Beltrán L, Cornejo-Mazón M, Beristain-Guevara C, Azuara-Nieto E and Gutiérrez-López G, *Revista Mexicana de Ingenierı́a Quı́mica*, **12,** 29-39 (2013).

[70] Devi N and Kakati DK, *J. Food Eng.*, **117,** 193-204 (2013).

[71] Kobayashi I, Wada Y, Uemura K and Nakajima M, *Microfluid Nanofluid.*, **8,** 255-262 (2010).

[72] Comunian TA, Abbaspourrad A, Favaro-Trindade CS and Weitz DA, *Food Chem.*, **152,** 271-275 (2014).

[73] Santana RC, Perrechil FA and Cunha RL, *Food Eng Rev*, **5,** 107-122 (2013).

[74] Farhang B, Kakuda Y and Corredig M, *Dairy Sci. & Technol.*, **92,** 353-366 (2012).

[75] Rozman B and Gašperlin M, *Drug deliv.*, **14,** 235-245 (2007).

[76] Comunian TA, Thomazini M, Alves AJG, de Matos Junior FE, de Carvalho Balieiro JC and Favaro-Trindade CS, *Food Res. Int.*, **52,** 373-379 (2013).

Chapter 4

Preparation and characterization of water-in-oil emulsions loaded

with high concentration of ʟ-ascorbic acid*

4.1 Introduction

Emulsions are defined as dispersions of droplets of one liquid in another, with a droplet diameter generally within the range of 0.1-100 μm [1]. According to the definition of International Union of Pure and Applied Chemistry (IUPAC) (1971), "In an emulsion liquid droplets and/or liquid crystals are dispersed in a liquid". An emulsion consists of at least two immiscible phases such as oil and water, with one of the phases dispersed in the other [2]. A dispersion consisting of oil droplets dispersed in an aqueous phase is called an oil-in-water (O/W) emulsion. O/W food emulsions include mayonnaise, milk, soups and sauces. On the other hand, a dispersion consisting of water droplets dispersed in an oil phase is called as water-in-oil (W/O) emulsion. Typical examples of W/O food emulsions are margarine, butter, and spreads.

Vitamins are complex organic compounds that the body needs in small quantities and are essential in carrying vital functions of human body. These vitamins must be supplied in the diet, as the human body cannot synthesize them. One such example is Vitamin C (L-ascorbic acid (L-AA)) which can be found in various fruits and leafy vegetables. The exact amount of vitamin C that the body needs is unknown, and is thought to be around 45 to 75 mg/day[3]. L-AA is a white, crystal-shaped organic compound, and can be synthesized from glucose or extracted from certain natural sources such as orange juice.

Vitamin C plays a vital role in our body synthesis of collagen tissue around bones, teeth, cartilage, skin, and damaged tissue[4]. Similarly, this vitamin is needed to activate various enzymes related to the nervous system, hormones, and detoxification of drugs and poison in the liver[5]. L-AA plays a role as antioxidant, as its solubility in water enables it to work as antioxidant within our body fluids. Vitamin C increases the rate of absorption of iron, calcium, and folic acid. Vitamin C reduces allergic reactions, boosts the immune system, stimulates the formation of bile in the gallbladder, and facilitates the excretion of various steroids[6]. Because of these favorable effects, vitamin C has been used in cosmetics and pharmaceutical applications[7]. However, its rapid degradation in aqueous solutions is still a major drawback to design a variety of functional products.

Vitamin C is highly soluble in water and alcohol, and is easily oxidized in the solubilized form and its oxidation occurs very quickly in an alkaline environment especially at higher temperatures (>50°C)[8]. Similarly, light and heat damage vitamin C in fruits and vegetables[9]. Degradation of vitamin C proceeds both aerobic and anaerobic pathways and depends upon many factors such as

oxygen, heat, light, storage temperature, and storage time[10,11]. The degradation processes of L-AA are very complex and contain a number of oxidation/reduction with some intermolecular rearrangements[5,12]. Fig. 4.1 shows pathway of L-AA degradation in aqueous solution[8]. Degradation of L-AA results in brownish color possibly due to interaction with amino acids[5].
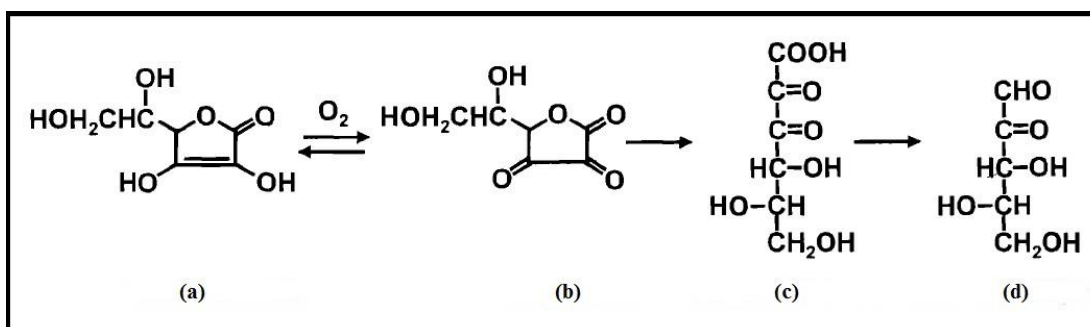
Figure 4.1: Degradation pathways of L-AA in aqueous solution (a) represents L-AA, (b) Dehydro-L-AA, (c) 2,3- diketo-L-gluconic acid and (d) represents L-xylosome (adopted from Lee *et al.* [5].

L-AA is very unstable in aqueous solution. Encapsulation and emulsification are widely used techniques for protection of this vital vitamin[13,14]. In most cases 1 to 5% of this vitamin is emulsified and encapsulated[5,13]. Both W/O and Water-in-Oil-in-Water (W/O/W) emulsification methods have been used for encapsulating vitamin C[4,5,13,15,16]. In these emulsions the interface acts as a barrier for oxygen to prevent encapsulated vitamin C from undergoing oxidation –induced degradation.

Foreseeing higher biological activity of L-AA, the authors formulated W/O emulsions containing high concentration of L-AA. The main purpose of this work is to elucidate that, up to what extent stable W/O emulsions can be prepared by incorporating higher amount of L-AA. The effect of homogenization speed, concentration of L-AA solubilized in a dispersed phase, stability of prepared emulsions, and retention kinetics of L-AA in the prepared emulsions were also investigated.

4.2 Materials and methods

Materials

L-AA (99.9% purity), magnesium sulfate, sodium bicarbonate, acetic acid, 2,6-dichlorophenol indophenol, metaphosphoric acid were purchased from Wako Pure Chemical Ind. (Osaka, Japan). All of these reagents were of analytical grade. Tetraglycerin monolaurate condensed ricinoleic acid ester (CR-310) was supplied by Sakamoto Yakuhin Kogyo (Osaka, Japan). Soybean oil (Wako Pure

Chemical Ind.) and *Moringa oleifera* oil (Yamakei Co., Ltd., Osaka, Japan) were used as continuous-phase medium.

Preparation of W/O emulsions

W/O emulsions were prepared from a dispersed aqueous phase and a continuous oil phase. The dispersed phase contained (5 to 30 g 100 mL^{-1}) ascorbic acid and (1 g 100^{-1}) magnesium sulfate. The magnesium sulfate was added to the dispersed phase to balance the ion-ion interaction and these magnesium ions acts as counter ions to stabilize the ascorbic acid by ion shielding effect as previously described by Lee *et al.*[5]. Soybean oil or *Moringa* oil, each containing (5 g 100 g^{-1}) CR-310 as emulsifier, was used as continuous phase separately. The volume fraction of the dispersed aqueous phase (ϕ_d) was fixed to 30 g 100 g^{-1}. . Thirty mL of dispersed phase were added to seventy mL of continuous phase at room temperature (~25°C), followed by emulsification at various rotation speed for 5 min with a polytron homogenizer (PT-3000 Kinematica-AG, Littace, Switzerland).

Determination of average droplet diameter

For analysis of prepared W/O emulsions, microscopic observations were made with an optical microscope (DM IRM, Leica Microsystems, Wetzler, Germany). From these micrographs droplet size was measured and expressed as average droplet diameter (d_{av}). To determine d_{av}, the diameters of 250 droplets were measured with an image processing software (WinRoof ver. 5.6, Mitani Co., Fukui, Japan). Coefficient of variation (CV) was used as an indicator of droplet size distribution of the prepared emulsion. The CV (%) was defined as follows:

$$CV = \left(\frac{\sigma}{d_{av}}\right) \times 100 \qquad (4.1)$$

where σ is the standard deviation of the droplet diameter (μm).

Measurement of fluid properties

Viscosity, density, and interfacial tension between the dispersed and continuous phases were measured at 25 °C. Viscosity was measured with a vibro viscometer (SV-10, A&D Co., Ltd., Tokyo, Japan). Density was measured with a density meter (DA-130 N, Kyoto Electronics Manufacturing Co., Ltd., Kyoto, Japan). The interfacial tension was measured with a Fully Automatic Interfacial Tensiometer (PD-W, Kyowa Interface Sciences Co., Ltd., Saitama, Japan) using a pendant drop method.

Physical stability of W/O emulsions

Stability studies were carried out either at 4 or 25 °C. The stability test were carried out for 30 days, and emulsions containing 10, 20 and 30 g 100 g^{-1} L-AA were analyzed with regard to droplet size, droplet size distribution, color, and physical state. The droplet size was measured using image processing software. Color and physical state were observed qualitatively [15].

Retention kinetics of L-AA in W/O emulsions

The concentration of vitamin C in W/O emulsions was determined according to 2,6- dichlorophenol indophenol titrimetric method No. 967.21 of AOAC[17] with slight modification. Briefly 1 g of W/O emulsion was mixed with 10 mL of ethanol, and then treated by sonication for 20 min, followed by centrifugation for 3 min at 3000 rpm. One mL of supernatant was used to measure L-AA concentration. All experiments were repeated in triplicate and mean value were calculated. The retention rate (*r*) calculated by using Eq. 4.2 was defined by the ratio of measured L-AA concentration (C_{AA}) to initial L-AA concentration ($C_{AA,0}$).

$$r = \left(\frac{c_{AA}}{c_{AA,0}}\right) \times 100 \qquad (4.2)$$

Statistical analysis

Analysis of variance (ANOVA) tests were used to analyze the characterization data at a confidence level of 95 %. Least significant difference (LSD) test with 95 % confidence level (P<0.05) was used to compare d_{av} at different homogenization speed and L-ascorbic acid concentration in the dispersed phase. The LSD was calculated using Statistix 8.1 software (Tallahassee, USA) and according to the method described by Steel *et al.*[18].

4.3 Results and discussion

Effect of homogenization speed on droplet size of W/O emulsions

Fig. 4.2a shows the effect of homogenization speed on d_{av} and CV of the prepared W/O emulsions containing 10 g 100 g^{-1} L-AA. W/O emulsions were successfully prepared using 5000 rpm or higher, whereas lowering homogenization speed resulted in incomplete homogenization with visible phase separation. d_{av} of the W/O emulsions prepared gradually decreased from 3.0 to 2.0 μm by increasing the homogenization speed. There was a significant difference (p<0.05) in their d_{av} with increasing

homogenization speed. The CV of the prepared W/O emulsions ranged between 13 % and 22 % with

polydispersity.

(a)

(b)

(c)
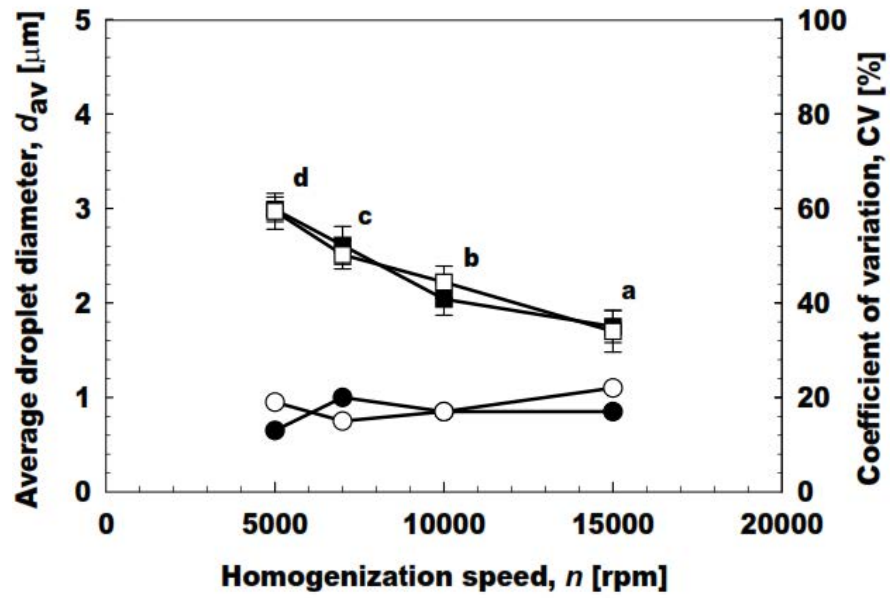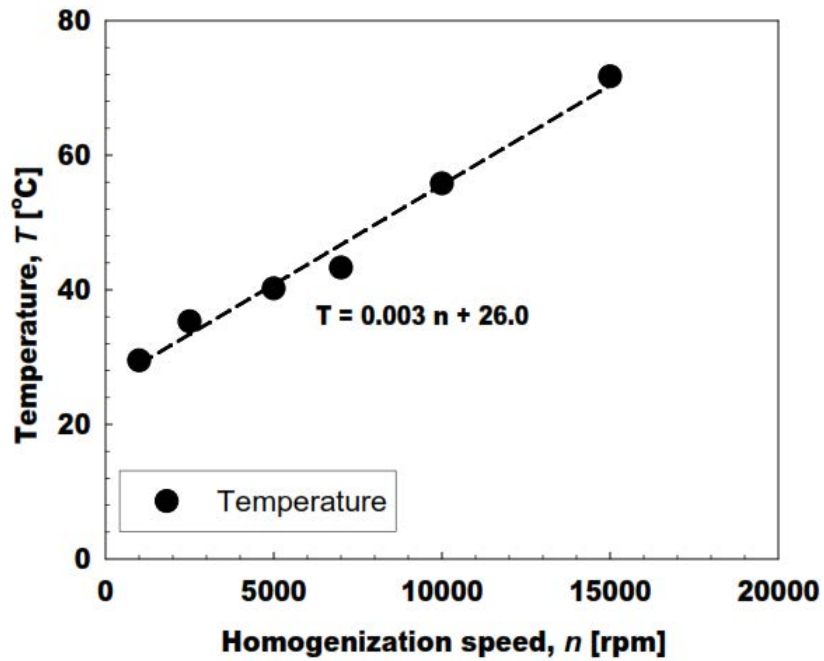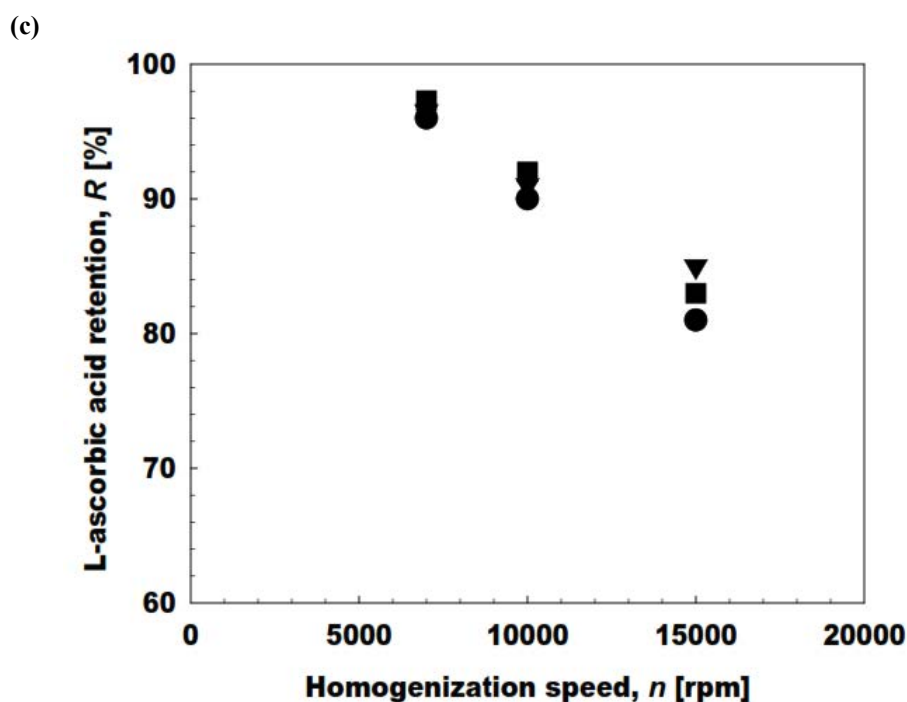
Figure 4.2: (a) Effect of homogenization speed on average droplet diameter (d_{av}) and coefficient of variation (CV) of W/O emulsions containing 10 g 100 g-1 L-AA. (■) represents soybean oil and (□) represents *Moringa* oil. Different letters (a, b, c, d) represent W/O emulsions (soybean and *Moringa* oil) have significantly difference d_{av} at the 95% confidence level (p=0.05). The symbol (●), (○) indicates CV of soybean oil and *Moringa* oil. (b) Effect of homogenization speed on temperature of prepared W/O emulsions. The fitted line had a coefficient of determination (R^2) of > 0.98. (c) Effect of homogenization speed on L-AA retention in prepared W/O emulsions. AA stands for L-AA. (●) represents 10 g 100 g^{-1}, (▼) represents 20 g 100g^{-1} AA and (■) presents 30g 100 g^{-1} L-ascorbic acid.

Homogenization at 15000 rpm increased the system temperature to more than 70 °C (Fig. 4.2b), leading towards reduction in L-AA retention to 82 to 85 g 100 g^{-1} in prepared W/O emulsions (Fig. 4.2c) which agrees well with results of Lee *et al.*[5]. The production of emulsion droplets requires high energy input. The droplet size of an emulsion produced by rotor-stator homogenization process depends on the rotational speed which represents the energy of homogenization. The higher the energy applied in the homogenization of emulsion, the smaller the droplet size produced. However, uniformity of droplet size distribution depended on the completion of droplet size reduction which required more energy [19]. W/O emulsions prepared at 7000 rpm incorporated mild heat (42 °C) in the system and showed better L-AA retention rate > 95 g 100 g^{-1}. This homogenization speed was considered adequate and therefore applied to prepare W/O emulsions in later sections. Increasing the homogenization speed results in incorporation of heat in emulsion system, and this heat might result in destruction of L-AA [5].

Effect of L-AA concentration in dispersed phase

Fig. 4.3 shows the effect of L-AA concentration in the dispersed phase on d_{av} and CV of prepared W/O emulsions. There was no significant difference (p>0.05) in their d_{av} with increasing L-AA concentration from (5 to 30 g 100 g^{-1}) in W/O emulsions. The oil type also did not affect droplet size of the prepared W/O emulsions. Both the soybean and *Moringa oleifera* oil has well balanced fatty acid profile (Table 4.1) with good amount of tocopherols. Their d_{av} ranged from 2.3 to 3.1 μm and slowly increased with increasing L-AA concentration. Akhtar *et al.*[15] reported that the oil droplet size of W/O/W emulsions containing 1 g 100 g^{-1} L-AA ranged between 14.8 to 17.0 μm. [4] also reported that the oil droplet size of different W/O/W emulsions containing 1 g 100 g^{-1} L-AA varied from 15.6 to 42.2 μm. These previous studies regarding W/O/W emulsions containing L-AA did not mention their internal aqueous droplet size. Major factors that affect d_{av} of emulsions are emulsion composition including the amount of emulsifier, and processing conditions. They play a vital role in determination of emulsions stability [5,13,15].

Table 4.1: Fatty acid composition of soybean and *Moringa* oil [20, 21].

Fatty acid profile	Range (g 100 g^{-1})	
	soybean oil	*Moringa oleifera* oil
Myristic (14:0)	0.1	0-0.13
Palmitic (16:0)	11	5.57-9.26
Palmitoleic (16:1)	0.1	1-3.7
Stearic (18:0)	4	2.27-8.3
Oleic (18:1)	23.4	67.7-76
Linoleic (18:2)	53.2	0.27-1.29
Linolenic (18:3)	7.8	0.18-0.45
Arachidic (20:0)	0.3	1.98-4.7
Gadoleic (20:1)	-	1.2-2.7
Behenic (22:0)	0.1	3.72-7.4
Total PUFA*	57.87	0.4-1.4

*Total polyunsaturated fatty acid
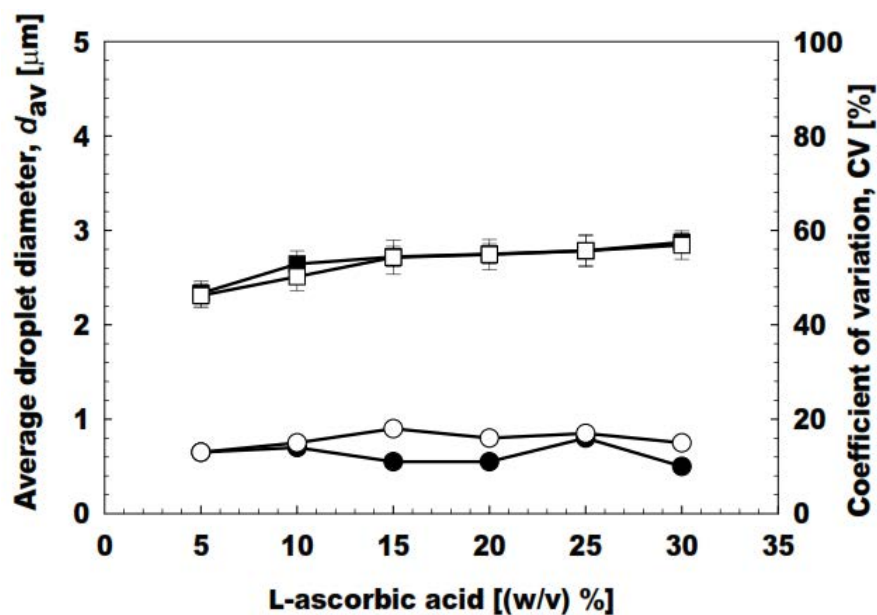
Figure 4.3: Effect of different concentration of L-AA on average droplet diameter (d_{av}) and coefficient of variation (CV) of W/O emulsions prepared at a homogenization speed of 7000 rpm. (■) indicates soybean oil and (□) indicates *Moringa* oil d_{av}. The symbol (●), (○) indicates CV of soybean oil and Moringa oil.

Viscosity (η), viscosity ratio (ζ) and interfacial tension (γ) are key fluid properties to investigate the droplet size of any emulsion. The soybean oil (η_c) had viscosity of 63.7 mPa s, while *Moringa* oil (η_c) had slightly higher viscosity of 68.7 mPa s. ζ (viscosity ratio) is a dimensionless parameter and defined as the ratio of the viscosity of the dispersed phase (η_d) to the viscosity of continuous phase (η_c), that gives idea about the droplet size under various conditions [22]. ζ in different concentrations of W/O emulsions containing L-AA was in between 0.05 to 0.1 (Fig. 4.4a). The gradual increase in η_d and ζ caused the slow increase in d_{av} of the prepared W/O emulsions (Fig. 4.4). γ between the soybean oil and Milli-Q water containing different concentration of L-AA (5 to 30 g 100 g^{-1}) was in between 4.5 to 6.3 mN m^{-1} (Fig. 4.4b), whereas it varied between 5.7 to 6.5 mN m^{-1} with increasing L-AA concentration in *Moringa* oil. The decrease in interfacial tension by hydrophobic emulsifier (CR-310) improves the stability of oil/water interface, that results in stable formation of W/O emulsions[23].

(a)

(b)
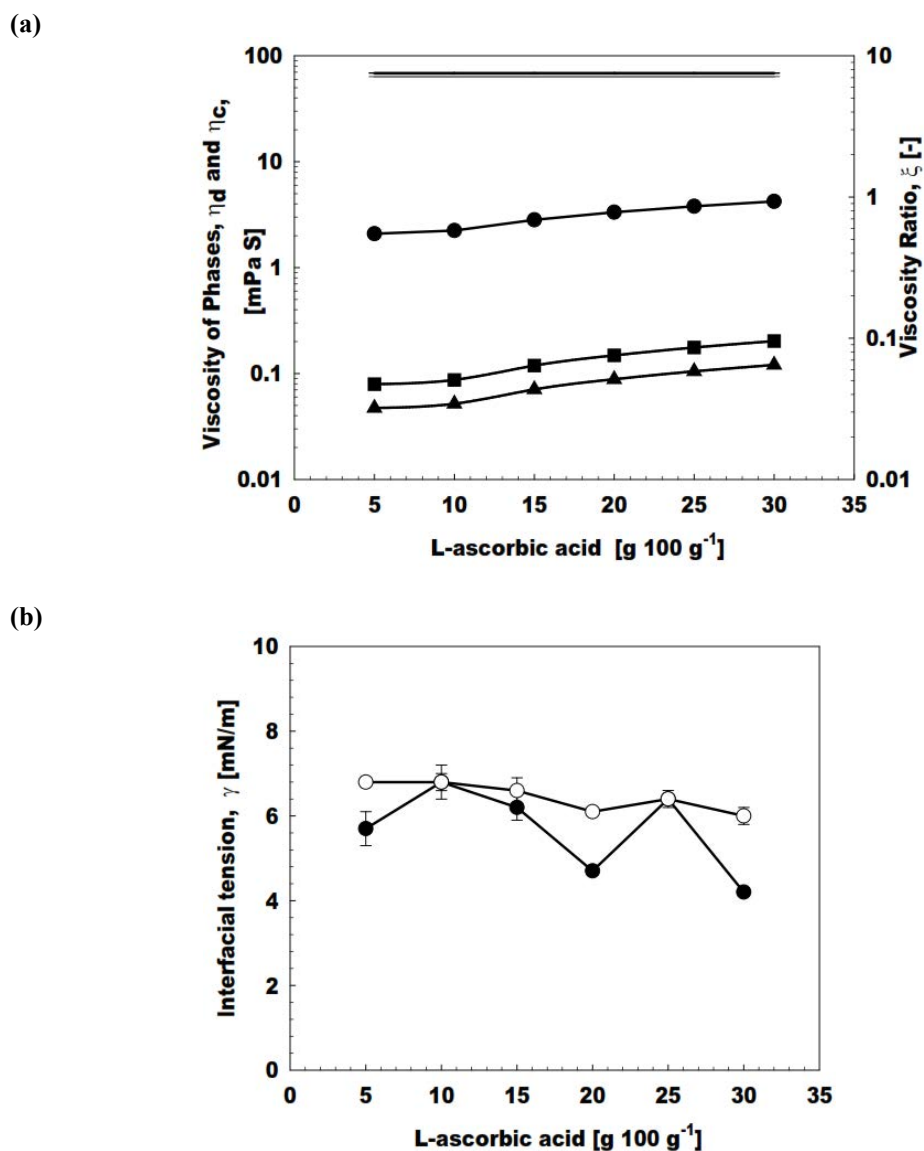
Figure 4.4: (a) Variation of viscosity of the dispersed phase, continuous phase and viscosity ratio of soybean and *Moringa* oil as a function of L-AA concentration in the dispersed phase. η_d is the viscosity of dispersed phase (●), η_c is the viscosity of continuous phases (black line *Moringa* oil and gray line soybean oil) and ξ is the viscosity ratio (soybean oil (■) and (▲) *Moringa* oil) defined as η_d/η_c (b) Variation of the interfacial tension (□) of soybean oil (●) and *Moringa* oil (○) as a function of L-AA concentration.

Physical stability of W/O emulsions containing L-AA at 4 and 25°C

Preparation of food-grade W/O emulsions containing vegetable oils (e.g., soybean oil and canola oil) is a challenging subject due to stability problems [15]. The emulsion stability is defined in terms of physical and chemical stability of the emulsion.

Fig. 4.5 shows the stability of W/O emulsions containing 10 to 30 g 100 mL^{-1} L-AA in the dispersed phase upon storage at 4 °C. There was little variation in their droplet size over 30 d of storage

period, and their d_{av} remained in the range of 2.3 to 3.0 μm either in case of *Moringa* oil or soybean oil. The oil type did not affect the resultant droplet size, regardless of L-AA concentration. All the W/O emulsions stored at 4ºC remained stable without any phase separation for more than 30 days. Fig. 4.6 depicts the stability of W/O emulsions containing 10 to 30 g 100 mL^{-1} L-AA in the dispersed phase stored at 25 ºC. Slight increases in d_{av} were seen in all the emulsions upon storage. The W/O emulsions stored at 25 ºC had d_{av} of 2.5 to 3.4 μm for the soybean oil-containing systems and of 2.6 to 2.9 μm for the *Moringa* oil-containing systems during 30 d of storage period. All emulsions remained stable over 30 d, followed by a formation of thin aqueous layer at the bottom. Slight increase in CV up to 20 % at 4 ºC and 25 ºC was seen in W/O emulsions containing *Moringa* oil. As for W/O emulsions containing soybean oil, their CV varied between 15 and 17 % at 4 ºC and 25 ºC, respectively.

(a)
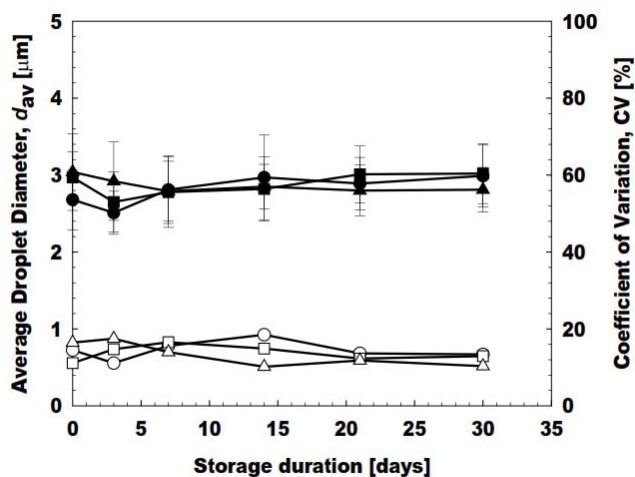
(b)
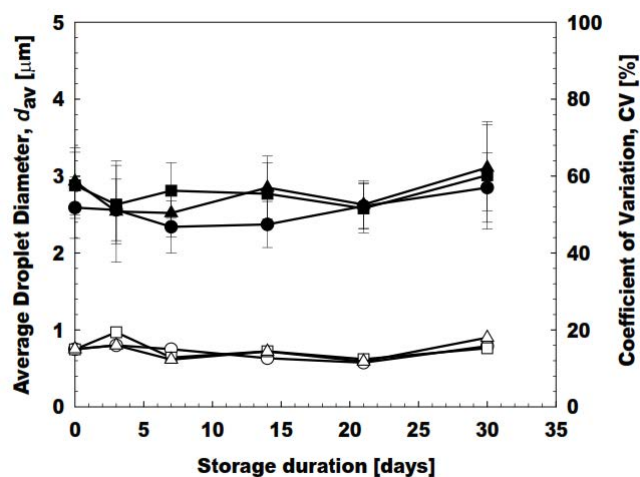
Figure 4.5: Stability of W/O emulsions at 4ºC. (a) Soybean oil. (b) *Moringa* **oil. The symbols (●) indicates 10 g 100 g^{-1} L-AA, (■) 20 g 100 g^{-1} L-AA, and (▲) 30 g 100 g^{-1} L-AA. The symbols (○) indicates CV of 10 g 100 g^{-1} L-AA, (□) 20 g 100 g^{-1} L-AA and (Δ) indicates 30 g 100 g^{-1} L-AA.**

(a)
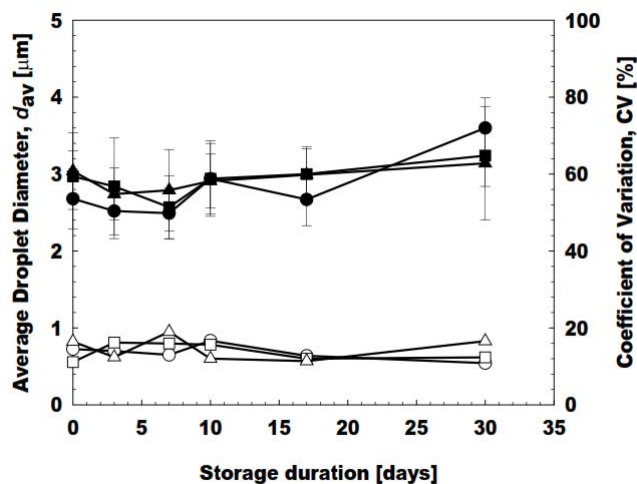
(b)
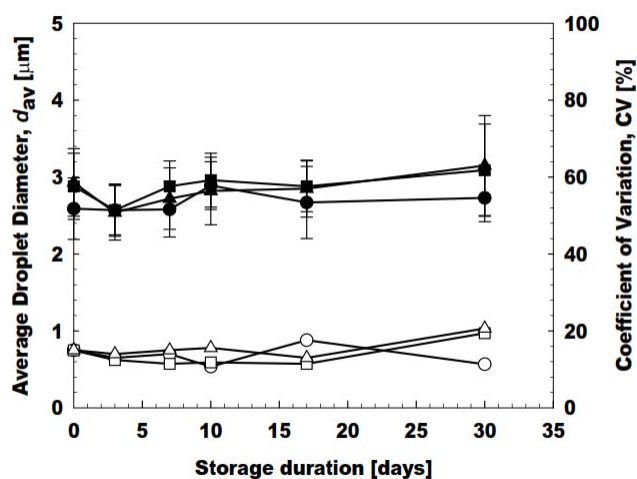
Figure 4.6: Stability of W/O emulsions at 25°C. (a) Soybean oil. (b) *Moringa* oil. The symbols (●) indicates 10 g 100 g^{-1} L-AA, (■) 20 g 100 g^{-1} L-AA, and (▲) 30 g 100 g^{-1} L-AA. The symbols (○) indicates CV of 10 g 100 g^{-1} L-AA, (□) 20 g 100 g^{-1} L-AA and (Δ) indicates 30 g 100 g^{-1} L-AA.

Organoleptic evaluation plays an important role in checking the physical stability of any emulsion[15]. As for organoleptic evaluation, we qualitatively observed color, physical appearance and physical state of prepared W/O emulsions. The emulsions store at 4 °C maintained whitish color for more than 30 d of storage, while those stored at 25 °C became first a lightly yellowish color after 17 d, followed by yellowish color that indicated destabilization of L-AA in the emulsions. As for physical appearance, the W/O emulsions containing soybean oil had flow-like consistency, regardless of storage temperature. By contrast, the W/O emulsions containing *Moringa* oil had solid like consistency at 4 °C and flow like consistency at 25 °C. The chemical stability of L-AA encapsulated in the W/O emulsions prepared in this study will be described in the next section.

Retention kinetics of W/O emulsions containing L-AA

The degradation of L-AA has been considered one of the major causes of quality and color changes during processing and storage of food products. The chemical stability of L-AA encapsulated in emulsions and creams has been studied in emulsions and creams by several research groups [4,5,13,24,25]. L-AA and its derivatives have been used in a variety of food products and cosmetic formulations as an antioxidant, pH adjuster, anti-aging and photoprotectant [25]. The control of instability of L-AA poses a significant challenge in the development of cosmetic and food-grade formulations. Fig. 4.7 shows L-AA retention in W/O emulsions stored at 4 °C in the presence of light. The prepared W/O emulsions containing 10 to 30 g 100 g^{-1} L-AA exhibited 50 g 100 g^{-1} retention of L-AA after 30 days of storage. There was no significant difference ($p>0.05$) between two different continuous phases, as they hardly affected L-AA retention after each storage period. By contrast, the W/O emulsions containing L-AA stored at 25 °C under darkness exhibited 30 g 100 g^{-1} retention of L-AA after 30 d storage (Fig. 4.7). The temperature has a major effect on L-AA degradation [8]. The observed retention rates were in accordance with a previous study by [5]. Those authors concluded that encapsulation of L-AA in W/O/W emulsions had beneficial effect on release profile of L-AA [9]. demonstrated that rate of oxidative degradation in L-AA cream formulation in the dark was about 70 times slower than that in presence of light. L-AA retention in Milli-Q water at 25 °C is also presented in Fig. 4.7. The L-AA retention in W/O emulsions was higher than that in Milli-Q water during their storage. Rapid ionization in aqueous solution results in rapid loss of L-AA [8,26].

(a)
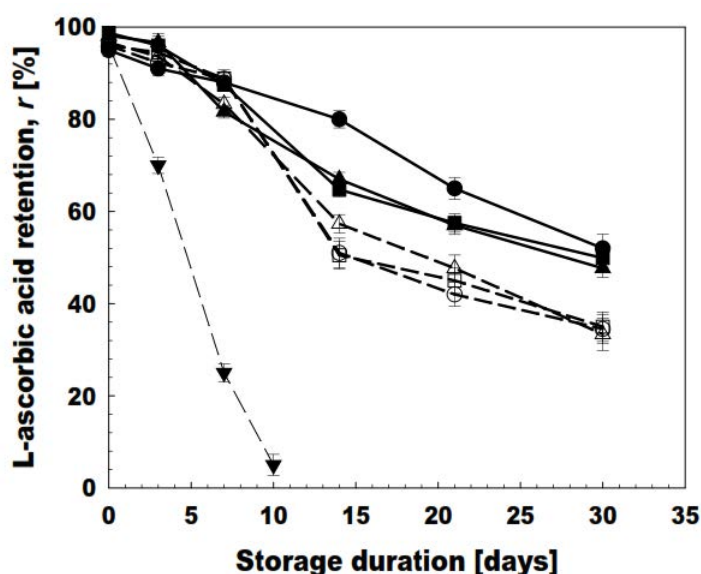
(b)
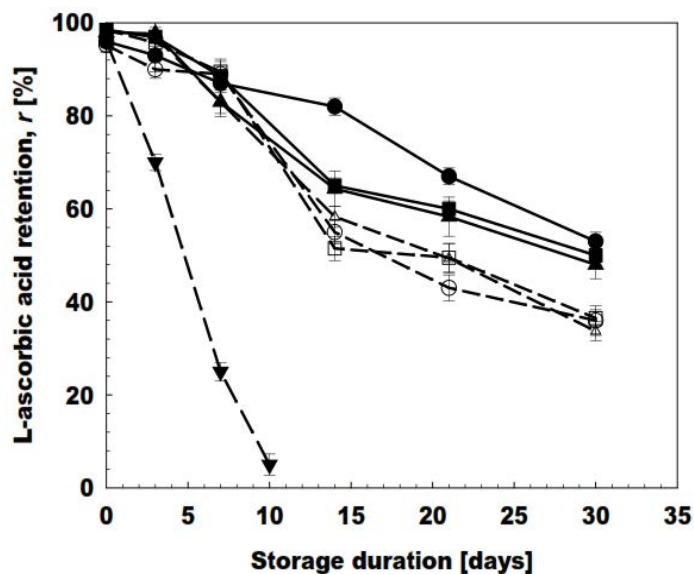
Figure 4.7: (a) L-AA retention in W/O emulsions containing soybean oil stored at 4 °C and 25 °C. **(b)** L-AA retention in W/O emulsions containing *Moringa* oil stored at 4 °C and 25 °C. The symbols (●) indicates 10 g 100 g^{-1} L-AA, (■) 20 g 100 g^{-1} L-AA, and (▲) 30 g 100 g^{-1} L-AA in W/O emulsions at 4 °C and the symbols (○) indicates 10 g 100 g^{-1} L-AA, (□) 20 g 100 g^{-1} L-AA and (Δ) indicates 30 g 100 g^{-1} L-AA in W/O emulsions at 25 °C. The symbol (▼) indicates L-AA retention in Milli-Q water stored at 25 °C.

Fig. 4.8 shows the retention kinetics of L-AA in W/O emulsions during storage. In (A/A_0) represents the fraction of remaining L-AA in the emulsions, where A is the L-AA concentration after storage and A_0 is the initial L-AA concentration. The results indicate that the L-AA retention follow first order kinetics with respect to time. The retention of L-AA as first-order kinetics was also reported by different research groups [27]. The retention kinetics of L-AA in W/O emulsions stored at 4 and 25 °C was also evaluated by the following first-order kinetics equation:

$$\frac{A}{A_0} = \exp(-kt) \qquad (4.3)$$

where k is the rate constant and t is the storage time. The rate constant of the first-order kinetics was calculated to best-fit the experimental results by the regression function of Microsoft Excel 2007. The lines fitted by eq. 2 are presented in Fig. 4.8. The calculated coefficients of determination (R^2) for all W/O emulsions were > 0.95, indicating that fitting application of the first-order kinetics is reasonable. Rate constants and half-life of L-AA retention in different W/O emulsions are also presented in Table 4.2. There was no significant difference (p>0.05) in the retention kinetics of two different continuous phases (soybean oil or *Moringa* oil). The observed half-life for W/O emulsions (soybean oil and *Moringa* oil) at 4 °C is > 30 d and >19 d for emulsions at 25 °C

112

respectively. The half-time values for the W/O emulsions stored at 4ºC show a better stability, compared to those stored at 25 ºC.

Table 4.2: Rate constants and half-life of ascorbic acid degradation in different W/O emulsions

Treatment	rate equation	R^2	rate constant k $(day)^{-1}$	Average value of rate constant k $(day)^{-1}$	half life (day) $t_{1/2}=0.693/k$
4°C (Soybean oil), 10 g 100 g^{-1}	$\ln(A/A_o) = -0.0183t$	0.95	0.018		
4°C (Soybean oil), 20 g 100 g^{-1}	$\ln(A/A_o) = -0.0242t$	0.96	0.024	0.022	31.5
4°C (Soybean oil), 30 g 100 g^{-1}	$\ln(A/A_o) = -0.0249t$	0.98	0.025		
25°C (Soybean oil), 10 g 100 g^{-1}	$\ln(A/A_o) = -0.0361t$	0.94	0.036		
25°C (Soybean oil), 20 g 100 g^{-1}	$\ln(A/A_o) = -0.0350t$	0.94	0.035	0.035	19.8
25°C (Soybean oil), 30 g 100 g^{-1}	$\ln(A/A_o) = -0.0347t$	0.98	0.035		
4°C (*Moringa* oil), 10 g 100 g^{-1}	$\ln(A/A_o) = -0.0178t$	0.95	0.018		
4°C (*Moringa* oil), 20 g 100 g^{-1}	$\ln(A/A_o) = -0.0247t$	0.97	0.025	0.023	30.1
4°C (*Moringa* oil), 30 g 100 g^{-1}	$\ln(A/A_o) = -0.0247t$	0.97	0.025		
25°C (*Moringa* oil), 10 g 100 g^{-1}	$\ln(A/A_o) = -0.034t$	0.95	0.034		
25°C (*Moringa* oil), 20 g 100 g^{-1}	$\ln(A/A_o) = -0.0346t$	0.98	0.035	0.035	19.8
25°C (*Moringa* oil), 30 g 100 g^{-1}	$\ln(A/A_o) = -0.0352t$	0.98	0.035		

(a)
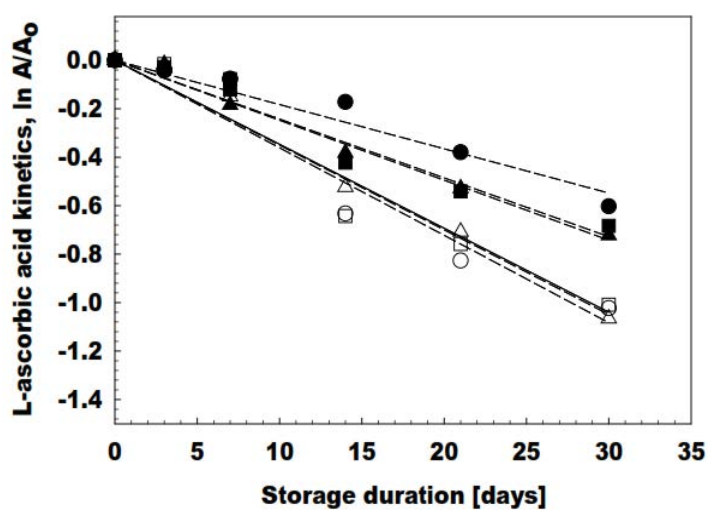
(b)
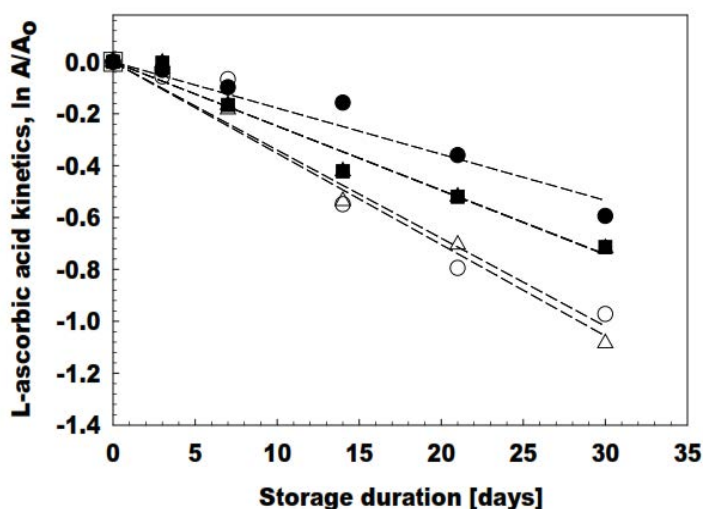
Figure 4.8: (a) Retention kinetics of W/O emulsions containing soybean oil stored at 4 ºC and 25 ºC. Rate constants, coefficients of determination, and half-life are presented in Table 2. (b) Retention kinetics of W/O emulsions containing *Moringa* oil stored at 4 ºC and 25 ºC . Rate constants, coefficients of determination, and half-life are presented in Table 2. The symbols (●) indicates 10 g 100 g^{-1} L-AA, (■) 20 g 100 g^{-1} L-AA, and (▲) 30 g 100 g^{-1} L-AA in W/O emulsions at 4 ºC and the symbols (○) indicates 10 g 100 g^{-1} L-AA, (□) 20 g 100 g^{-1} L-AA and (Δ) indicates 30 g 100 g^{-1} L-AA in W/O emulsions at 25 ºC.

The photolysis kinetics of L-AA in cream formulations was investigated by Ahmad *et al.*[9]. They concluded that L-AA retention follows first-order kinetics and this retention is affected by the concentration of active ingredients, pH, and viscosity of the medium. Watanabe *et al.*[28] concluded that retention of catechins follows first-order kinetics in O/W emulsions containing L-AA. More research is needed to completely elucidate the retention profile of L-AA in W/O emulsions containing higher concentration of L-AA.

References

[1] Calderon L, Schmitt F, Bibette V and Jerome, Emulsion Science, Basic Principles, in, Springer Science, New York, USA, 2007, pp. 1-50.

[2] McClements D, Food Emulsions: Principles, Practice and Techniques, in, CRC Press, Boca Raton, Florida, 2004, pp. 20-50.

[3] Fennema O, Food Chemistry, in, Marcel Dekker, Inc., New York, USA, 1996, pp. 559-567.

[4] Gallarate M, Carlotti M, Trotta M and Bovo S, *Int. J. Pharm.*, **188,** 233-241 (1999).

[5] Lee J, Kim J, Han S, Chang I, Kang H, Lee O, Oh S and Suh K, *J. Cosmet Sci.*, **55,** 1-12 (2004).

[6] Abbasi M and Niakousari M, *Electronic J. Environ. Agric. Food Chem*, **6,** 1735-1741 (2007).

[7] Pinnell SR, Yang H, Omar M, Riviere NM, DeBuys HV, Walker LC, Wang Y and Levine M, *Dermatologic Surgery*, **27,** 137-142 (2001).

[8] Yuan J-P and Chen F, *J. Agric. Food Chem.*, **46,** 5078-5082 (1998).

[9] Ahmad I, Sheraz M, Ahmed S, Shaikh R, Vaid F, ur Rehman Khattak S and Ansari S, *AAPS PharmSciTech*, **12,** 917-923 (2011).

[10] Satoh K, Sakagami H, Terasaka H, Ida Y and Fujisawa S, *Antican. Res*, **20,** 1577-1581 (2000).

[11] Nunes MCN, Brecht JK, Morais AMMB and Sargent SA, *J. Food Sci.*, **63,** 1033-1036 (1998).

[12] Kimoto E, Tanaka H, Ohmoto T and Choami M, *Anal. Biochem.*, **214,** 38-44 (1993).

[13] Farahmand S, Tajerzadeh H and Farboud ES, *Pharm. Develop. Technol.*, **11,** 255-261 (2006).

[14] Uddin M, Hawlader M and Zhu H, *J. Microencapsul.*, **18,** 199-209 (2001).

[15] Akhtar N, Ahmad M, Khan HA, J, Gulfishan, Mahmood A and Uzair M, *Bull. Chem. Soc. Ethiopia*, **24,** 1-10 (2010).

[16] Xia Q and Yao Y, *Mat. Sci. Forum*, **649,** 783-787 (2011).

[17] AOAC, Official Methods of Analysis of Association of Official Analytical Chemists International, in: W. Horwitz (Ed.), AOAC Press, Arlington, VA, USA, 2003.

[18] Steel R, Torrie J and Dickey D, Principles and procedures of statistics: A biometrical approach in, McGraw Hill Book Co., New York, USA, 1997.

[19] Affandi M, Julianto T and Majeed A, *Asian J. Pharm. Clin. Res.*, **4,** 142-148 (2011).

[20] Rahman IMM, Barua S, Nazimuddin M, Begum ZA, Rahman MA and Hasegawa H, *J. Food Lipid.*, **16,** 540-553 (2009).

[21] Wang T, Soybean Oil, in: F. Gunstone (Ed.) Vegetable Oils in Food Technology: Composition, Properties and Uses, Wiley-Blackwell Publishing Ltd., Oxford, UK, 2011.

[22] van Dijke K, Kobayashi I, Schroën K, Uemura K, Nakajima M and Boom R, *Microfluidics and Nanofluidics*, **9,** 77-85 (2010).

[23] Scamehorn J, Phenomena in Mixed Surfactant Systems, in, American Chemical Society, Washington, AD, 1986, pp. 1-27.

[24] Raschke T, Koop U, Düsing H, Filbry A, Sauermann K, Jaspers S, H W and Wittern K, *J. Skin Pharmacol. Physiol.,* **17,** 200-206 (2004).

[25] Elmore A, *Int. J. Toxicol.*, **24,** 51-111 (2005).

[26] Matei N, Soceanu A, Dobrinas S and Magearu V, *Ovidius Univ. Ann. Chem.*, **20,** 132-136 (2009).

[27] Watanabe Y, Suzuki T, Nakanishi H, Sakuragochi A and Adachi S, *J. Am. Oil Chem. Soc*, **89**, 269-274 (2012).

[28] Watanabe Y, Suzuki T, Nakanishi H, Sakuragochi A and Adachi S, *J. Am. Oil Chem. Soc.*, **89,** 269-274 (2012).

Chapter 5

Preparation and characterization of water-in-oil-in-water emulsions containing a high concentration of L-ascorbic acid*

5.1 Introduction

Double emulsions are categorized as complex dispersion systems and are regarded as emulsions of emulsions [1]. Double emulsions are further classified into water-in-oil-in-water (W/O/W) and oil-in-water-in-oil (O/W/O) emulsions. Most industrial applications utilize W/O/W emulsions, whereas the applicability of O/W/O emulsions is still limited, mainly due to solubility issues. W/O/W emulsions have attracted a great deal of interest for various applications, including foods,[2] pharmaceuticals,[3] and cosmetics.[4] For instance, they have been utilized as controlled-release drug-delivery systems (DDS),[5] as templates for preparing microcapsules with enhanced stability and controlled release of functional food components,[6,1] and in the formulation of reduced-calorie food emulsions [7].

Food-grade W/O/W emulsions are usually prepared by two-step emulsification using conventional mechanical emulsification devices (e.g., rotor-stator homogenizers and high-pressure homogenizers). They are mostly polydisperse, and structurally heterogeneous. W/O/W emulsions with high monodispersity can be prepared by membrane emulsification[8,9] or microchannel emulsification[10,11] as the second-step emulsification. In W/O/W emulsions, oil droplets containing inner aqueous droplets as dispersed phase are further dispersed in an outer aqueous phase. Compared to single emulsions, W/O/W emulsions are capable of encapsulating hydrophilic components with higher entrapment yields and stability against degradation [1]. These advantages make them useful as dispersion systems for encapsulating food-grade hydrophilic components.

Stabilizing double emulsions is a major challenge for the food, cosmetic, and pharmaceutical industries. In general, several major factors (e.g., Ostwald ripening, coalescence, flocculation, and creaming) are responsible for destabilizing emulsions. Moreover, the stability of W/O/W emulsions is critically influenced by the osmotic pressure balance between the inner and the outer aqueous phase,[12] the volume ratio balance between the oil and the outer aqueous phase, and the selection of hydrophilic and hydrophobic emulsifiers [13,14].

L-ascorbic acid (vitamin C), an important water-soluble vitamin, is the most widely used vitamin supplement in the world.[15] It plays an important role in the biosynthesis of collagen, carnitine, and neurotransmitters.[16] Plants and most animals synthesize L-ascorbic acid (L-AA) for their own requirements, but primates and humans are unable to synthesize L-AA due to lack of the enzyme gulonolactone oxidase [17]. L-AA is a labile molecule, so it can be lost from foods during cooking, processing, and preservation [15]. Cooking loss of L-AA depends upon many factors (e.g., heating at

high temperature, surface area exposed to water, oxygen, pH, and the presence of transition metals) [18].

Synthetic L-AA is available in a wide variety of supplements in the forms of tablets, capsules, chewable tablets, crystalline powder, effervescent tablets, and liquids.

L-ascorbic and dehydroascorbic acid are the major dietary forms of vitamin C. All forms of L-AA are soluble in water, except for ascorbyl palmitate, which is used in commercial antioxidant preparations due to its greater lipid solubility [19]. L-AA and its fatty acid esters are used as food additives, antioxidants, browning inhibitors, reducing agents, flavor stabilizers, dough modifiers, and color stabilizers [20,21].

Encapsulating L-AA in emulsion systems is highly recommended due to its hydrophilic nature and rapid degradation in bulk aqueous systems. Both single- and double-emulsion systems are used to encapsulate L-AA. Several research groups have encapsulated L-AA at low concentrations (up to 5%) in aqueous droplets using the W/O/W and O/W/O techniques [22-26]. Nevertheless, in order to formulate food-based products such as high energy drinks, high concentrations of active components are required.

The primary objective of this study was to prepare stable W/O/W emulsions containing a high concentration of L-AA in the inner aqueous phase. The study investigated the effects of type of sugar in the outer aqueous phase and the addition of gelatin in the inner aqueous phase on the preparation and stability of W/O/W emulsions and the retention kinetics of L-AA in W/O/W emulsions. The W/O/W emulsions prepared were also characterized by microscopic analysis, and the results were employed to evaluate physical stability.

5.2 Materials and Methods

Materials

L-AA (> 99.6% purity), refined soybean oil, magnesium sulfate ($MgSO_4$), gelatin, glucose, fructose, sucrose, and methanol were purchased from Wako Pure Chemical Industries (Osaka, Japan). Xanthan gum was purchased from Tokyo Chemical Industry (Tokyo, Japan). These reagents were of analytical grade. Tetraglycerin monolaurate condensed ricinoleic acid ester (TGCR, CR-310) was from Sakamoto Yakuhin Kogyo (Osaka, Japan). Decaglycerol monolaurate (DGM, Sunsoft A-12E) was from Taiyo Kagaku (Yokkaichi, Japan).

Preparation of W/O/W emulsions

W/O/W emulsions were prepared by two-step emulsification using a Polytron (rotor-stator) homogenizer (PT-3000 Kinematica-AG, Littau, Switzerland) (Fig. 5.1). In W/O/W emulsions, the osmotic pressure generated by the presence of electrolytes (e.g., NaCl or MgSO$_4$) in the inner water phase can cause swelling and ultimately bursting of the inner aqueous droplets, with negative impact on W/O/W emulsion stability. In order to avoid these effects, the concentration of electrolytes must be high enough to counteract the Laplace pressure but sufficiently low to avoid osmotic effects [13]. Osmotic pressure (Π) can be calculated by the Morse equation:

$$\Pi = iMRT \qquad\qquad (5.1)$$

Morse equation is a modified form of the van't Hoff equation,[27] where i is the van't Hoff factor, with a value of 2 for MgSO$_4$; M is the molecular concentration of MgSO$_4$, L-AA, and various sugars; R is a constant with a value of 8.31KPa m^3 K^{-1}mol^{-1}; and T is the thermodynamic temperature (K). The osmotic pressure of both the inner and outer aqueous phase was adjusted to 0.17MPa at 25°C (298K).

Firstly W/O emulsions were prepared using an inner aqueous phase containing L-AA (10 to 30% w/v), MgSO$_4$ (1% w/w), and gelatin (0 to 1% w/v), and an oil phase containing a hydrophobic emulsifier (TGCR, 5% w/w). Milli-Q water with a resistivity of 18 MΩ cm was used as the medium for all the aqueous phases. The volume fraction of the inner aqueous phase (ϕ_w) was fixed to 30%. Thirty mL of the inner aqueous phase was added to 70 mL of the oil phase at room temperature (about 25°C), followed by first-step emulsification at 7 000 rpm for 5 min with the Polytron homogenizer.

Next, W/O/W emulsions were obtained by dispersing the W/O emulsion in an outer aqueous phase containing a hydrophilic emulsifier (DGM, 1% w/w), MgSO$_4$ (1% w/w), and a sugar (glucose, fructose, or sucrose, 10 to 30% w/w). The volume fraction ($\phi_{w/o}$) of the W/O emulsion was fixed at 30%. The W/O emulsion phase was added to the outer aqueous phase at a total volume of 100 mL at room temperature , followed by second-step emulsification at 5 000 rpm for 5 min with the Polytron homogenizer. During emulsification, 10 mL of an aqueous solution containing xanthan gum (1% w/v) was added to stabilize the W/O droplets that formed.

Determination of average droplet diameter

Microscopic observations were made with an optical microscope (DM IRM, Leica Microsystems, Wetzlar, Germany) to analyze the W/O and W/O/W emulsions prepared. Samples of W/O/W

emulsions were diluted 10 times in the outer aqueous phase, prior to analysis. In order to determine the average droplet diameter (d_{av}), the diameters of 250 droplets in the micrographs captured were manually measured using image analysis software (WinRoof ver. 5.6, Mitani Co., Fukui, Japan). The coefficient of variation (CV) was used as an indicator of the droplet size distribution of the emulsions prepared:

$$CV = \left(\frac{\sigma}{d_{av}}\right) \times 100 \qquad (5.2)$$

where σ is the standard deviation of the droplet diameter (μm).
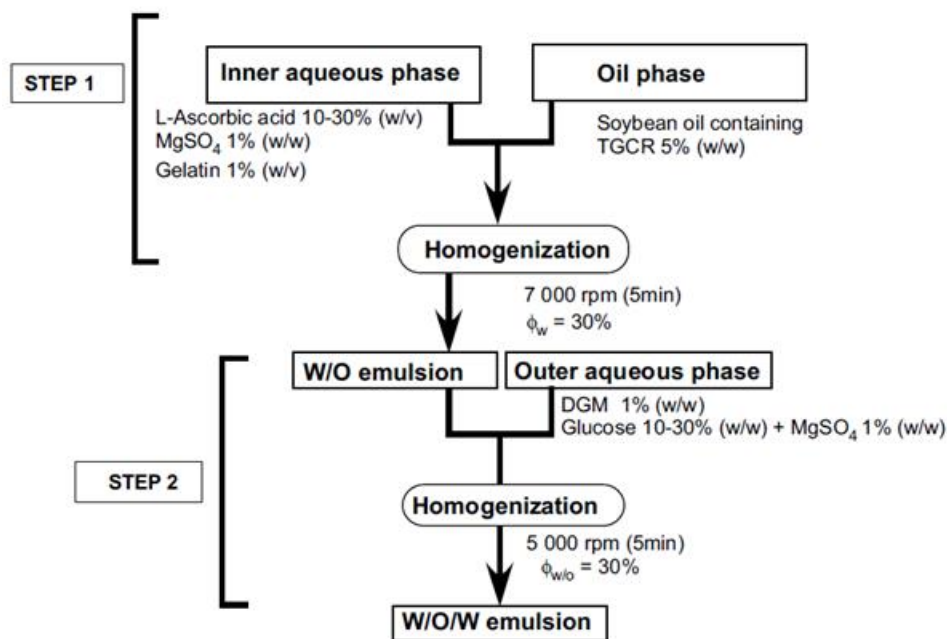
Figure 5.1: Schematic diagram for preparing W/O/W emulsions containing high concentrations of L-AA. ϕ_w denotes the volume fraction of the inner aqueous phase in the W/O emulsion, and $\phi_{w/o}$ denotes the volume fraction of the W/O emulsion phase in the W/O/W emulsion.

Measurement of fluid properties

The viscosity and density of each phase and the interfacial tension between two contacting phases were measured at 25°C. Viscosity was measured with a vibroviscometer (SV-10, A&D, Tokyo, Japan). Density was measured using a density meter (DA-130 N, Kyoto Electronics Manufacturing, Kyoto, Japan). Interfacial tension was measured with a Fully Automatic Interfacial Tensiometer (PD-W, Kyowa Interface Sciences, Saitama, Japan) by the pendant drop method. Table 5.1 lists the major fluid properties of the three-phase systems used to prepare the W/O/W emulsions.

Stability of W/O/W emulsions

The W/O/W emulsions prepared were observed in order to evaluate consistency, color, homogeneity, and eventually phase separation during 35 d of storage under refrigeration at 4°C. All samples (10-g aliquots) were centrifuged at 3,000 rpm for 30 min using a laboratory centrifuge (KN-70, Kubota, Tokyo). After centrifugation, samples were inspected for eventual phase separation. Testing was replicated at time intervals previously determined.

Retention kinetics of L-AA in W/O/W emulsions

L-AA encapsulated in the W/O/W emulsions was determined by the spectrophotometric method reported by Zeng *et al.*,[28] which was originally used to measure L-AA solubilized in aqueous solution. All spectral measurements of methanolic extracts of W/O/W emulsions were carried out with a UV/VIS/NIR spectrophotometer (V-570, Jasco, Hachioji, Japan). Next, 1 mL of W/O/W emulsion was extracted with 10 mL of methanol, followed by ultrasonication for 20 min. The methanolic extract was then centrifuged (KN-70, Kubota) at 2 000 rpm for 15 min. A 1 mL aliquot of the supernatant was diluted to 20 mL with methanol, and the diluted solution was then injected into a quartz cell with a 10-mm pass length. The absorbance of L-AA in this solution was measured at 247 nm using an appropriate blank. A representative standard curve of absorbance versus concentration gave linear least-squares regression with a coefficient of determination (r^2) of 0.9996. All experiments were repeated in triplicate and mean values were calculated. The retention ratio, defined as:

$$R = \left(\frac{c_{AA}}{c_{AA,0}}\right) \times 100 \qquad (5.3)$$

Where C_{AA} is the measured L-AA concentration at a given storage time and $C_{AA,0}$ is the initial L-AA concentration.

Statistical analysis

Analysis of variance (ANOVA) tests were used to analyze the characterization data at a confidence level of 95% ($p < 0.05$). A least-significant difference (LSD) test was used to compare the effect of adding gelatin on the average oil droplet diameter of the W/O/W emulsions and the effect of storage time on the droplet diameter of the W/O and W/O/W emulsions. LSD was calculated by the method described by Steel *et al.*[29]

5.3 Results and Discussion

Effects of the compositions of aqueous phases on the preparation of W/O/W emulsions

Osmotic pressure plays a very important role in the stability of W/O/W emulsions, and Laplace pressure works against the stability of W/O emulsions.[30] The addition of a small quantity of electrolyte to the disperse phase has a stabilizing effect on W/O emulsions, by counteracting the Laplace pressure effect. Kanouni *et al.*[12] found that stabilization of W/O/W emulsions required a balance between the osmotic pressures of the outer and the inner aqueous phase. Considering these results, the outcomes of adding various sugars in the outer aqueous phase and adding gelatin in the inner aqueous phase were investigated.

Effects of adding sugars in the outer aqueous phase

A well-balanced composition of aqueous phases is needed in order to prepare stable W/O/W emulsions. Fig. 5.2 indicates the variation in the average W/O droplet diameters ($d_{av,w/o/w}$) of freshly prepared W/O/W emulsions in the presence and the absence of a sugar (fructose, sucrose, or glucose) containing L-AA (10 % w/v) in the inner aqueous droplets. The W/O emulsions prepared by first-step homogenization had an average aqueous droplet diameter ($d_{av,w/o}$) of 2.5 μm and a $CV_{w/o}$ of 20%. The W/O droplets of the resulting W/O/W emulsions had a $d_{av,w/o/w}$ of 12 to 20 μm and a $CV_{w/o/w}$ of 20 to 25%. Adding sugar caused a 20 to 30% reduction in the $d_{av,w/o/w}$ value. These CV values for the W/O/W emulsions containing fructose or sucrose were somewhat greater than the values for those containing glucose and no sugar. Freshly prepared W/O/W emulsions containing no sugar or glucose did not undergo creaming for 2 d but those containing sucrose and fructose underwent rapid creaming soon after preparation (Fig. 5.3a). This creaming may have occurred due to considerable flocculation of the W/O droplets, which causes much faster creaming of aggregated droplets (flocs). The micrographs in Fig. 5.3b depict aggregation of W/O droplets in the outer aqueous phase containing fructose or sucrose. Stokes' law gives a good description of the terminal creaming rate of isolated emulsion droplets and flocs, provided that there is little movement of the liquid within the droplets [31]. This condition is fulfilled when the viscosity of the droplets (the dispersed phase) is significantly greater than that of the continuous phase, or when the droplets are surrounded by an emulsifier membrane that resists deformation [31]. The terminal creaming rate of an individual droplet is defined as:

$$v_{dr} = \frac{g d_{dr}^2 \Delta \rho}{18 \eta_c} \qquad (5.3)$$

and that of a floc is defined as:

$$v_{\text{floc}} = \frac{-g d_{\text{floc}}^2 \Delta\rho}{18\eta_c} \qquad (5.3)$$

where g is gravitational acceleration, d_{dr} is droplet diameter, d_{floc} is floc diameter, $\Delta\rho$ is the density difference between the droplet or floc and the continuous phase, and η_c is the viscosity of the continuous phase. The formation of flocs caused by droplet aggregation greatly increases the creaming rate of emulsions.

Adding glucose leads to increased molecular movement, interfacial film formation, and the setting up of physical barriers with components due to the non-Newtonian behavior of emulsions[32,33]. Creaming and oiling-off are the results of a variety of physicochemical mechanisms that occur within W/O/W emulsions, including gravitational separation, flocculation, and coalescence. Schmidts et al.[34] reported that it was difficult to obtain physically stable W/O/W emulsions using hydrophilic sucrose esters in the continuous aqueous phase. Added fructose or sucrose in the continuous aqueous phase can interact with the hydrophobic emulsifier at the oil-water phase and weaken the repulsive interaction between the adjacent interfacial films that prevents rapid creaming.

(a)
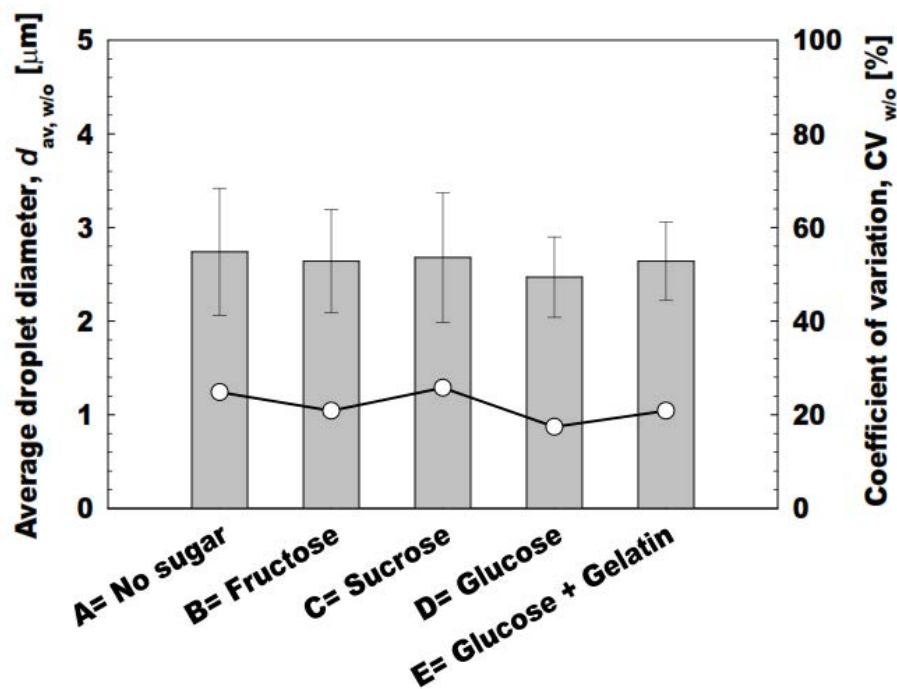
(b)
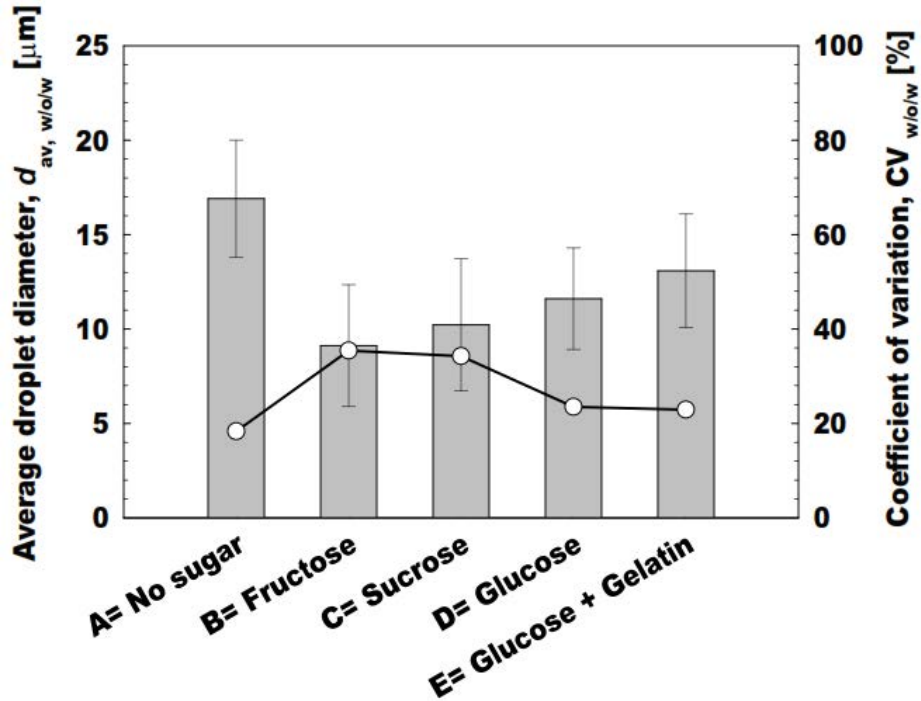
Figure 5.2: Effects of sugars on the average droplet diameters and coefficients of variation of the W/O and W/O/W emulsions prepared. (a) The average aqueous droplet diameter ($d_{av,w/o}$) and coefficient of variation ($CV_{w/o}$) of the W/O emulsions prepared. (b) The average oil droplet diameter ($d_{av,w/o/w}$) and $CV_{w/o/w}$ of the W/O/W emulsions prepared. Gray bars indicate the $d_{av,w/o}$ and $d_{av,w/o/w}$ of the W/O/W emulsions, and ($\circ$) indicates CV of emulsions.

(a)
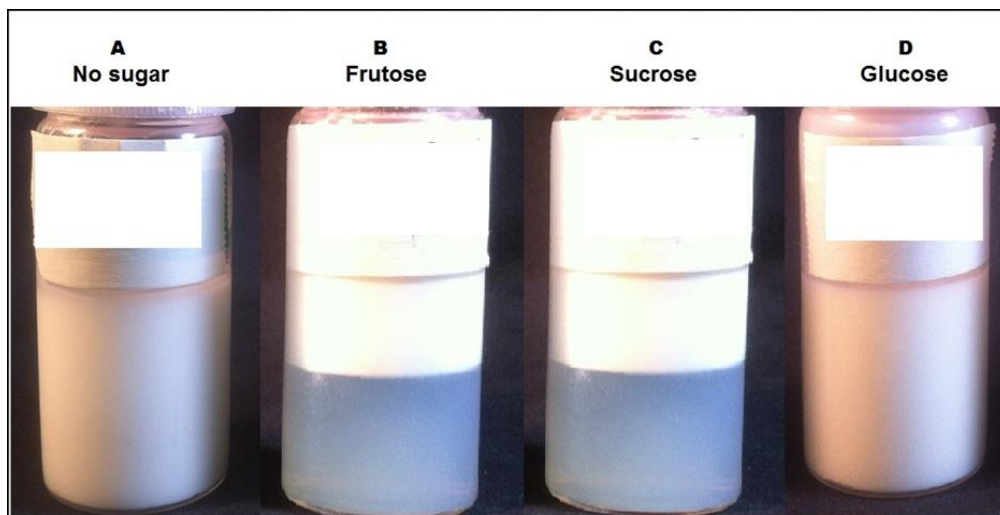
(b)
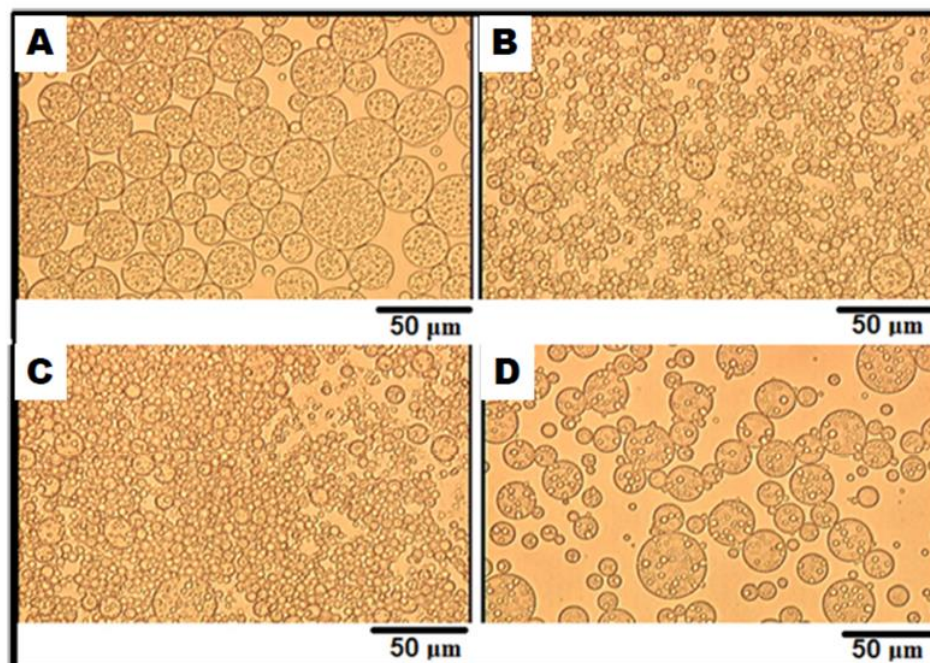
Figure 5.3: Photographs and optical micrographs of the W/O/W emulsions prepared in the presence and absence of a sugar in the continuous aqueous phase. (a) Photographs. (b) Symbols: A, no sugar, B with fructose, C with sucrose, and D with glucose.

Effects of adding gelatin to the inner aqueous phase

The effects of adding gelatin to the inner aqueous phase on the droplet size and droplet size distribution of the W/O/W emulsions prepared is depicted in Fig. 5.2. Adding gelatin did not significantly affect ($p > 0.05$) the $d_{av,w/o}$ of the W/O emulsions (Fig. 5.2a). The $d_{av,w/o/w}$ of the W/O/W emulsion in the presence of gelatin was greater than that of the W/O/W emulsion in the absence of gelatin, whereas the CV of the W/O/W emulsions was unaffected by added gelatin. The W/O/W emulsion containing gelatin had smooth mobility with a good organoleptic profile in terms of color, flowability, and stability in comparison to that without gelatin. The W/O/W emulsion prepared in the presence of gelatin had better stability against creaming than that in the absence of gelatin.

Adding gelatin to the aqueous phase of the W/O emulsions resulted in a narrow size distribution with improved stability and a good organoleptic profile [35]. Evison *et al.*[36] have reported that adding 1% (w/w) gelatin in the inner aqueous phase of W/O/W emulsions led to a substantial increase in the yield of an encapsulated compound and better stability against the coalescence of both inner aqueous and oil droplets. Biopolymers such as gelatin that are incorporated in W/O/W emulsions also act as

chelating agents that can reduce the release rate of encapsulated compounds [2, 37]. In our study, this gelation and chelating action of gelatin were assumed to be responsible for increasing the stability of the W/O/W emulsions against sedimentation and creaming. The additional gelatin can also act as a buffer to balance the effect of a high concentration of L-AA in W/O/W emulsions.

Effects of L-AA concentration on the preparation of W/O/W emulsions

Fig. 5.4 presents the average diameters ($d_{av,w/o}$ and $d_{av,w/o/w}$) and CV of the oil droplets and inner aqueous droplets in prepared W/O/W emulsions containing various concentrations of L-AA. The concentration of L-AA in the inner aqueous phase was varied from 10 to 30% (w/v), and gelatin was added to all the inner aqueous phase solutions at a concentration of 1% (w/v). The concentration of glucose in the outer aqueous phase was also varied from 10 to 30% (w/v), depending on the preceding L-AA concentration. The W/O emulsions, with a ϕ_w of 30%, used in second-step homogenization, had a $d_{av,w/o}$ of 2.3 to 2.8 μm and a CV of 10 to 16%. The $d_{av,w/o}$ value increased slightly with increasing L-AA concentrations, probably due to the increased viscosity of the inner aqueous phase (Table 5.1). The interfacial tension between the inner aqueous phase and the oil phase was independent of the L-AA concentration (Table 5.1). W/O/W emulsions were successfully prepared regardless of the L-AA concentration applied. The $d_{av,w/o/w}$ of the resulting W/O/W emulsions increased gradually from 12 to 18 μm as the concentration of L-AA increased. The increase in $d_{av,w/o/w}$ of the W/O/W emulsions corresponds to an increase in the viscosity of the outer aqueous phase (Table 5.1), as the interfacial tension between the oil phase and the continuous aqueous phase was unaffected by the L-AA concentration. The results shown in Fig. 5.4 indicate the successful preparation of W/O/W emulsions containing a high concentration of L-AA (up to 30% w/v) in the inner aqueous phase, considerably higher than those previously reported.[22,24]

(a)
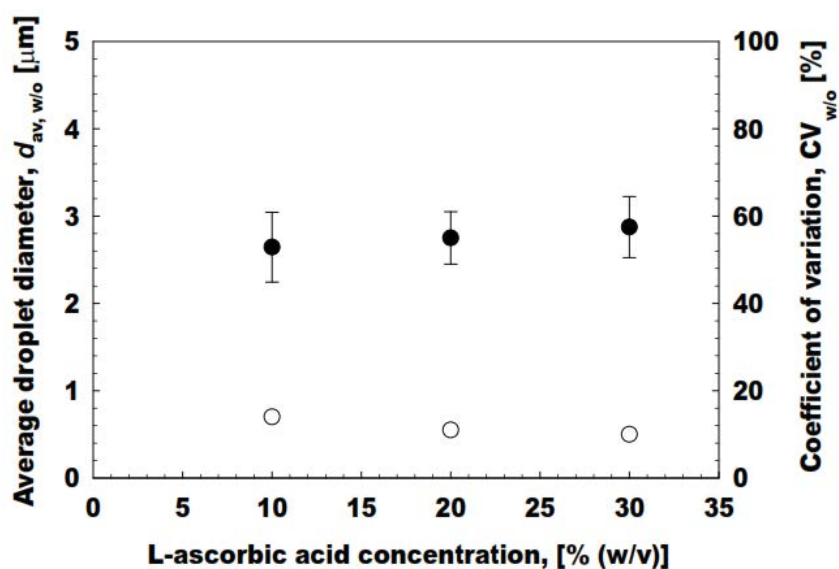
(b)
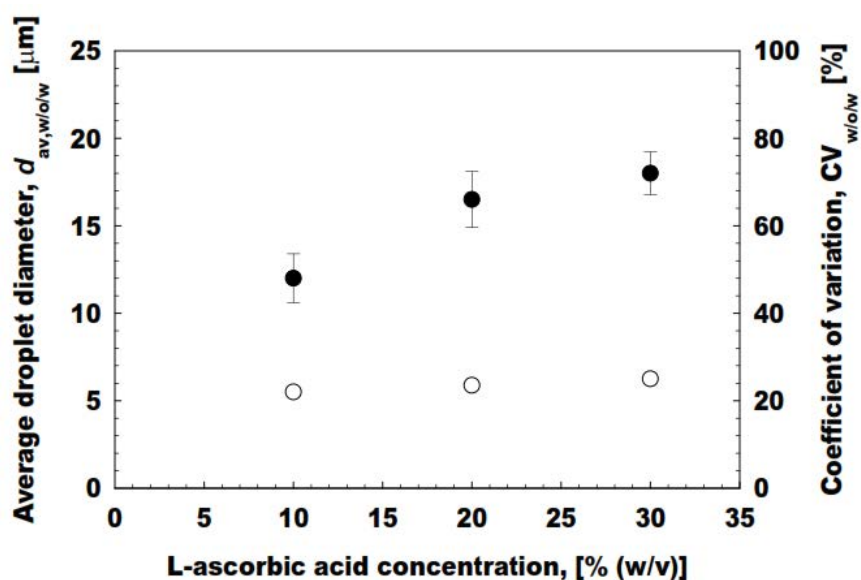
Figure 5.4: Effects of concentration of L-AA on the average droplet diameter and coefficient of variation of the W/O and W/O/W emulsions. (a) $d_{av,w/o}$ and $CV_{w/o}$ of the W/O emulsions. (b) $d_{av,w/o/w}$ and $CV_{w/o/w}$ of W/O/W emulsions. All emulsions contained 1% (w/v) gelatin in the inner aqueous phase. ● $d_{av,w/o}$ and $d_{av,w/o/w}$ of emulsions; and ○ indicates CV of emulsions.

Table 5.1: Fluid properties of three-phase systems containing high concentrations of L-AA, glucose, and gelatin used for preparing W/O/W emulsions.

L-ascorbic acid concentration[a] % (w/v)	Viscosity (mPa s)			Interfacial tension (mN/m)	
	Inner aq. phase[b]	Oil phase[c]	Outer aq. phase[d]	Oil and inner aq. phases	W/O and outer aq. phases
10	2.0 ± 0.01	66.1 ± 0.10	1.9 ± 0.05	6.2 ± 0.4	1.6 ± 0.2
20	2.8 ± 0.02	66.1 ± 0.10	2.7 ± 0.01	6.4 ± 0.2	1.6 ± 0.2
30	3.3 ± 0.01	66.1 ± 0.10	3.1 ± 0.01	6.6 ± 0.4	1.6 ± 0.4

[a]Initial concentration of L-AA in the inner aqueous phase., [b]containing 10-30% (w/v) L-AA with 1% (w/w) $MgSO_4$ and gelatin 1% (w/v)., [c]containing TGCR 5% (w/w) in soybean oil., [d]containing $MgSO_4$ 1% (w/w), glucose 10-30% (w/v), and DGM 1% (w/w).

Stability of W/O/W emulsions containing high concentrations of L-AA

Physical stability of the W/O/W emulsions

The W/O/W emulsion samples were stored at 4°C for 35 d. Immediately after preparation, those containing concentrations of L-AA were whitish in color and showed good flowability. In addition, the W/O/W emulsions did not exhibit any change in physical appearance or homogeneity during the storage period, confirming increased stability. A centrifugation test indicated no phase separation in the W/O/W emulsions containing gelatin in the inner aqueous phase even after 30 d of storage. In contrast, those without gelatin resulted in phase separation after 36 h of storage as indicated by the centrifugation test. This suggests a beneficial effect of gelatin on the stabilization of W/O/W emulsions containing 30% (w/v) L-AA.

Fig. 5.5 indicates the time changes in the $d_{av,w/o}$ and $CV_{w/o}$ of the inner aqueous droplets and in the $d_{av,w/o/w}$ and $CV_{W/O/W}$ of the oil droplets in the prepared W/O/W emulsions containing concentrations of L-AA. There was a non-significant difference ($p > 0.05$) in $d_{av,w/o}$ during storage, which can be attributed to the migration of L-AA from the inner aqueous droplets to the continuous aqueous phase. Their $CV_{w/o}$ increased from 19 to 25% (Fig. 5.5a). For the resulting W/O/W emulsions, there was a non-significant difference in $d_{av,w/o/w}$ and almost no change in $CV_{w/o/w}$ between days 1 and 35 (Fig. 5.5b). The variation in $d_{av,w/o/w}$ can be ascribed to coalescence of the W/O droplets and/or an osmotic pressure effect that becomes important after a certain duration.

(a)
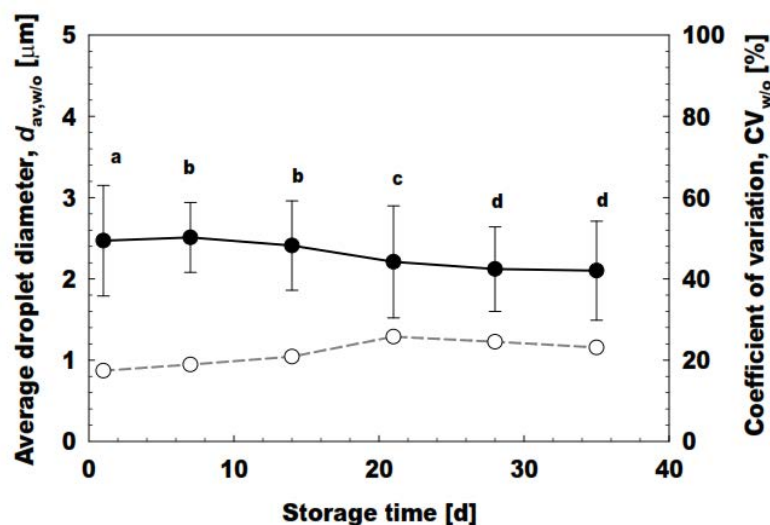
(b)
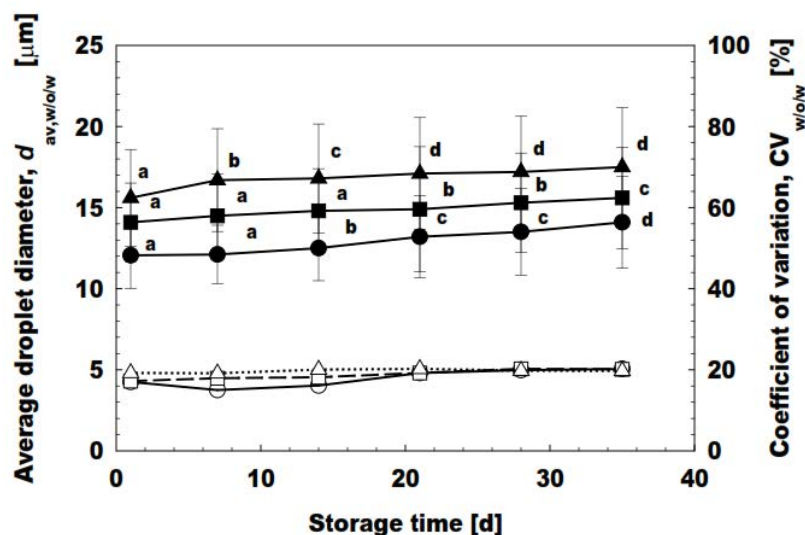
Figure 5.5: Time changes in average droplet diameter and coefficient of variation of the W/O and W/O/W emulsions. (a) $d_{av,w/o}$ and $CV_{w/o}$ of the W/O emulsions containing 10 to 30% (w/v) L-ascorbic acid in the inner aqueous phase. (b) The $d_{av,w/o/w}$ and $CV_{w/o/w}$ of the W/O/W emulsions. ● their $d_{av,W/O}$, and ○ their $CV_{W/O}$. $C_{AA,0}$ initial concentration of L-AA in the inner aqueous phase. Time change of $d_{av,w/o/w}$ of W/O/W emulsions with $C_{AA,0}$ of 10% is indicated by ●, 20 % by ■, and 30 % by ▲, whereas, their CV is represented by ○ for 10 %, □ for 20, % and, by △ for 30%. Similar letters (a, b, c, d) indicate that the W/O and W/O/W emulsions had shown non-significant differences in d_{av} at the 95% confidence level ($p = 0.05$).

Retention kinetics of L-AA in the W/O/W emulsions

Fig. 5.6 shows L-AA retention in the W/O/W emulsions during storage under refrigeration at 4°C. The freshly prepared W/O/W emulsions had an initial retention of L-AA (10-30% w/v) of higher than 90%. The L-AA levels in the W/O/W emulsions decreased gradually with time and exhibited about 40% retention at day 28. The L-AA in a bulk Milli-Q water stored at 4°C had retention of < 5% at day 28, as

130

rapid ionization in aqueous solutions results in a rapid loss of L-AA. Lee *et al.*[25] encapsulated 5% (w/w) L-AA in W/O/W emulsions using electrolytes, and concluded that W/O/W emulsions were revealed as efficient tool for improving L-AA stability. The prepared W/O/W emulsions had L-AA concentrations (*R*) of 3.88 g/100 mL, 8.02 g/100 mL and 12.06 g/100 mL at 10, 20, and 30% (w/v), after 30 d of storage time. They were subjected to centrifugation at 15 000 rpm for 20 min to determine the amounts of phase separation. There was hardly any phase separation in them during 30 d of storage, and the degradation of L-AA took place with a rate constant of 0.03 (0.75%) (Table 5.2). The formation of an oil-emulsifier interface across the inner aqueous phase containing L-AA may protect the linkage of L-AA to the outer aqueous phase. Similarly, L-AA also appear to act as a pro-antioxidant protecting against L-AA leakage and enhancing the stability W/O/W emulsions.
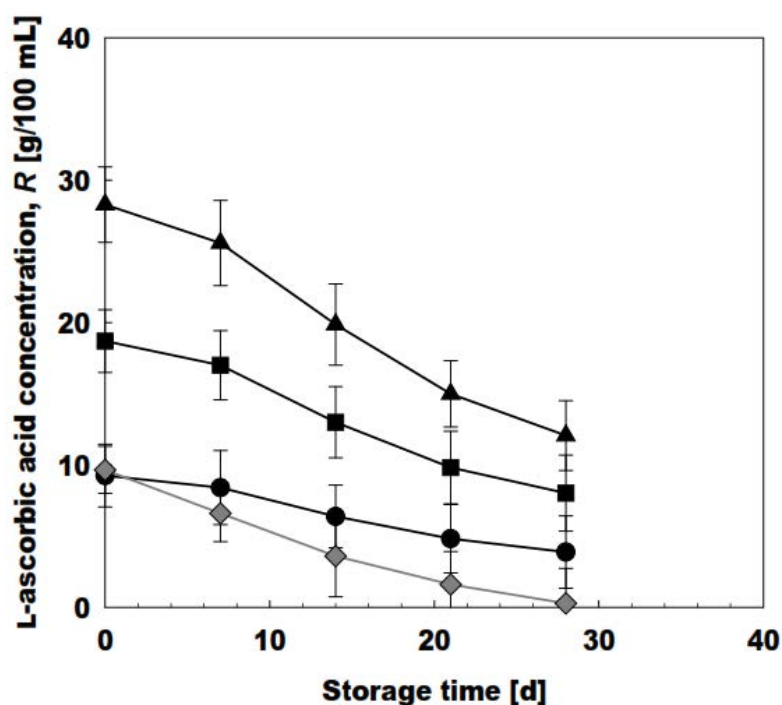
Figure 5.6: Time change of L-AA retention (*R*) in the W/O/W prepared emulsions and in bulk Milli-Q water. The samples containing L-AA were stored at 4ºC. $C_{AA,0}$ initial concentration of L-AA in the inner aqueous phase. $C_{AA,0}$ of 10 % is indicated by ●, 20 % by ■, and, 30 % by ▲. (♦) $C_{AA,0}$ in Milli-Q water.

Table 5.2: Rate constants and half-life of L-AA retention in various W/O/W emulsions

L-ascorbic acid concentration % (w/v)	Rate equation[a]	Coefficient of determination (r^2)	Rate constant k (d^{-1})	Half-life (d) $t_{1/2} = 0.693/k$
10	$\ln C_{AA}/C_{AA,0} = -0.0298t$	0.96	0.03	23.7
20	$\ln C_{AA}/C_{AA,0} = -0.0292t$	0.97	0.029	23.8
30	$\ln C_{AA}/C_{AA,0} = -0.0292t$	0.97	0.029	23.9

[a]C_{AA}, L-AA concentration at a given time; $C_{AA,0}$, initial L-AA concentration.

The retention kinetics of L-AA in the W/O/W emulsions stored at 4°C was also evaluated as:

$$\ln \frac{C_{AA}}{C_{AA,0}} = -kt \qquad (5.4)$$

where k is the rate constant and t is the storage time. The rate constant of first-order kinetics was calculated by applying the regression function of Microsoft Excel 2010, obtaining best-fit results. The lines fitted by the retention kinetics equation are presented in Fig. 5.7. The calculated r^2 values for all the W/O/W emulsions were > 0.95, indicating that the fitting application of the first-order kinetics is plausible. The observed half-life for W/O/W emulsions containing high concentrations of L-AA at 4°C was about 24 d (Table 5.2). Our results indicate that the L-AA retention kinetics depended on the composition of the external aqueous phase used in the W/O/W emulsion preparation. Diffusion of L-AA across the interface can play an important role in retention kinetics. The diffusive transfer of L-AA through the oil phase is a very complex process and its origin remains controversial. Based on first-order kinetics, it can be stated that L-AA transfer involves various steps, and that interfacial and aqueous phase composition have an influence on the release rate. This behavior have been reported by different research groups for O/W emulsions containing L-AA in the outer aqueous phase [38]. The factors affecting the retention kinetics of L-AA in different systems include the concentration of L-AA (active ingredient), the pH and viscosity of the liquid phase and the preparation process. The release pattern of L-AA follows zero-order kinetics in W/O and O/W/O emulsions [23]. In most food matrices (juices and fruits) and in water, L-AA oxidation and decomposition follow first-order kinetic [39].
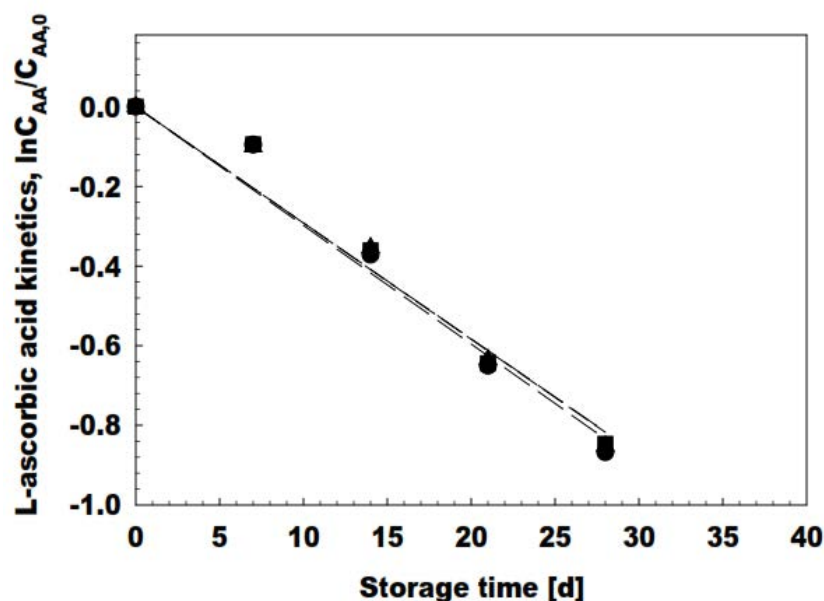
Figure 5.7: Retention kinetics of L-AA in the W/O/W emulsions stored at 4 °C. Rate constants, coefficients of determination, and half-life of the fitted lines are presented in Table 5.2. $C_{AA,0}$ initial concentration of L-AA in the inner aqueous phase. $C_{AA,0}$ of 10% is indicated by ●, 20% by ■ and, 3% by ▲.

References

[1] Vasiljević D, Parojčić VJ, Primorac M, and Vuleta MG, *J. Serb. Chem. Soc.,* **74**, 801–816 (2009)

[2] Dickinson E, *Food Biophys.,* **6**, 1-11 (2011).

[3] Nakashima T, Shimizu M, and Kukizaki M, *Adv. Drug Deliv. Rev.,* **45**, 47-56 (2000).

[4] Hanson JA, Chang CB, Graves SM, Li Z, Mason TG, and Deming TJ, *Nature,* **455**, 85-88 (2008).

[5] Okochi H and Nakano M, *Adv. Drug Deliv. Rev.,* **45**, 5-25 (2000).

[6] Vladisavljević GT and Weiss J, "Microencapsulation Systems with Emphasis on Successful Applications in Foods," ed. Heldman DR, Marcel Dekker, New York, pp. 1-8 (2007).

[7] De Cindio B and Cacace D, *Int. J. Food Sci. Technol.,* **30**, 505-514 (1995).

[8] Vladisavljević GT and Schubert J, *J. Membr. Sci.,* **225**, 15-23 (2003).

[9] Vladisavljević GT, Kobayashi I, Nakajima M, Williams RA, Shimizu M, and Nakashima T, *J. Membr. Sci.,* **302**, 243-253 (2007).

[10] Kobayashi I, Mukataka S, and Nakajima M, *Ind. Eng. Chem. Res.,* **44**, 5852-5856 (2005).

[11] Sugiura S, Nakajima M, Yamamoto K, Iwamoto S, Oda T, Satake M, and Seki M, *J. Colloid. Interface Sci.,* **270**, 221-228 (2004).

[12] Kanouni M, Rosano HL, and Naouli N, *Adv. Colloid. Interface Sci.,* **99**, 229-254 (2002).

[13] Jiao J, Rhodes DG, and Burgess DJ, *J. Colloid. Interface Sci.,* **250**, 444-450 (2002).

[14] Mezzenga R, Folmer BM, and Hughes E, *Langmuir,* **20**, 3574-3582 (2004).

[15] Naidu KA, *Nutr. J.,* **2**, 7-15 (2003).

[16] Olson RE, "Water Soluble Vitamins," ed. Munson PL, Mueller RA, and Bresse GR, Chapman and Hall, New York, pp. 30-66 (1999).

[17] Frei B and Traber MG, *Redox Rep.,* **6**, 5-9 (2001).

[18] Yuan JP and Chen F, *J. Agric. Food Chem.,* **46**, 5078-5082 (1998).

[19] Špiclin P, Gašperlin M, and Kmetec V, *Int. J. Pharm.,* **222**, 271-279 (2001).

[20] Lee DI, Huh YJ, Hwang KW, Choi Y, Choi JS, Han SY, Gyoung YS, and Joo SS, *J. Pharm. Pharmacol.,* **63**, 1327-1335 (2011).

[21] Hfaiedh N, Murat JC, and Elfeki A, *J. Trace Elem. Med. Biol*., **26**, 273-278 (2012).

[22] Akhtar N, Ahmad M, Khan H, Akram J, Gulfishan MA, and Uzair M, *Bull. Chem. Soc. Ethiopia,* **24**, 1-10 (2010).

[23] Farahmand S, Tajerzadeh H, and Farboud ES, *Pharm. Develop. Technol.,* **11**, 255-261 (2006).

[24] Gallarate M, Carlotti M, Trotta M, and Bovo S, *Int. J. Pharm.,* **188**, 233-241 (1999).

[25] Lee J, Kim J, Han S, Chang I, Kang H, Lee O, Oh S, and Suh K, *J. Cosmet. Sci.,* **55**, 1-12 (2004).

[26] Xia Q and Yao Y, *Mat. Sci. Forum,* **649**, 783-787 (2011).

[27] Strathmann H, "Membrane Processes," ed. Rautenbach VR, Albrecht R, and Cottrell ÜV, John Wiely & Sons, Chicester , (1990).

[28] Zeng W, Martinuzzi F, and MacGregor A, *J. Pharm. Biomed. Anal.,* **36**, 1107-1111 (2005).

[29] Steel R, Torrie J, and Dickey D, "Principles and Procedures of Statistics: A Biometrical Approach," McGraw Hill Book Co, New York(1997).

[30] Davis SS, Round HP, and Purewal TS, *J. Colloid. Interface Sci.,* **80**, 508-511 (1981).

[31] McClements D, "Food Emulsions: Principles, Practice and Techniques," CRC Press, Boca Raton, pp. 20-50 (2004).

[32] Washington C, Athersuch A, and Kynoch DJ, *Int. J. Pharm.,* **64**, 217-222 (1990).

[33] Palazolo G, Sobral P, and Wagner J, *International Conference on Food Innovation*, Valencia, Spain, pp. 1-4 (2010).

[34] Schmidts T, Dobler D, Nissing C, and Runkel F, *J. Colloid. Interface Sci.,* **338**, 184-192 (2009).

[35] Iwamoto S, Nakagawa K, Sugiura S, and Nakajima M, *AAPS PharmSciTech,* **3**, 72-76 (2002).

[36] Evison J, Dickinson E, Owusu RK, Apenten, and Williams A, "Food Macromolecules and Colloids," ed. Dickinson E and Lorient D, Royal Society of Chemistry, Cambridge, pp. 235- 239 (1995).

[37] Su J, Flanagan J, Hemar Y, and Singh H, *Food Hydrocoll.*, **20**, 261-268 (2006)

[38] Watanabe Y, Suzuki T, Nakanishi H, Sakuragochi A, and Adachi S, *J. Am. Oil Chem. Soc.*, **89**, 269-274 (2012).

[38] Rahmawati S and Bundjali B, *Prosiding Seminar Kimia Bersama UKM-ITB,* **8**, 535-546 (2009).

Chapter 6

The preparation characteristics and stability evaluation of oil-in-water emulsions loaded with ergocalciferol by microchannel emulsification*

_____

6.1 Introduction

Vitamin D plays a vital role in maintaining and developing healthy skeletal system, since it maintains calcium level in the body. Deficiency of vitamin D results in increased risk of diabetes, hypertension, cancer and autoimmune diseases [1-4]. Broad spectrum deficiencies of vitamin D includes rickets in children, osteomalacia in adults and osteoporosis in women, all of these lead to softening and weakening of bones [5-7]. Nutritional and cultural factors leading to vitamin D deficiency include insufficient fortified food consumption, sunblock usage, limited body exposure to sun and fear for excessive intake of vitamin D [7,8]. Vitamin D is synthesized in the skin and involves the phytochemical conversion of provitamin D by the action of ultra-violet (UV-B) rays. This process takes place if the UV-B rays fall between 290-315 nm of spectrum. These rays are only emitted in the regions that lie below 35º latitude and includes Northern Africa and Los Angeles [9,10].

The terminology and classification related to vitamin D is confusing and can be classified into 5 different forms and metabolites, among these vitamin D_2 (ergocalciferol) and D_3 (cholecalciferol) are important (Fig. 6.1) [11,12]. Vitamin D_2 is naturally present in some plants and is produced commercially by irradiation of yeast. Vitamin D_2 is substantially used for fortification and supplementation in food and pharmaceutical industries [12]. Several researchers pointed out rapid metabolism of vitamin D_2 in comparison to vitamin D_3, but if taken daily the action become bioequivalent [13, 14]. Both forms of vitamin D are converted to 25-hydoxyvitamin [25-(OH)D] in the liver. The quantification of 25-(OH)D in blood gives the quantitation of vitamin D status. A cutoff value of 30 ng/mL is sometimes used for optimal vitamin status [12]. Ergocalciferol was produced in 1920s through UV-B exposure of foods, and resulted in the formation of first medicinal preparation called Viosterol [15]. Ergocalciferol has limited natural sources and the most significant source is wild mushrooms [16]. Ergocalciferol is prone to oxidation and is also isomerized to isotachysterol in the presence of sunlight and mostly under acidic conditions [16,17]. Erogcalciferol is mostly supplemented and fortified in fat based products due to its fat soluble nature.
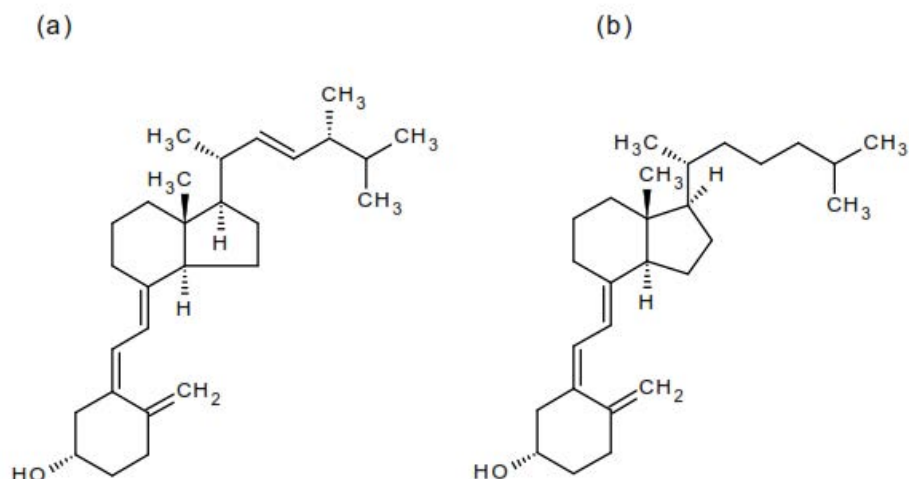
Figure 6.1: Chemical structures of important forms of vitamin D. (a) ergocalciferol and (b) cholecalciferol.

Emulsification technologies play an important role in the production of encapsulated foods, pharmaceuticals, cosmetics and chemicals [18,19]. The produced emulsions are either simple (O/W and W/O) emulsions, multiple emulsions (W/O/W and O/W/O), nanoparticles or core shell micelles [19]. These different emulsification processes are either carried by conventional devices (colloidal mills, high pressure homogenizers and rotor stator) and modern devices like microfluidic devices (Lab-on-a-chip), membrane emulsification and microchannel emulsification (MCE) [19,20]. The conventional devices produce emulsions with broader size distribution and polydispersity in system, these in term reduces the stability and functionality of system. Microfabricated emulsification devices have potential to produce monodisperse emulsions with droplet size variation less than 10% with membrane emulsification and around 5% with other microfluidic devices [20].

MCE is a progressive method that produce monodisperse droplets by spontaneous transformation of oil-water interface specifically driven by interfacial tension on a micron scale [21] and comprehensively reviewed by Vladisavljevic, *et al.* [20] and Vladisavljevic' *et al.* [22]. Similarly, this emulsification technique allow integration of hundreds of thousands of droplet forming units on a single silicon or stainless steel chips [23,24]. MCE produces O/W, W/O and W/O/W emulsions with diameter ranged from 1 μm to 550 μm [22]. Based on microfabrication design, the MCE devices can either be categorized into grooved MC arrays consisting of uniform microgrooves and a slit-like terrace and straight-through MC arrays having uniform, symmetric or asymmetric microholes together with

microslots [22]. Grooved type MCs are further classified into either dead end type and cross flow grooved MCs. Cross flow grooved MC modules are more suited for higher droplet production with low flow rates around 1.5 mL h^{-1} [25]. Grooved MC arrays are designed to study the droplet generation process, droplet characterization and to observe the interface movement around microchannels [26]. On the other hand, straight-through MC arrays are designed to increase the throughput capacity of emulsions and to work with low viscosity fluids. The straight-through MC arrays has ability to increase the production capacity up to 2000 L m^{-2} h^{-1} with monodisperse droplets having CV less than 2% [22].

MCE has been used to produce monodisperse microdispersions (e.g., solid lipid microspheres [27], gel microbeads [28], and giant vesicles [29]). MC emulsification has promising potential for producing uniformly sized oil droplets containing such functional lipids as β-carotene [30], γ-oryzanol [31], L-ascorbic acid [32], ascorbic acid derivatives [33] and oleuropein [34]. Different food grade materials (e.g., refined vegetable oils, a medium-chain triglyceride oil, hydrophilic and hydrophilic emulsifiers, proteins, and hydrocolloids) were utilized to produce monodisperse O/W, W/O, W/O/W emulsions and microparticles by MCE.

In this study, ergocalciferol loaded O/W emulsions were prepared with MCE. The basic characterization and optimization of these emulsions were performed on grooved type MCs. The effect of dispersed and continuous phase flux together with stability and release profile were carried out with straight-though MCE. Moreover, in this research, the effect of different vegetable oils and emulsifiers on production characteristics of O/W emulsions were evaluated. The results of this research will help to prepare and optimized new aqueous based functional foods.

6.2 Material and methods

Chemicals

Ergocalciferol (396.66 g/mol), soybean and olive oil were purchased from Wako Pure Chemical Ind. (Osaka, Japan). Medium chain triacylglycerol (MCT, sunsoft MCT-8) with a fatty acid residue composition of 75% caprylic acid and 25% capric acid was procured from Taiyo Kagaku Co. Ltd. (Mie, Japan). Safflower oil was purchased from MP biomedicals (lllkirch, France). All of above mentioned chemicals were used as dispersed phase. Polyoxyethylene (20) sorbitan monolaurate (Tween 20) was purchased from Wako Pure Chemical Ind. (Osaka, Japan), β-lactoglobulin (β-lg) from bovine milk (>90% purity) was purchased from Sigma Aldrich (St. Louis, Mo., USA) and decaglycerol

monolaurate (Sunsoft A-12, HLB: 12) was supplied by Taiyo Kagaku Co., Ltd. (Yokkaichi, Japan). Tween 20, β-lg and Sunsoft A-12 were used as emulsifiers in this study. These emulsifiers were separately dissolved in Milli-Q water with a resistivity of 18MΩ cm and served as continuous phase. All other chemicals used in this study were of analytical grade and used as received.

Preparation of solutions

The continuous phase was prepared by dissolving either 1-2% (w/w) Tween 20, 1% (w/w) Sunsoft A-12 or 1% (w/w) β-lg in Milli-Q water. The dispersed phase was prepared by dissolving 0.2-1.0% (w/w) ergocalciferol in preheated MCT, soybean, olive or safflower oil at 85 ± 3°C for 20 min and afterwards cooling at room temperature for 2 h before storage at 4 ± 1°C. During storage, we expected that dissolved ergocalciferol molecules would form nuclei that would grow and eventually form crystals large enough to sediment. Before initiating experiments, the samples were therefore shaken slightly to resuspend any ergocalciferol crystals if present. Although no crystallization was observed during storage at 4 ± 1°C.

Silicon chips

The experiments have been carried out by using silicon 24 × 24 mm and 25 × 28 mm MC plates (model WMS 11-1 and CMS 6-2, manufactured by EP. Tech Co., Ltd., Hitachi, Japan). WMS 11-1 contain 27,400 active MCs arranged within a 10 × 10 mm square region in the center of MC plate, and CMS 6-2 contain 540 parallel channels on 10 consecutive MC arrays. WMS 11-1 and CMS 6-2 were etched to 100 μm in all directions. The MC plates were microfabricated by photolithography and deep reactive ion etching.

Fig. 6.2a is a schematic representation of a silicon CMS 6-2 plate, each MC array contain 54 parallel channels with a depth of 5 μm, with a width of 18 μm and a length of 140 μm and a terrace depth of 5 μm and a length of 60 μm. Each continuous-phase channel outside the terrace outlet has a depth of 100 μm. Fig. 6.2b shows the schematic representation of WMS 11-1. Each MC consisted of a cylindrical 10 μm diameter straight microhole with a depth of 200 μm and a 10 x 80 μm microslot with a depth of 40 μm. The slot aspect ratio of 8 was above the threshold value of 3 for monodisperse emulsion droplets. The distance between the two adjacent MCs in the vertical was 105 μm and the distance between the centers of MCs in the adjacent rows was 70 μm.

The MC plates were subjected for plasma oxidation in plasma reactor (PR41, Yamato Science Co. Ltd., Tokyo, Japan) to develop a silicon dioxide layer on the surface of MC plates. The silicon

dioxide layer maintain the hydrophilicity of silicon during MCE. After each experiment the MC plates were cleaned in three steps. In the first step the MC plates were washed with neutral detergent together with Milli-Q water in an ultrasonic bath (VS-100 III, As One Co., Osaka, Japan) for 20 min, afterwards treatment with 50% Milli-Q water and 50% ethanol in an ultrasonic bath, lastly cleaned in an ultrasonic bath with Milli-Q water and stored in 50 mL of Milli-Q water prior to reuse for MC emulsification.

(a)
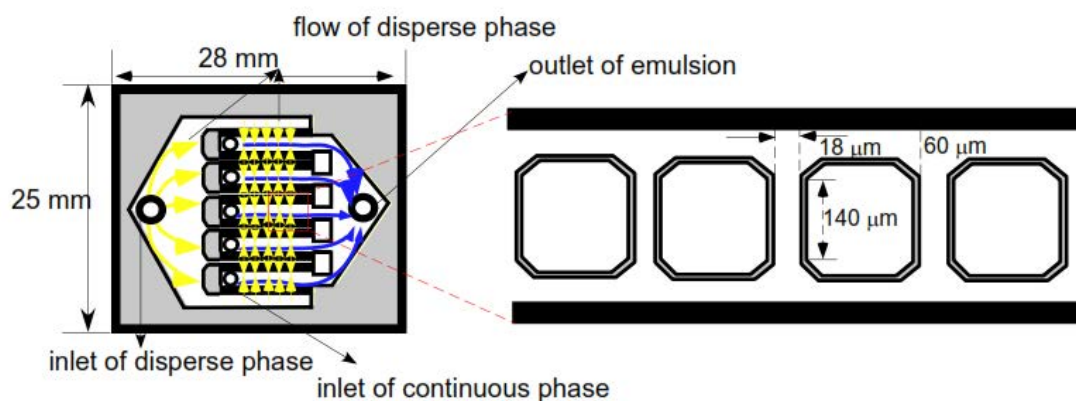
(b)
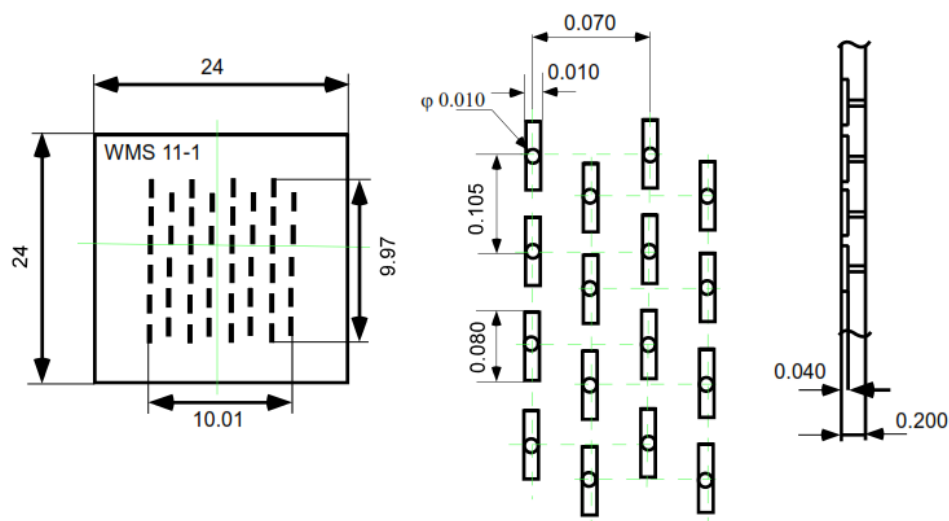
Figure 6.2: (a) Schematic drawings of the MC array chip (CMS 6-2) and part of an MC array together with different dimensions. (b) Schematic drawings of the MC array (WMS 11-1) and MCs dimensions. All dimensions were presented in micrometers.

Experimental procedure for MCE

At the initiation of experiment, MC plates were degassed in continuous phase (emulsifier in Milli-Q water) by ultrasonic bath for 20 min. For grooved type MCE, the setup consists of MC module, a 10

mL liquid chamber that contain the disperse phase and a syringe pump (Model 11, Harvard Apparatus Inc., Holliston, USA) that feeds the continuous phase with a 50 mL glass syringe (Fig. 6.3a). The emulsification process was carried out for approximately 3 h and monitored through inverted metallographic microscope (MD-300EF; Nikon Co., Tokyo, Japan) equipped with an objective lens of 2.5x to 20x and a CCD camera (KP-C550; Hitachi, Tokyo, Japan). The whole process was recorded with a video recorder (RDR-HX67; Sony Co., Tokyo, Japan).

Droplet-generation experiments were performed with the grooved type MCE setup depicted in Fig. 6.3b. The module was initially filled with continuous phase before mounting the CMS 6-2 plate. The pressurized dispersed phase was introduced into the module. The pressure applied to the dispersed phase (ΔP_d) was gradually increased. ΔP_d can be given by

$$\Delta P_d = \rho_d \Delta h_d g \qquad (6.1)$$

where ρ_d is the dispersed-phase density, Δh_d is the difference in the hydraulic heads between the chamber containing the dispersed phase and the channels of the module, and g is the acceleration due to gravity. To generate droplets, the dispersed phase was forced through the MCs onto the terrace and into the continuous phase channel.

(a)
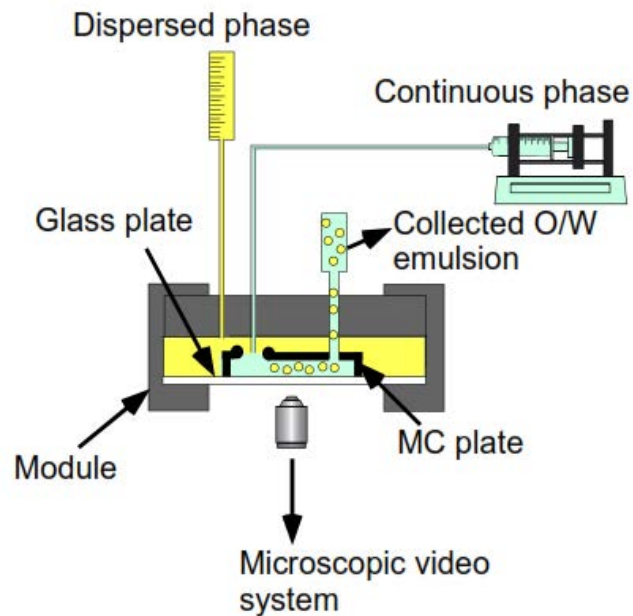
(b)
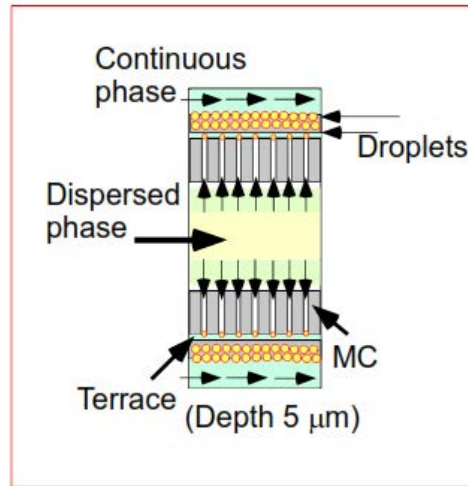
Figure 6.3: (a) Schematic drawing of the experiment setup for grooved type MCE. (b) Schematic drawing of droplet generation via part of an MC array having 5 μm depth.

For straight-through MCE, the setup consists of MC module (comprising of 6 steel parts, two glass plate of different dimensions and rubber seals) and a syringe pumps (Model 11, Harvard Apparatus Inc., Holliston, USA) that feeds the continuous phase and dispersed phase (Fig. 6.4a). The emulsification process was carried out for approximately 1 h and monitored through FASTCAM-1024 PCI high speed video system at 250 to 500 fps (Photron, Tokyo, Japan) attached to an inverted metallographic microscope (MD-300EF; Nikon Co., Tokyo, Japan).

The droplet generation process was observed by injecting the disperse phase through a syringe pump (Model 11, Harvard Apparatus Inc., Holliston, USA) at the flow rate ranging from 0.5 to 2.0 mL h^{-1} (flux (J_d); 5 to 20 L m^{-2} h^{-1}). The generated droplets were removed by supplying continuous phase ranging from 100 to 500 mL h^{-1} through the gap between the MC plate and the gap. The shear stress (τ) at the WMS 11-1 plate is given by

$$\tau = \frac{3Q_c n_c}{2h^2 W} \qquad (6.2)$$

Where h =1 mm is the gap height and W = 12 mm is the gap width, Q_c is the continuous phase flow rate (m^3 sec^{-1}) and η_c is the continuous phase viscosity (Pa. sec). τ had a negligible value of 0.011 to 0.021 Pa at 250 to 500 mL h^{-1}.

(a)
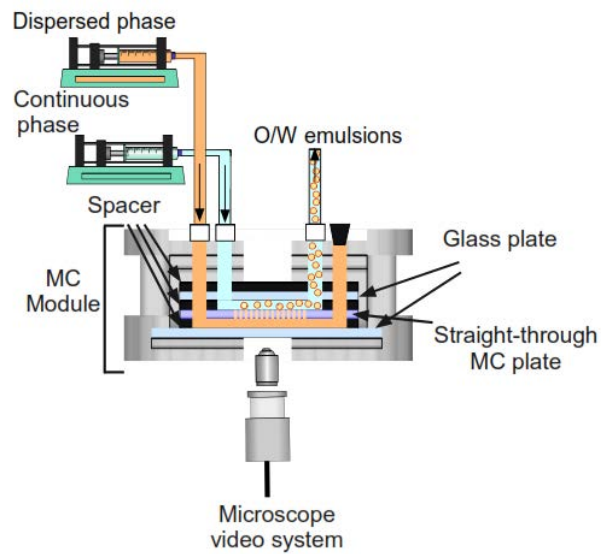
(b)
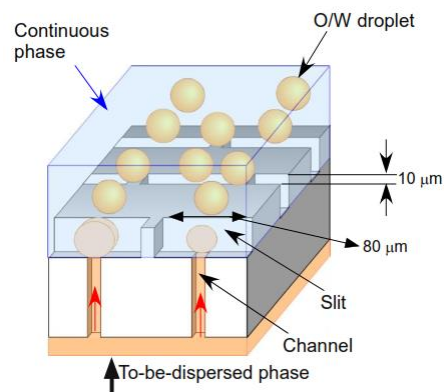
Figure 6.4: (a) Schematic representation of an asymmetric straight through MCE setup. (b) Droplet generation representation through straight through MC arrays.

Measurement and analysis

The size and size distribution of the resultant O/W emulsion droplets from grooved MC emulsification were determined as follows. The average droplet diameter (d_{av}) was defined by:

$$d_{av} = \sum_{i=1}^{n} d_i / n \qquad (6.3)$$

where d_i is the diameter of the ith droplet measured using WinRoof software (Mitani Co., Ltd., Fukui, Japan) and n is the number of the droplets measured (n= 250). The droplet dispersity (droplet size distribution) was expressed as CV, and is defined as: where σ is the standard deviation and d_{av} is the average droplet diameter (μm).

$$CV = \frac{\sigma}{d_{av}} \times 100 \qquad (6.4)$$

The particle size distribution of O/W emulsions from straight-through MC emulsification was measured by using light scattering instrument, that work on the principle of Polorization Intensity Differential Scattering Technology (Beckman Coulter LS 13 320, Miami, USA). This instrument have ability to measure the size ranging from 0.04 to 2000 μm with a resolution of 116 particle size channels. The mean droplet size was expressed as Sauter mean diameter ($d_{3,2}$) i.e. the diameter of a droplet having the same area per unit volume as that of the total collection of droplets in emulsions. The width of droplet size distribution was expressed as relative span factor (RSF) and is defined as:

$$RSF = \frac{D_{v0.9} - D_{v0.1}}{D_{v0.5}} \qquad (6.5)$$

Where $D_{v0.9}$ and $D_{v0.1}$ are the representative diameters where 90%, 10% and 50% of the total volume of the liquid is made up of droplets with diameters smaller than or equal to the stated value. While $D_{v0.5}$ is the representative diameter where 50% of the total volume of the liquid is made up of droplets with diameters larger than the stated value and 50% is made up of droplets with diameters smaller than the stated value.

Measurement of fluid properties

The densities of dispersed and continuous phases were measured using a density meter (DA-130 N, Kyoto Electronics Manufacturing Co., Ltd., Kyoto, Japan) at 25 ± 2°C. The viscosities of dispersed and continuous phases were measured with a vibro viscometer (SV-10, A&D Co., Ltd., Tokyo, Japan) at 25 ± 2°C by taking either 10 or 35 mL of samples in a measuring vessel followed by immersion of sensor plates in that vessel. Viscosity was measured by detecting the electric current needed to resonate the sensor plates. The absolute viscosity (η) was calculated by

$$Absolute\ viscosity = \frac{n_{mea}}{\rho} \qquad (6.6)$$

where η_{mea} is the measured fluid viscosity and ρ is the fluid density. The static interfacial tension between the oil and the aqueous phases was measured with a fully automatic interfacial tensiometer (PD-W, Kyowa Interface Sciences Co., Ltd., Saitama, Japan) using a pendant drop method. The key physical properties of dispersed and continuous phase were presented in Table 6.1.

Physical and chemical stability of O/W emulsions

The O/W emulsions loaded with ergocalciferol formulated through straight-through MCE were observed with light scattering Bechman Coulter Counter to evaluate $d_{3,2}$, RSF, consistency, homogeneity, and coalescence during 15d of refrigerated storage at 4 °C.

The amount of ergocalciferol encapsulated in the O/W emulsions was determined spectrophotometrically. All spectral measurements of ethanolic extracts of O/W emulsions were carried out using a UV/VIS/NIR spectrophotometer (UV-1700, Shimadzu Co., Japan). First, 1 mL of the emulsion was extracted with 9 mL of ethanol, followed by ultrasonication for 20 min. The ethanolic extracts were then centrifuged (Avanti HP-25, Beckman Coulter, Miami, USA) at 20,000 g for 15 min. A 1 mL aliquot of the subnatants was diluted ten times with ethanol and then injected into a quartz cell with a 10 mm pass length. The absorbance of ergocalciferol in emulsion extract was measured at 310 nm using an appropriate blank. A representative standard curve of absorbance versus concentration gave linear least-squares regression with a coefficient of determination (r^2) of 0.9996. All experiments were repeated in triplicate and mean values were calculated. The Beer's law was obeyed in the concentration range of 0.1-0.5 mg mL^{-1} and the sensitivity of measurement has relative standard deviation of 0.85% (n=15). The Molar absorptivity (ε) for ergocalciferol during this study was 2.52 mM^{-1} cm^{-1}. The encapsulation efficiency of ergocalciferol in samples were calculated with the equation:

$$EE_{vita_{D_2}} = \frac{weight\ of\ free\ vitamin_{D_2}}{Weight\ of\ encapsulated\ vitamin_{D_2}} \times 100 \qquad (6.7)$$

6.3 Results and discussion

Basic characterization through grooved type MCE

Effect of disperse phase composition on O/W emulsions

Fig. 6.5a illustrates the effect of different oils on d_{av} and CV of O/W emulsions. The grooved MC emulsification was carried out by dissolving 0.5% (w/w) ergocalciferol in MCT, soybean, olive and safflower oil, while the continuous phase constitutes 1% (w/w) Tween 20 in Milli-Q water. The dispersed phase was introduced into MC module by head on pressure (ΔP_d) difference. A gradual increase in ΔP_d caused the dispersed phase to enter the terrace in front of the MC inlets. When ΔP_d reached the break-through pressure ($\Delta P_{d,bt}$ = 3.0 kPa), the dispersed phase started to pass through the

MCs, leading to the periodic generation of aqueous droplets. The MC emulsification was performed at slightly above break-through pressure of 3.2 kPa. The continuous phase flow rate was fixed at 2 mL h^{-1} throughout the experiment. Successful emulsification was conducted with different oil types. The d_{av} of resultant emulsions ranged between 28.3 to 30.0 μm with CV between 3.6 to 6.1%. More narrow size droplet distribution was seen in emulsions prepared with slightly higher viscous oils like olive oil and soybean oil in comparison to MCT (Fig. 6.5b). The O/W emulsions prepared with MCT have CV more than 6%. The d_{av} of emulsions prepared with 5 μm channel depth was higher than 18-20 μm previously reported by Fujiu et al. [35] that only contain Milli-Q water droplets in water saturated decane. The results of this study was well in line with Souilem, et al. [34]. They encapsulated oleuropein in W/O/W emulsions and produced W/O droplets with d_{av} around 27 μm with channel depth of 5 μm and width of about 18 μm. More narrow size droplet formation take place in MCE, if the inflow of the continuous phase is sufficiently fast compared to the outflow of the liquid that is forming the droplet (dispersed phase) [36]. The viscosity ratio ($\zeta = \eta_d/\eta_c$) is one the key factor determining the monodispersity of emulsions [36]. The viscosity ratio of all vegetable oils in this study were sufficiently high (Table 6.1) leading to successful monodisperse emulsion droplets encapsulating ergocalciferol. The slightly higher d_{av} of olive oil emulsions might corresponds toward higher viscosity (62.1 mPa s) in comparison to other oils, this high viscosity have no impact on monodispersity and droplet size distribution, more narrow size distribution was observed in olive oil emulsions in comparison to MCT, soybean and safflower oil. The possible interpretation of above mention reason is the higher viscosity of olive oil that leads toward more monodisperse droplets.

(a)
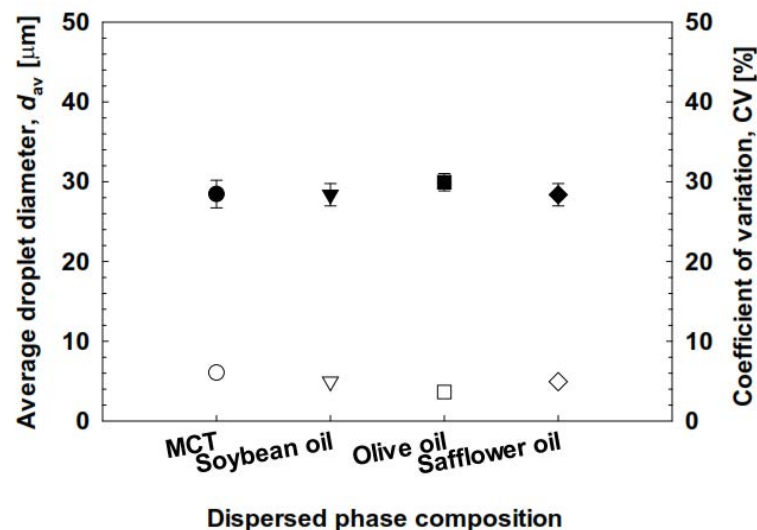
(b)
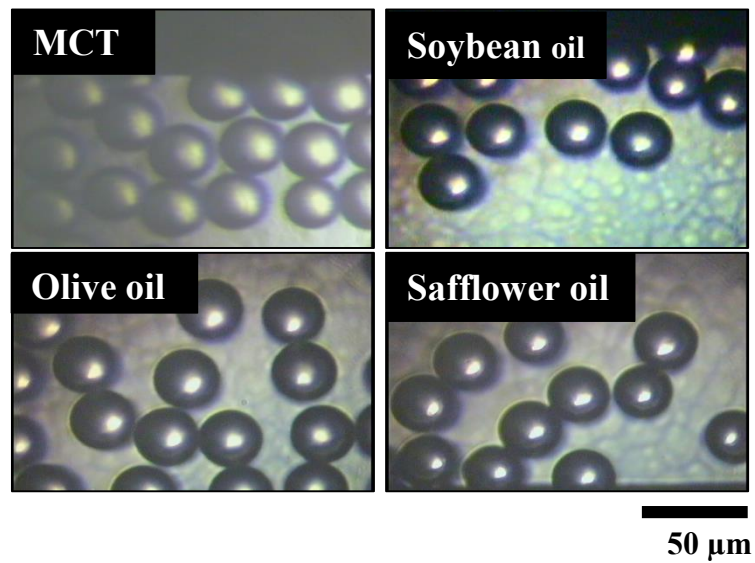
Figure 6.5: (a) Effect of different dispersed phase composition on d_{av} and CV of O/W emulsions. (●) denote MCT, (▼) soybean oil, (■) olive oil and (◆) denote safflower oil, while there open keys denote CV. (b) Typical generation behaviors of O/W emulsions droplets encapsulating ergocalciferol by using different dispersed phase oils.

Effect of different emulsifiers on O/W emulsions loaded with ergocalciferol

The effect of the emulsifiers on oil droplet formation from the grooved MC was also investigated. Food grade emulsifiers (Tween 20, Sunsoft A-12 and β-lg) with a noticeable ability to prepare O/W emulsions were used at a concentration of 1% (w/w) in the Milli-Q water. These aqueous emulsifier solutions were used as continuous phase. All of these emulsifier solutions exhibited successful emulsification with smooth detachment of droplets at the interface (Fig. 6.6a(*i-iii*)). Uniform emulsion droplets were stably generated from the MCs especially in the presence of Tween 20 and Sunsoft A-12. There was neither the formation of bigger droplets nor a continuous out flow of dispersed phase. Fig. 6.6b illustrate the effect of emulsifiers on d_{av} and CV of O/W emulsions. The d_{av} and CV of the resultant emulsion droplets were 28.5 μm and 5.9% for Tween 20 and 28.1 μm and 6.6% for Sunsoft A-12. Although droplet generation and detachment process was quite stable with β-lg with smallest droplet diameter (26.6 μm) but after 5 min few droplets start sticking at the terrace of MC plate (Fig. 6.6b(*iii*)) and grow in size with passage of time, as a result the CV of emulsion droplets increased to 7.2%.

Kobayashi and Nakajima [37] investigated the effect of emulsifiers on droplet generation characteristics by using a straight-through extrusion filter. They pointed Tween 20 and polyglycerol

fatty acid ester as optimum food grade emulsifiers for MCE. Similarly, in another study by Patel and San Martin-Gonzalez [17] demonstrate successful preparation of solid lipid nanoparticles loaded with ergocalciferol stabilized by Tween 20. The results of above section demonstrate that Tween 20 and Sunsoft A-12 as potential emulsifiers for generating ergocalciferol loaded O/W emulsions, either with conventional homogenization techniques (data not shown) or MCE.

(a)
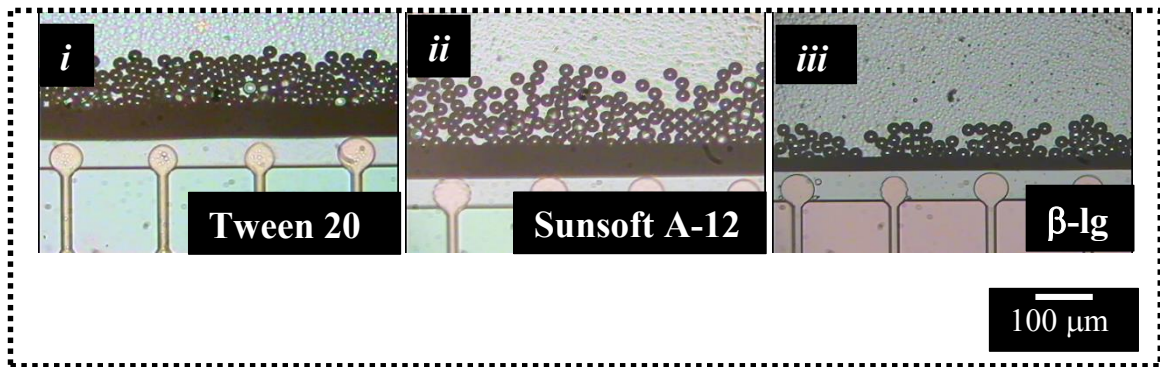
(b)
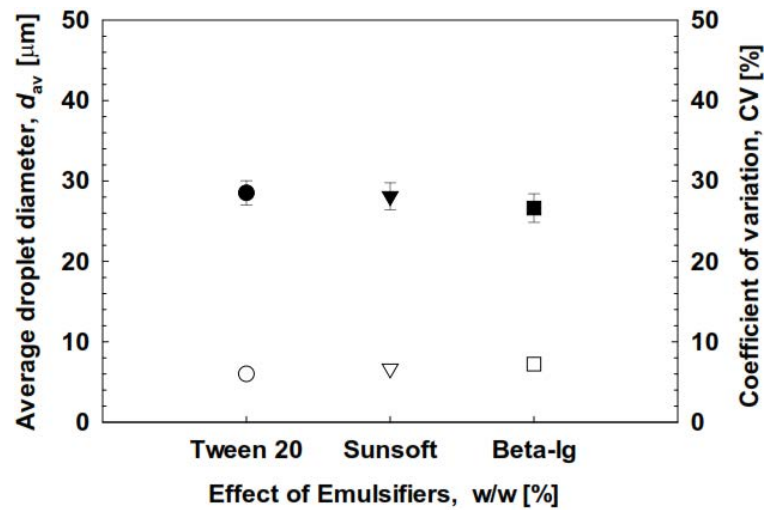
(c)
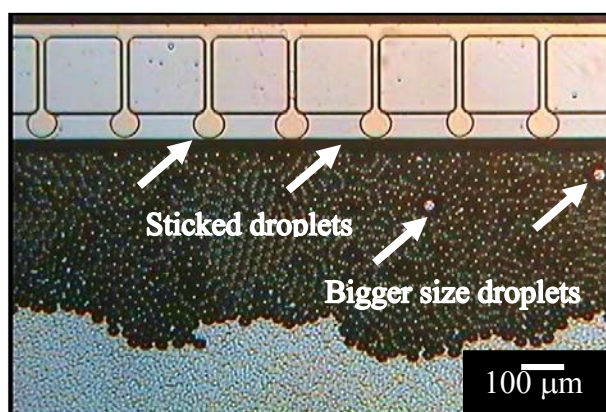
Figure 6.6: Effect of different emulsifiers on droplet generation behavior in grooved type MC emulsification. (a) Droplet generation with (*i*) Tween 20, (*ii*) Sunsoft A-12 and (*ii*) β-lactoglubulin. (b) Effect of different emulsifiers on d_{av} and CV of O/W emulsions, (●) denote Tween 20, (▼) Sunsoft A-12 and (■) β-lactoglubulin. (c) Typical droplet generation characteristics with β-lactoglubulin as emulsifier.

Effect of concentration of ergocalciferol on O/W emulsions

Fig. 6.7 illustrates the effect of concentration of ergocalciferol on d_{av} and CV of O/W emulsions. The concentration of ergocalciferol varied from 0.2% to 1.0% (w/w) in soybean oil. According to US Pharmacopeia, ergocalciferol can sparingly soluble in different oils, and have maximum solubility in organic solvents except hexane. In our study, we noticed maximum solubility of 1% (w/w) ergocalciferol in different oils at 85 ± 2°C with no solubility at room temperature. Successful MCE was conducted with different concentrations of ergocalciferol by keeping dispersed phase pressure at 3.2 kPa and continuous phase flow rate around 2 mL h^{-1}. In this section we also evaluated the effect of Tween 20 and Sunsoft A-12 with different concentrations of ergocalciferol in soybean oil. The d_{av} of O/W emulsions increased linearly with increasing concentration of ergocalciferol when emulsified with 1% (w/w) Tween 20. The resultant droplet diameter ranged between 23.8 to 28.5 μm with CV between 5.9 to 6.2%.

Comparatively similar results were obtained with Sunsoft A-12 (Fig. 6.7). The emulsions stabilized with 1% (w/w) Sunsoft A-12 have d_{av} ranged between 24.5 to 27.5 μm and have CV in between 6.5 to 8.4%. More monodisperse droplet size distribution were seen in emulsions emulsified with Tween 20 in comparison to Sunsoft A-12 (Fig. 6.6). Monodispersity of droplets stabilized with 1% (w/w) Tween 20 were previously reported by Kobayashi *et al.* [38] and Kobayashi *et al.* [39] in MCE.
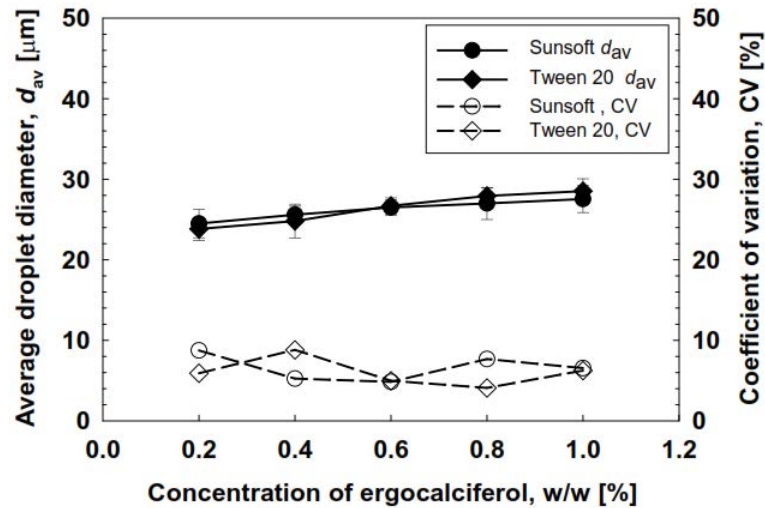
Figure 6.7: Effect of ergocalciferol concentration in soybean oil on d_{av} and CV of O/W emulsions either stabilized by 1% (w/w) Tween 20 or Sunsoft A-12.

Effect of dispersed phase flow rate on O/W emulsions encapsulating erogcalciferol

Dispersed phase flow rate is an important parameter in MCE that correlates with droplet productivity at sable droplet generation rate. Fig. 6.8a depicts the effect of dispersed phase (Q_d) flow rate on the d_{av} and CV of the generated droplets. Q_d constitute 0.5% (w/w) ergocalciferol in soybean oil, while continuous phase (Q_c) includes 1% (w/w) Tween 20 in Milli-Q water.

At the lowest Q_d of 2×10^{-3} mL h^{-1}, the resultant droplets had a d_{av} of 23.5 μm and a CV of 5.4%. They also had a monomodal and very narrow size distribution. When Q_d was increased stepwise, monodisperse emulsions with CV of 4 to 7% were produced at Q_d of 9×10^{-2} mL h^{-1} or less. In this Q_d range, d_{av} of the resultant droplets ranged from 23.7 μm to 29.0 μm. The microscopic observations during MCE confirmed that the resultant droplet size hardly changed between Q_c of 0 mL h^{-1} and 5.0 mL h^{-1}. The generation of droplets even without continuous flow rate depicts the unique spontaneous transformation of interface in MCE. In contrast, at Q_d of > 0.1 mL h^{-1}, the d_{av} and CV of O/W emulsions dramatically increased to > 33.4 μm with CV values more than 10%, moreover the droplet size distribution became wider and lead towards large droplet size area (Fig. 6.8a). The MC plate (CMS 6-2) used in this study enabled the production of O/W emulsions with uniform fine droplets at a critical Q_d of 9×10^{-2} mL h^{-1}, which was slightly higher than a maximum Q_d (5×10^{-3} mL h^{-1}) for the previously reported studies from MC emulsification [40].

After reaching the critical Q_d, some of the dispersed phase that passed through a MCs expanded instead of generating droplets, suggesting that the flow state of the dispersed phase was

affected by the dispersed-phase velocity inside the MC. Sugiura, *et al.* [21] reported that the droplet generation behavior inside MCs are significant to the capillary number of the dispersed phase that flows inside a MCs. The capillary number (Ca), indicates the balance between viscous force and interfacial force, can be determined by:

$$Ca = n_d U_d / \gamma \qquad (6.8)$$

where η_d is the dynamic viscosity (Pa.s) of the dispersed phase, U_d is the dispersed phase velocity (m sec^{-1}) and γ is the interfacial tension between the two phases (N m^{-1}). Ca at the critical Q_d of 9×10^{-2} mL h^{-1} was 0.019. The observed Ca was similar to the pervious findings with grooved type MCE [21, 41]

The influence of Q_d on the droplet generation frequency per MC plate (active area; f) was presented in Fig. 6.8b) can be estimated by:

$$f = \frac{Q_d}{V_{av}} = \frac{6Q_d}{\pi d_{av}^3} \qquad (6.9)$$

Where V_{av} is the average droplet volume. The f increased with increasing Q_d in the range of 0.3 mL h^{-1} or less. The further increase in Q_d lowered the f, uniform fine droplets were generated at a maximum f of 144.8 144.8×10^5 h^{-1} (Fig. 6.8b).

(a)

152
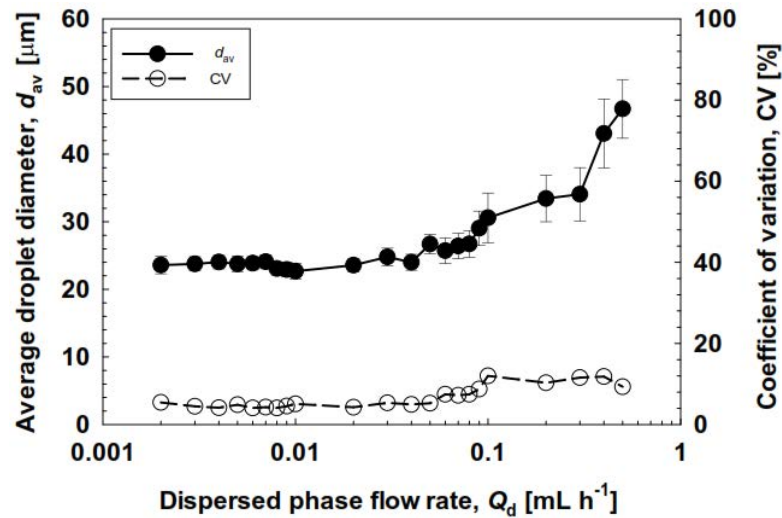
(b)
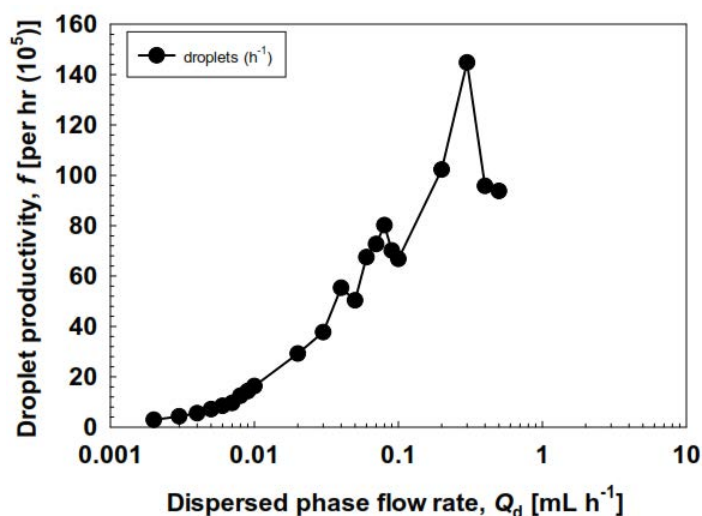
Figure 6.8: (a) Influence of Q_d on d_{av} and CV of the O/W emulsions encapsulating ergocalciferol produced using the CMS 6-2 MC array. (b) Influence of Q_d on the droplet generation frequency per hour.

Stability evaluation of O/W emulsions through straight through MCE

Grooved type MCE provides useful information regarding basic characterization of droplets but the drawback lies in low droplet productivity up to 1.5×10^{-3} l h^{-1} [25]. In comparison straight-through MCE can increase the through-put capacity of droplets and work even at Q_d of 0.27 l h^{-1} with uniform droplet productivity [26]. These asymmetric MC arrays comprises of straight-through microholes can accommodate $>10^4$ MCs per 1 cm^3 [42]. This part of wok focused on the stability and encapsulation efficiency of ergocalciferol loaded O/W emulsions.

Emulsifier concentration on stability of O/W emulsions

The most effective emulsifiers are non-ionic surfactants (Tween 20 etc.) that can be used emulsify O/W or W/O emulsions. In addition, they can stabilize the emulsion against flocculation and coalescence. The effect of Tween 20 concentration in the continuous phase has been investigated over a concentration range between 0.5 and 2.0% (w/w) using 0.5% (w/w) ergocalciferol in soybean oil as a dispersed phase. As shown in Fig.6.9a and b, uniform droplet production were obtained with a span of particle size distribution in the range of 0.204-0.208 up to the concentration range of 0.5 to 1.5% (w/w), although droplet generation was quite stable with 2% (w/w) Tween 20 but the distribution was fairly larger and have span width of about 0.237 with $d_{3,2}$ of 35.7 μm.

The production of uniform droplets even at low emulsifier concentration could be clarified by the presence of surface active agents in soybean oil, like free fatty acid (e.g., linoleic and linolenic

acid). The production of these free fatty acid might increase during mixing of ergocalciferol at 85 °C. The other factor that promote successful droplet generation at low emulsifier concentration is the asymmetric structure of MCs that enhance the droplet formation and increase monodispersity. At higher Tween 20 concentration (2% (w/w)) significant amount of droplets were attached to the plate surface during emulsification and after generation. This attachment process might be due to high interfacial forces that prevails over the tangential drag force generated by cross flow and slightly increased the steric hindrance effect and decrease the monodispersity (Fig. 6.10b) in comparison such steric hindrance effect was not observed with low concentration of Tween 20 (Fig. 6.10a).

(a)
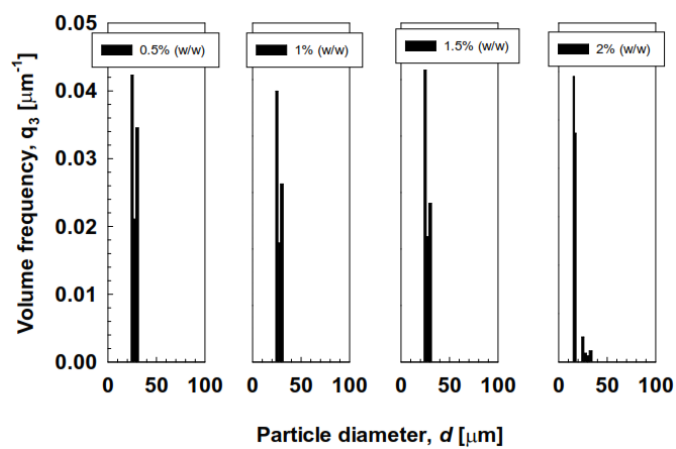
(b)
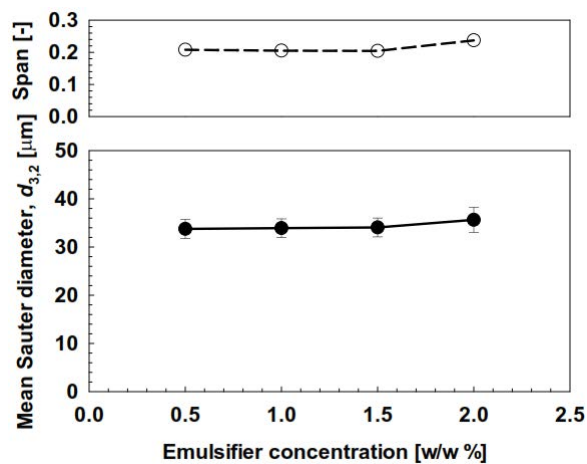
Figure 6.9: (a) Particle size distribution of the generated soybean oil droplets encapsulating ergocalciferol at the constant flux of 5 L m^{-2} h^{-1} for four different Tween 20 concentration (0.5-2.0% (w/w)). (b) Effect of Tween 20 concentration in the aqueous phase on the mean size of ergocalciferol loaded emulsions at J_d = 5 L m^{-2} h^{-1}.
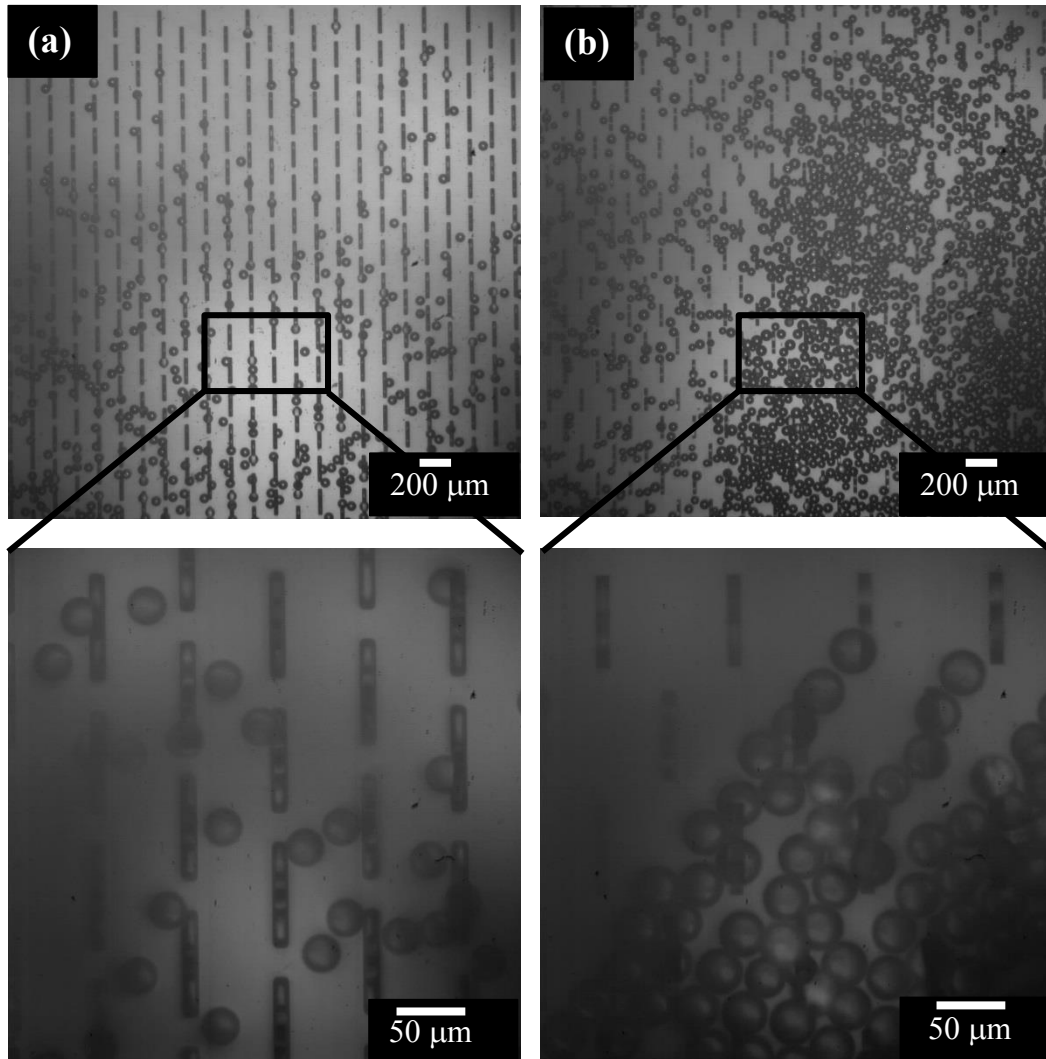
Figure 6.10: (a) Generation of ergocalciferol loaded droplets at low Tween 20 concentration (0.5% (w/w)). The droplets detached smoothly from the plate surface as soon as they formed (higher magnification). (b) Generation of droplets at high Tween 20 concentration (2.0% (w/w)). The droplet remains attached to plate surface for some time, before they detached from the microslots (higher magnification).

Vladisavljevic *et al.* [43] reported the observed effect at low concentration of SDS (0.01-0.1%) in straight-through MCE. This deviation might attributed with the emulsifier nature, since SDS is the strong ionic emulsifier in comparison to non-ionic nature of Tween 20. At 0.5-1.5% (w/w) Tween 20, the mean droplet diameter ($d_{3,2}$) was in between 33.7-34.1 μm (Fig. 6.9b). The mean droplet/channel size ratio lies in between 3.37 to 3.41 and fairly smaller than other membrane emulsification devices [44]. The $d_{3,2}$ value of 33.7-34.1 μm is significantly higher than d_{av} of 24.5 μm reported in straight-through MC emulsification for the system containing 1% (w/w) Tween 20 and argan oil using a symmetric MC plate with 10×50 μm channels [45]. The results of successful emulsification at low

Tween 20 concentration are well in line with the previous study of El-Abbassi *et al.* [45]. They formulated argan oil stabilized O/W emulsions with low concentration of Tween 20 (1-6%).

Effect of dispersed phase flux and storage stability of O/W emulsions

Fig. 6.11a shows the effect of ergocalciferol loaded soybean oil flux on the $d_{3,2}$ and the size distribution. The dispersed phase flux (J_d) is the useful indicator of droplet productivity via MCs as well as other microfluidic devices. J_d is defined as:

$$J_d = \frac{Q_d}{A_{MCA}} \qquad (6.10)$$

Where A_{MCA} is the total active area of the MC arrays (10 × 10 mm). The maximum Q_d used here was 2 mLh^{-1} which corresponds to J_d of 20 L m^{-2} h^{-1} and it was the critical flux in this study, after crossing this flux there was continuous outflow of dispersed phase and leading to unstable droplet production. There was continuous increase in $d_{3,2}$ of produced emulsions with increasing dispersed phase flux (Fig. 6.11a). The $d_{3,2}$ with increasing flux ranged in between 33.9 to 35.4 μm, correspondingly there span width (indicator of droplet dispersity) also increased with increasing dispersed phase flux. The droplet production behavior with increasing flux was presented in Fig. 6.11b. There was smooth detachment of droplets with increasing flux before reaching critical J_d.

The results of J_d on ergocalciferol loaded O/W emulsions deviates with previous findings of Vladisavljevic*, et al.* [26]. They reported size stable zone of soybean oil loaded emulsions in between 0-50 L m^{-2} h^{-1}, moreover they reported critical J_d of 260 L m^{-2} h^{-1} for soybean oil loaded emulsions without loading any bioactive. The results are somewhat similar to the findings of [31], they formulated polyunsaturated fatty acid (PUFA) loaded O/W emulsions and observed increase in d_{av} of emulsions as a function of J_d. They reported critical J_d of 80 L m^{-2} h^{-1}.

The monodisperse O/W emulsions encapsulating 0.5% (w/w) ergocalciferol formulated with 1% (w/w) Tween 20 were stored at 4 ± 1°C for 15 d. These emulsions were formulated by keeping J_d at 5 L m^{-2} h^{-1} and continuous phase flow rate at 150 mL h^{-1}. Immediately after formulation, emulsions with ergocalciferol had a colorless turbid appearance with good flowability. The appearance of the O/W emulsions did not change with storage time. Fig. 6.10 depicts time changes in the $d_{3,2}$ and span values of the formulated O/W emulsions encapsulating ergocalciferol. There was hardly any increase in $d_{3,2}$ of emulsion during evaluated storage time, indicating high physical stability of O/W emulsions. The $d_{3,2}$ of emulsions remain in range of 33.9 mm with span width between 0.203 to 0.208 (Fig. 6.12).

(a)
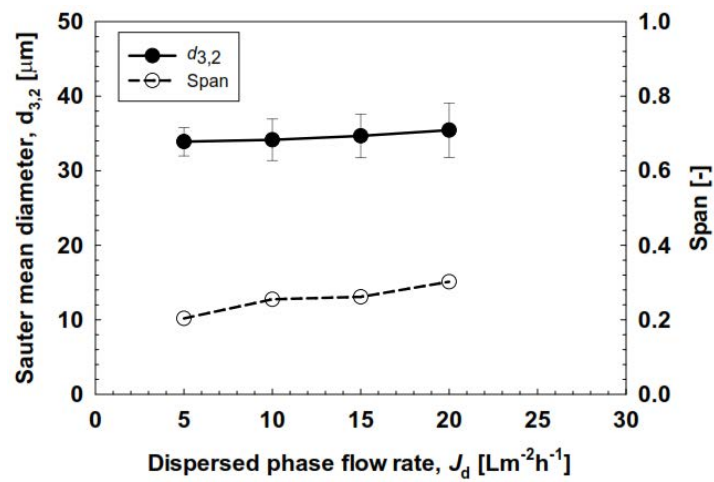
(b)
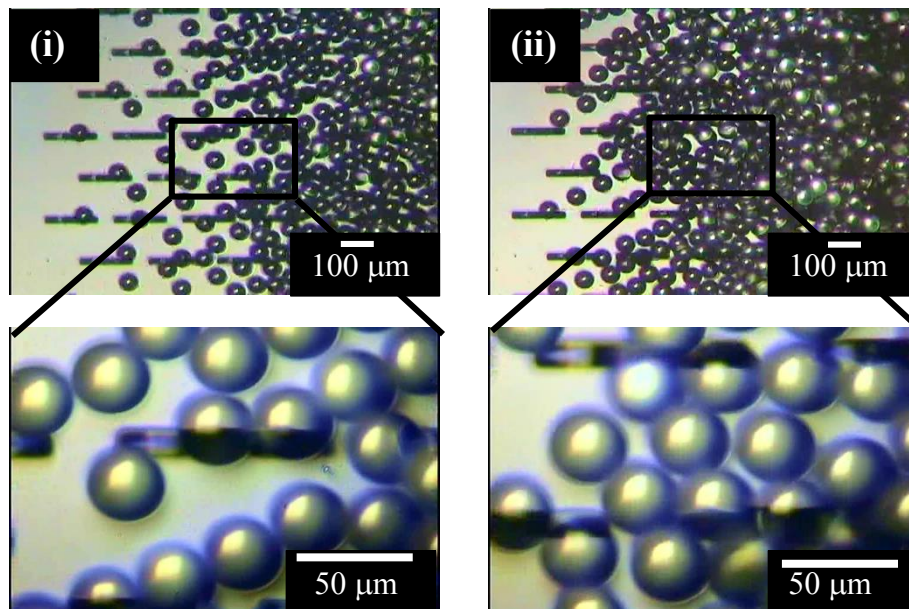
Figure 6.11: (a) Effect of J_d on mean droplet diameter and span width of O/W emulsions encapsulating ergocaliferol. (b) Typical droplet generation behavior at (i) low flux of 5 L m^{-2}h^{-1} and (ii) critical flux of 20 L m^{-2}h^{-1}.
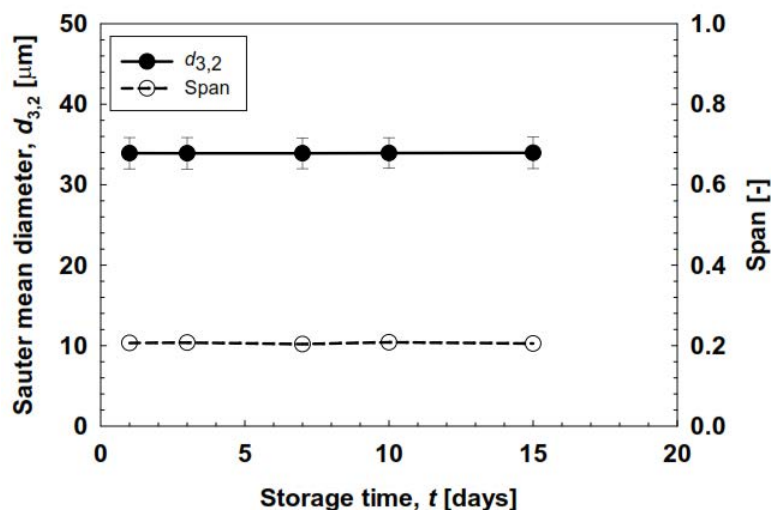
Figure 6.12: Storage stability of O/W emulsions encapsulating ergocalfierol stored at 4 ±1°C. The data was presented in term of mean droplet diameter and span width.

Encapsulation efficiency of ergocalciferol in O/W emulsions

The freshly formulated O/W emulsions had an initial retention of 0.06 mg mL^{-1} and regarded as 100% encapsulated efficiency, since in MC emulsification it was difficult to maintain the volume fraction with passage of time in comparison to conventional emulsification procedures. Fig. 6.13 indicates the retention and encapsulation efficiency (EE) of O/W emulsions. The EE slightly decreased with storage time and exhibited 76% retention of ergocalciferol after 15 d of storage at 4 °C. The results are comparable with EE of previously encapsulated bioactives in MC emulsification. The EE of L-ascorbic acid in W/O/W emulsions prepared through MC emulsification was more 80% after 10 d of storage period [32]. This higher retention can be ascribed to the narrow size distribution of the O/W droplets formulated by MCE, since the generation of droplets in MCE was based upon difference in interfacial tension rather than high-energy homogenization procedures. Semo *et al.* [46] and Ron *et al.* [47] encapsulated ergocalciferol in casein and β-lactoglobulin and observed that reduction rate of encapsulated ergocalciferol was slower than solved ergocalciferol in ethanol-water mixture. Encapsulated ergocalciferol in mentioned studies perform better against oxygen diffusion, interaction with oxidizing agents and harmful effects of UV radiations. The evaluation of these mechanisms are beyond the scope of present study.
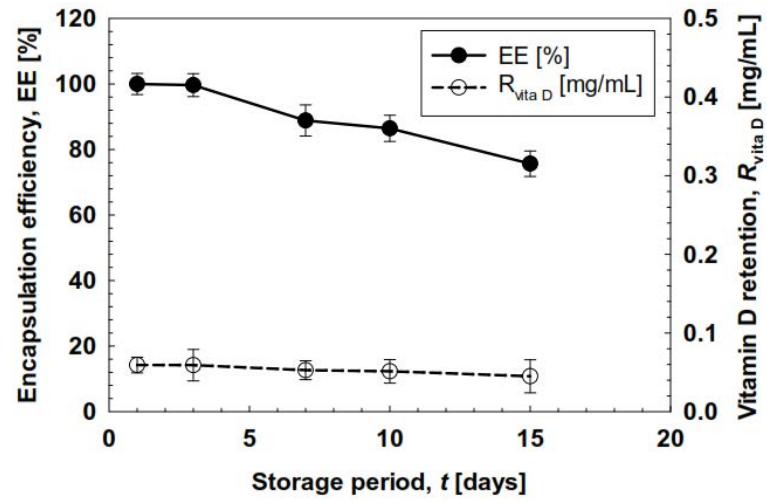
Figure 6.13: Encapsulating efficiencies and retention profile of O/W emulsions with storage time. The emulsions were prepared at J_d of 5 L m^{-2} h^{-1} and the data was presented over 15 days of storage time

Table 6.1: Fluid properties of systems containing ergocalciferol together with different oils used for preparing O/W emulsions

	Dispersed phase				Continuous phase			
	η_d (mPa s)	ρ_d (kg m^{-3})	γ_d (mN m^{-1})	**ζ (–)	Emulsifiers in Milli-Q water	η_d (mPa s)	ρ_d (kg m^{-3})	γ_d (mN m^{-1})
MCT	22.5±0.3	946.9±0.2	5.3±0.4	24.7	0.5% Tween 20	0.89±0.1	997.3±0.6	5.1±0.2
Soybean oil	53.0±0.1	921.9±0.4	5.6±0.1	58.2	1.0% Tween 20	0.91±0.1	998.4±0.6	5.2±0.1
Olive oil	68.2±0.1	911.9±0.2	6.2±0.2	75.0	1.5% Tween 20	0.96±0.1	999.1±0.8	5.2±0.2
Safflower oil	53.2±0.1	918.9±0.1	5.3±0.2	58.5	2.0% Tween 20	0.99±0.1	1000.1±0.1	5.4±0.3
					1.0% β-lg	0.95±0.1	999.9±0.2	12.6±0.9
					1.0% Sunsoft A-12	0.97±0.1	998.5±0.6	4.8±0.2

* Dispersed phase contains 0.5% (w/w) ergocalciferol and interfacial tension was observed in the presence of 1% (w/w) Tween 20 in Milli-Q water, ** Viscosity ratio (ζ) was defined as the ratio of to-be-dispersed phase viscosity over the continuous phase viscosity.

References

[1] Cantorna MT and Mahon BD, *Exp. Biol Med.*, **229,** 1136-1142 (2004).

[2] Hypponen E, Laara E, Reunanen A, Jarvelin MR and Virtanen SM, *Lancet*, **358,** 1500-1503 (2001).

[3] Kendrick J, Targher G, Smits G and Chonchol M, *Atherosclerosis*, **205,** 255-260 (2009).

[4] Lappe JM, Travers-Gustafson D, Davies KM, Recker RR and Heaney RP, *Am. J. Clin. Nutr.*, **85,** 1586-1591 (2007).

[5] Bandeira F, Costa AG, Soares Filho MA, Pimentel L, Lima L and Bilezikian JP, *Arquivos brasileiros de endocrinologia e metabologia*, **58,** 504-513 (2014).

[6] Song IG and Park CJ, *Blood Res.*, **49,** 84 (2014).

[7] Ward LM, Gaboury I, Ladhani M and Zlotkin S, *CMAJ : Canadian Med. Assoc. J.,* **177,** 161-166 (2007).

[8] Chesney RW, *Pediatrics Int.*, **45,** 509-511 (2003).

[9] Holick MF, *J. Cell. Biochem.*, **88,** 296-307 (2003).

[10] Holick MF, *J. Investigative Med.*, **59,** 872-880 (2011).

[11] Japelt RB and Jakobsen J, *Frontiers Plant Sci.*, **4,** 136 (2013).

[12] Thacher TD and Clarke BL, *Mayo Clinic proceed.*, **86,** 50-60 (2011).

[13] Armas LA, Hollis BW and Heaney RP, *J. Clin. Endocrinol. Metabol.*, **89,** 5387-5391 (2004).

[14] Trang HM, Cole DE, Rubin LA, Pierratos A, Siu S and Vieth R, *Am. J. Clin. Nutr.*, **68,** 854-858 (1998).

[15] Houghton LA and Vieth R, *Am. J. Clin. Nutr.*, **84,** 694-697 (2006).

[16] Eitenmiller RR, Landen Jr W and Ye L, Vitamin analysis for the health and food sciences, CRC press, 2007.

[17] Patel MR and San Martin-Gonzalez MF, *J. Food Sci.*, **77,** N8-13 (2012).

[18] Schramm LL, Microscience and Applications of Emulsions, Foams, Suspensions, and Aerosols, John Wiley & Sons, 2014.

[19] McClements DJ, *Crit. Rev. Food Sci. Nutr.*, **47,** 611-649 (2007).

[20] Vladisavljevic GT, Khalid N, Neves MA, Kuroiwa T, Nakajima M, Uemura K, Ichikawa S and Kobayashi I, *Adv. Drug Deliv. Rev.,* **65,** 1626-1663 (2013).

[21] Sugiura S, Nakajima M, Kumazawa N, Iwamoto S and Seki M, *J. Phys. Chem. B*, **106,** 9405-9409 (2002).

[22] Vladisavljevic' GT, Kobayashi I and Nakajima M, *Microfluid Nanofluid.*, **13,** 151-178 (2012).

[23] Kobayashi I, Mukataka S and Nakajima M, *Ind. Eng. Chem. Res.*, **44,** 5852-5856 (2005).

[24] Kobayashi I, Wada Y, Hori Y, Neves MA, Uemura K and Nakajima M, *Chem. Eng. Technol.*, **35,** 1865-1871 (2012).

[25] Kobayashi I, Wada Y, Uemura K and Nakajima M, *Microfluid. Nanofluid.*, **8,** 255-262 (2010).

[26] Vladisavljevic GT, Kobayashi I and Nakajima M, *Microfluid. Nanofluid.*, **10,** 1199-1209 (2011).

[27] Sugiura S, Nakajima M, Tong JH, Nabetani H and Seki M, *J. Colloid Interface Sci.*, **227,** 95-103 (2000).

[28] Ikkai F, Iwamoto S, Adachi E and Nakajima M, *Colloid Polymer Sci.*, **283,** 1149-1153 (2005).

[29] Sugiura S, Kuroiwa T, Kagota T, Nakajima M, Sato S, Mukataka S, Walde P and Ichikawa S, *Langmuir*, **24,** 4581-4588 (2008).

[30] Neves MA, Ribeiro HS, Kobayashi I and Nakajima M, *Food Biophys.*, **3,** 126-131 (2008).

[31] Neves MA, Ribeiro HS, Fujiu KB, Kobayashi I and Nakajima M, *Ind. Eng. Chem. Res.*, **47,** 6405-6411 (2008).

[32] Khalid N, Kobayashi I, Neves MA, Uemura K, Nakajima M and Nabetani H, *Colloid Surface A.*, **458,** 69-77 (2014).

[33] Khalid N, Kobayashi I, Neves MA, Uemura K, Nakajima M and Nabetani H, *Colloid Surface A.*, **459,** 247-253 (2014).

[34] Souilem S, Kobayashi I, Neves M, Sayadi S, Ichikawa S and Nakajima M, *Food Bioprocess Technol*, **7,** 2014-2027 (2014).

[35] Fujiu KB, Kobayashi I, Neves MA, Uemura K and Nakajima M, *Colloid Surface A.*, **411,** 50-59 (2012).

[36] van Dijke K, Kobayashi I, Schroen K, Uemura K, Nakajima M and Boom R, *Microfluid Nanofluid.*, **9,** 77-85 (2010).

[37] Kobayashi I and Nakajima M, *Eur. J. Lipid Sci. Technol.*, **104,** 720-727 (2002).

[38] Kobayashi I, Uemura K and Nakajima M, *Food Biophys.*, **3,** 132-139 (2008).

[39] Kobayashi I, Nakajima M and Mukataka S, *Colloid Surface A.*, **229,** 33-41 (2003).

[40] Kawakatsu T, Tragardh G, Kikuchi Y, Nakajima M, Komori H and Yonemoto T, *J. Surfactant Detergent*, **3,** 295-302 (2000).

[41] Kobayashi I, Neves MA, Wada Y, Uemura K and Nakajima M, *Procedia Food Sci.*, **1,** 109-115 (2011).

[42] Kobayashi I, Mukataka S and Nakajima M, *Langmuir*, **21,** 7629-7632 (2005).

[43] Vladisavljevic GT, Kobayashi I and Nakajima M, *Powder Technol.*, **183,** 37-45 (2008).

[44] Vladisavljević GT, Kobayashi I, Nakajima M, Williams RA, Shimizu M and Nakashima T, *J. Membrane Sci.*, **302,** 243-253 (2007).

[45] El-Abbassi A, Neves MA, Kobayashi I, Hafidi A and Nakajima M, *Eur. J. Lipid Sci. Technol,*, **115,** 224-231 (2013).

[46] Semo E, Kesselman E, Danino D and Livney YD, *Food Hydrocolloid*, **21,** 936-942 (2007).

[47] Ron N, Zimet P, Bargarum J and Livney YD, *Int. Dairy J.*, **20,** 686-693 (2010).

Chapter 7

Formulation of monodisperse O/W emulsions loaded with ergocalciferol and cholecalciferol by microchannel emulsification: Insights of production characteristics and stability*

_____

7.1 Introduction

There are an estimated one billion people worldwide who are either vitamin D deficient or have insufficient vitamin D intake [1]. This deficiency can be addressed by food fortification and supplementation. Vitamin D is a hydrophobic bioactive and has numerous uses in various industries including cosmetics, foods and pharmaceutics. Vitamin D is basically a seco-steroid hormone that possesses two active forms namely ergocalciferol (vitamin D_2) and cholecalciferol (vitamin D_3) [2]. Vitamin D_3 is produced intradermally in the skin upon exposure to light and has many structural forms [3], while vitamin D_2 is formed by the irradiation of ergosterol [4].

After release from the food matrix, vitamin D is included to mixed micelle and enters the enterocytes via passive diffusion through unsaturable mechanism. Afterwards, it is included in chylomicrons and is activated by liver [5]. The liver converts vitamin D to calcidiol [25(OH)D], the inactive blood circulating form or more precisely the indicator of vitamin D status in living bodies [5, 6]. Calcidiol is converted to calcitriol [1, 25(OH)$_2$D] in the kidneys, and afterwards controls bone metabolism, calcium and phosphorus hemostasis, renal calcium reabsorption, blood pressure in addition to intestinal transport and insulin secretion [1, 2, 6].

The recommended daily intake of vitamin D is around 5 μg day^{-1} [2]. Most researchers define vitamin D deficiency as a serum calcidiol concentration less than 50 nmol L^{-1}, insufficiency as a concentration of less than 80 nmol L^{-1} and toxicity as a concentration of greater than 375 nmol L^{-1} [1, 6]. Most dietary products are poor source of vitamin D, including breast milk [7]. Vitamin D intake is found to be low in vegetarians and vegans [8, 9]. The high phytate and fiber content of vegetarian diets may also reduce the vitamin D absorption, while consumption of fish at least four times a week (wild fatty fish) helps prevent vitamin D deficiency [10]. Similarly, vitamin D deficiency occurs due to lack of exposure of sun light, extensive use of UV protecting creams, lactose intolerance, and so on [11-13].

Kawakatsu *et al.* [14] proposed microchannel emulsification (MCE) capable of generating monodisperse emulsion droplets by using microchannel (MC) arrays precisely fabricated on a single-crystal silicon microchip. These MC arrays have also been fabricated on polymer [15] and stainless steel chips [16]. On MC array chips, numerous droplets can be generated simultaneously from a maximum of hundreds or thousands of parallel MCs [17]. These MC arrays are either fabricated onto the chip surface as microgrooves

(grooved MC array) or straight-through holes (straight-through MC array) [18]. MCE enables formulating monodisperse emulsions by forcing a dispersed phase into a continuous phase through uniformly sized channels of well-defined geometry. The droplet generation process in MCE was comprehensively reviewed by Vladisavljevic *et al.* [19]. Monodisperse emulsions with droplet diameters of 1 to 500 μm and the smallest coefficient of variation below 5% have been successfully formulated through MCE [18].

MCE is a useful technique for many fundamental studies on emulsions, e.g., emulsion stability [20] and crystallization behavior of emulsion droplets [21]. This technique has been used to prepare microdispersions such as solid lipid microspheres [22], coacervate microcapsules [23] gel microbeads [24] and giant vesicles [25]. Similarly, previous studies have demonstrated the formulation of microdispersions encapsulating bioactives such as β-carotene [26], oleuropein [27], γ-oryzanol [28], L-ascorbic acid [29] and ascorbic acid derivatives [30].

There is a considerable interest in fortifying food and beverage products with vitamin D, while fortifying foods with vitamin D is not straightforward due to its high hydrophobicity in food matrixes [31], degradability at high temperatures [32], better efficacy at higher pH [33], oxidation [34] and variable oral bioavailability [11]. There was no pervious study describing the encapsulation of both active forms of vitamin D. Encapsulation of both forms of vitamin D have synergetic effect on retention of vitamin D in body for longer period of time [35,36]. Keeping this idea in mind the present study was conducted to formulate oil-in-water (O/W) emulsions containing both ergocalciferol (VD_2) and cholecalciferol (VD_3) by using straight-through MCE. We investigated the effect of sodium cholate as potential emulsifier on stabilization of these emulsions. We also evaluate the physical and chemical stability of the O/W emulsions containing VD_2 and VD_3 formulated from MCE.

7.2 Material and methods

Chemicals

Ergocalciferol, cholecalciferol, soybean oil, olive oil and polyoxyethylene (20) sorbitan monolaurate (Tween 20) were purchased from Wako Pure Chemical Ind. (Osaka, Japan). Medium chain triacylglycerol (MCT, sunsoft MCT-7) with a fatty acid residue composition of 75% caprylic acid and 25% capric acid was procured from Taiyo Kagaku Co. Ltd. (Mie, Japan). Sodium salt of colic acid (Na-cholate, > 97%

purity) was purchased from Sigma Aldrich (St. Louis, USA). Milli-Q water with a resistivity of 18 MΩ cm (pH 7.1) was used to dissolve the emulsifiers and served as continuous phase. All other chemicals used in this study were of analytical grade and used as received.

Microchannel array chip

In this study we used a 24×24-mm MC array chip (Model WMS 1-2) consisting of 10,313 MCs (Fig. 7.1) in a 10-mm^2 in the center of the chip and two 1.5 mm diameter holes at the corners of the chip. This MC array chip was fabricated by repeated processes of photolithography and deep-reactive-ion etching (DRIE) on 5 in. silicon wafer. Each MC consisted of a circular microhole (10 μm diameter and 70 μm depth) located on the inlet side and a microslot (11 × 104 μm cross section and 30 μm depth) located on the outlet side. The slot aspect ratio of 9.5 was above the threshold value of 3 for successfully formulating monodisperse emulsions [37]. Oxygen plasma treatment (PR41, Yamato Science Co. Ltd., Tokyo, Japan) was then performed to grow a hydrophilic silicon dioxide layer on the fabricated plate before carrying out the emulsification.

Preparation of dispersed and continuous phases

0.5% (w/w) VD$_2$ was dissolved in soybean oil, olive oil and MCT heated to 75±2°C for 20 min and then quickly cooled to room temperature. Afterwards, 0.5% (w/w) VD$_3$ was added to each oil solution pre-loaded with VD$_2$ at ambient temperature, and the oil solution loaded with VD$_2$ and VD$_3$ were stirred for 20 min for proper dissolution. The influence of temperature on VD$_2$ solubility in different oils was ascertained by measuring the turbidity as a function of temperature. Briefly, a known concentration of VD$_2$ was dispersed in different oils (0.5 mg mL^{-1}) at room temperature, which leads to the formation of turbid suspensions. The turbidity of these samples was then measured as function of temperature from 25 to 100°C by using an UV/VIS/NIR spectrophotometer (V-570, Jasco Co., Hachioji, Japan) at 600 nm. As this experiment showed that the samples above 70°C become clear (original oil color), we chose 75°C as optimum temperature to dissolve VD$_2$ in different oils. The continuous phase contained 1% (w/w) Na-cholate or 1% (w/w) Tween 20 in Milli-Q water and used as such during MCE. The pH of the continuous phase during MCE was 7.1.
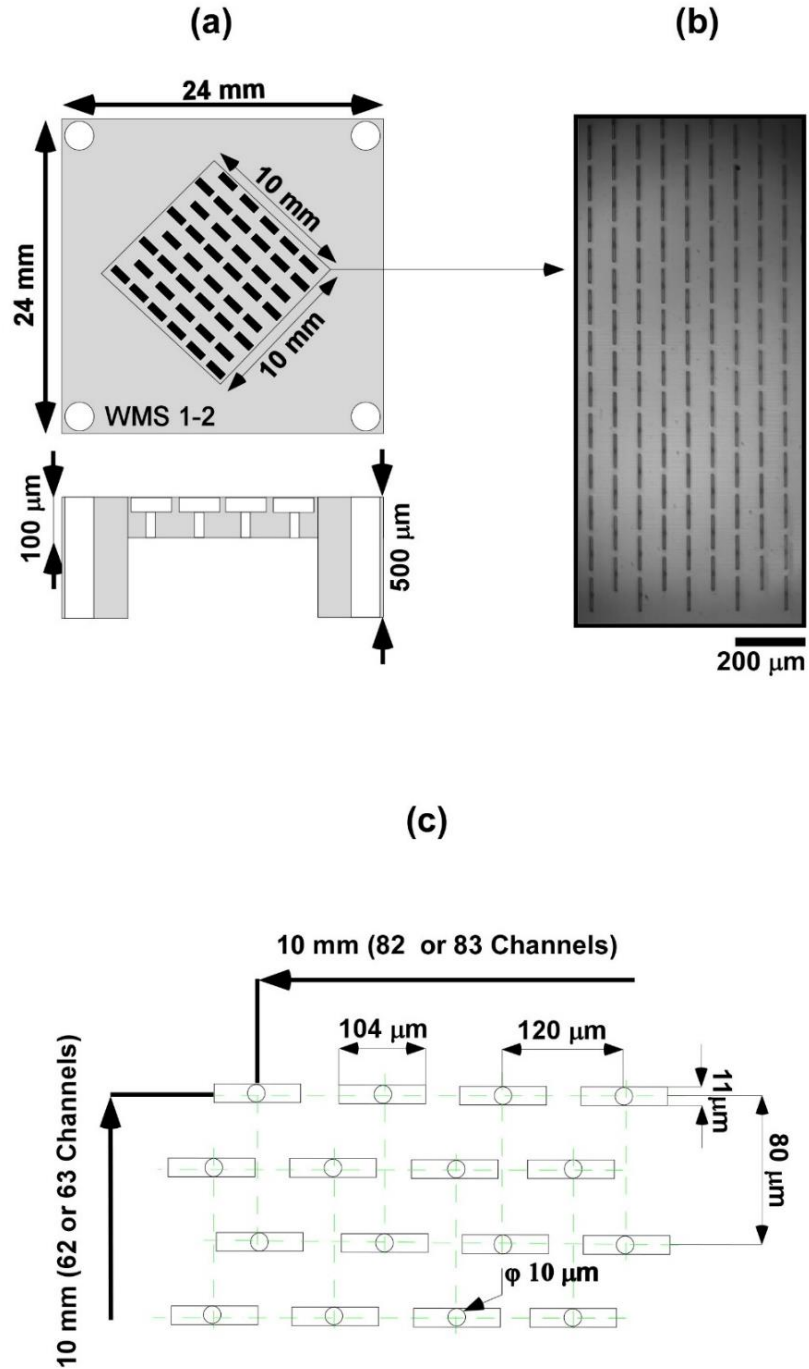
Figure 7.1: Schematic representation of microchannel (MC) array chip used in microchannel emulsification. (a) WMS 1-2 silicon chip. (b) Optical micrograph of the bottom-illuminated chip surface. The microholes are highlighted in dark black color in the center of light grey color microslot. (c) Arrangement of channels on the top side of a WMS 1-2 chip. Each horizontal row contains alternatively 82 or 83 channels and vertical rows contain alternatively 62 or 63 channels.

Emulsification procedure

Each emulsification experiment was started with degassing of a WMS 1-2 chip soaked in the continuous phase under ultrasonication (VS-100III, As One Co., Osaka, Japan) at 100 kHz for 20 min. During module assembly, the degassed MC array chip was mounted in a module compartment previously filled with the continuous phase. Fig. 7.2a shows a simplified schematic diagram of the experimental setup used for MCE. A syringe pump (Model 11, Harvard Apparatus Inc., Holliston, USA) was used to supply both the continuous and dispersed phases. The emulsification process was carried out for approximately 1 h at ambient temperature and monitored through a high speed video system at 250 to 500 fps (FASTCAM-1024 PCI, Photron Ltd., Tokyo, Japan) attached to an inverted metallographic microscope (MS-511B, Seiwa Kougaku Sesakusho Ltd., Tokyo, Japan). The droplet generation process during MCE is illustrated in Fig. 7.2b. The dispersed phase flux (J_d) (L m^{-2} h^{-1}) during emulsification was calculated using the following equation:

$$J_d = \frac{Q_d}{A_{MCA}} \qquad (7.1)$$

where Q_d is the dispersed phase flow rate (L h^{-1}) and A_{MCA} is the effective area of the MC array (10^{-4} m^2). The average flow velocity of the continuous phase along the plate surface (V_c) (m h^{-1}) was calculated with the following equation:

$$V_c = \frac{Q_c}{A_{a,s}} \qquad (7.2)$$

where Q_c is the continuous phase flow rate (L h^{-1}), and $A_{a,s}$ is the flow area along the plate surface (m^2) and is calculated by measuring the dimensions of the spacer between the MC array chip and glass plate:

$$A_{a,s} = W \times H \qquad (7.3)$$

where W is the spacer internal width (10^{-2} m), and H is the spacer thickness (10^{-3} m). The J_d was varied between 5 to 120 L m^{-2} h^{-1}. The V_c was set between 6.9 to 27.8 mm s^{-1}. After experiments, the MC array chip was cleaned using an ultrasonic bath at a frequency of 100 kHz based on the following sequences: an MC array chip was cleaned in an aqueous solution of non-ionic detergent for 20 min, afterwards, the chip was again cleaned in Milli-Q water containing ethanol (1:1 v/v proportion) for the next 20 min and another round of cleaning with Milli-Q water for the final 20 min.

Measurement and analysis

The size distribution of the O/W emulsion droplets containing VD_2 and VD_3 was measured by using a laser light scattering instrument which works on the principle of Polorization Intensity Differential Scattering Technology (LS13320, Beckman Coulter, Fullerton, USA). This instrument has ability to measure the size ranging from 0.04 to 2000 μm with a resolution of 116 particle size channels. The mean droplet size was expressed as Sauter mean diameter ($d_{3,2}$); i.e., the diameter of a droplet having the same area per unit volume as that of the total collection of droplets in emulsions. The width of droplet size distribution was expressed as relative span factor (RSF) and is defined as:

$$\text{RSF} = \frac{d_{v90} - d_{v10}}{d_{v50}} \qquad (7.4)$$

where d_{v90} and d_{v10} are the representative diameters where 90% and 10% of the total volume of the liquid is made up of droplets with diameters smaller than or equal to the stated value. d_{v50} is the representative diameter where 50% of the total volume of the liquid is made up of droplets with diameters larger than the stated value and 50% is made up of droplets with diameters smaller than the stated value.

Measurement of fluid properties

The densities of dispersed and continuous phases were measured using a density meter (DA-130 N, Kyoto Electronics Manufacturing Co., Ltd., Kyoto, Japan) at 25±2°C. The viscosities of dispersed and continuous phases were measured with a sine wave vibro viscometer (SV-10, A&D Co., Ltd., Tokyo, Japan) at 25±2°C by taking 10 samples in a measuring vessel followed by immersion of sensor plates in that vessel. This viscometer uses a frequency of 30 Hz which is maintained at a constant amplitude. Viscosity was measured by detecting the electric current needed to resonate the sensor plates. The absolute viscosity (η) was calculated by

$$\eta = \frac{\eta_{mea}}{\rho} \qquad (7.5)$$

where η_{mea} is the measured fluid viscosity and ρ is the fluid density. The static interfacial tension between the oil and aqueous phases was measured with a fully automatic interfacial tensiometer (PD-W, Kyowa Interface Sciences Co., Ltd., Saitama, Japan) using a pendant drop method. The key physical properties of the continuous and dispersed phases are presented in Table 7.1.
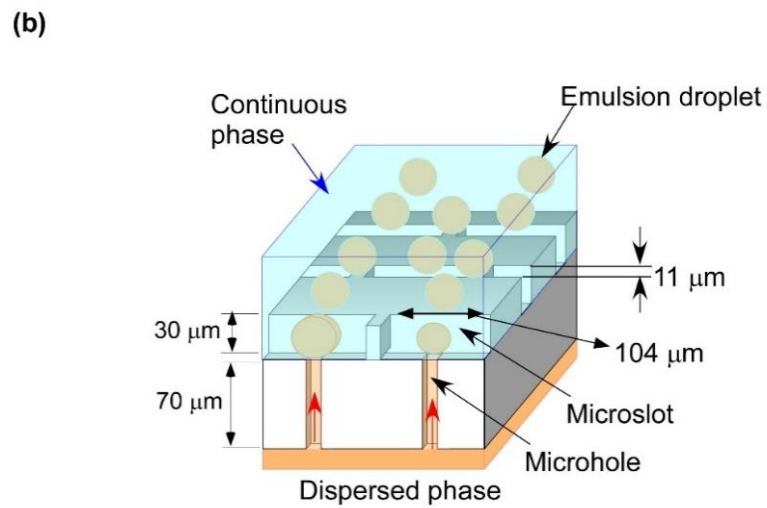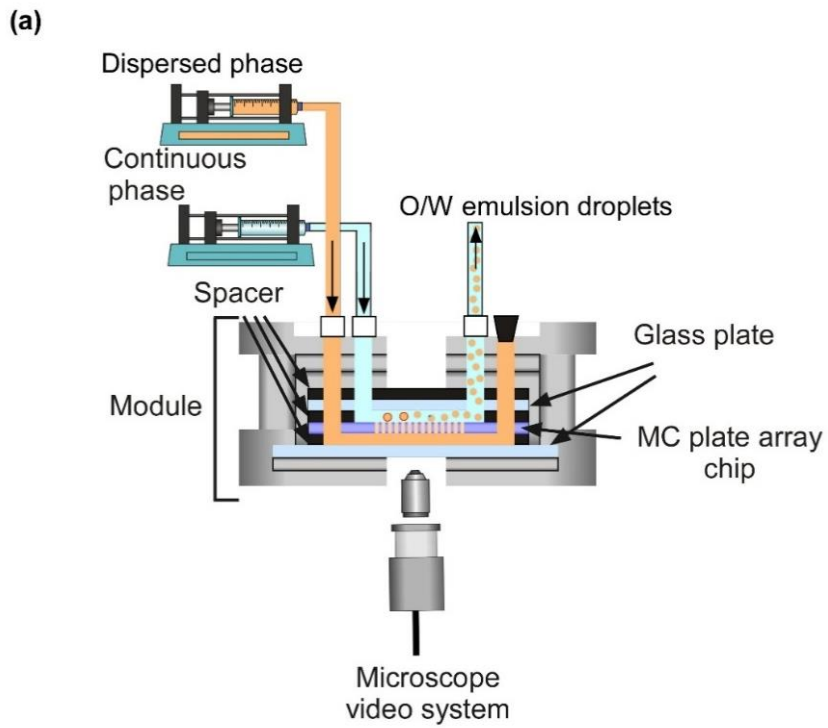
Figure 7.2: Simplified representation of microchannel emulsification (MCE). (a) Experimental set-up used in this work for straight-through MCE. (b) Generation of O/W emulsion droplets in MCE.

Table 7.1: Fluid properties of the two-phase systems containing ergocalciferol (VD₂) and chorecalciferol (VD₃) together with different oils used for formulating O/W emulsions.

Emulsion phase	Density (kg m⁻³)	Viscosity (mPa s)	Interfacial tension (mN m⁻¹)
Dispersed phase*	918.23 ± 0.55	51.06 ± 0.20	-
Continuous phase** (1% (w/w) Tween 20)	998.90 ± 0.10	0.86 ± 0.01	5.30 ± 0.30
Continuous phase** (1% (w/w) Na-cholate)	999.20 ± 0.30	1.29 ± 0.01	10.80 ± 0.30

* Dispersed phase contains 0.5% (w/w) ergocalciferol and cholecalciferol in soybean oil; **Interfacial tension was measured between 1% (w/w) Tween 20 or 1% (w/w) Na-cholate in Milli-Q water and 0.5% (w/w) ergocalciferol and cholecalciferol in soybean oil

Physical and chemical stability of O/W emulsions encapsulating VD₂ and VD₃

The physical stability of the O/W emulsion droplets encapsulating VD_2 and VD_3 was evaluated according to the method described in an earlier section. The $d_{3,2}$, RSF, consistency and coalescence during 30 days of storage were observed at 4 ± 1 and $25\pm1°C$. The chemical stability of VD_2 and VD_3 in the emulsion droplets was determined spectrophotometrically. All spectral measurements of ethanol and hexane extracts of the preceding O/W emulsions were carried out using a UV/VIS/NIR spectrophotometer (UV-1700, Shimadzu, Co., Kyoto, Japan). First, 1 mL of the emulsion was extracted either with 9 mL of ethanol or hexane, followed by ultrasonication at 100 kHz for 20 min. The extracts were then centrifuged (Avanti HP-25, Beckman Coulter) at 20,000 g for 15 min. A 1 mL aliquot of the supernatant was diluted five times with ethanol (VD_2) and hexane (VD_3) and then injected into a quartz cell with a 10 mm pass length. The absorbance of VD_2 and VD_3 in emulsion extract was measured at 310 nm using an appropriate blank (ethanol and hexane). A representative standard curve of absorbance versus concentration gave linear least-squares regression with a coefficient of determination (r^2) of 0.999. All experiments were repeated in triplicate, and mean values were calculated. The Beer's law was obeyed in the concentration range of 0.01-0.5 mg mL⁻¹ for VD_2 and VD_3, and the sensitivity of measurement has relative standard deviation of 0.85% (n=15). The molar absorptivity (ε) for VD_2 during this study was 0.61 mM⁻¹ cm⁻¹ and for VD_3 was 0.4 mM⁻¹ cm⁻¹. The encapsulation efficiency of VD_2 and VD_3 in samples n samples was calculated using the following equations, respectively:

$$EE_{VD_2} = \frac{W_{VD2,t}}{W_{VD2,0}} \times 100 \qquad (7.6)$$

$$EE_{\text{VD}_3} = \frac{W_{\text{VD3,t}}}{W_{\text{VD3,0}}} \times 100 \qquad (7.7)$$

where $W_{\text{VD2,t}}$ is the total amount of VD$_2$ in the O/W emulsions and $W_{\text{VD2,0}}$ is the total amount of VD$_2$ added initially during preparation. Similarly, $W_{\text{VD3,t}}$ is the total amount of VD$_3$ in the O/W emulsions and $W_{\text{VD3,0}}$ is the total amount of VD$_3$ added initially during emulsion preparation.

7.3 Results and discussion

Effect of different oils of the disperse phase on droplet generation characteristics

The formulation characteristics of O/W emulsions encapsulating VD$_2$ and VD$_3$ were evaluated by using three different oils as the dispersed phase: soybean oil, olive oil and MCT. The continuous phase included either 1% (w/w) Tween 20 or 1% (w/w) Na-cholate in Milli-Q water. The dispersed phase was injected into the module at Q_d of 2 mL h^{-1}, while Q_c was maintained at 250 mL h^{-1}. Uniformly sized oil droplets encapsulating VD$_2$ and VD$_3$ were stably generated from the slot outlets without any significant wetting, regardless of the types of oils and emulsifiers used. Moreover, this droplet generation was completely based on spontaneous transformation of the oil-water interface in and over the slots (Fig. 7.3a), which is quite similar to previous studies on encapsulating β-carotene in O/W emulsions and L-ascorbic acid in W/O/W emulsions with straight-through MCE [28, 29].

Fig. 7.3b shows the $d_{3,2}$ and RSF width of the formulated O/W emulsion droplets encapsulating VD$_2$ and VD$_3$ in different oils. Their $d_{3,2}$ for Tween 20 ranged between 26.4 to 29.0 μm with RSF width less than 0.3. In contrast, their $d_{3,2}$ and RSF for Na-cholate had greater values and ranged between 30.9 to 31.5 μm with RSF width less than 0.6. Many past studies reported RSF of <0.5 as indictor of monodispersity in microfluidic devices [38, 39]. Although narrower droplet size distributions were observed when using soybean oil and MCT rather than olive oil, the resultant emulsions containing olive oil droplets maintained monodispersity with RSF <0.5 (Figs. 7.3c and d). This finding might be attributed to the difference in fatty acid composition and free fatty acids of olive oil and soybean oil. As shown in Figs. 7.3c and 4d narrower droplet size distributions were observed for the O/W emulsions stabilized by Tween 20 in comparison to Na-cholate. Na-cholate is a biological surfactant extensively used for the formulation of mixed micelles and plays important role in many physiological processes; however, its efficiency to stabilize the emulsion interfaces is far less in comparison to Tween 20 due to low aggregation number [40].

Tween 20 has fatty acid ester moiety that could provide extra stability during emulsification process together with long-term stability [41].

(a)
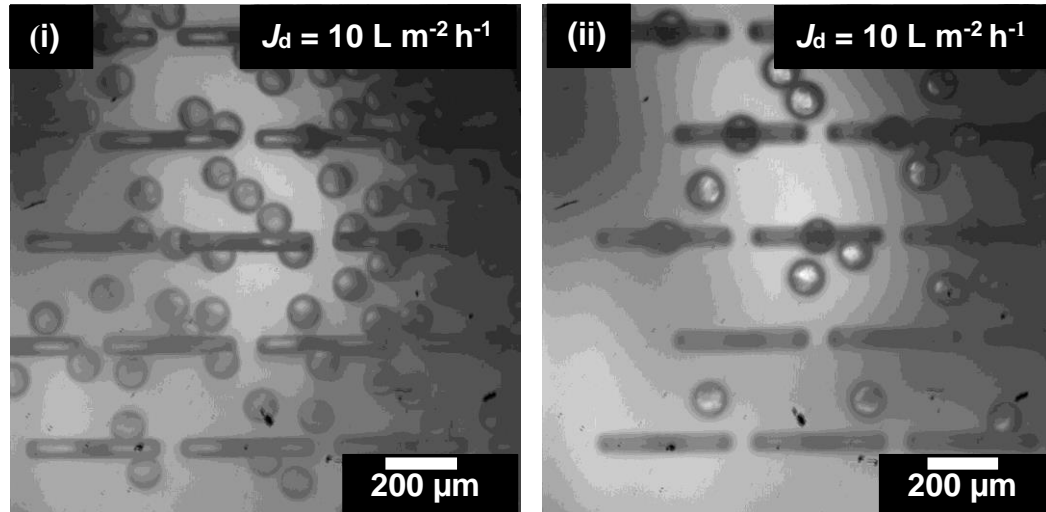
(b)
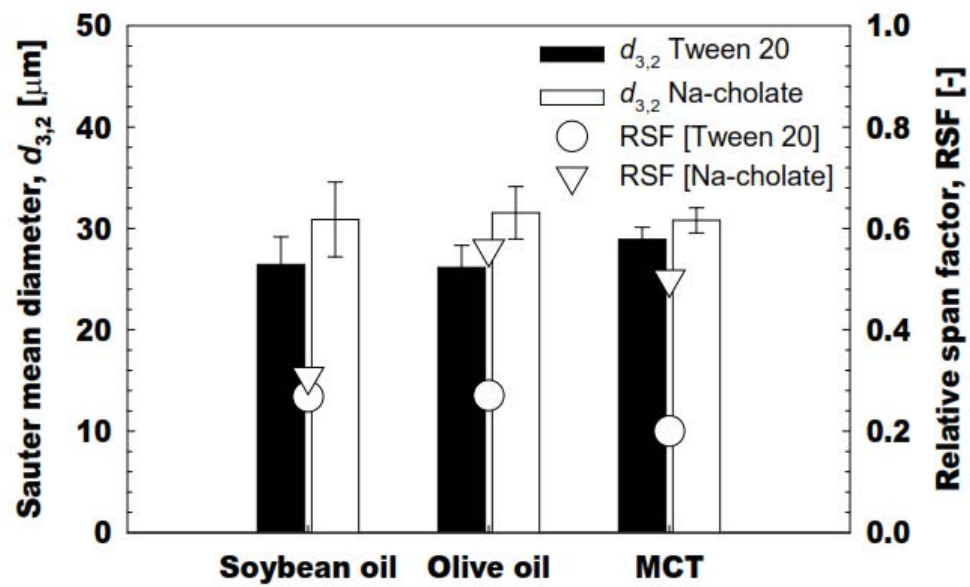
(c)
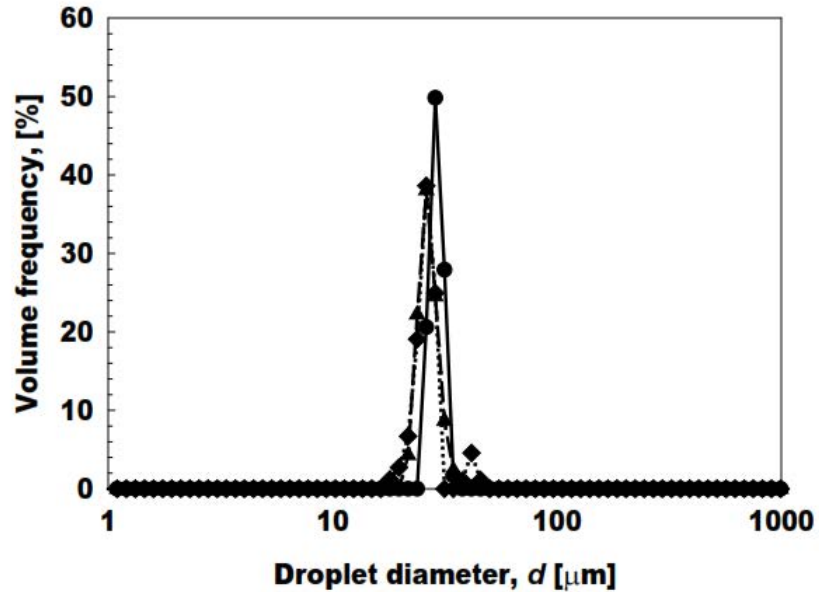
(d)
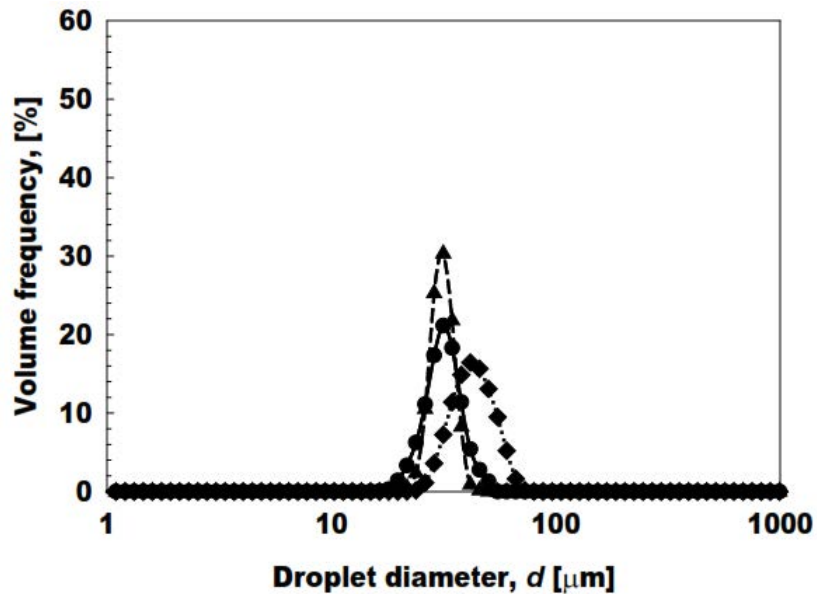
Figure 7.3: (a) Typical generation behaviors of O/W emulsion droplets containing VD_2 and VD_3 stabilized by 1% (w/w) Na-cholate (i) and Tween 20 (ii). (b) Effect of different dispersed phase composition on mean droplet diameter ($d_{3,2}$) and RSF width of O/W emulsions. (c) Droplet size distribution of different disperse phases stabilized by Na-cholate. (d) Droplet size distribution of dispersed phases stabilized by Tween 20. (—●—) MCT, (·—▲—·) soybean oil and (····◆····) denote olive oil in both Na-cholate and Tween 20.

Effect of dispersed phase flux on droplet generation characteristics

Droplet productivity in MCE is directly related with J_d, being considered as important parameter in scaling up microfluidic devices. Fig. 7.4a depicts the effect of J_d on the $d_{3,2}$ and RSF width of the resultant droplets stabilized either with Tween 20 or Na-cholate. The dispersed phase constitutes 0.5% (w/w) VD_2 and VD_3 in soybean oil. MCE was conducted by varying J_d in between 5 and 100 L m^{-2} h^{-1}, while V_c was varied between 6.9 and 19.4 mm s^{-1}. In Fig, 7.4a, the O/W emulsion droplets stabilized by Tween 20 have size stable zone between 10 and 40 L m^{-2} h^{-1}. In this stable zone the $d_{3,2}$ varies between 29.3 to 29.7 μm with RSF width <0.25. In comparison the emulsions stabilized with Na-cholate have size stable zone in J_d of 10 to 30 L m^{-2} h^{-1}. The $d_{3,2}$ in size stable zone remain in range from 30.3 to 30.7 μm with RSF width below 0.25. After crossing the size stable zone, the $d_{3,2}$ slowly increased with increasing J_d in its range of 50 to 80 L m^{-2} h^{-1} for Tween 20 and 40 to 60 L m^{-2} h^{-1} for Na-cholate. In this case, the RSF was kept below 0.25 for Tween 20 but gradually increased for Na-cholate. Further increase in J_d resulted in steeper increase in the $d_{3,2}$ for both emulsifiers, and the $d_{3,2}$ ranged between 35.4 to 37.4 μm with RSF above 0.5 at J_d of 100 L m^{-2} h^{-1}.

The influence of J_d on the droplet generation frequency per MC array chip (*f*) is presented in Fig. 7.4b. *f* can be estimated by:

$$f = \frac{Q_d}{V_{av}} = \frac{6Q_d}{\pi d_{3,2}^3} \qquad (7.8)$$

where V_{av} is the average droplet volume (m^3). The monodisperse droplets produced had a maximum productivity of 4.9×10^5 h^{-1} at J_d of 80 L m^{-2} h^{-1} for Tween 20, and 2.8×10^5 h^{-1} at J_d of 50 L m^{-2} h^{-1} for Na-cholate. During MCE, we observed the generation of uniformly sized oil droplets from more than 90% of the whole channels at J_d of 80 L m^{-2} h^{-1} in emulsions stabilized with Tween 20. In comparison, uniformly sized oil droplets from more than 90% of the whole channels were observed at J_d of 50 L m^{-2} h^{-1} in emulsions stabilized with Na-cholate. In MCE the droplet generation from the channel is depended on the capillary number (Ca) defined as the ratio of the viscous force to the interfacial tension force and is expressed as:

$$\mathrm{Ca} = \frac{\eta_d \bar{U}_{d,ch}}{\gamma} \qquad (7.9)$$

where η_d is the viscosity of the dispersed phase (Pa s), $\bar{U}_{d,ch}$ is the average flow velocity of the dispersed phase in the channel (m s^{-1}), and γ is the interfacial tension between the dispersed and continuous phases (N m^{-1}). $\bar{U}_{d,ch}$ can be estimated by the following equation:

$$\bar{U}_{d,ch} = \frac{4Q_d}{d^2 \pi N_{ch}} \qquad (7.10)$$

where d_{ch} is the hydraulic diameter of each channel and N_{ch} is the total number of channels (10, 313). Monodisperse emulsion droplets were generated from the channels below the critical Ca, where the interfacial tension force was dominant for droplet generation [42]. The soybean oil loaded with VD$_2$ and VD$_3$ had a η_d of 50.2 mPa s, but γ for the two-phase system containing Na-cholate (10.8 mN m^{-1}) was much higher than that containing Tween 20 (4.5 mN m^{-1}). At the critical $\bar{U}_{d,MC}$ (1.4 mm s^{-1}), the calculated critical Ca value was 1.8×10^{-2} in emulsions stabilized by Tween 20. The emulsions stabilized by Na-cholate have much lower critical Ca value of 8.8×10^{-3} at $\bar{U}_{d,MC}$ of 1.0 mm s^{-1}.

(a)
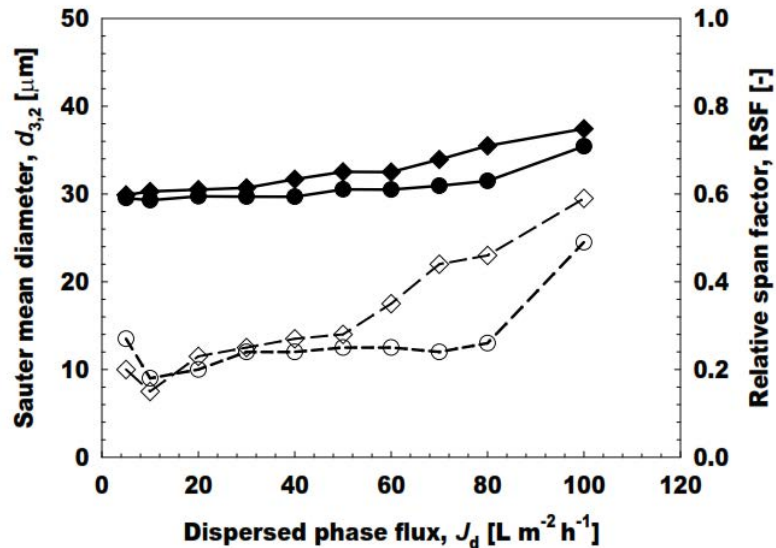
(b)
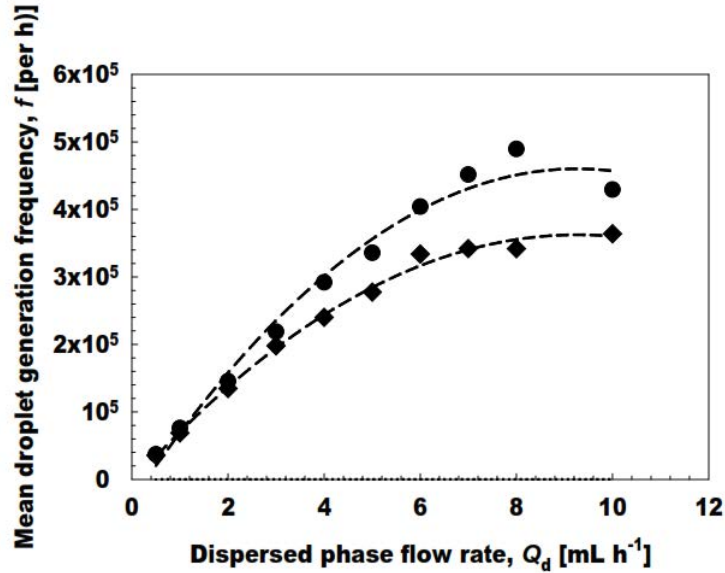
Figure 7.4: (a) Effect of dispersed phase flux on mean droplet diameter ($d_{3,2}$) and RSF width of O/W emulsions stabilized by Na-cholate and Tween 20. (●) denote Tween 20 and (▼) denote Na-cholate, while same open keys represent RSF width of O/W emulsions. **(b)** Effect of dispersed phase flux on droplet productivity. (●) denote Tween 20 and (▼) denote Na-cholate.

Stability evaluation of O/W emulsion droplets encapsulating VD₂ and VD₃

The monodisperse O/W emulsions encapsulating 0.5% (w/w) VD_2 and VD_3 formulated at J_d of 10 L m^{-2} h^{-1} were stored at 4±1 and 25±1°C for 30 days. Immediately after formulation, the collected emulsions containing VD_2 and VD_3 had a light turbid appearance with good flowability and consistency. Their physical appearance did not change with storage time. Fig. 7.5 depicts time changes in the $d_{3,2}$ and RSF width of the monodisperse O/W emulsions encapsulating VD_2 and VD_3. There was no difference in their $d_{3,2}$ and RSF width for Tween 20 at 4 and 25°C and Na-cholate only at 25°C. On the contrary, destabilization was observed in emulsions stabilized by Na-cholate stored at 4°C after 15 days of storage. There was gradual increases in the $d_{3,2}$ and RSF of emulsions stabilized by Na-cholate stored at 4°C. Initially there was slight increase in the $d_{3,2}$ up to 15 days from 29.7 to 31.7 μm with RSF of <1.0. After 15 days there was sharp increase in the $d_{3,2}$ of emulsions and the droplet size reached to 65.3 μm with RSF of >1.7. This sharp increase in $d_{3,2}$ indicates weaker emulsifier layer around the droplets. In comparison the

$d_{3,2}$ slightly increased from 29.5 to 31.8 μm at 4 and 25°C in emulsions stabilized by Tween 20 and 28.3 to 31.5 μm at 25°C in emulsions stabilized by Na-cholate.

The steep increase in $d_{3,2}$ of the O/W emulsions stabilized by Na-cholate at 4°C can be well explained by low aggregation number (average number of molecules in a micelle) of Na-cholate. The aggregation number of pure Na-cholate (3 to 16) is highly influenced by the environmental parameters [43, 44]. At low temperature some of the Na-cholate aggregates may crystallize the droplet surface and destabilize the emulsions, which could cause the increase in their $d_{3,2}$. In contrast, such destabilization was not observed at ambient temperature. Tween 20 has higher aggregation number (<60) and also has strong hydrophobic moiety that stabilized the oil-water interfaces for longer period of time in comparison to ionic emulsifiers [45]. Recently, Guttoff et al. [46] formulated nanoemulsions encapsulating vitamin D that were physically stable for one month at ambient temperature, whereas they were susceptible to droplet growth when exposed to elevated temperatures. Similarly, Ziani et al. [47] prepared food-grade O/W emulsions loaded with VD$_3$ by running a blend of 10% (w/w) oil and 90% (w/w) water containing 1% (w/w) of non-ionic emulsifiers (Tweens) over cycles in the high pressure homogenizer. The resulting emulsion had an average droplet size of around 0.22 μm and was resistant to particle growth after formulation. To our knowledge, there are no previous reports describing the encapsulation of both forms of vitamin D using either conventional or microfluidic approaches. We used extremely mild emulsification procedure, which produced O/W emulsions with precise monodispersity.

(a)

179
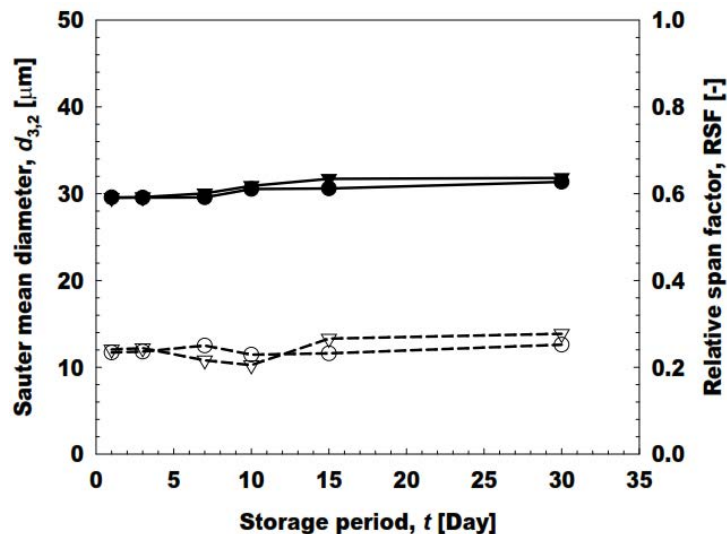
(b)
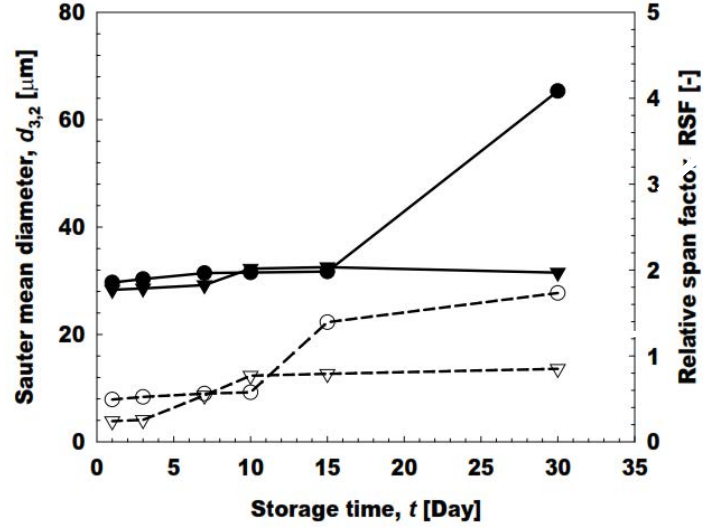
Figure 7.5: Storage stability of O/W emulsions encapsulating VD₂ and VD₃ stored at 4±1 and 25±1°C. The data was presented in term of mean droplet diameter ($d_{3,2}$) and RSF width. (a) Storage stability of emulsion droplets stabilized by Tween 20. (⬤) denote stability at 4°C and (▼) denote stability at 25°C, while same open keys denote RSF width. (b) Storage stability of emulsion droplets stabilized by Na-cholate. (◆) denote stability at 4°C and (▼) denote stability at 25°C, while same open keys denote RSF width.

Encapsulation efficiency of VD₂ and VD₃ in O/W emulsion droplets

The freshly formulated O/W emulsions containing VD₂ and VD₃ had initial concentrations of 59.3 μg mL⁻¹ for VD₂ and 62.1 μg mL⁻¹ for VD₃ regarded as 100% EE, since in MCE it was difficult to maintain the dispersed phase volume fraction (φ_d) in these emulsions with passage of time in comparison to conventional emulsification procedures. The calculated φ_d at the end of emulsification corresponds to 0.79%. Fig. 7.6a depicts the EE of the VD₂ and VD₃ kept in the resultant O/W emulsions stabilized with 1% (w/w) Tween 20. The EE slowly decreased with storage time and exhibited 75.7% for VD₂ and 77.1% for VD₃ at 4°C and 66.2% for VD₂ and 69.1% for VD₃ after 15 days of storage at 25°C. In comparison the O/W emulsions stabilized with 1% (w/w) Na-cholate exhibited only 49.5% for VD₂ and 51.21% for VD₃ at 4°C after 15 days of storage (Fig. 7.6b). The emulsions stored at 25°C had EE of 68.2% for VD₂ and 70.1% for VD₃ after 15 days of storage.

The present study correlates well with the previously reported EEs of bioactives in MCE. For instance, the EE of L-ascorbic acid in the monodisperse W/O/W emulsions prepared through MCE was more than 80% after 10 d of storage at 4°C [29]. Semo *et al.* [48] and Ron *et al.* [49] encapsulated VD_2 in casein and β-lactoglobulin micelles and observed that reduction rate of encapsulated VD_2 was slower than VD_2 solubilized in ethanol-water mixture. Recently, Almouazen *et al.* [50] encapsulated VD_3 in polymeric nanoparticles for potential applications in chemotherapy and found its EE of around 90% with sustained release over a period of 7 days. The EE of VD_3 in poly(lactic-co-glycolic acid)-coated nanoparticles was around 74.8% [51]. Tippetts *et al.* [52] fortified milk with different emulsions containing VD_3, and the retention profile was observed in cheese curd. The emulsified cheese curd showed higher EE of VD_3 (74-78%) in comparison to non-emulsified cheese curd.

(a)
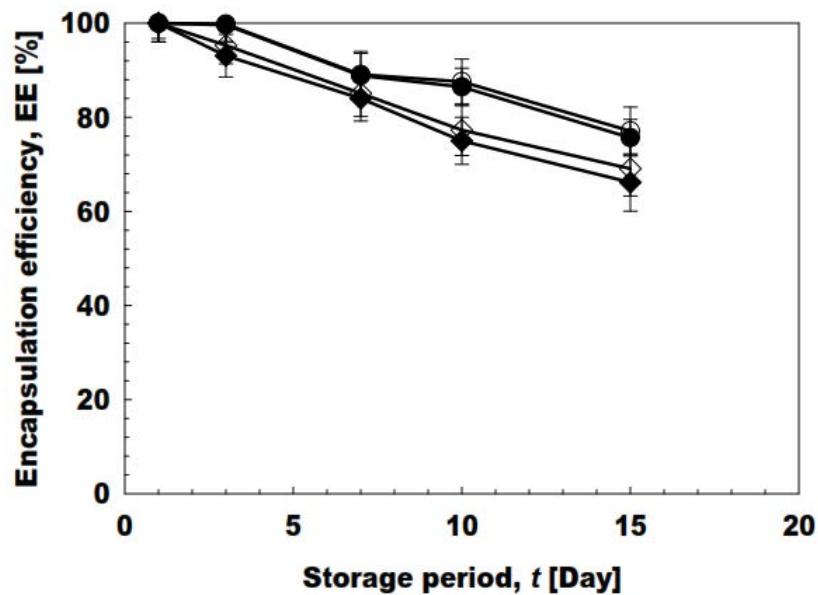
(b)
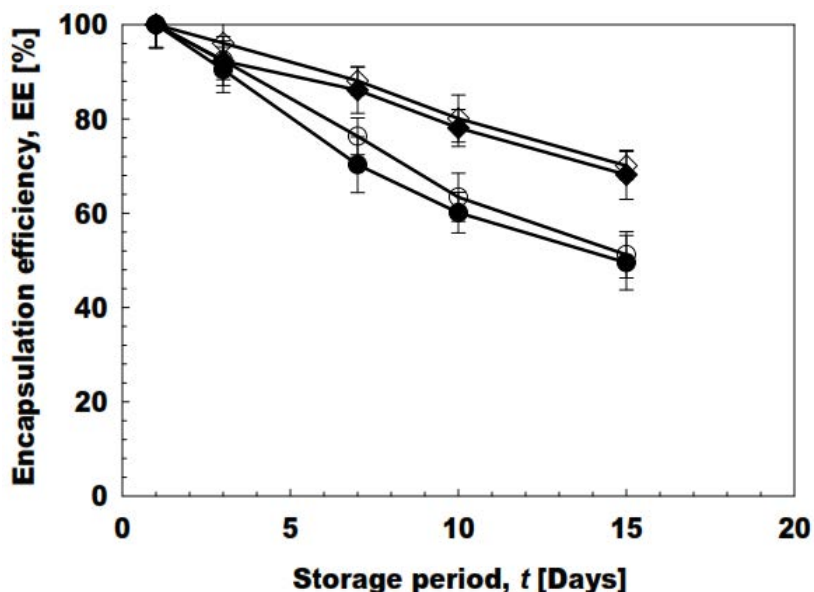
Figure 7.6: Encapsulating efficiencies (EEs) of ergocalciferol (VD₂) and chorecalciferol (VD₃) in the resultant O/W emulsions as a function of storage time. These emulsions were formulated at J_d of 5 L m^{-2} h^{-1} and the data are presented over 15 days of storage time. (a) EEs of Tween 20 stabilized emulsions and (b) EEs of Na-cholate stabilized emulsions. (━●━) denote EE of VD₂ at 4ºC, (━○━) EE of VD₃ at 4ºC, (━◆━) EE of VD₂ at 25ºC and (━◇━) denote EE of VD₃ at 25ºC.

References

[1] Holick MF, *New Engl J. Med.*, **357,** 266-281 (2007).

[2] Gonnet M, Lethuaut L and Boury F, *J.Controlled Release.*, **146,** 276-290 (2010).

[3] Lund J and DeLuca HF, *J. Lipid Res.*, **7,** 739-744 (1966).

[4] Rosenheim O and Webster TA, *Biochem J.*, **22,** 762-766 (1928).

[5] Christakos S, Ajibade DV, Dhawan P, Fechner AJ and Mady LJ, *Endocrinol. Metabol. Clin. North Am.*, **39,** 243-253, table of contents (2010).

[6] Holick MF, *Ann. Epidemiol.*, **19,** 73-78 (2009).

[7] Wagner CL, Hulsey TC, Fanning D, Ebeling M and Hollis BW, *Breastfeeding Med.*, **1,** 59-70 (2006).

[8] Davey GK, Spencer EA, Appleby PN, Allen NE, Knox KH and Key TJ, *Public health Nutr.*, **6,** 259-269 (2003).

[9] Outila TA, Karkkainen MU, Seppanen RH and Lamberg-Allardt CJ, *J. Am. Diet. Assoc.*, **100,** 434-441 (2000).

[10] Nakamura K, Nashimoto M, Hori Y and Yamamoto M, *Am. J. Clin. Nutr.*, **71,** 1161-1165 (2000).

[11] Haham M, Ish-Shalom S, Nodelman M, Duek I, Segal E, Kustanovich M and Livney YD, *Food Function*, **3,** 737-744 (2012).

[12] Holick MF, *Am. J. Clin. Nutr.*, **79,** 362-371 (2004).

[13] Tsiaras WG and Weinstock MA, *Acta dermato-venereologica*, **91,** 115-124 (2011).

[14] Kawakatsu T, Kikuchi Y and Nakajima M, *J. Am. Oil Chem. Soc.*, **74,** 317-321 (1997).

[15] Liu HJ, Nakajima M and Kimura T, *J. Am. Oil Chem. Soc.*, **81,** 705-711 (2004).

[16] Kobayashi I, Wada Y, Hori Y, Neves MA, Uemura K and Nakajima M, *Chem. Eng. Technol.*, **35,** 1865-1871 (2012).

[17] Kobayashi I, Mukataka S and Nakajima M, *Langmuir*, **21,** 7629-7632 (2005).

[18] Vladisavljevic' GT, Kobayashi I and Nakajima M, *Microfluid Nanofluid.*, **13,** 151-178 (2012).

[19] Vladisavljevic GT, Khalid N, Neves MA, Kuroiwa T, Nakajima M, Uemura K, Ichikawa S and Kobayashi I, *Adv. Drug Deliv. Rev.*, **65,** 1626-1663 (2013).

[20] Purwanti N, Neves MA, Uemura K, Nakajima M and Kobayashi I, *Colloid Surface A.*, **466,** 66-74 (2015).

[21] Hamada Y, Kobayashi I, Nakajima M and Sato K, *Crystal Growth Design*, **2,** 579-584 (2002).

[22] Sugiura S, Nakajima M, Tong JH, Nabetani H and Seki M, *J. Colloid Interface Sci.*, **227,** 95-103 (2000).

[23] Nakagawa K, Iwamoto S, Nakajima M, Shono A and Satoh K, *J. Colloid Interface Sci.*, **278,** 198-205 (2004).

[24] Chuah AM, Kuroiwa T, Kobayashi I, Zhang X and Nakajima M, *Colloid Surface A.*, **351,** 9-17 (2009).

[25] Kuroiwa T, Fujita R, Kobayashi I, Uemura K, Nakajima M, Sato S, Walde P and Ichikawa S, *Chem. Biodiversity*, **9,** 2453-2472 (2012).

[26] Neves MA, Ribeiro HS, Kobayashi I and Nakajima M, *Food Biophys.*, **3,** 126-131 (2008).

[27] Souilem S, Kobayashi I, Neves M, Sayadi S, Ichikawa S and Nakajima M, *Food Bioprocess Technol*, **7,** 2014-2027 (2014).

[28] Neves MA, Ribeiro HS, Fujiu KB, Kobayashi I and Nakajima M, *Ind. Eng. Chem. Res.*, **47,** 6405-6411 (2008).

[29] Khalid N, Kobayashi I, Neves MA, Uemura K, Nakajima M and Nabetani H, *Colloid Surface A.*, **458,** 69-77 (2014).

[30] Khalid N, Kobayashi I, Neves MA, Uemura K, Nakajima M and Nabetani H, *Colloid Surface A.*, **459,** 247-253 (2014).

[31] Loftsson T and Hreinsdottir D, *AAPS PharmSciTech*, **7,** E4 (2006).

[32] Grady LT and Thakker KD, *J. Pharm. Sci.*, **69,** 1099-1102 (1980).

[33] Markman G and Livney YD, *Food Function*, **3,** 262-270 (2012).

[34] DeRitter E, *J. Pharm. Sci.*, **71,** 1073-1096 (1982).

[35] Schwartz Z, Sylvia VL, Dean DD and Boyan BD, *Endocrinol.*, **139,** 534-545 (1998).

[36] Stio M, Celli A and Treves C, *IUBMB life*, **53,** 175-181 (2002).

[37] Vladisavljevic GT, Kobayashi I and Nakajima M, *Powder Technol.*, **183,** 37-45 (2008).

[38] Vladisavljević GT, Kobayashi I and Nakajima M, *Microfluid Nanofluid.*, **10,** 1199-1209 (2011).

[39] Laouini A, Fessi H and Charcosset C, *J. Membrane Sci.*, **423,** 85-96 (2012).

[40] Varade D, Patel V, Bahadur A, Bahadur P and Vethamuthu MS, *Indian J. Biochem. Biophys.*, **41,** 107-112 (2004).

[41] Kishore RS, Kiese S, Fischer S, Pappenberger A, Grauschopf U and Mahler HC, *Pharm Res.*, **28,** 1194-1210 (2011).

[42] Sugiura S, Nakajima M, Kumazawa N, Iwamoto S and Seki M, *J. Phys. Chem. B*, **106,** 9405-9409 (2002).

[43] Calabresi M, Andreozzi P and La Mesa C, *Molecules*, **12,** 1731-1754 (2007).

[44] Jojart B, Posa M, Fiser B, Szori M, Farkas Z and Viskolcz B, *PloS one*, **9,** e102114 (2014).

[45] Carnero Ruiz C, Molina-Bolívar J, Aguiar J, MacIsaac G, Moroze S and Palepu R, *Colloid Polym Sci*, **281,** 531-541 (2003).

[46] Guttoff M, Saberi AH and McClements DJ, *Food Chem.*, **171,** 117-122 (2015).

[47] Ziani K, Fang Y and McClements DJ, *Food Chem*, **134,** 1106-1112 (2012).

[48] Semo E, Kesselman E, Danino D and Livney YD, *Food Hydrocolloid*, **21,** 936-942 (2007).

[49] Ron N, Zimet P, Bargarum J and Livney YD, *Int. Dairy J.*, **20,** 686-693 (2010).

[50] Almouazen E, Bourgeois S, Jordheim LP, Fessi H and Briancon S, *Pharm. Res.*, **30,** 1137-1146 (2013).

[51] Domingues NJA, Carrier systems for vitamin D, in: Department of Biological Engineering, University of Porto, Porto, 2013.

[52] Tippetts M, Martini S, Brothersen C and McMahon DJ, *J. Dairy Sci.*, **95,** 4768-4774 (2012).

Chapter 8

Formulation and characterization of food grade oil-in-water emulsions encapsulating mixture of cholcalciferol and ergocalciferol by different homogenization techniques*

_____

8.1 Introduction

Vitamin D is called the antirachitic vitamin, since it counteracts rickets, helps to breaking-down mineral substance in fully grown bones (Osteodistrophy), bone and joint deformations and spontaneous brittleness of bones [1]. The term vitamin D refers to a pair of biologically inactive precursors; these are vitamin D_3, also known as cholecalciferol, and vitamin D_2 known as ergocalciferol. Cholecalciferol (D_3) is produced in the skin by a photoreaction on exposure to UV light from the sun (wavelength 290 to 320nm), while ergocalciferol (D_2) is produced in plants and enters human diet through consumption of plant sources [2, 3]. Vitamin D_2 and D_3 forms are inactive but once present in the circulation enter the liver and kidneys where they are hydroxylated to form active forms of D_2 and D_3 [4].

Vitamin D_2 and D_3 plays an important part in human and animal nutrition. It regulates the absorption, metabolism and excretion of calcium and phosphorus from the intestine and kidneys. Further it controls the incorporation of calcium and phosphorus in the skeleton [4]. The recommended daily intake of vitamin D is around 5 μg/day [5]. Most dietary products are poor source of vitamin D, including breast milk [6]. Vitamin D intake is found to be low in vegetarians and vegans [7, 8]. The high phytate and fiber content of vegetarian diets may also reduce the vitamin D absorption, in contrast consumption of fish at least four times a week (wild fatty fish) helps prevent vitamin D deficiency [9]. Similarly, vitamin D deficiency occurs due to lack of exposure of sun light, extensive use of UV protecting creams, lactose intolerance and religious restrictions [10-12].

Low fat or reduced fat products are highly desirable in human nutrition, but the processing of low fat products resulted in reduction of several micronutrients like fat soluble vitamins. Enrichment of low fat products with vital micronutrients is the challenging task in food industries. Encapsulation, emulsification, salting out, solvent evaporation and polymerization are the popular enrichment methods frequently used in food industries [13, 14]. All of these methods have positive and negative aspects, but in general each delivery system must be specifically designed for each application depending on the characteristics of the active agent to be encapsulated, e.g., solubility, physical and chemical stability. Previously, vitamin D is encapsulated in numerous systems like spontaneous emulsification [15], nanoparticles [16], casein micelles [17] and Poly(D, L)Lactic acid (PLA) nanoparticles prepared from nanoprecipitation method [18].

Fat soluble bioactives in its pure form, can be handled only with difficulty or not at all, because it is oxidation-sensitive substance. Furthermore, a fine dispersion of the fat soluble bioactive is advantageous for optimal absorbability and as well as bioavailability. These substances are therefore often supplied in the form of emulsions or in the dry powders or as solution in physiologically tolerated oil or embedded in a fine dispersion in a protective colloid. The challenges associated with vitamin D fortification are: poor water solubility; chemical degradation when exposed to light, oxygen, or elevated temperatures; and variable oral bioavailability [10,15]. In the current study, we aimed to formulate oil-in-water (O/W) emulsion-based delivery systems for vitamin D containing a mixture of both vitamin D_2 and D_3 by using a simple rotar-stator homogenizer and high pressure homogenization techniques. Moreover, we conducted comparative studies with both techniques on stability and release profile of vitamin D loaded emulsions.

8.2 Material and methods

Chemicals

Cholecalciferol (VD_3), ergocalciferol (VD_2), soybean oil, olive oil, disodium hydrogen phosphate dodecahydrate (sodium phosphate, dibasic), sodium dihydrogen phosphate dehydrate and polyoxyethylene (20) sorbitan monolaurate (Tween 20) were purchased from Wako Pure Chemical Ind. (Osaka, Japan). Medium chain triacylglycerol (MCT, sunsoft MCT-7) with a fatty acid residue composition of 75% caprylic acid and 25% capric acid was procured from Taiyo Kagaku Co. Ltd. (Mie, Japan). Milli-Q water with a resistivity of 18MΩ cm (pH 7.1) was used to dissolve the emulsifiers and served as continuous phase. All other chemicals used in this study were of analytical grade and used as received.

Dispersed and continuous phase preparation

0.5% (w/w) VD_2 was dissolved in heated soybean oil, olive oil and MCT at 75± 2°C and quickly cooled to room temperature. Afterwards, 0.5% (w/w) VD_3 was added to pre-loaded VD_2 solutions (soybean oil, olive oil and MCT) and stirred for 20 min for proper dissolution. The influence of temperature on VD_2 solubility in different oils was ascertained by measuring the turbidity as a function of temperature. Briefly, a known concentration of VD_2 was dispersed in different oils (0.5 mg mL^{-1}) at room temperature, which lead to the formation of turbid suspension. The turbidity of these samples was then measured as function of

temperature from 25 to 100°C by using an UV/VIS/NIR spectrophotometer (V-570, Jasco, Hachioji, Japan) at 600 nm. This experiment shows that the samples above 70°C become clear (original oil color), and so we choose 75°C as optimum temperature to dissolve VD_2 in different oils. The continuous phase comprises 1% (w/w) Tween 20 in Milli-Q water and used as such during emulsification. The pH of continuous phase during emulsification was 7.1.

Preparation of O/W through rotar-stator homogenization

The O/W emulsions were prepared from a dispersed oil and continuous phase. The dispersed phase constitutes 0.5% (w/w) VD_2 and VD_3 in soybean oil, olive oil or MCT, while the continuous phase contain 1% (w/w) Tween 20 in Milli-Q water. The volume fraction of the dispersed aqueous phase (ϕ_d) was fixed to 30 g 100 g^{-1}. Thirty mL of dispersed phase were added to seventy mL of continuous phase at room temperature (~25°C), followed by emulsification at various rotation speed (5000 to 20,000 rpm) for 5 min with a polytron homogenizer (PT-3000 Kinematica-AG, Littace, Switzerland).

Preparation of O/W through high-pressure homogenization

Two step homogenization technique was adopted to prepare O/W emulsions with high pressure homogenizer. In the first step a premix emulsions were obtain by homogenizing dispersed and continuous phases at 7,000 rpm for 5 min by using polytron homogenizer (PT-3000 Kinematica-AG, Littace, Switzerland), and immediately followed by high-pressure homogenization (Microfluidizer Processor Model M-110EH, Microfluidics Corporation, Newton, ME, USA) in a single pass at 100 MPa. The pH of all prepared O/W emulsions was 7.1.

Physicochemical properties of the continuous and dispersed phases

The densities of the liquid phases were measured with a digital density meter (DA-130 N, Kyoto Electronics Manufacturing Co., Ltd., Kyoto, Japan) at 25 ± 2°C. The viscosities of the emulsified fluids were measured with a vibro viscometer (SV-10, A&D Co., Ltd., Tokyo, Japan) at 25 ± 2°C by taking 35 mL of samples in a measuring vessel followed by immersion of sensor plates in that vessel. The frequency

and amplitude of the resonating gold plates were maintained at 30 Hz during measurement. Absolute

viscosity (η) was then calculated from the real viscosities of fluids by

$$\eta = \frac{\eta_{mea}}{\rho} \qquad (8.1)$$

where η_{mea} is the measured fluid viscosity and ρ is the fluid density. The static interfacial tension between

the two emulsified phases were measured with a fully automatic interfacial tensiometer (PD-W, Kyowa

Interface Sciences Co., Ltd., Saitama, Japan) using a pendant drop method. The key physical properties of

liquid phases were presented in Table 8.1.

Droplet size determination and ζ-potential measurements

The particle size distribution of sub-micron O/W emulsion droplets encapsulating VD_2 and VD_3 was

measured by using laser diffraction particle size analyzer, that works on the principle of Polorization

Intensity Differential Scattering (PIDS) Technology (Beckman Coulter LS 13 320, Miami, FL, USA). This

instrument has ability to measure the size ranging from 0.04 to 2000 μm. The mean droplet size was

expressed as volume mean diameter ($d_{4,3}$) i.e. the diameter of a droplet having the same volume in total

weight of emulsions and expressed as:

$$d_{4,3} = \frac{\sum n_i \, d_i^4}{\sum n_i d_i^3} \qquad (8.2)$$

where n_i is the number of droplets of diameter d_i. The width of droplet size distribution was

expressed as relative span factor (RSF) and is defined as:

$$\text{RSF} = \frac{D_{v0.9} - D_{v0.1}}{D_{v0.5}} \qquad (8.3)$$

Where $D_{v0.9}$ and $D_{v0.1}$ are the representative diameters where 90%, 10% and 50% of the total

volume of the liquid is made up of droplets with diameters smaller than or equal to the stated value. While

$D_{v0.5}$ is the representative diameter where 50% of the total volume of the liquid is made up of droplets with

diameters larger than the stated value and 50% is made up of droplets with diameters smaller than the

stated value.

The ζ-potential of O/W emulsions encapsulating VD_2 and VD_3 was measured by Dynamic Light

Scattering (Zetasizer Nano ZS, Malvern Instruments Ltd., Worcestershire, UK). All measurements were

recorded in triplicate and reported as the average and standard deviation.

Physical and chemical stability of O/W emulsions

The physical stability of O/W emulsions encapsulating 0.5% (w/w) VD_2 and VD_3 were observed by using laser diffraction particle size analyzer as described in section 2.5 to evaluate $d_{4,3}$, RSF, consistency and coalescence during 30 d of storage at $4 \pm 1°C$. The chemical stability of emulsion extracts either in ethanol or hexane was determined spectrophotometrically using a UV/VIS/NIR spectrophotometer (UV-1700, Shimazdu, Co. Japan).

The 1 mL of the emulsion was extracted either with 9 mL of ethanol or hexane and followed by ultrasonication for 20 min. The extracts were then centrifuged (Avanti HP-25, Beckman Coulter, Miami, FL) at 20,000 g for 15 min. 1 mL aliquot of the subnatants was diluted five times with ethanol for quantification of VD_2 and hexane for quantification of VD_3. Afterwards, 3 mL of aliquot was injected into a quartz cell with a 10 mm pass length. The absorbance of VD_2 and VD_3 in emulsion extract was measured at 310 nm using an appropriate blank.

A representative standard curve of absorbance versus concentration gave linear least-squares regression with a coefficient of determination (r^2) of 0.999. All experiments were repeated in triplicate and mean values were calculated. The Beer's law was obeyed in the concentration range of 0.01-0.5 mg mL^{-1} for VD_2 and VD_3 the sensitivity of measurement has relative standard deviation of 0.85% (n=15). The Molar absorptivity (ε) for VD_2 during this study was 0.61 mM^{-1} cm^{-1} and for VD_3 was 0.4 mM^{-1} cm^{-1}. The encapsulation efficiency of VD_2 and VD_3 in samples was calculated with the equation:

$$EE_{vita_{D_2}} = \frac{weight\ of\ free\ vitamin_{D_2}}{Weight\ of\ encapsulated\ vitamin_{D_2}} \times 100 \qquad (8.4)$$

$$EE_{vita_{D_3}} = \frac{weight\ of\ free\ vitamin_{D_3}}{Weight\ of\ encapsulated\ vitamin_{D_3}} \times 100 \qquad (8.5)$$

8.3 Results and discussion

Effect of emulsifying techniques on preparation of O/W emulsions

Rotar-stator homogenization

Fig. 8.1 shows the effect of homogenization speed on $d_{4,3}$ and span width of O/W emulsions containing 0.5% (w/w) VD_2 and VD_3. The O/W emulsions were successfully prepared at 5,000 rpm or higher, whereas

lower speed of homogenization resulted in incomplete homogenization and phase separation in short time. $d_{4,3}$ of resultant emulsions gradually decreased from 28.34 μm to 6.86 μm by increasing speed of homogenization form 5,000 to 20,000 rpm. The O/W emulsions prepared at 5,000 and 7,000 rpm completely phase separated within 2 h of formation, while all other emulsions remained stable without any prominent phase separation or physical deformation. The span width of O/W emulsions was in between 1.03 to 3.40. The higher span width indicates polydispersity in formulated emulsions.
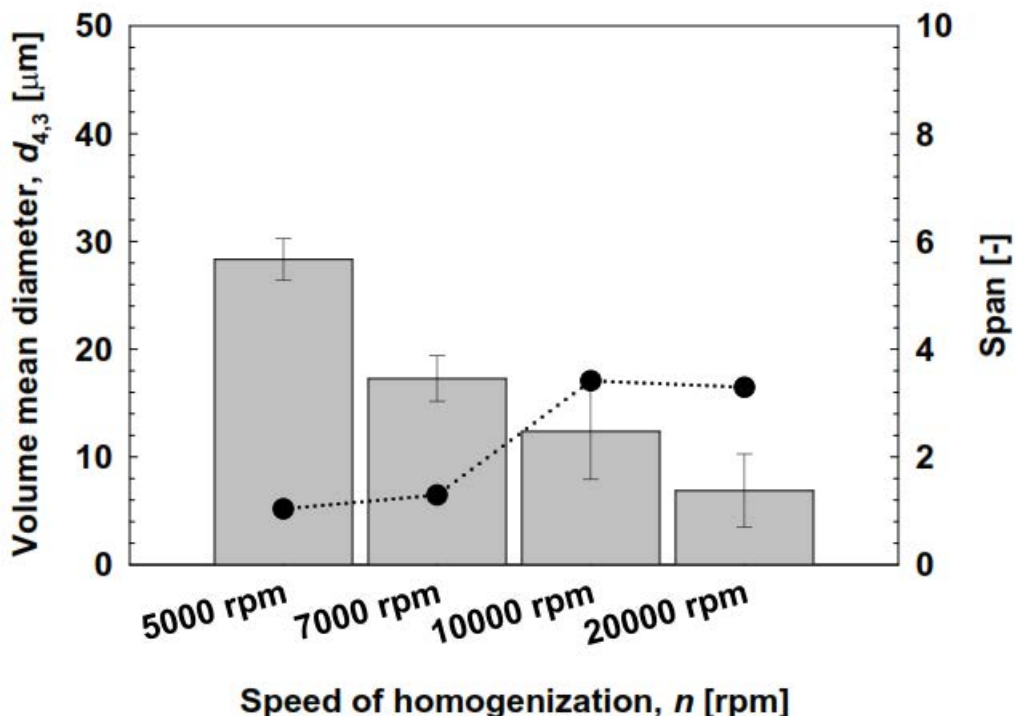
Figure 8.1: Effect of rotor-stator homogenization speed on $d_{4,3}$ and span width of O/W emulsions encapsulating vitamin D₂ and D₃. Grey bar denote $d_{4,3}$ of emulsions and (˙●˙) span width of O/W emulsions.

Homogenization at 20,000 rpm slightly increased the temperature to more than 40.2°C in comparison to 28-35°C in emulsions produced at low speed of homogenization. However, such variation in temperature has no prominent effect on encapsulation efficiencies (EE) of VD_2 and VD_3 (Fig. 8.2). The initial EEs of VD_2 and VD_3 were more than 80% just after emulsification with different speed of homogenization. Moreover, a slightly higher yield of VD_2 was observed in emulsions in companion to VD_3. The higher yield of VD_2 was in order of 3-4% in comparison to VD_3.
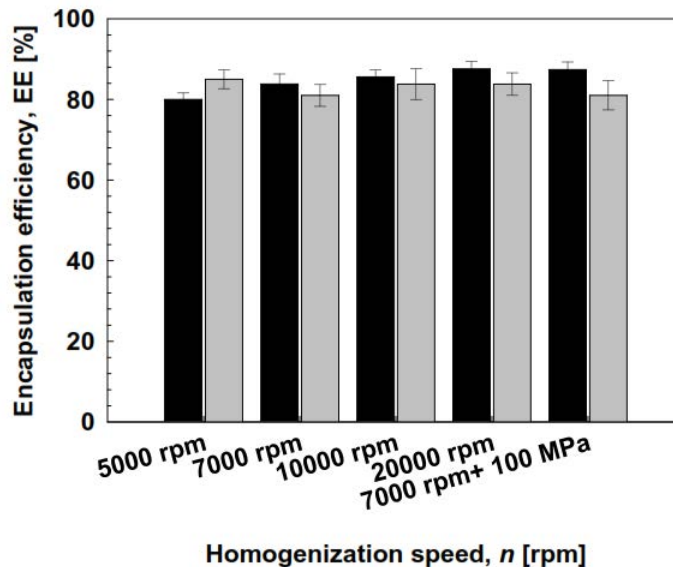
Figure 8.2: Encapsulation efficiencies (EEs) of O/W emulsions produced from rotor-stator and high pressure homogenization techniques. The EEs were quantified in soybean oil by two step extraction process. Black bars denote EEs of VD_2, while grey bars present EEs of VD_3.

The production of emulsions with rotar-stator homogenizer (RSH) depends upon the rotational speed of shaft, which can easily be co-related with energy of homogenization. The higher the input energy, the smaller will be the droplet size. However, uniformity of droplet size distribution depends upon the type of emulsion (O/W or W/O) formulated and the strength of emulsifier [19, 20]. High emulsion stability for O/W emulsions is obtained by using emulsifiers having hydrophilic and lipophilic balance (HLB) greater than 10 [21]. In our study we used polyoxyethylene (20) sorbitan monolaurate as emulsifier and have HLB value around 16.7. The high HLB value reduces the interfacial tension and gives extra stability to O/W emulsions even at low speed of homogenization.

High-pressure homogenization

To conduct a comparative study with RSH, O/W emulsions were also prepared with high pressure homogenization (HPH). A premix emulsion ($\phi_d = 30\%$) was prepared with RSH at 7,000 rpm for 5 min and immediately carried out HPH at 100 MPa in a single pass. This treatment resulted in a well stable O/W emulsion having smooth consistency with bright whitish color. Fig. 8.3 shows droplet size distribution of premix and high pressure treated O/W emulsions. The normal distributed curve in emulsions treated with

193

HPH shows monodispersity in emulsion system in comparison to RSH. The high pressure treated emulsions have $d_{4,3}$ of 0.40 μm with span width < 1.
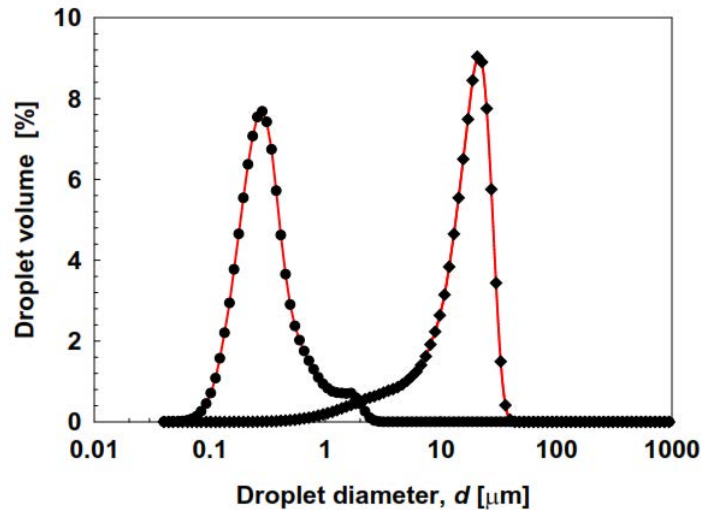
Figure 8.3: Droplet size distribution of premix O/W emulsion at 7,000 rpm and high pressure homogenized O/W emulsion at 100 MPa in single pass. The dispersed phase contains vitamin D_2 and D_3 in soybean oil. (——◆——) denote droplet size distribution of premix O/W emulsion and (——●——) denote droplet size distribution of high pressure homogenized O/W emulsion.

HPH has no marked effect on EEs of VD_2 and VD_3 (Fig. 8.2). The initial EEs of VD_2 and VD_3 were more than 80% in both premix and high pressure treated O/W emulsions. HPH is a non-thermal technology capable of producing O/W and W/O emulsions on sub-micron scale and have potential benefit in food industries. The narrow size droplet distribution with HPH have marked influence on shelf life and texture of different emulsion systems [22]. Recently, Ziani *et al.* [23] formulated VD_3 loaded O/W emulsions by using blend of 10% (w/w) oil and 90% (w/w) aqueous phase containing 1% (w/w) non-ionic surfactants over 5 cycles in the high pressure homogenizer at 62 MPa. The obtained O/W emulsion was resistant to particle growth and had average particle size of around 0.2 μm.

Effect of oil type on droplet sizes of O/W emulsions prepared from RSH and HPH

The ability of different oils to encapsulate VD_2 and VD_3 in O/W emulsions prepared with RSH was investigated by using soybean oil, olive oil and MCT. These oils were selected on the basis of functionality. Soybean and olive oil contain varieties of phospholipids, sterols and fatty acids, while MCT comprises only of caprylic and capric acid. Successful emulsification was conducted with different oil type from 5,000 to 20,000 rpm for 5 min. Fig. 8.4 shows the $d_{4,3}$ of different O/W emulsions in relation to oil type and speed of

homogenization. The droplet size decreases with speed of homogenization in all oil types. The smallest $d_{4,3}$ was obtained with soybean oil in comparison to olive oil and MCT. The prepared emulsions at low speed of homogenization phase separated quickly, while emulsions prepared at 10,000 and 20,000 rpm remain stable for more than 30 days without showing any physical deformity. Emulsions prepared at low speed of homogenization phase separated probably due to Ostwald ripening. Ostwald ripening leads to droplet growth due to mass transport of oil molecules, from smaller to larger droplets, since RSH produce emulsions with polydisperse droplets and normally has span width greater than 1.5 [22]. Fig. 8.5 shows the optical micrographs of O/W emulsions prepared with different oil types. The presence of large droplets clearly reflect polydisperse emulsions, while at higher speed of homogenization, relatively monodisperse droplets were seen in MCT oil type, the possible reason for such monodispersity is the low viscosity of MCT in comparison to soybean and olive oil. The generation of smaller droplets during homogenization depends upon the ratio of viscosity of the dispersed phase to that of the continuous phase [24]
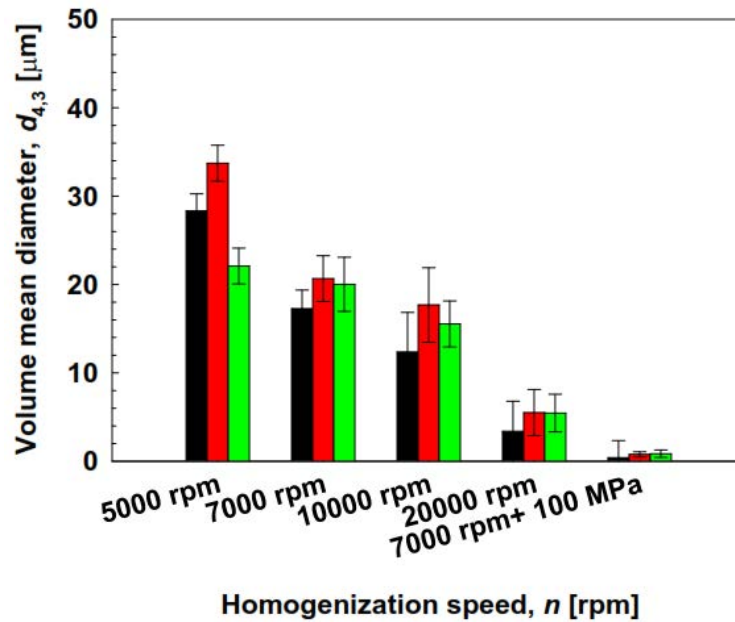
Figure 8.4: Effect of rotor-stator homogenization speed on $d_{4,3}$ of O/W emulsions containing different oil types. (■) shows O/W emulsions containing soybean oil, (■) denote olive oil and (■) denote O/W emulsions containing MCT.
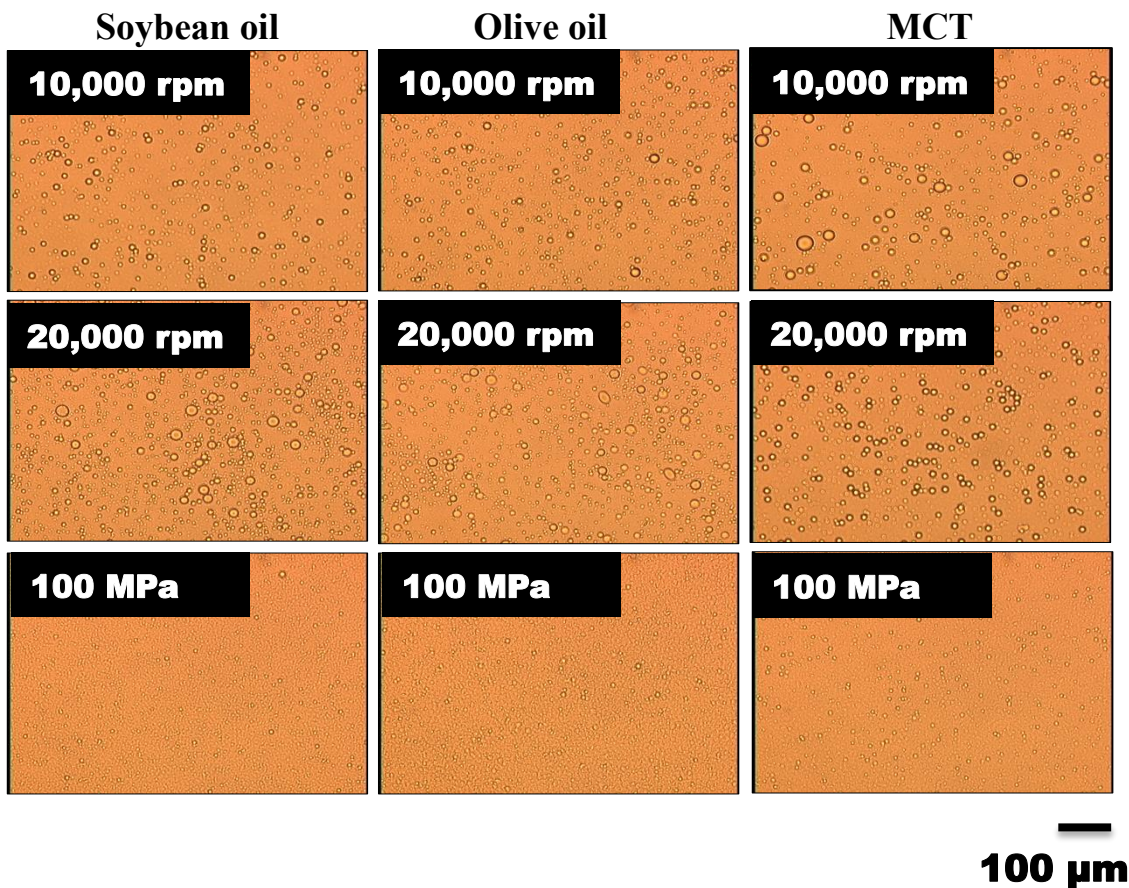
Figure 8.5: Optical micrographs of O/W emulsions with different oil types prepared with rotor-stator homogenizer at 10,000 and 20,000 rpm and with high pressure homogenizer at 100 MPa in single pass.

The premix O/W emulsions prepared with MCT, soybean and olive oil at 7,000 rpm for 5 min was subject to HPH at 100 MPa. Significant reduction in $d_{4,3}$ was observed with all oil types. Among them the smallest $d_{4,3}$ was obtained with soybean oil (0.40 μm) followed by olive oil (0.77 μm) and MCT (0.85 μm). Similarly, monomodal droplet size distribution was observed with soybean oil (Fig. 8.6) in comparison to olive oil and MCT. Olive oil and MCT has distant bimodal peaks, indicating droplet growth even after HPH. An increased $d_{4,3}$ with olive oil can be attributed to the high viscosity of the oil phase (Table 8.1), the high viscosity makes droplet distribution with in HPH more difficult [22, 24]. The above results slightly deviates from previous study of Ziani, *et al.* [23], they obtained monomodal peak of O/W emulsions encapsulating VD$_3$ in MCT with average droplet size diameter around 220 nm. However, they pointed

bimodal distribution of droplets with viscous oil loaded with vitamin E and the above findings correlated

with their results [23].

Table 8.1: Fluid properties of two-phase system containing vitamin D$_2$ and D$_3$ used for preparing O/W emulsions

Emulsion phase	Density (Kg m^{-3})	Viscosity (mPa s)	Interfacial tension (mN m^{-1})	Zeta potential (-mV)
Dispersed phase*				
Soybean oil	917.8 ± 0.55	52.9 ± 0.06	5.5 ± 0.40	-56.5 ± 0.09
Olive oil	929.5 ± 0.23	62.2 ± 0.10	6.2 ± 0.20	-51.5 ± 1.63
MCT	943.8 ± 0.26	22.1 ± 0.10	5.2 ± 0.40	-55.3 ± 0.21
Continuous phase**				
1% (w/w) Tween 20	999.0 ± 0.20	0.87 ± 0.01		

*Dispersed phase contains 0.5% (w/w) ergocalciferol and cholecalciferol in different oil types
**Continuous phase includes 1% (w/w) Tween 20 in phosphate buffer (pH 7.0)
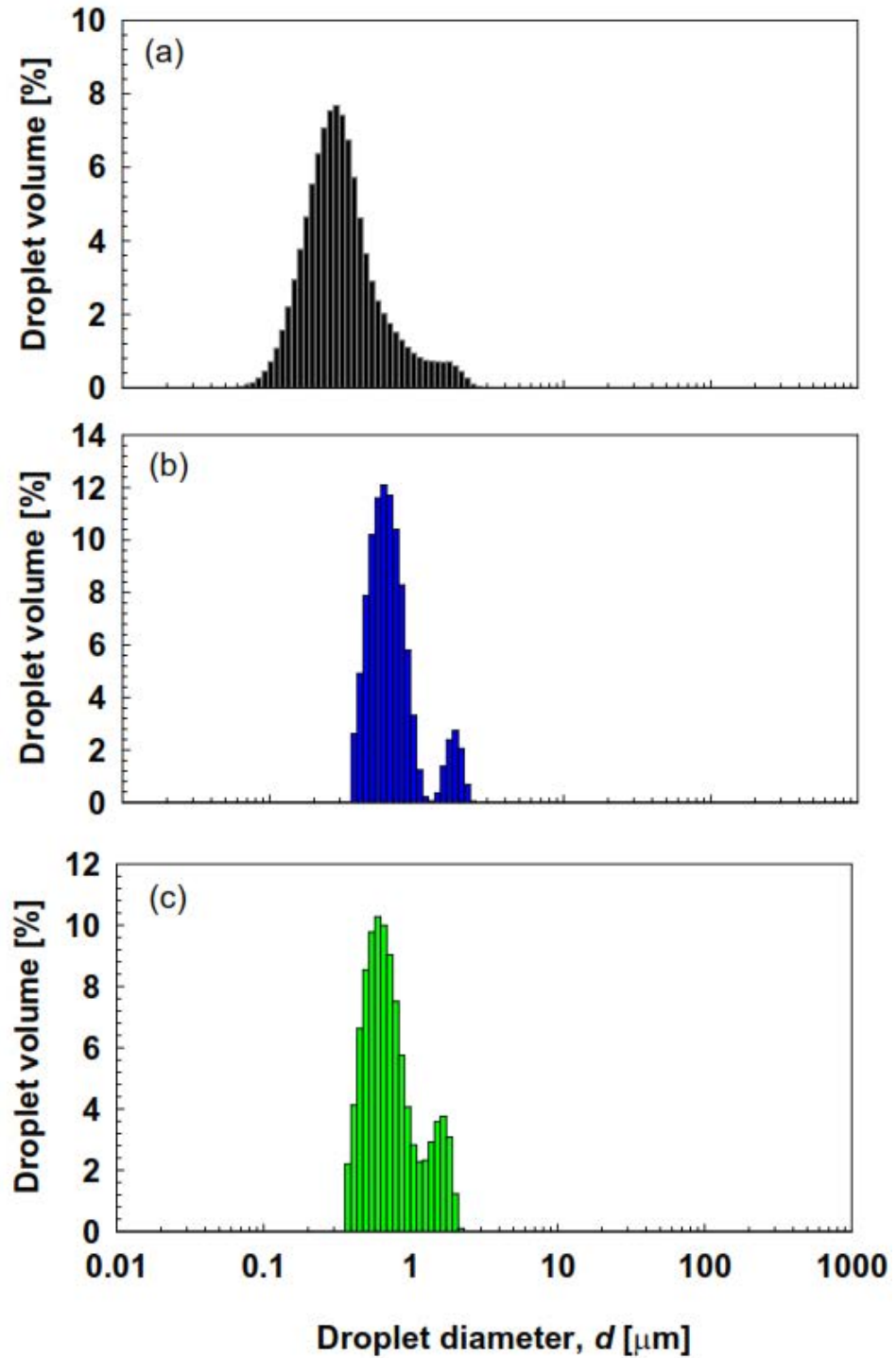
Figure 8.6: Droplet size distribution of emulsions formulated with different oil types with high pressure homogenizer at 100 MPa. (■) shows emulsions containing soybean oil, (■) denote olive oil and (■) denote O/W emulsions containing MCT.
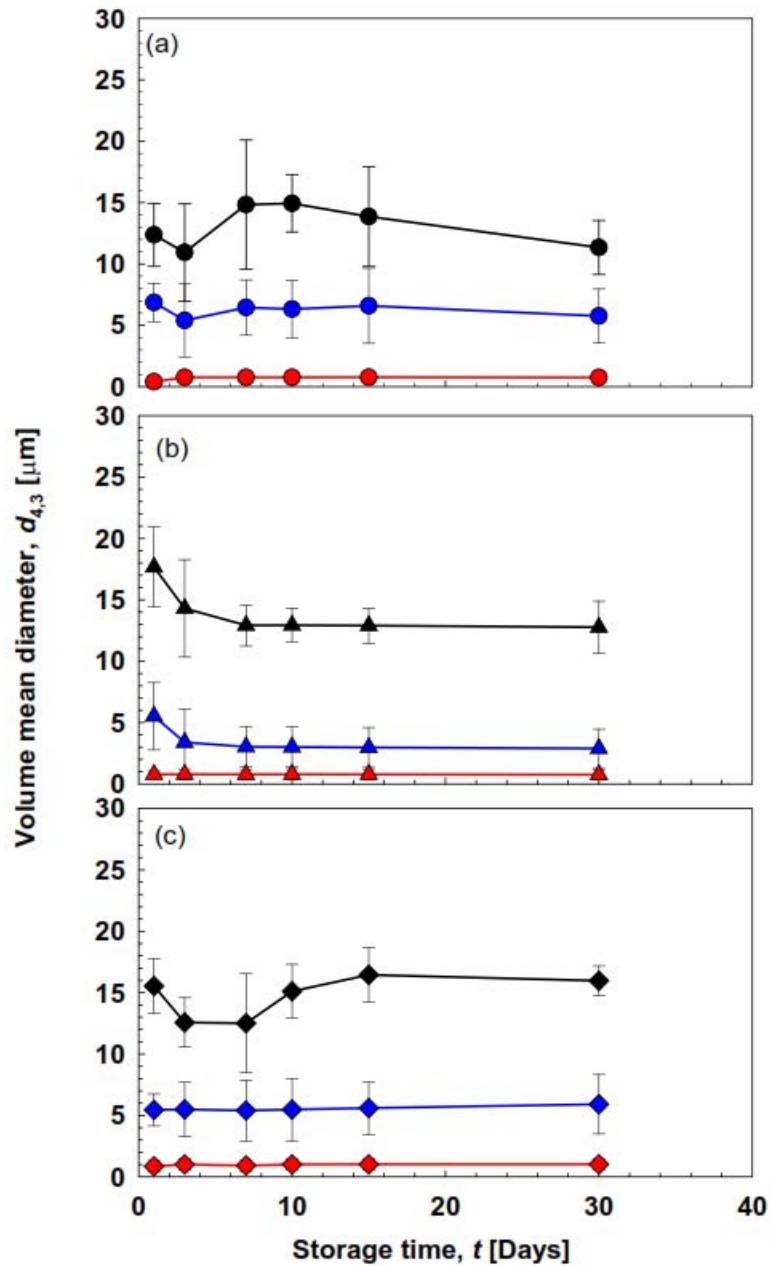
Figure 8.7: Storage stabilities of O/W emulsions with different oil types for a period of 30 days. (a) Soybean oil stability (–●–) denotes emulsions formulated at 10,000 rpm, (–●–) denote emulsions formulated at 20,000 rpm and (–●–) denotes emulsions formulated at 100 MPa. b) Olive oil stability, (–▲–) denotes emulsions formulated at 10,000 rpm, (–▲–) denote emulsions formulated at 20,000 rpm and (–▲–) denotes emulsions formulated at 100 MPa. (c) MCT stability, (–◆–) denotes emulsions formulated at 10,000 rpm, (–◆–) denote emulsions formulated at 20,000 rpm and (–◆–) denotes emulsions formulated at 100 MPa.

Encapsulation efficiency of O/W emulsions encapsulating vitamin D_2 and D_3

Fig. 8.8 shows encapsulation efficiencies (EEs) VD_2 in different O/W emulsions. The freshly prepared rotor-stator homogenized emulsions with soybean oil have EE over 85 and 87% at 10,000 and 20,000 rpm respectively. The olive oil containing emulsions have EE over 71 and 67.5% at 10,000 and 20,000 rpm, while MCT containing emulsions retains about 42% VD_2 at 10,000 and 20,000 rpm respectively. There was significant reduction in EEs of VD_2 in O/W emulsions with storage time. At day 30, soybean oil retains <10%, olive oil <3% and MCT <23% VD_2 respectively. Polydisperse droplet size distribution and diffusion of oil droplets to aqueous phase resulted in significant loss of VD_2 from O/W emulsions.

Slightly higher initial EEs were observed in emulsions prepared with HPH. The initial EE with soybean oil was 87%, 65% with olive oil and 57% with MCT. These emulsions retain about 50% VD_2 after 15 days of storage at 4ºC. Afterwards, there was sharp decline in EEs and at day 30; the EEs were in order of 2%, 6% and 23.3% with soybean, olive oil and MCT respectively. Dahan and Hoffman [30] evaluated the impact of short (C_2triacetin), medium (C_{8-10}, glyceryl tricaprylate/caprate) and long chain (C_{18}, peanut oil) triglyceride (SCT. MCT and LCT respectively) on VD_3 absorption. The bioavailability (*in vitro* lipolysis) indicated a rank order of MCT > LCT > SCT, but the *in vivo* bioavailability followed LCT > MCT > SCT. A slightly higher retention in MCT in our studies correlated with the study of Dahan and Hoffman [30].

Fig. 8.9 shows EEs of VD_3 in different O/W emulsions. The freshly prepared emulsions from RSH containing soybean oil have EE of 83 and 73% at 10,000 and 20,000 rpm. A slightly lower EE of 70% was observed with olive oil at 10,000 and 20,000 rpm respectively. In contrast, MCT containing emulsions have higher EEs of 91 and 94% at 10,000 and 20,000 rpm. All of these emulsions retains good amount of VD_3 up to 7 days of storage, after then there was sharp decline in EEs of VD_3 the trend can more obvious in olive oil and MCT in comparison to soybean oil emulsions. After 30 days of storage the retention was about 10% in all O/W emulsions prepared with RSH. The initial EEs with HPH were more than 80% in all emulsions containing soybean, olive oil and MCT. Soybean oil retains about 70% VD_3 after 10 days of storage, whereas olive oil retains 39% and MCT 50% after same storage period. The Sharpe decline in EEs were also observed in emulsion prepared with HPH and follows the order olive oil > MCT > soybean oil. The possible interpretation of sharp decline can be deduced from two reasons, firstly the prepared emulsions either with RSH or HPH contains polydisperse droplets. This polydisperity allows the small

droplets to grow with time due to Oswald ripening; moreover this process is accelerated due to viscosity difference between oil and aqueous phases [22]. Secondly, vitamin D might migrate to the interface of O/W emulsions with respect to storage time that resulted in rapid decline in EEs of emulsions. VD_2 has a predicted intrinsic solubility value of log S = -5.96, which indicate that part of the molecule possess hydrophilic characters due to its OH groups [31]. Menéndez-Aguirre, et al. [17] encapsulated VD_2 in casein micelles with application of high pressure treatments. They concluded that application of high pressure treatment with a slow release rate increased VD_2 retention, while fast release of pressure reduces the retention of VD_2. The lower stability of vitamin D loaded emulsions were also reported by Ziani, et al. [23] and the addition of co-surfactant might increase the thermal stability of vitamin D loaded emulsions [23].
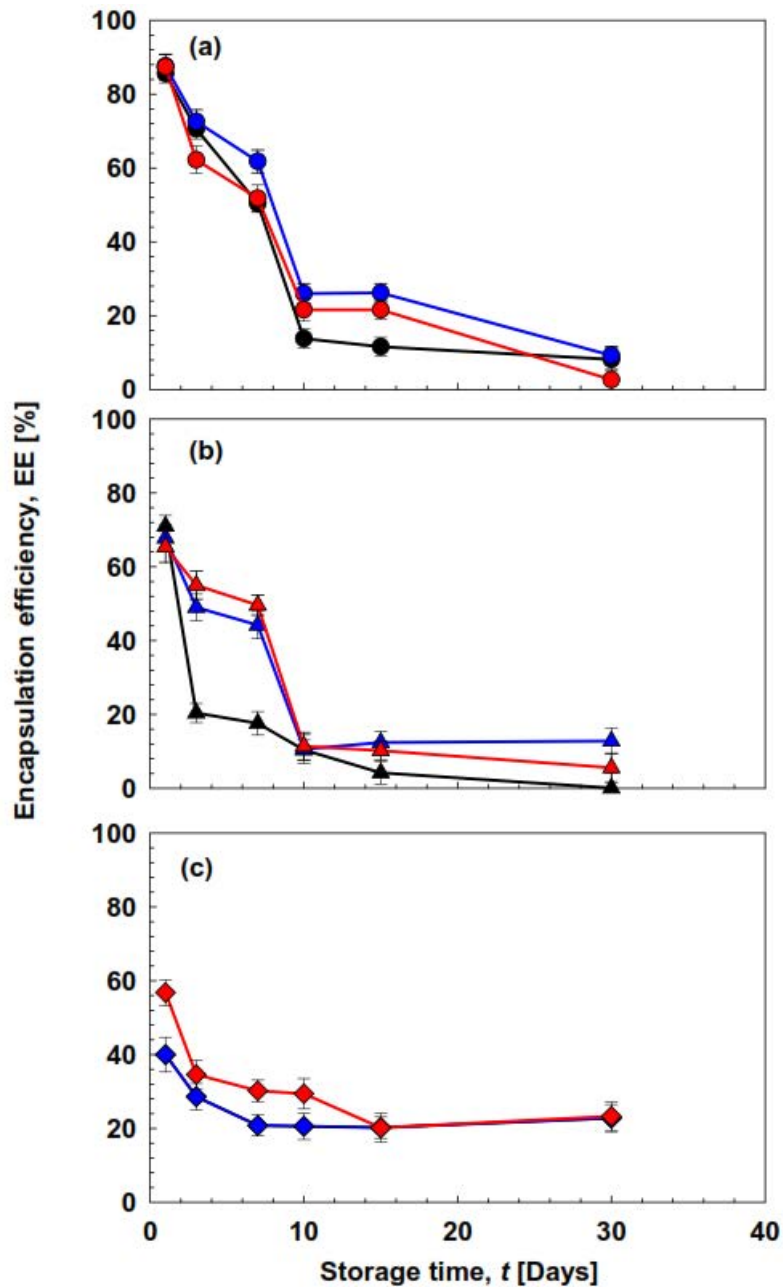
Figure 8.8: Encapsulation efficiencies (EEs) of O/W emulsions encapsulating ergocalciferol (VD$_2$). (a) Soybean oil containing emulsions, (●) denotes emulsions formulated at 10,000 rpm, (●) denote emulsions formulated at 20,000 rpm and (●) denotes emulsions formulated at 100 MPa. (b) Olive oil emulsions, (▲) denotes emulsions formulated at 10,000 rpm, (▲) denote emulsions formulated at 20,000 rpm and (▲) denotes emulsions formulated at 100 MPa. (c) MCT containing O/W emulsions, (◆) denotes emulsions formulated at 10,000 rpm, (◆) denote emulsions formulated at 20,000 rpm and (◆) denotes emulsions formulated at 100 MPa.
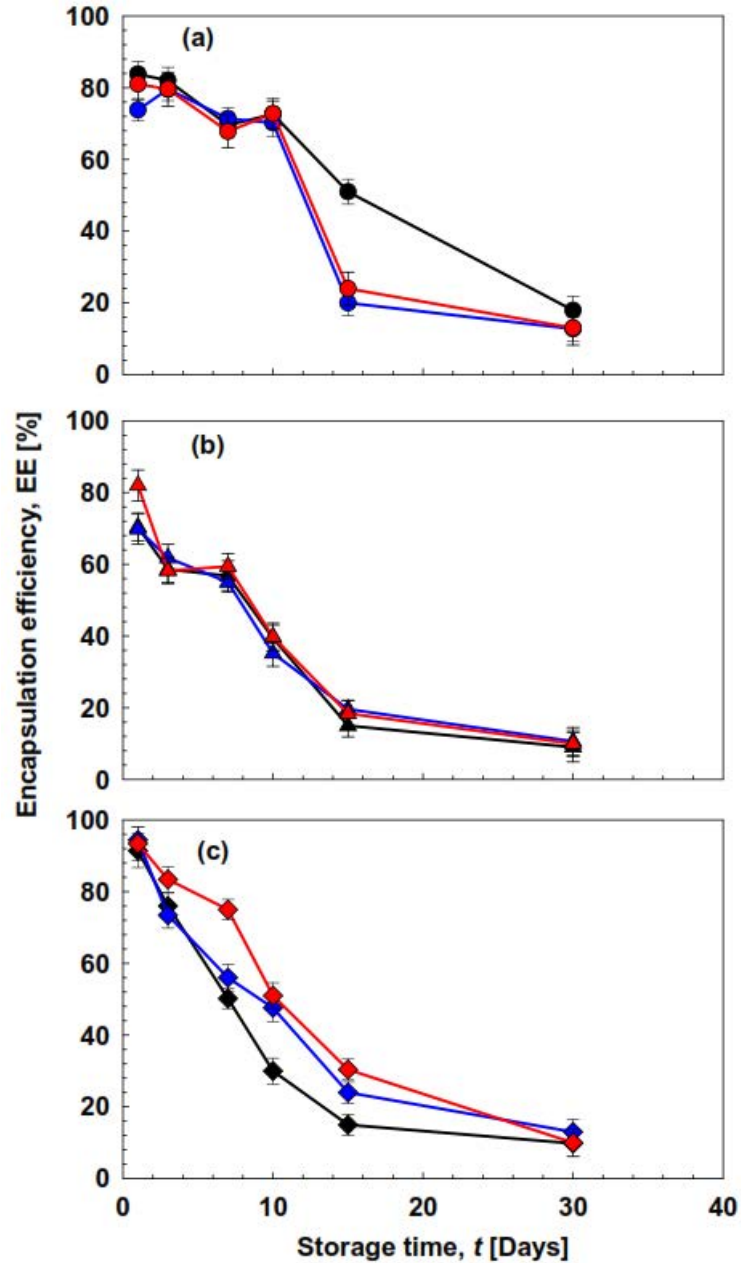
Figure 8.9: Encapsulation efficiencies (EEs) of O/W emulsions encapsulating cholecalciferol (VD₃). (a) Soybean oil containing emulsions, (–●–) denotes 10,000 rpm, (–●–) denote e 20,000 rpm and (–●–) denotes 100 MPa. (b) Olive oil emulsions, (–▲–) denotes 10,000 rpm, (–▲–) denote 20,000 rpm and (–▲–) denotes 100 MPa. (c) MCT containing O/W emulsions, (–◆–) denotes emulsions formulated at 10,000 rpm, (–◆–) denote emulsions formulated at 20,000 rpm and (–◆–) denotes emulsions formulated at 100 MPa.

References

[1] Bandeira F, Costa AG, Soares Filho MA, Pimentel L, Lima L and Bilezikian JP, *Arquivos brasileiros de endocrinologia e metabologia*, **58,** 504-513 (2014).

[2] Holick MF, *J. Cell Biochem.*, **88,** 296-307 (2003).

[3] Holick MF, *J. Investigate Med.*, **59,** 872-880 (2011).

[4] Christakos S, Ajibade DV, Dhawan P, Fechner AJ and Mady LJ, *Endocrinol. Metabol. Clin. North Am.*, **39,** 243-253, (2010).

[5] Gonnet M, Lethuaut L and Boury F, *J. Controlled Release.*, **146,** 276-290 (2010).

[6] Wagner CL, Hulsey TC, Fanning D, Ebeling M and Hollis BW, *Breastfeed Med.*, **1,** 59-70 (2006).

[7] Davey GK, Spencer EA, Appleby PN, Allen NE, Knox KH and Key TJ, *Public health Nutr.*, **6,** 259-269 (2003).

[8] Outila TA, Karkkainen MU, Seppanen RH and Lamberg-Allardt CJ, *J. Am. Diet. Assoc.*, **100,** 434-441 (2000).

[9] Nakamura K, Nashimoto M, Hori Y and Yamamoto M, *Am. J. Clin. Nutr.*, **71,** 1161-1165 (2000).

[10] Haham M, Ish-Shalom S, Nodelman M, Duek I, Segal E, Kustanovich M and Livney YD, *Food Function*, **3,** 737-744 (2012).

[11] Holick MF, *Am. J. Clin. Nutr.*, **79,** 362-371 (2004).

[12] Tsiaras WG and Weinstock MA, *Acta dermato-venereologica*, **91,** 115-124 (2011).

[13] Huang Q, Yu H and Ru Q, *J. Food Sci.*, **75,** R50-R57 (2010).

[14] Weiss J, Takhistov P and McClements DJ, *J. Food Sci.*, **71,** R107-R116 (2006).

[15] Guttoff M, Saberi AH and McClements DJ, *Food Chem.*, **171,** 117-122 (2015).

[16] Abbasi A, Emam-Djomeh Z, Mousavi MA and Davoodi D, *Food Chem.*, **143,** 379-383 (2014).

[17] Menéndez-Aguirre O, Stuetz W, Grune T, Kessler A, Weiss J and Hinrichs J, *High Pressure Res.*, **31,** 265-274 (2011).

[18] Almouazen E, Bourgeois S, Jordheim LP, Fessi H and Briancon S, *Pharm. Res.*, **30,** 1137-1146 (2013).

[19] Wang Z, Neves MA, Yin L-J, Kobayashi I, Uemura K and Nakajima M, *Food Sci. Technol. Res.*, **18,** 149-156 (2012).

[20] Khalid N, Kobayashi I, Neves MA, Uemura K and Nakajima M, *LWT-Food Sci. Technol*, **51,** 448-454 (2013).

[21] Schott H, *J. Pharm. Sci.*, **84,** 1215-1222 (1995).

[22] McClements DJ, Food emulsions: principles, practice, and techniques, 2nd ed., CRC press, Boca Raton, USA, 2005.

[23] Ziani K, Fang Y and McClements DJ, *Food Chem*, **134,** 1106-1112 (2012).

[24] Walstra P, *Chem. Eng. Sci.*, **48,** 333-349 (1993).

[25] Prinderre P, Piccerelle P, Cauture E, Kalantzis G, Reynier JP and Joachim J, *Int. J. Pharm.*, **163,** 73-79 (1998).

[26] Vladisavljević GT and Schubert H, *J. Membrane Sci.*, **225,** 15-23 (2003).

[27] Elwell MW, Roberts RF and Coupland JN, *Food Hydrocolloid*, **18,** 413-418 (2004).

[28] Floury J, Desrumaux A and Lardières J, *Innov. Food Sci. Emerg. Technol.*, **1,** 127-134 (2000).

[29] Tadros TF, Applied surfactants: principles and applications, John Wiley & Sons, 2006.

[30] Dahan A and Hoffman A, *Pharm. Res.*, **23,** 2165-2174 (2006).

[31] Box KJ and Comer JE, *Curr. Drug Metabol.*, **9,** 869-878 (2008).

Chapter 9

Oil-in-water emulsions encapsulating quercetin using microchannel emulsification: Effect of different emulsifiers on generation characteristics and stability*

_____

9.1 Introduction

Quercetin is categorized as a flavonol and belongs to the family of flavonoids. The International Union of Pure and Applied Chemistry (IUPAC) nomenclature for quercetin is 3,3',4',5,7 –pentahydroxyflavanone [1]. By definition quercetin is an aglycone (lacking an attached sugar) having brilliant citron yellow color and is entirely insoluble in water, sparingly souble in oil medium and readily soluble in variety of polar solvents [2]. The solubility of quercetin can greatly be improved by attaching glycosyl group at hydroxyl positions [3]. Flavonols are present in variety of fruits, vegetables, seeds, flowers and nuts [4]. These are also abundant in variety of medicinal plants like *Ginko bioloba*, *Solanum trilobatum* and many others [2]. The estimated daily intake of flavonols is in the range of 20-50 mg. day^{-1}. Most of the dietary intake is as flavonol glycosides of quercetin, kaempferol and myricetin [5].

Quercetin exhibit a wide range of biological activities, including anti-oxidant, anti-cancer, anti-toxic, anti-thrombotic, anti-aging, metal chelating and anti-microbial activities [2, 6-8]. Similarly, it has impact on obesity, sleep and mood disorders [2,9]. Recently, quercetin is used in many sport supplements in order to reduce post-exercise immune system perturbations [10]. The bioavailability and absorption of quercetin depends upon the nature of attached sugar, solubility modifications and type of emulsifiers used in different systems [11]. Despites of great biological activities, quercetin has very poor oral bioavailability. The main disadvantages of using quercetin in therapeutics and functional foods are, poor solubility in aqueous and oil medium, crystallization behavior at ambient and body temperatures, poor permeability and low bioavailability [12-14]. To overcome these disadvantages, it is necessary to develop an efficient delivery system for quercetin that improves the stability and release of quercetin at appropriate target site.

A wide variety of colloidal systems have been developed to encapsulate vital lipophilic compounds, including micro and nano-emulsions, solid lipid micro and nano-particles, filled hydrogel particles and polymeric nanoparticles [15,16]. These colloidal delivery systems were formulated either with conventional emulsification tools or microfluidic devices[17]. In this study we used microchannel emulsification (MCE) to encapsulate quercetin in different oil-in-water (O/W) emulsions. MCE is a promising technique to generate extremely monodisperse emulsion droplets with droplet size variation less than 5% [18]. MCE chips consist of either MC arrays with parallel microgrooves and a terrace, or many

straight-through holes [18,19]. The distinguishing features of MCE involves no shear forces during droplet generation process, size of the droplets is determined by the microchannel geometry and composition of dispersed phase and flow rate [20]. In MCE, droplet generation is driven by spontaneous transformation of dispersed phase that passed through the microchannels and is further driven by interfacial tension [21]. MCE has been successfully applied for preparation of simple and multiple emulsions, microspheres and microcapsules. Many hydrophilic and lipophilic compounds were encapsulated in these systems like β-carotene, [22] oleuropein, [23] γ-oryzanol, [24], L-ascorbic acid [25, 26] and ascorbic acid derivatives [27].

The aim of this study was to design food grade O/W emulsions encapsulating quercetin using straight-through MCE. The present study investigates the effect of different emulsifiers on generation characteristics and stability of O/W emulsions encapsulating quercetin. Moreover, the study investigates the effect of different dispersed phase composition on quercetin encapsulation, together with storage stability and encapsulation efficiency of formulated O/W emulsions. The output of this research improves the understanding of different factors that influence the formation, stabilization and utilization of crystalline bioactive compounds in food, cosmetics and pharmaceutical products.

9.2 Material and methods

Chemicals

3,3',4',5,7 –pentahydroxyflavanone (quercetin) was procured from Nacalai Tesque, Inc. (Kyoto, Japan). Soybean oil, sesame oil, dimethyl sulfoxide, bovine serum albumin (BSA) and polyoxyethylene (20) sorbitan monolaurate (Tween 20) were purchased from Wako Pure Chemical Ind. (Osaka, Japan). Safflower oil was purchased from MP biomedicals (lllkirch, France). Medium chain triacylglycerol (MCT, sunsoft MCT-7) with a fatty acid residue composition of 75% caprylic acid and 25% capric acid and polyglyceryl-5-laurate (Sunsoft A-12E, HLB 15.6) were procured from Taiyo Kagaku Co. Ltd. (Mie, Japan). Sodium salt of colic acid (Na-cholate > 97% purity) was purchased from Sigma Aldrich (St. Louis, Mo., USA). Decaglycerol monolaurate (ML-750, HLB 14.8) was procured from Sakamoto Yakuhin Kogyo Co., Ltd (Osaka, Japan). Milli-Q water with a resistivity of 18MΩ cm was used to dissolve the emulsifiers and served as continuous phase. All other chemicals used in this study were of analytical grade and used as received.

Dispersed and continuous phase preparation

A continuous phase was prepared by dissolving either 1% (w/w) Tween 20, Na-cholate, ML-750, Sunsoft A-12E or BSA in Milli-Q water at ambient temperature, stirring for 20 min and stored for 60 min before using as continuous phase. A disperse phase was prepared by dispersing quercetin (0.1-0.6 mg mL^{-1}) either into soybean oil, MCT, mixture of MCT and soybean oil (50:50% (v/v)), sesame oil or safflower oil at ambient temperature, then heating the mixture under water bath at 90°C (with stirring for 40 min, ultra-sonication (VS-100III, As One Co., Osaka, Japan) at 45kHz for 10 min, again heating for 40 min, followed by ultra-sonication for 10 min and lastly storage for 40 min at ambient temperature).

Silicon microchannel chip

The encapsulation experiment has been conducted using silicon 24 × 24-mm MC array chip (Model WMS 1-2; EP. Tech Co., Ltd., Hitachi, Japan) containing 10,313 MCs arranged within a 10-mm^2 central region. The MC chip was 500 μm thick, but it was thinned to 100 μm in the central region (Fig. 9.1a). The four 1.5-mm diameter holes at the corner of chip permit a disperse phase to flow beneath the plate. The MC plate and MC arrays were fabricated by repeated processes of photolithography and deep-reactive-ion etching (DRIE) on 5-in. silicon wafer. Dimension wise each MC consisted of a circular microhole (10-μm diameter and 70-μm depth) located on the outlet side and a microslot (11 × 104-μm cross section and 21-μm depth, an aspect ratio = 9) located on the inner side (Fig. 9.1b). Before first usage, the MC chip was plasma oxidized in a plasma reactor (PR41, Yamato Science Co. Ltd., Tokyo, Japan) to grow a hydrophilic silicon dioxide layer on the surface. After each experiment, the MC chip was cleaned with neutral detergent and ethanol using an ultrasonic bath (VS-100III, As One Co., Osaka, Japan) at a frequency of 100 kHz and later stored in Milli-Q water.

(a)

(b)
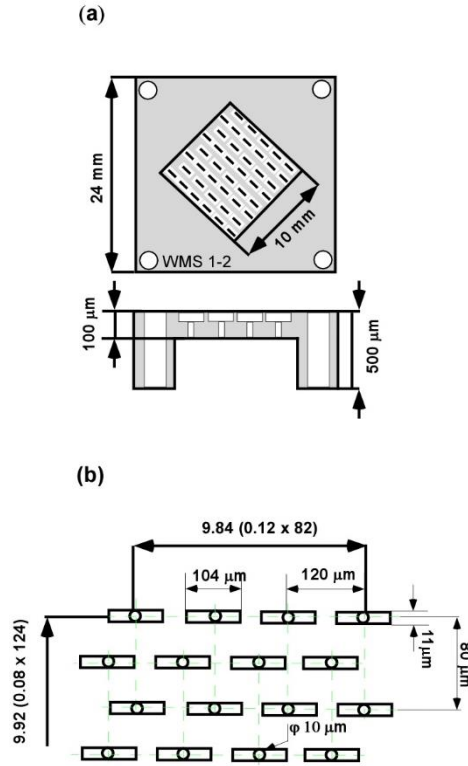
Figure 9.1: Schematic representation of MC chip used in MCE. (a) WMS 1-2 silicon chip. (b) Arrangement of MCs in WMS 1-2 chip. Each horizontal row contains alternatively 82 or 83 channels and vertical rows contain alternatively 62 or 63 channels.

Emulsification procedure

Before conducting each experiment, the MC chip was degassed in the continuous phase under ultra-sonication at a 100 kHz for 20 min. The degassed MC chip was mounted in a MC module compartment previously filled with continuous phase. Fig. 9.2a shows a simplified schematic diagram of the experimental setup used for MCE. The dispersed phase was injected through the MCs by a syringe pump (Model 11, Harvard Apparatus Inc., Holliston, USA) using a 10 mL glass syringe at the flux ranging (J_d) from 10 to 300 L m^{-2}h^{-1}, while continuous phase was delivered from an elevated reservoir through the gap between the MC chip and cover slip. The emulsification process was carried out for approximately 1 h and monitored through FASTCAM-1024 PCI high speed video system at 250 to 1000 fps (Photron Ltd., Tokyo, Japan) attached to an inverted metallographic microscope (MS-511B, Seiwa Kougaku Sesakusho Ltd., Tokyo, Japan). The droplets generation process during MCE is illustrated in Fig. 9.2b.
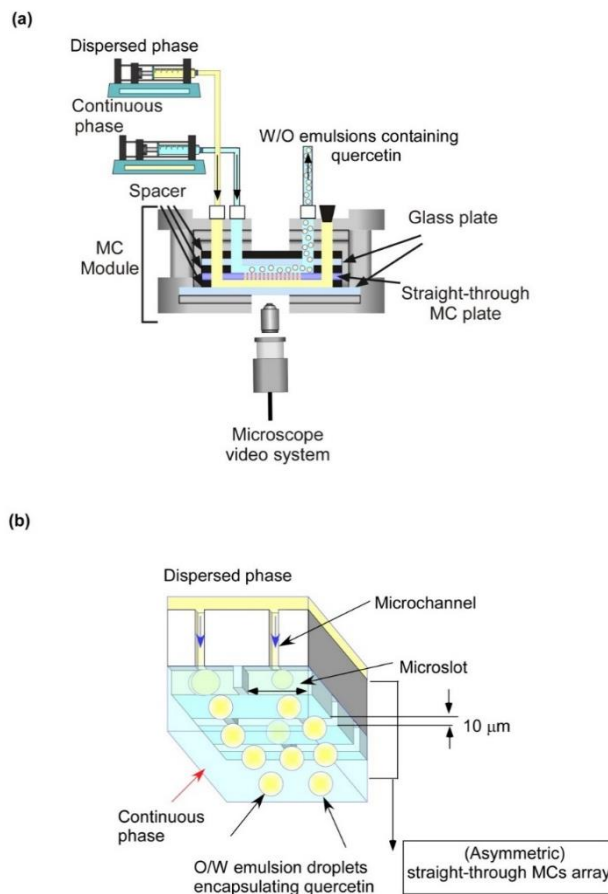
Figure 9.2: Schematic presentation of MCE used for encapsulation of quercetin. (a) Experimental set-up used for quercetin encapsulation. (b) O/W emulsion droplets generation process in MCE.

Measurement and analysis

The particle size distribution of the resultant O/W emulsions encapsulating quercetin was measured by using a light scattering instrument (LS 13 320, Beckman Coulter, Fullerton, USA). This instrument works on the principle of Polorization Intensity Differential Scattering Technology and has ability to measure the size ranging from 0.04 to 2000 μm with a resolution of 116 particle size channels. The mean droplet size was expressed as Sauter mean diameter ($d_{3,2}$), which is the diameter of a droplet having the same area per unit volume as that of the total collection of droplets in emulsions. The width of droplet size distribution was expressed as relative span factor (RSF) and is defined as:

$$\text{RSF} = \frac{d_{v0.9} - d_{v0.1}}{d_{v0.5}} \qquad (9.1)$$

where $d_{v0.9}$ and $d_{v0.1}$ are the representative diameters where 90% and 10% of the total volume of the liquid is made up of droplets with diameters smaller than or equal to the stated value. $d_{v0.5}$ is the representative diameter where 50% of the total volume of the liquid is made up of droplets with diameters larger than the stated value and 50% is made up of droplets with diameters smaller than the stated value.

Measurement of fluid properties

The densities of dispersed and continuous phases were measured using a density meter (DA-130 N, Kyoto Electronics Manufacturing Co., Ltd., Kyoto, Japan) at 25±2°C, while the viscosities of dispersed and continuous phases were measured with a sine wave vibro viscometer (SV-10, A&D Co., Ltd., Tokyo, Japan) at 25±2°C by taking 35 mL samples in a measuring vessel followed by immersion of sensor plates vibrating at constant frequency and amplitude in that vessel. The absolute viscosity (η) was calculated by

$$\eta = \frac{\eta_{mea}}{\rho} \qquad (9.2)$$

where η_{mea} is the measured fluid viscosity and ρ is the fluid density. The static interfacial tension between the oil and aqueous phases was measured with a fully automatic interfacial tensiometer (PD-W, Kyowa Interface Sciences Co., Ltd., Saitama, Japan) using a pendant drop method. The key physical properties of the continuous and dispersed phases are presented in Table 9.1.

Physical and chemical stability of O/W emulsions encapsulating quercetin

The physical stability in terms of consistency and coalescence was observed at 4 and 25 ± 1°C with microscopic observations using an optical microscope (DM IRM, Leica Microsystems, Wetzlar, Germany), while the particle size distribution and RSF with storage period was measured by using a light scattering instrument (LS 13 320, Beckman Coulter, Fullerton, USA).

The amount of quercetin present in O/W emulsions and dispersed phases was quantified using UV/VIS/NIR spectrophotometry (V-570, Jasco, Hachioji, Japan). Standard curves were made by using a 1 mM quercetin solution as a stock solution and dimethyl sulfoxide (DMSO) as a blank. Calibration curves were linear ($r^2 > 0.996$) over the quercetin concentration (1-10 μg mL^{-1}). The slope of best-fit line was $0.066 ± 0.020$ cm^{-1} (μg mL^{-1})$^{-1}$ and the intercept was $0.016 ± 0.004$ cm^{-1}. The Molar absorptivity (ε) for quercetin during this study was 21.86 mM^{-1} cm^{-1}.

The amount of quercetin that was encapsulated in O/W emulsions was evaluated using absorbance measurements. 1 mL of sample from the middle of bottle was dissolved in DMSO (ratio 1:10), then centrifuged at 3000 rpm for 15 min. Aliquots of supernatant were taken and then filtered using 0.45 micron syringe filter (Millipore Corp. USA). The quercetin concentration was then determined by measuring the absorbance at 372 nm using a UV/VIS/NIR spectrophotometry (V-570, Jasco, Hachioji, Japan). The encapsulation efficiency (EE_Q) of quercetin encapsulated in O/W emulsions was calculated using the following equation:

$$EE_Q = \frac{QC_s}{QC_i} \times 100 \qquad (9.3)$$

Where QC_s is the quercetin concentration remained in O/W emulsion at a specific time and QC_i is the initial quercetin concentration.

9.3 Results and discussion

Effect of quercetin concentration on formulation of O/W emulsions

To formulate an efficient delivery system, the most important criteria to determine the loading capacity of the functional compound in the system. The physical state of a functional compound is known to have a major impact on its bioavailability [28]. The melting point of quercetin is relatively very high (> 310 °C) and has a relative low water solubility (< 1g L^{-1}). The low water solubility and high melting point of quercetin limits its use as functional ingredients in food and pharmaceutical products [13]. Quercetin was solubilized in different oil medium at 90 °C according to the procedure described by Pool *et al.* [29] with slight modifications. The maximum solubility of quercetin in different oil medium was in between 0.1 to 0.6 mg mL^{-1}. The solutions of quercetin with these concentrations remain stable for more than 30 days without showing any visible crystallization. To elevate the effect of quercetin concentration on O/W emulsions, we prepared dispersed phase containing 0.1 to 0.6 mg mL^{-1} in MCT, while 1% (w/w) Tween 20 in Milli-Q water served as continuous phase during MCE. The dispersed phase was injected into MC module at J_d of 20 L m^{-2} h^{-1}. Successful emulsification was conducting with different concentrations of quercetin. Fig. 9.3a shows the $d_{3,2}$ and RSF width of O/W emulsions containing different concentrations of quercetin. The $d_{3,2}$ ranged between 28.59 to 29.18 μm with RSF width < 0.25. The narrow span width indicates extreme monodispersity in the O/W emulsions encapsulating different concentrations of quercetin. There was

smooth generation of emulsion droplets from the MCs with different quercetin concentrations (Fig. 9.3b) and these emulsions retain about 20-40 µg mL^{-1} of quercetin.

The quercetin solubility in dispersed phase was slightly higher than previously reported by Pool, *et al.* [29], there study indicates nucleation of quercetin in MCT beyond 0.1 mg mL^{-1}. However, such nucleation of quercetin was observed at 0.7 mg mL^{-1} in our study. Karadag *et al.* [30] reported two times higher solubility of quercetin in limonene oil in comparison to MCT when combined with Tween 80 and heated to 130°C for 30 min.

(a)
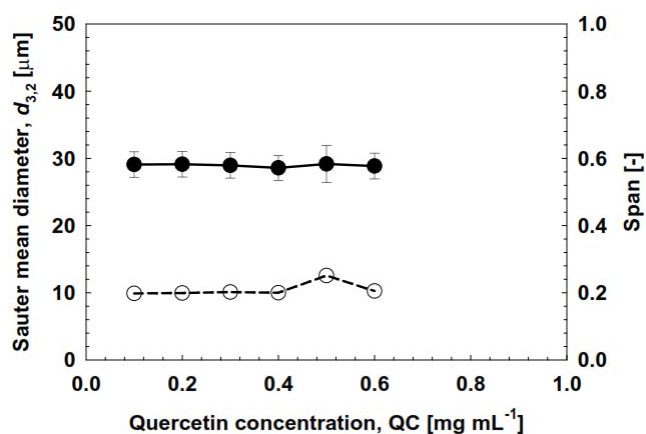
(b)
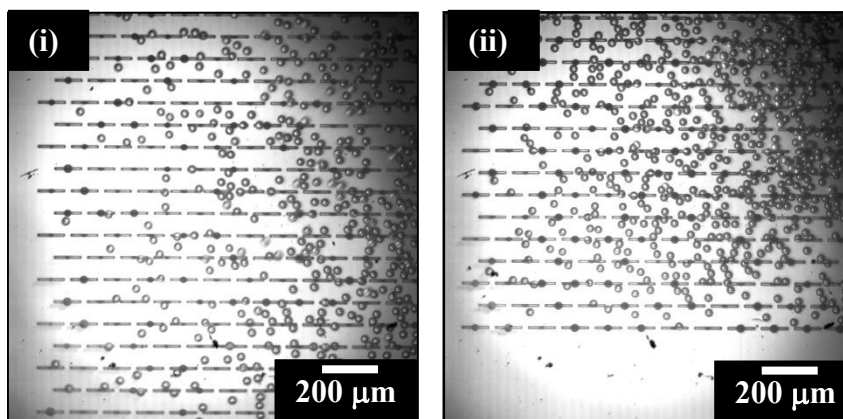
Figure 9.3: (a) Effect of quercetin concentration on O/W emulsions. The concentration effect was evaluated in MCT. (—●—) denote $d_{3,2}$ of O/W emulsions, while open key denote their span width. (b) Optical micrographs indicating droplet generation with different concentrations of quercetin (i) at 0.1 mg mL^{-1} (ii) 0.6 mg mL^{-1}.

Effect of different dispersed phases on droplet generation characteristics

The ability of different food grade oils to encapsulate quercetin in O/W emulsions was investigated by using MCT, soybean oil, mixture of soybean oil and MCT (50:50% (v/v)), safflower oil and sesame oil. These oils were used on the basis of their broad usage and functionality in different food products. 0.4 mg mL^{-1} quercetin was solubilized in different oils and served as dispersed phase, while 1% (w/w) Tween 20 in Milli-Q water was used as continuous phase in MCE. The experiments were conducted by keeping J_d at 20 L m^{-2} h^{-1} and the flow rate of continuous phase was maintained between 250 to 500 mL h^{-1}. The physical properties of different dispersed phases were presented in Table 9.1. All of these oils have viscosities (η_d) lower than the threshold value of 100 mPa s needed in MCE for successful droplet generation [31].

Table 9.1: Fluid properties of emulsion system containing quercetin together with different food grade oil used for O/W emulsions formation.

Emulsion phase	Density (kg m^{-3})	Viscosity (mPa s)	Interfacial tension (mN m^{-1})***
Dispersed phase*			
Medium chain triglyceride (MCT)	943.8 ± 0.55	22.50 ± 0.10	6.0 ± 0.3
Soybean oil	916.9 ± 0.45	49.46 ± 0.20	6.8 ± 0.2
Mixture of MCT and soybean oil	930.1 ± 0.40	33.60 ± 0.22	6.5 ± 0.3
Safflower oil	920.0 ± 0.30	51.50 ± 0.20	6.4 ± 0.1
Sesame oil	916.1 ± 0.45	54.80 ± 0.10	6.5 ± 0.1
Continuous phase**			
Tween 20	998.9 ± 0.10	0.86 ± 0.01	
Decaglycerol monolaurate	999.7 ± 0.15	1.18 ± 0.01	
Sunsoft A-12E	999.9 ± 0.10	1.19 ± 0.01	
Sodium cholate	999.2 ± 0.12	1.29 ± 0.01	
Bovine serum albumin	998.0 ± 0.10	0.83 ± 0.01	

*Dispersed phase contains 0.4 mg mL^{-1} quercetin in different food grade oils, ** Continuous phase contains 1% (w/w) of each emulsifiers in Milli-Q water, *** Interfacial tension was observed in the presence of 1% (w/w) Tween 20 in Milli-Q water and 0.4 mg mL^{-1} quercetin in different oils.

Fig. 9.4a shows the effect of different dispersed phases on $d_{3,2}$ and RSF width of O/W emulsions. Successful emulsification was conducted with different dispersed phase, and the $d_{3,2}$ of emulsions ranged between 27.75 to 33.20 μm with RSF width < 0.23. Fig. 9.4b depicts droplet formation from asymmetric straight-through MCs for different dispersed phases, all of these oil phases transformed spontaneously into uniform droplets without any physical deformation. A slightly higher $d_{3,2}$ was observed with safflower and sesame oil in comparison to other soybean oil and MCT. This slight variation in droplet sizes might corresponds to different fatty acid composition, distribution of various bioactives and physical properties of oils [32]. Kobayashi, et al. [31] pointed that that average droplet diameter of emulsions in straight-through MCE was greatly influenced by η_d not the type of oil. However, in our study we observed variation in droplet sizes with different oil types. Soybean, sesame and safflower oil have slight higher viscosities in comparison MCT and mixture of soybean oil and MCT. The higher η_d leads toward higher $d_{3,2}$. This slight increase in droplet sizes has no marked influenced on droplet generation or monodispersity. All of the generated O/W emulsions in MCE have extreme monodispersity with RSF width < 0.23.

(a)
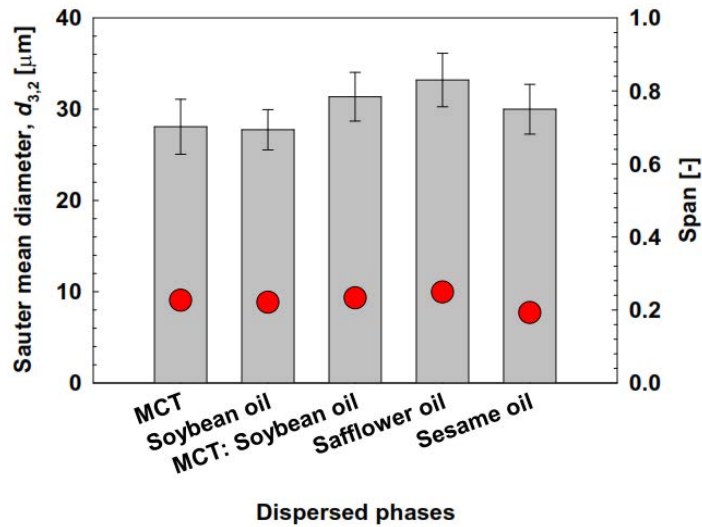
(b)
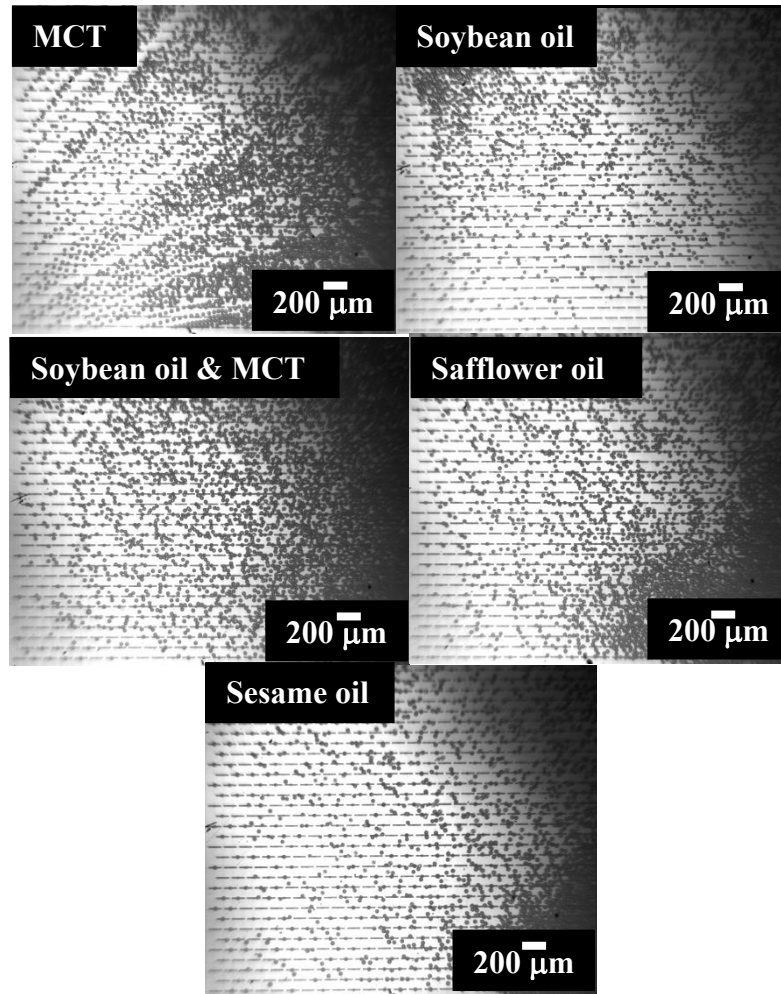
Figure 9.4: (a) Effect of different dispersed phases on $d_{3,2}$ and span width of O/W emulsions. ▭ **denote $d_{3,2}$ of O/W emulsions and** 🔴 **denote span width. (b) Droplet generation in MCE with different dispersed phases encapsulating quercetin.**

Effect of dispersed phase flux and continuous phase flow velocity on droplet generation characteristics

Cross-flow membrane emulsification and MCE has great potential to produce monodisperse emulsions and emulsions with sensitive bioactive compounds. However, low flux of dispersed phase may be a limiting factor for emulsion production on a commercial scale [33].

The effect of various levels of J_d (10-300 L m^{-2} h^{-1}) and continuous phase velocity ($\overline{V}_c$), (ranging from 2.8 mm s^{-1} to 22.8 mm s^{-1}) on the droplet generation behavior, $d_{3,2}$ and RSF were evaluated. The flow velocity along the MC chip surface ($\overline{V}_c$, mm s^{-1}) was determined as follows:

$$\overline{V}_c = \frac{Q_c}{A} \qquad (9.4)$$

Where Q_c is the continous phase flow rate (mm³ s⁻¹) and A is the flow area along the MC chip surface (mm²). As depicted in Fig. 9.5a, the gradual increase in J_d, resulted in increased $d_{3,2}$ and RSF of emulsions encapsulating quercetin. The size stable zone was in between J_d of 20-70 L m⁻² h⁻¹. In this stable zone the $d_{3,2}$ was in between 28.22 to 29.57 μm with RSF width < 0.33. Moreover, the emulsification using a J_d of above 100 L m⁻² h⁻¹ and a $\overline{V}_c$ of 22.8 mm s⁻¹ resulted in polydispersed droplets with a $d_{3,2}$ of > 31.77 and a RSF of > 0.70 (Fig 9.5b). At higher J_d the $d_{3,2}$ depends on the oil flux inside the MCs. The size stable of quercetin loaded emulsions were slightly higher in comparison to previous study of γ-oryzanol loaded emulsions [24], they reported size stable zone in J_d between 10-40 L m⁻² h⁻¹. Whereas, increased droplet size with increasing flux agreed well with previous literature [34]. Fig. 9.5c depicts the effect of $\overline{V}_c$ on $d_{3,2}$ and RSF of O/W emulsions encapsulating quercetin. The monodisperse emulsions formulated at low and high $\overline{V}_c$ shows no prominent difference in $d_{3,2}$ and RSF. The size of emulsion droplets was independent of $\overline{V}_c$ in straight-through MCE and agreed well with previous findings. [35]

(a)
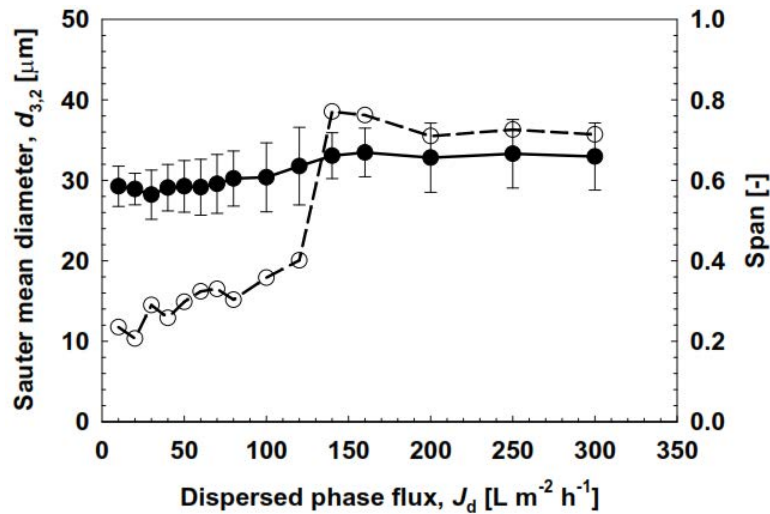
(b)
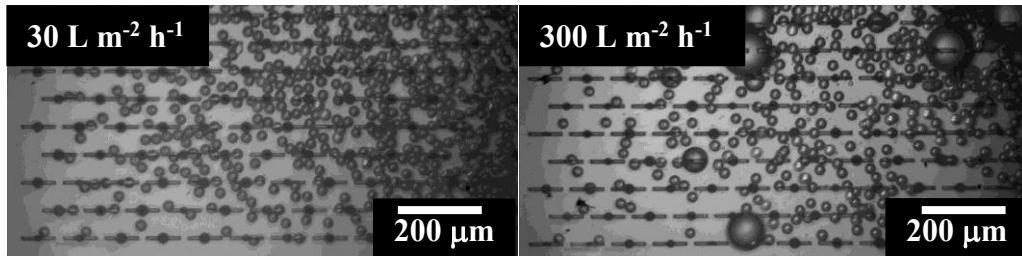
(c)
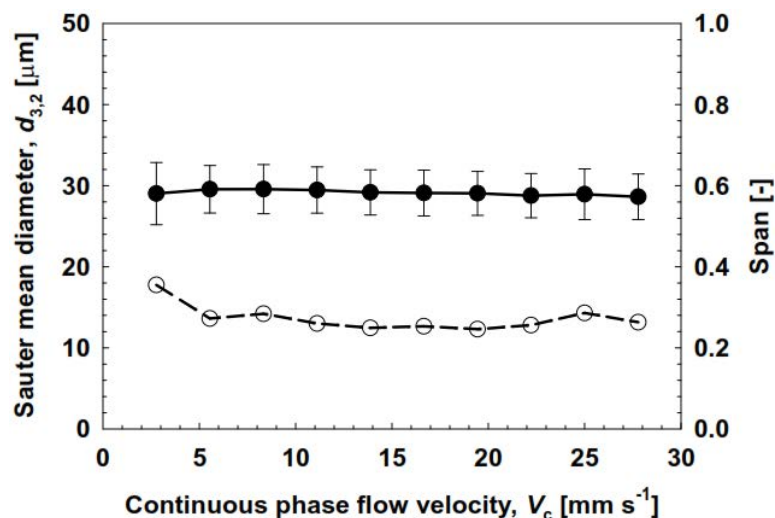
Figure 9.5: (a) Effect of disperse phase flux on $d_{3,2}$ and RSF width of O/W emulsions. (━●━) denote $d_{3,2}$ and (━ ⊖ ━) denote RSF of O/W emulsions encapsulating quercetin. **(b)** Micrographs at disperse phase flux at 30 and 300 L m^{-2} h^{-1} captured at 1000 fps. continuous phase velocity was in between 14 and 23 mm s^{-1}. **(c)** Effect of continuous phase flow velocity on $d_{3,2}$ and RSF width of O/W emulsions. (━●━) denote $d_{3,2}$ and (━ ⊖ ━) denote RSF of O/W emulsions.

Effect of different emulsifiers on stability of O/W emulsions

Emulsifier molecules have a critical role in the stability of oil droplets in MCE. The charge on the MC chip surface and electrostatic interactions of emulsifiers must kept in mind during MCE. Uniform oil droplets can be generated in MCE when MC chip surface has a non-attractive interaction with emulsifier molecules. Moreover, the stability of droplets correlate with the continuous phase, if it preferentially wet the surface of MC chip during emulsification [36].

0.4 mg mL^{-1} quercetin was solubilized in MCT, while 1% (w/w) of different emulsifiers in Milli-Q water were used as continuous phase in MCE. The experiments were conducted by keeping J_d at 20 L m^{-2} h^{-1} and the flow rate of continuous phase was maintained between 250 to 500 mL h^{-1}. Stable droplet generation with uniform size was observed in all working channels with different food grade emulsifiers. There was neither the formation of irregularly size droplets, nor a continuous growth of the dispersed phase, which could result in a broad size distribution and polydispersity (Fig. 9.6a). The formed particles were detached rapidly from the channel tip with different emulsifiers. Fig. 9.6b depicts the $d_{3,2}$ and RSF of O/W emulsions stabilized by different emulsifiers. The $d_{3,2}$ of emulsions stabilized by non-ionic

emulsifiers (Tween 20, Sunsoft A-12E and ML-750) were in between 28.50 to 28.85 μm with RSF width < 0.21. More stable droplet generation was observed (Fig. 9.6c) with non-ionic emulsifiers in droplet stable zone (J_d = 20-50 L m^{-2} h^{-1}) in comparion to ionic (Na-cholate) and protein based emulsifiers (BSA). Slightly higher $d_{3,2}$ (29.40 μm, RSF <0.21) was observed in emulsions stabilized by Na-cholate, while BSA stabilized emulsions have much higher droplet diameter, the $d_{3,2}$ increases to 34.48 μm with RSF width < 0.24. The results with non-ionic emulsifiers agreed well with previous studies of emulsification reporting that hydrophile-lipophile balance exceeding 10 produced unifrom droplets in MCE [37, 38]. The effect of proteins as an emulsifiers on MCE was previously reported by Saito *et al.* [39]. They reported increased in droplet diameter from 41.0 to 44.1 μm in BSA stabilized emulsions with increasing J_d. Moreover, the generated emulsions droplets with BSA maintained monodispersity at high J_d. Our experiments with BSA was conducted at pH 7.1, indicating negative charge on BSA. The negative charge allows droplets to detached more smoothly from MCs [39].

(a)
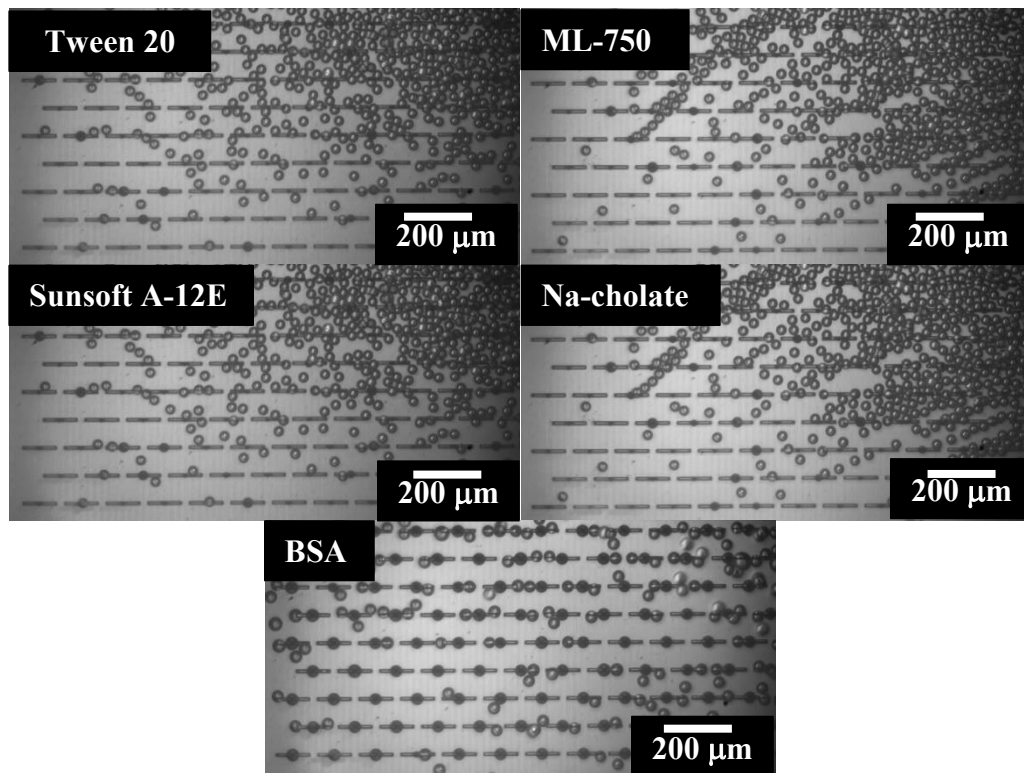
(b)
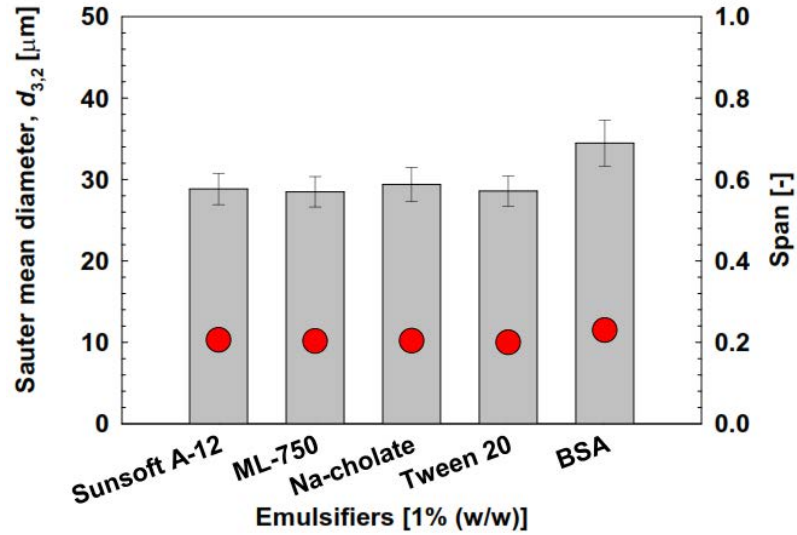
(c)
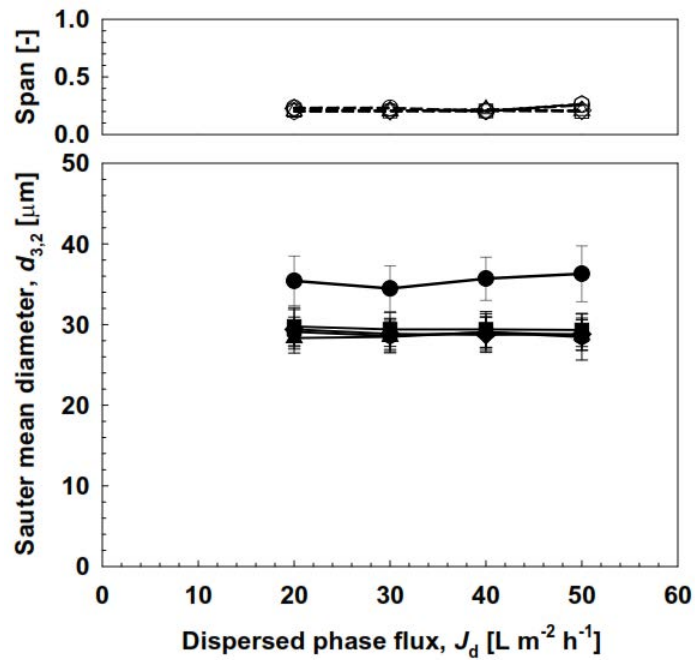
Figure 9.6: (a) Droplet generation behavior in straight-throught MCE encapsulating quercetin in O/W emulsions stabilized by different emulsifiers. (b) Effect of different emulsifers on $d_{3,2}$ and RSF of O/W emulsions. ▭ denote $d_{3,2}$ of O/W emulsions and ⬤ denote RSF width. (c) Effect of J_d on $d_{3,2}$ and RSF of emulsions in size stable zone. (—●—) deonte Tween 20, (—◆—) Sunsoft A-12E, (—▲—) ML-750, (—■—) Na-cholate, (—●—) donote BSA. The opens key donote RSF of O/W emulsions stabilized with Tween 20.

221

Long term stability of O/W emulsions encapsulating quercetin

The monodisperse O/W emulsions encapsulating 0.4 mg mL^{-1} quercetin and stabilized with 1% (w/w) different emulsifiers were stored at 4 and 25 ± 1 ºC for a period of 30 days. The emulsions were formulated by keeping J_d at 20 L m^{-2} h^{-1} and the continuous phase flow rate between 250 to 500 mL h^{-1}. Fig. 9.7a shows the $d_{3,2}$ and RSF width of the O/W emulsions encapsulating quercetin at 4 ± 1 ºC. There was a gradual decrease in $d_{3,2}$ of emulsions stabilized with Sunsoft A-12E after 30 days of storage period in comparison to other emulsifiers. The decrease in droplet size can be attributed to Sunsoft A-12E absorption in the interfacial film [40]. The $d_{3,2}$ of emulsions stabilized by Na-cholate increased to 36.0 μm after 7 days of storage. The increased in $d_{3,2}$ of emulsions stabilized by Na-cholate at low temperature can be attributed to low aggregation number of Na-cholate. The aggregation number of pure Na-cholate (3 to 16) is highly influenced by the environmental parameters [41, 42]. There was hardly any change in the $d_{3,2}$ and RSF width of emulsions stabilized by Tween 20, ML-750 and BSA. The droplet size of emulsions stabilized by Tween 20 and ML-750 remain in range from 28.31 to 28.88 μm, while those stabilized by BSA was in range of 34.09 to 34.59 μm after 30 days of storage at 4 ± 1 ºC.

Fig. 9.7b depicts the stability profile of quercetin loaded emulsions stabilized by different emulsifiers at 25 ± 1 ºC. There was slight decrease in $d_{3,2}$ of emulsions stabilized with Tween 20, ML-750, Sunsoft A-12E and Na-cholate. The emulsions stabilized with different emulsifiers maintained monodispersity with RSF < 0.35 after 30 days of storage at 25 ± 1 ºC. There was sharp decrease in droplet diameter of emulsions stabilized with BSA and $d_{3,2}$ decreased from 33.35 to 27.79 μm with RSF width of > 0.45 after 30 days of storage at 25ºC. The decreased droplet size might be attributed to denaturation of BSA at 25ºC. Moreover, partial denaturation of the adsorbed BSA on the surface of emulsions might decreased the droplet diameter [43]. Saito *et al.* [44] reported good thermal stability of BSA stabilized emulsions in MCE ranged between 30-80ºC. However, their study do not evaulate long term storage stability of BSA stabilized emulsions.

(a)
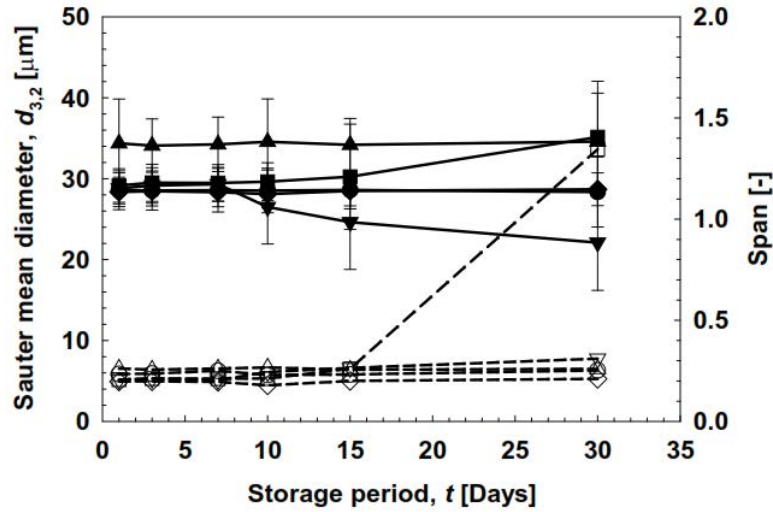
(b)
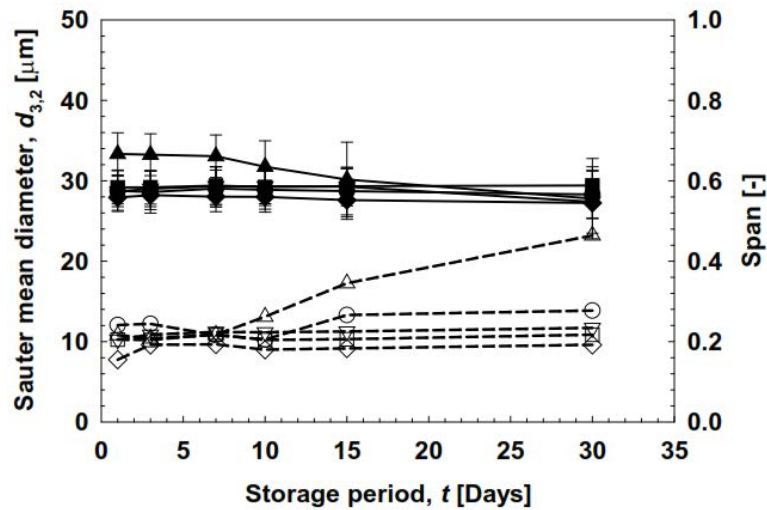
Figure 9.7: Storage stability of O/W emulsions encapsulating querectin. The data was presented in terms of $d_{3,2}$ and RSF. (a) storage stability at 4 ± 1^oC (b) storage stability at 25 ± 1^oC. (–●–) denote Tween 20, (–▼–) Sunsoft A-12E, (–◆–) ML-750, (–■–) Na-cholate and (–▲–) denote BSA. The same open keys denote RSF of O/W emulsions encapsulating quercetin.

Encapsulation efficiency of O/W emulsions encapsulating quercetin

O/W emulsions stabilized with 1% (w/w) Tween 20 have better storage stability at 4 and 25°C in comparison to other emulsifiers, based upon better storage stability, encapsulation efficiency (EE) was investigated in emulsions stabilized with 1% (w/w) Tween 20. O/W emulsions were formulated by keeping J_d at 20 L m^{-2} h^{-1} and the continuous phase flow rate at 500 mL h^{-1}. The optical micrographs of emulsion

223

droplets at 4 and 25°C after 30 days of storage were presented in Fig. 9.8a. The monodispersity was complete observed in these micrographs. At both storage temperatures the $d_{3,2}$ varied between 28. 37 to 28.90 μm with RSF width < 0.27. The EEs of emulsions stabilized with 1% (w/w) Tween 20 were depicted in Fig. 8b. The freshly formulated O/W emulsions retains about 31.50 μg mL^{-1} of quercetin. There was gradual decrease in EE of quercetin with storage time at both 4 and 25°C. The EEs was about 79.68% and 70.15% at 4 and 25°C after 30 days of storage. The slightly higher EE in emulsions formulated by MCE can be attributed to narrow size droplet distribution (Fig. 9.8b). Moreover, in MCE the droplet generation was based upon difference in interfacial tension rather than high energy shear forces. The energy efficiency (E_e) in MCE using the WMS 1-2 was estimated by the following equation:

$$\Delta E_{exp} = \frac{\Delta P_d}{\rho_d} \qquad (9.5)$$

Where ΔE_{exp} is the actual energy input for droplet generation in the straight-through MCE, ΔP_d is the applied dispersed phase pressure (4.62 kPa) during MCE for 1 hour and ρ_d is the dispersed phase density containing 0.4 mg mL^{-1} quercetin in MCT. The calculated ΔE_{exp} during emulsification was 4.9 J kg^{-1}. The ΔE_{exp} was comparable with oblong type straight-through MCE (5.0-14.2 J kg^{-1}), previously reported by Kobayashi et al. [45]. According to the ΔE_{exp} must exceed the theoretical minimum energy (ΔE_{Thr}). The ΔE_{Thr} was calcuated from following equation:

$$\Delta E_{Thr} = \Delta A \gamma_{ow} = \frac{6\gamma_{ow}}{\rho_d d_{3,2}} \qquad (9.6)$$

Where ΔA is the increase in interfacial area, γ_{ow} is the interfacial tension between two phases, ρ_d is the dispersed phase density and $d_{3,2}$ is the Sauter mean diameter of O/W emulsions. The ΔE_{Thr} at ambient temperature corresponds to 1.35 J kg^{-1}. The E_e can be calculated from above equation:

$$E_e = \frac{\Delta E_{Thr}}{\Delta E_{exp}} \times 100 \qquad (9.7)$$

The calculated E_e was 27.5% and was comparatively less than E_e of oblong type straight-through MCE [45]. The E_e of oblong type MCE setups were 47-60% and grooved type MCE was 65% [21, 45]. Quercetin was previously encapsulated in poly D, L-lactide (PLA) nanoparticles and have EE of 96.7% [46]. Gilles et al. [47] studied the encapsulation of linoleic acid (LA) in the presence or absence of quercetin into a dual polymer system of whey protein and Kappa-carrageenan. The stability of quercetin stabilized LA was

examined to be 83%. Watanabe *et al.* [48] investigated lecithin-chitosan nanoparticles as a topical delivery system for quercetin. The quercetin-loaded nanoparticles showed higher permeation ability with entrapment efficiency of 48.5%. Pool*, et al.* [29] encapsulated 0.1 mg mL^{-1} quercetin in O/W emulsions and observed 95% retention at different storage temperatures, however they noticed appreciable decrease in the level of quercetin in O/W emulsions initially containing 0.5 mg mL^{-1} quercetin after one month of storage.

(a)
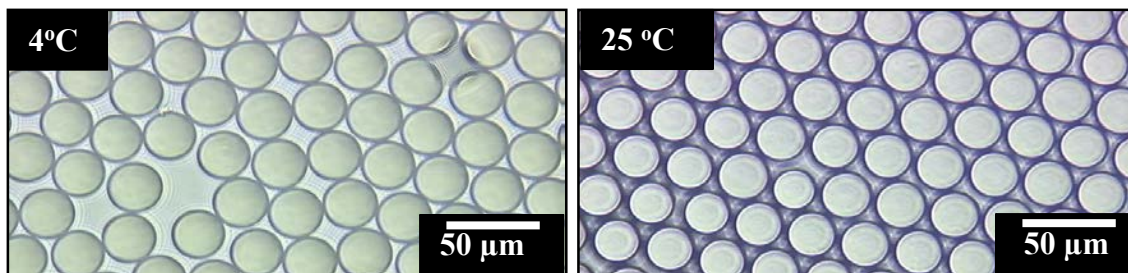
(b)
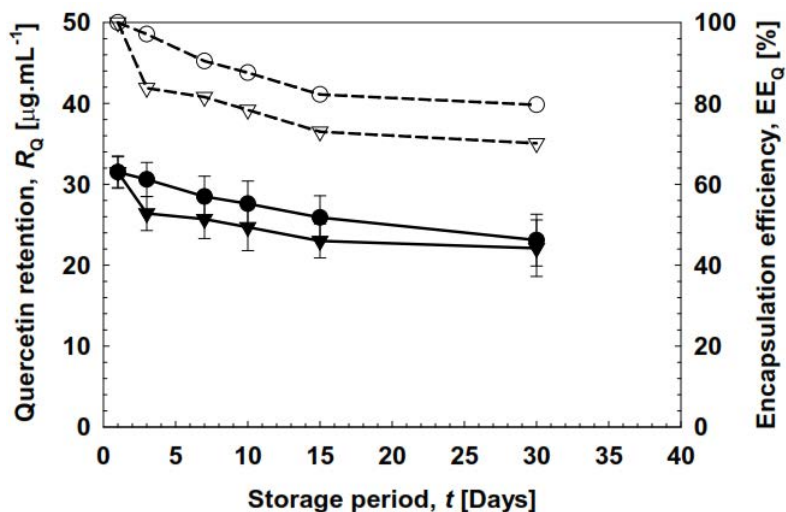
Figure 9.8: (a) Optical micrographs of O/W emulsions encapsulating quercetin after 30 days of storage at 4 and 25°C. (b) Encapsulating efficiency (EE$_Q$) and retention profile (R$_Q$) of O/W emulsions encapsulating quercetin at 4 and 25°C. (—●—) denote R$_Q$ at 4°C and (—▼—) denote R$_Q$ at 25°C. (-⊖-) presents EE$_Q$ at 4°C and (-▽-) presents EE$_Q$ at 25°C.

References

[1] Ross JA and Kasum CM, *Ann. Rev. Nutr.*, **22,** 19-34 (2002).

[2] Kelly GS, *Monograph. Altern. Med. Rev*, **16,** 172-194 (2011).

[3] Hollman PC, Bijsman MN, van Gameren Y, Cnossen EP, de Vries JH and Katan MB, *Free Rad. Res.*, **31,** 569-573 (1999).

[4] Häkkinen SH, Kärenlampi SO, Heinonen IM, Mykkänen HM and Törrönen AR, *J. Agric. Food Chem.*, **47,** 2274-2279 (1999).

[5] Cao J, Zhang Y, Chen W and Zhao X, *Brit. J. Nutr.*, **103,** 249-255 (2010).

[6] Meyers KJ, Rudolf JL and Mitchell AE, *J. Agric. Food Chem.*, **56,** 830-836 (2008).

[7] Borska S, Drag-Zalesinska M, Wysocka T, Sopel M, Dumanska M, Zabel M and Dziegiel P, *Folia Histochemica et Cytobiologica*, **48,** 222-221 (2010).

[8] Das S, Mandal AK, Ghosh A, Panda S, Das N and Sarkar S, *Curr Aging Sci*, **1,** 169-174 (2008).

[9] Joshi D, Naidu P, Singh A and Kulkarni S, *J. Med. Food*, **8,** 392-396 (2005).

[10] Davis JM, Carlstedt CJ, Chen S, Carmichael MD and Murphy EA, *Int. J. Sport Nutr. Exercise Metabol.*, **20,** 56-62 (2010).

[11] Scholz S and Williamson G, *Int. J. Vitamin Nutr. Res.*, **77,** 224-235 (2007).

[12] Ader P, Wessmann A and Wolffram S, *Free Rad. Biol. Med.*, **28,** 1056-1067 (2000).

[13] Borghetti GS, Lula IS, Sinisterra RD and Bassani VL, *AAPS PharmSciTech*, **10,** 235-242 (2009).

[14] Pouton CW, *Eur. J. Pharm. Sci.*, **29,** 278-287 (2006).

[15] Flanagan J and Singh H, *Crit. Rev. Food Sci. Nutr.*, **46,** 221-237 (2006).

[16] McClements DJ and Rao J, *Crit. Rev. Food Sci. Nutr.*, **51,** 285-330 (2011).

[17] Vladisavljevic GT, Khalid N, Neves MA, Kuroiwa T, Nakajima M, Uemura K, Ichikawa S and Kobayashi I, *Adv. Drug Deliv. Rev.*, **65,** 1626-1663 (2013).

[18] Kawakatsu T, Kikuchi Y and Nakajima M, *J Amer Oil Chem Soc*, **74,** 317-321 (1997).

[19] Kobayashi I, Nakajima M, Chun K, Kikuchi Y and Fujita H, *AIChE J.*, **48,** 1639-1644 (2002).

[20] Vladisavljević GT, Kobayashi I and Nakajima M, *Microfluid. Nanofluid.*, **13,** 151-178 (2012).

[21] Sugiura S, Nakajima M, Iwamoto S and Seki M, *Langmuir*, **17,** 5562-5566 (2001).

[22] Neves MA, Ribeiro HS, Kobayashi I and Nakajima M, *Food Biophys.*, **3,** 126-131 (2008).

[23] Souilem S, Kobayashi I, Neves M, Sayadi S, Ichikawa S and Nakajima M, *Food Bioprocess Technol*, **7,** 2014-2027 (2014).

[24] Neves MA, Ribeiro HS, Fujiu KB, Kobayashi I and Nakajima M, *Ind. Eng. Chem. Res.*, **47,** 6405-6411 (2008).

[25] Khalid N, Kobayashi I, Neves MA, Uemura K, Nakajima M and Nabetani H, *Colloid Surface A.*, **458,** 69-77 (2014).

[26] Khalid N, Neves A, Kobayashi I, Uemura K, Nakajima M and Nabetani H, Preparation of monodisperse aqueous liquid microspheres containing high-concentration of L-ascorbic acid by microchannel emulsification, in: The Annual Meeting of Japan Society for Bioscience, Biotechnology and Agrochemistry, Japan Society for Bioscience, Biotechnology and Agrochemistry, Meiji University, Tokyo, Japan., 2014, pp. 2B02p08, p. 534.

[27] Khalid N, Kobayashi I, Neves MA, Uemura K, Nakajima M and Nabetani H, *Colloid Surface A.*, **459,** 247-253 (2014).

[28] Muller RH and Keck CM, *J. Biotechnol.*, **113,** 151-170 (2004).

[29] Pool H, Mendoza S, Xiao H and McClements DJ, *Food Function*, **4,** 162-174 (2013).

[30] Karadag A, Yang X, Ozcelik B and Huang Q, *J Agric. Food Chem.*, **61,** 2130-2139 (2013).

[31] Kobayashi I, Mukataka S and Nakajima M, *Langmuir*, **21,** 5722-5730 (2005).

[32] McClements DJ, Food emulsions: principles, practice, and techniques, 2nd ed., CRC press, Boca Raton, USA, 2005.

[33] Gijsbertsen-Abrahamse AJ, van der Padt A and Boom RM, *J. Membrane Sci.*, **230,** 149-159 (2004).

[34] Vladisavljevic GT, Kobayashi I and Nakajima M, *Microfluid. Nanofluid.*, **10,** 1199-1209 (2011).

[35] Kobayashi I, Mukataka S and Nakajima M, *Ind. Eng. Chem. Res.*, **44,** 5852-5856 (2005).

[36] Kobayashi I, Nakajima M and Mukataka S, *Colloid Surface A.*, **229,** 33-41 (2003).

[37] Kobayashi I and Nakajima M, *Eur. J. Lipid Sci. Technol.*, **104,** 720-727 (2002).

[38] Tong JH, Nakajima M, Hiroshi, Nabetani and Kikuchi Y, *J. Surfactant Detergent*, **4,** 85-85 (2001).

[39] Saito M, Yin LJ, Kobayashi I and Nakajima M, *Food Hydrocolloid*, **19,** 745-751 (2005).

[40] Yin L-J, Kobayashi I and Nakajima M, *Food Biophys.*, **3,** 213-218 (2008).

[41] Calabresi M, Andreozzi P and La Mesa C, *Molecules*, **12,** 1731-1754 (2007).

[42] Jojart B, Posa M, Fiser B, Szori M, Farkas Z and Viskolcz B, *PloS one*, **9,** e102114 (2014).

[43] Kim HJ, Decker EA and McClements DJ, *Langmuir*, **18,** 7577-7583 (2002).

[44] Saito M, Yin L-J, Kobayashi I and Nakajima M, *Food Hydrocolloid*, **20,** 1020-1028 (2006).

[45] Kobayashi I, Takano T, Maeda R, Wada Y, Uemura K and Nakajima M, *Microfluid Nanofluid*, **4,** 167-177 (2008).

[46] Kumari A, Yadav SK, Pakade YB, Singh B and Yadav SC, *Colloid Surface B.*, **80,** 184-192 (2010).

[47] Gilles KK, Vinod KT, Christopher LM, Tarab A, Mark SB, Netkal MG and Ronald JT, *J, Encapsulation Adsorption Sci,*, **2012,** (2012).

[48] Watanabe Y, Suzuki T, Nakanishi H, Sakuragochi A and Adachi S, *J. Am. Oil Chem. Soc.*, 1-6 (2011).

Chapter 10

Encapsulation of γ-oryzanol plus β-sitosterol in oil-in-water emulsions: Insights of formulation characteristics with microchannel emulsification*

_____

*This chapter is to be submitted as **<u>Khalid N</u>**, Kobayashi I, Neves M, Uemura K, Nakajima M, Nabetani H. Encapsulation of γ-oryzanol plus β-sitosterol in oil-in-water emulsions: Insights of formulation characteristics with microchannel emulsification

229

10.1 Introduction

An emulsion is a mixture of two immiscible liquids containing one liquid dispersed in the form of small droplets in another liquid that forms a continuous phase [1]. These different phases constitute oil-in-water (O/W) or water-in-oil (W/O) emulsions like milk or butter [2]. The emulsions play extremely important role in different applications like food processing [3], oil recovery [4], toxic material handling [5] and different drug deliveries [6]. The emulsions are stabilized by using different emulsifiers and these emulsifiers migrates to the liquid-liquid interface and inhibit droplet coalescence and flocculation [2].

Conventional methods for making emulsions involve drop breakup using high energy shear forces. These forces are not uniform entirely in emulsion system and contribute polydispersity in system [7]. Moreover, these high shear forces have low energetic efficiencies and well as encapsulation efficiencies [7]. Modern emulsification methods like microthread generation [8], viscoelastic shear [9], membrane extrusion [10] and microchannel emulsification [11] have been developed and optimized for better control over droplet size and system properties. These methods are more energy efficient and have better encapsulation efficiencies over time. The other attractive feature of microfluidic devices are fabrication of double, triple or even higher order emulsions with extreme monodispersity and unprecedented accuracy [12, 13].

In this study we uses the striking features of microchannel emulsification (MCE) to encapsulate γ-oryzanol together with β-sitosterol in O/W emulsions. The term MCE was coined by Kawakatsu, *et al.* [11] and the system has capacity to form monodisperse emulsion droplets by using microchannel (MC) arrays precisely fabricated on single-crystal silicon microchip [11] or stainless steel microchips [14]. These MC arrays can be fabricated as microgrooves horizontally to the microchip surface [11] or vertically as straight-through microholes [15]. The grooved microchips exhibits low droplet productivity due to limited number of MCs but extremely productive in elucidating droplet generation behavior in MCs. The straight-thorough microchips consist of several hundreds of thousands of MCs and have monodisperse droplet productivity even at dripping regime of 50 mL h^{-1} [15]. The droplet generation process in MCE was comprehensively reviewed by Vladisavljevic *et al.* [16] and Vladisavljevic' *et al.* [17]. Monodisperse emulsion droplets with diameters of 1 μm to 500 μm and coefficient of variation below 5% have been successfully formulated through MCE [17]. The MCE has been used to produce many encapsulated dispersions with improved properties such as β-carotene [18], oleuropein [19], γ-oryzanol [20], L-ascorbic acid [21] and ascorbic acid derivatives [22].

γ-oryzanol (Fig. 10.1a) is a naturally occurring component in rice bran and rice germ which consist of a mixture of ferulic acid esters of sterols and triterpene alcohols [23]. There are increasing number of reports indicating the benefits, efficacy and safety of γ-oryzanol. The antioxidant effect of γ-oryzanol was well documented and excellent in inhibiting lipid peroxidation. Kanno *et al.* [24] reported that γ-oryzanol (0.5% ~1%) inhibited thermal oxidative polymerization of soybean oil. Wilson *et al.* [25] reported that γ-oryzanol reduced plasma cholesterol in hypercholesterolemic hamsters. There are number of clinical studies reported that γ-oryzanol is beneficial in the treatment of relieving menopausal (climacteric) symptom [26]. β-sitosterol (Fig. 10.1b) is a predominant phytosterol found in higher plants and as well as in human foods [27]. β-sitosterol is the most extensive studied phytosterol due to its role in hypercholesterolemia [28], cardiovascular diseases [29] and benign prostatic hyperplasia [30]. β-sitosterol is used in a variety of enriched commercial foods such as fruits juice, milk, yoghurt and spreads. Safety concerns regarding the use of β-sitosterol have been well addressed in different *in vivo* and clinical studies [31, 32].

There is a considerable interest in structuring, fortifying and supplementing food, oils and beverages with plant based phytochemicals. The difficulties behind phytosterols encapsulation includes hydrophobicity in food matrixes [33], degradability at high temperatures [34], low water solubility [35] and moisture contents [36]. The present study was conducted to formulate O/W emulsions containing both γ-oryzanol and β-sitosterol. We investigated the effect of different concentrations of γ-oryzanol and β-sitosterol on droplet formation characteristics. Moreover, the physical and chemical stability of O/W emulsions stabilized by two different emulsifiers were also investigated during MCE.
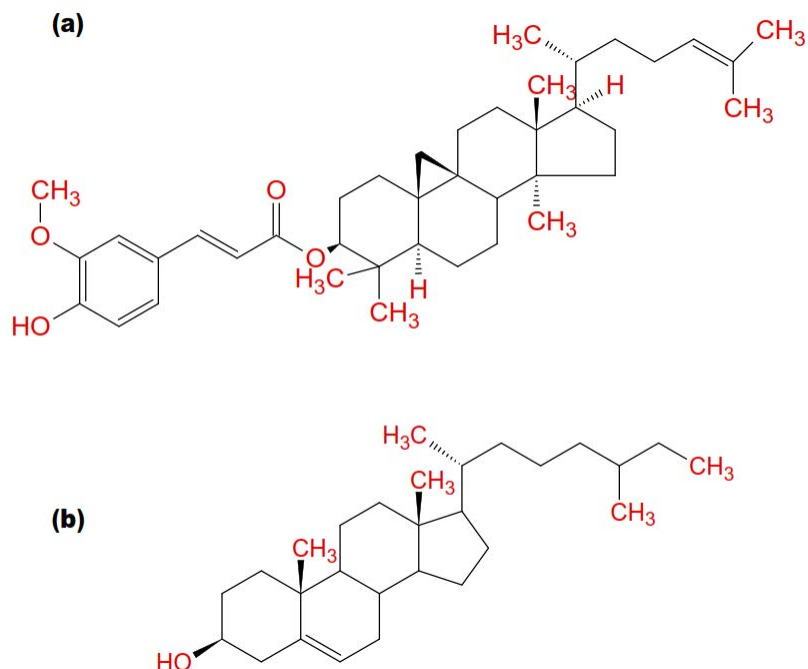
Figure 10.1: Structural representation of bioactives (a) γ-oryzanol (b) β-sitosterol.

10.2 Material and methods

Chemicals

γ-oryzanol, ethyl acetate, chloroform, acetic anhydride, sulfuric acid and polyoxyethylene (20) sorbitan monolaurate (Tween 20) were purchased from Wako Pure Chemical Ind. (Osaka, Japan). Medium chain fatty acid triglyceride oil (MCT, sunsoft MCT-7) with a fatty acid residue composition of 75% caprylic acid and 25% capric acid was procured from Taiyo Kagaku Co. Ltd. (Mie, Japan). β-sitosterol was purchased from MP biomedicals (lllkirch, France). Decaglycerol monolaurate (ML-750, HLB 14.8) was procured from Sakamoto Yakuhin Kogyo Co., Ltd (Osaka, Japan). Milli-Q water with a resistivity of 18MΩ cm (pH 7.1) served as the continuous phase. All other chemicals used in this study were of analytical grade and used as received.

A-symmetric microchannel array plate

The emulsification experiments were conducted using 24 × 24 mm silicon MC plate (Model WMS 1-4, manufactured by EP. Tech Co., Ltd., Hitachi, Japan) containing 23, 348 MCs and four 2.0 mm diameter

holes at the corners of the plate, these holes were used to feed both phases and collect the produced emulsions. These MCs were fabricated by repeated process of photolithography and deep-reactive-ion etching (DRIE) and located within 10×10 mm square region in center of plate. The MC plate was 500 μm thick (Fig. 10.2a), but was etched down to thickness of 100 μm in the central region where MCs were located. Each MC consist of cylinderal microhole of 10 μm with 70 μm depth on the outer side and a microslot (10×50 μm cross section and 30 μm depth) located on the inner side (Fig. 10.2c,d). The distance between the centers of adjacent MCs in the vertical rows was 70 μm and the distance between the centers of MCs in the adjacent rows was 60 μm (Fig. 10.2d). The MC plate was plasma oxidized to grow hydrophilic silicondioxide layer using oxygen plasma reactor (PR41, Yamato Science Co. Ltd., Tokyo, Japan).

Dispersed and continuous phase preparation

0.5-4.0% (w/w) β-sitosterol was dissolved in heated MCT oil at 60± 2ºC under water bath (HWA-50D, As One Co., Osaka, Japan) and stirred for 10 min at ambient temperature. Afterwards, 0.5-4.0% (w/w) γ-oryzanol was added to pre-loaded β-sitosterol solution and stirred for 20 min for proper dissolution. The β-sitosterol and γ-oryzanol loaded MCT oil was used as dispersed phase during MCE. The continuous phase comprises 1% (w/w) Tween 20 or 1% (w/w) ML-750 as emulsifiers in Milli-Q water and used as such during emulsification. The pH of continuous phase during emulsification was 7.2.
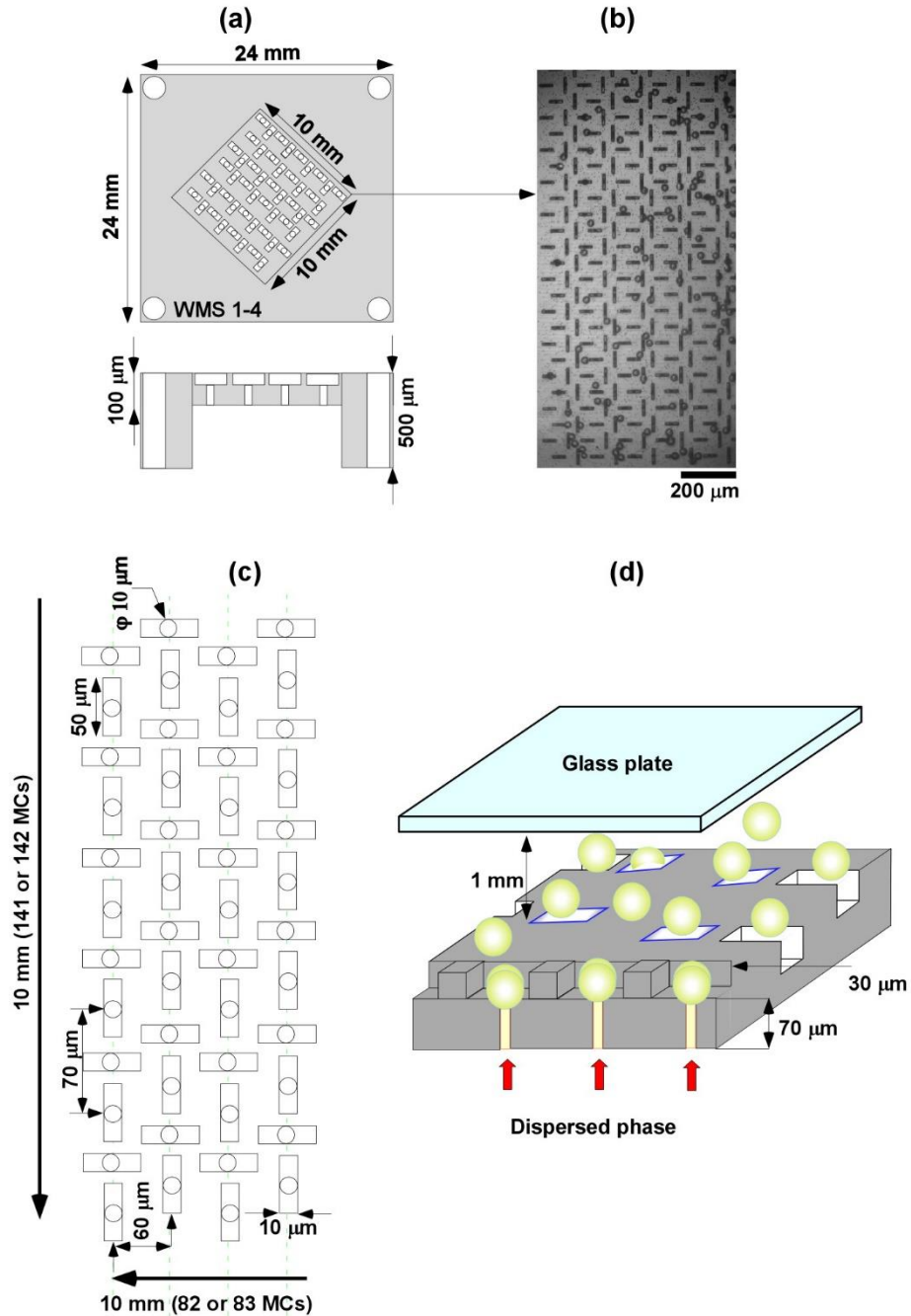
Figure 10.2: (a) Schematic representation of MC chip used in MCE. (b) Microscopic image of WMS 1-4 silicon chip surface. Cylindered holes can be seen as black dots in the center of each slot. (c) Arrangement of MCs in WMS 1-4 chip. Each vertical row contains alternately 142 and 141 MCs. There are 83 vertical rows with 142 MCs and 82 rows with 141 MCs making the total number of MCs equal to 23,348 = 83 × 142 + 82 × 141. (d) Schematic view of the WMS 1-4 chip depth.

Emulsification procedure

The MC plate was degassed in the continuous phase using ultrasonic water bath (VS-100 III, As One Co., Osaka, Japan) at a 100 kHz for 20 min, and then mounted in the six piece module assembly previously filled with continuous phase. Afterwards, the dispersed phase was injected through the MC plate at the flow rate ranging from 1 to 14 mL h^{-1} using syringe pump (Model 11, Harvard Apparatus Inc., Holliston, USA). The droplets were removed from the module by the continuous phase delivered from an elevated reservoir through the gap between the MC plate and cover slip. The droplets generation process during MCE in illustrated in Fig. 10.3a. The emulsification process was carried out for approximately 1 h and monitored through FASTCAM-1024 PCI high speed video system at 250 to 1000 fps (Photron, Tokyo, Japan) attached to an inverted metallographic microscope (MD-300EF; Nikon Co., Tokyo, Japan), as shown in Fig. 10.3b.

Measurement and analysis

A laser light scattering particle size analyzer (Beckman Coulter LS 13 320, Miami, FL) was used to measure the Sauter mean diameter ($d_{3,2}$) of O/W emulsion droplets encapsulating γ-oryzanol and β-sitosterol. The particle size analyzer have ability to measure the size ranging from 0.04 to 2000 μm with a resolution of 116 particle size channels. The width of droplet size distribution was expressed as relative span factor (RSF) and is defined as:

$$\text{RSF} = \frac{D_{v,90} - D_{v,10}}{D_{v,50}} \qquad (10.1)$$

Where $D_{v,90}$ and $D_{v,10}$ and $D_{v,50}$ are the equivalent volume diameters at 90, 10 and 50% cumulative diameter, respectively. The droplet generation rate was estimated from the recorded videos obtained from FASTCAM-1024 PCI high speed video system at 1000 fps.

(a)

Continuous phase

Emulsion droplets

10 μm

Channel

Slit 50 μm

Dispersed phase

(b)

Continuous phase

Dispersed phase

O/W emulsions

Spacer

Glass plate

MC Module

Straight-through MC plate

Microscope video system
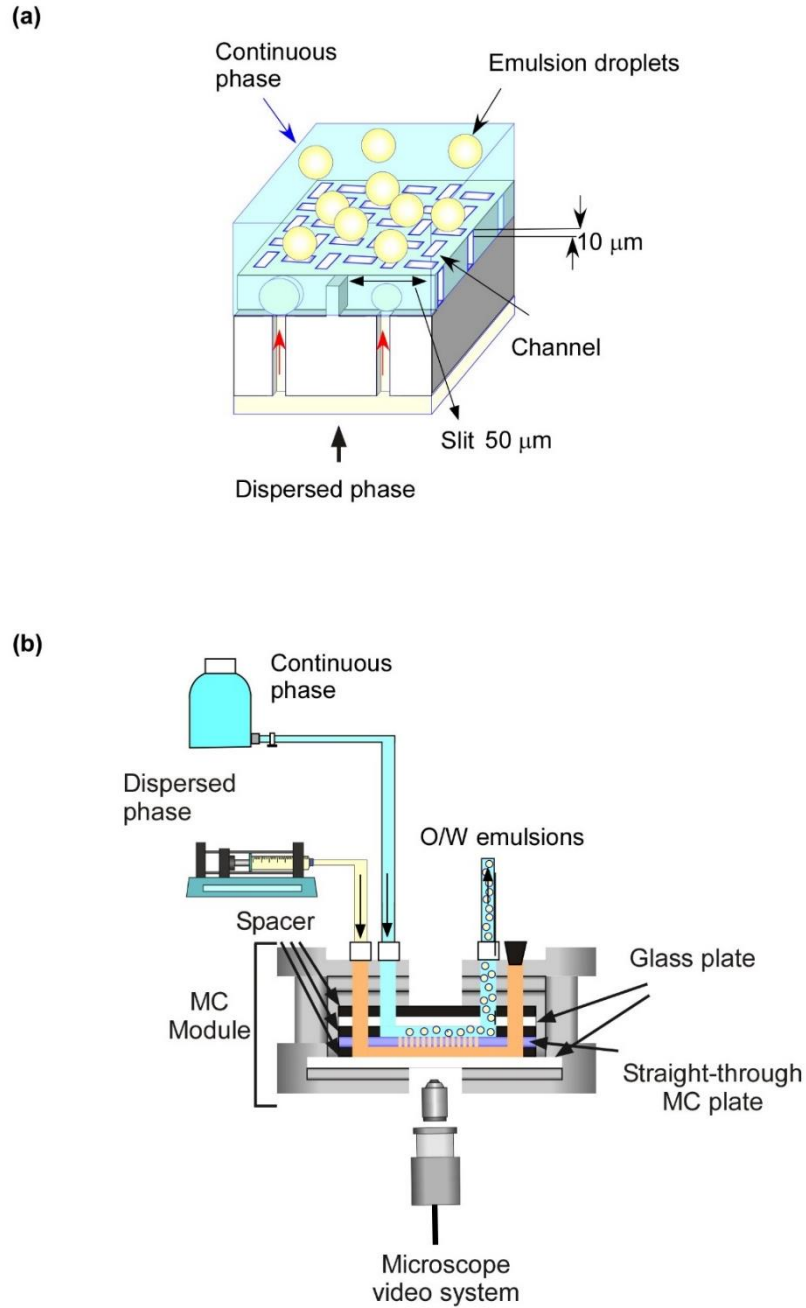
Figure 10.3: (a) Droplet generation representation through straight through MC arrays. (b) Schematic representation of an asymmetric straight through MCE setup.

Measurement of fluid properties

The densities of dispersed and continuous phases were measured using a density meter (DA-130 N, Kyoto Electronics Manufacturing Co., Ltd., Kyoto, Japan) at $25 \pm 2^\circ$C. The viscosities of dispersed and

236

continuous phases were measured with a sine wave vibro viscometer (SV-10, A&D Co., Ltd., Tokyo, Japan) at $25 \pm 2\,^{\circ}\text{C}$, later on absolute viscosity (η) was calculated by

$$\eta = \frac{\eta_{\text{mea}}}{\rho} \qquad (10.2)$$

where η_{mea} is the measured fluid viscosity and ρ is the fluid density. The static interfacial tension between the oil and the aqueous phases was measured with a fully automatic interfacial tensiometer (PD-W, Kyowa Interface Sciences Co., Ltd., Saitama, Japan) using a pendant drop method. The key physical properties of dispersed and continuous phase were presented in Table 10.1.

Table 10.1: Fluid properties of β-sitosterol and γ-oryzanol used for preparing O/W emulsions.

Concentration of bioactives*	Dispersed phase			Continuous phase		
	η_d (mPa s)	ρ_d (kg m^{-3})	γ_d (mN m^{-1})	Emulsifiers in Milli-Q water	η_c (mPa s)	ρ_c (kg m^{-3})
0.5% (w/w)	20.96 ± 0.06	945.96 ± 0.38	6.2 ± 0.2	1.0% (w/w) Tween 20	0.86 ± 0.01	998.86 ± 0.06
1.0% (w/w)	22.03 ± 0.06	946.03 ± 0.21	5.9 ± 0.2	1.0% (w/w) ML-750	0.80 ± 0.01	999.70 ± 0.15
2.0% (w/w)	23.80 ± 0.10	947.93 ± 0.06	5.1 ± 0.2			
3.0% (w/w)	26.70 ± 0.06	949.50 ± 0.10	4.1 ± 0.2			
4.0% (w/w)	29.73 ± 0.10	951.00 ± 0.10	2.7 ± 0.1			

* Dispersed phase contains both β-sitosterol and γ-oryzanol. The interfacial tension was observed in the presence of 1% (w/w) Tween 20 in Milli-Q water

Physical and chemical stability of O/W emulsions

The physical stability of emulsion droplets at 4 and $25 \pm 1\,^{\circ}\text{C}$ was observed from $d_{3,2}$ and RSF values. Moreover, droplet coalescence or flocculation was observed from microscopic observations using an optical microscope (DM IRM, Leica Microsystems, Wetzlar, Germany). The chemical stability of emulsion droplets at 4 and $25 \pm 1\,^{\circ}\text{C}$ was determined spectrophotometrically. γ-oryzanol was quantified in ethyl acetate, while chloroform was used to quantity β-sitosterol. The spectral measurements of ethyl acetate and chloroform extracts were carried out using a UV/VIS/NIR spectrophotometer (V-570, Jasco, Hachioji, Japan).

γ-oryzanol quantification

2 mL of the emulsion was extracted with 8 mL of ethyl acetate, followed by ultrasonic water bath at a 45 kHz for 10 min (VS-100 III, As One Co., Osaka, Japan). The extract was then centrifuged (KN-70, Kubota, Japan) at 3500 rpm for 15 min. A 1 mL aliquot of the supernatant was diluted five times with ethyl acetate and filtered through 0.45 micron syringe filter (Millipore Corp. USA). The filtered extract was then injected into a quartz cell with a 10 mm pass length. The absorbance of γ-oryzanol in emulsion extract was measured at 320 nm using an appropriate blank. A representative standard curve of absorbance versus concentration gave linear least-squares regression with a coefficient of determination (r^2) of 0.9966. All experiments were repeated in triplicate and mean values were calculated. The Beer's law was obeyed in the concentration range of 1-10 μg mL^{-1}. The encapsulation efficiency of γ-oryzanol in samples was calculated with the equation:

$$EE_{OG}(\%) = \frac{Weight\ of\ free\ \gamma-oryzanol}{Weight\ of\ formulated\ \gamma-oryzanol} \times 100 \qquad (10.3)$$

β-sitosterol quantification

2 mL of the emulsion was extracted with 4 mL of chloroform, followed by ultrasonic water bath at a 45 kHz for 10 min (VS-100 III, As One Co., Osaka, Japan). The extract was then centrifuged (KN-70, Kubota, Japan) at 3500 rpm for 15 min. A 1mL aliquot of the subnatant was diluted five times with chloroform and filtered through 0.45 micron syringe filter (Millipore Corp. USA). 2 mL of the Libermann-Burchard reagent (composed of 10 mL acetic anhydride and 0.5 mL sulfuric acid), was added to the filtered extract and stored in dark at ambient temperature for 15 min. The presence of β-sitosterol produces a characteristic green color whose absorbance was measured in a spectrophotometer at 640 nm using an appropriate blank [37]. A representative standard curve of absorbance versus concentration gave linear least-squares regression with a coefficient of determination (r^2) of 0.9970. All experiments were repeated in triplicate and mean values were calculated. The Beer's law was obeyed in the concentration range of 10-400 μg mL^{-1}. The encapsulation efficiency of β-sitosterol in samples was calculated with the equation:

$$EE_{BS}(\%) = \frac{Weight\ of\ free\ \beta-sitosterol}{Weight\ of\ formulated\ \beta-sitosterol} \times 100 \qquad (10.4)$$

10.3 Results and discussion

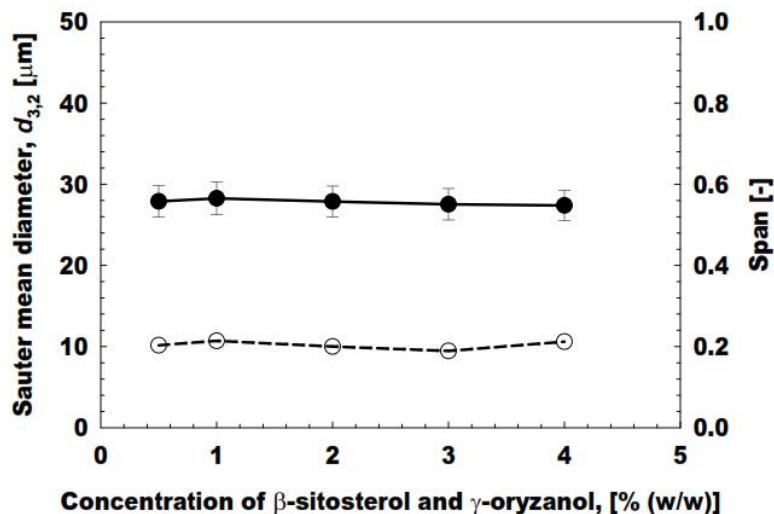*Effect of β-sitosterol and γ-oryzanol concentration on production characteristics of O/W emulsions*

The crystalline bioactives were detrimental to the stability of emulsion system, as they could greatly increase the droplet size and eventually reduce the encapsulation efficiency of emulsion system [38]. The solubility of β-sitosterol and γ-oryzanol in oil medium plays a critical role in the stability of emulsion droplets. The maximum solubility of β-sitosterol and γ-oryzanol in MCT was evaluated from series of dilution experiments. Firstly, different concentrations (0.5-4.0% (w/w)) of β-sitosterol was dissolved in MCT under water bath at $60 \pm 2^{\circ}C$ for a period of 20 min, the heating efficiently dissolve different concentrations within 10 min. The resistivity against crystallization was observed at $4^{\circ}C$ for a period of 24 h, all dilutions having concentration above 2% (w/w) shows large amount β-sitosterol crystals just after 1 h of storage. Afterwards, different concentrations of (0.5-4.0% (w/w)) γ-oryzanol was added to pre-loaded β-sitosterol MCT oil at ambient temperature with continuous stirring for 20 min. All of oil samples completely dissolve γ-oryzanol and later stored at $4^{\circ}C$ for a period of 24 h. The oil samples show crystallization beyond 2% (w/w) concentrations after 24 h.

The MCE were conducted immediately after dissolving (0.5-4.0% (w/w)) of β-sitosterol and γ-oryzanol in MCT in order to assess the droplet generation characteristics and effect of different concentrations on $d_{3,2}$ and RSF width of O/W emulsions. The continuous phase includes 1% (w/w) Tween 20 in Milli-Q water. The dispersed phase was injected into the MC module at flow rate (Q_d) of 1-5 mL h^{-1}, while the continuous flow rate (Q_c) was maintained at 500 mL h^{-1}. Uniformly sized O/W emulsion droplets were generated from the asymmetric through holes with different concentrations of β-sitosterol and γ-oryzanol. Fig. 10.4a shows the concentration effect of β-sitosterol and γ-oryzanol on $d_{3,2}$ and RSF width of O/W emulsions generated at Q_d of 1 mL h^{-1}. There was almost no influence of concentration of dispersed phase on $d_{3,2}$ of O/W emulsions (Fig. 10.4a). The $d_{3,2}$ of emulsions remain in range from 27.90 to 27.40 μm with RSF with less than 0.2 with increasing concentration of β-sitosterol and γ-oryzanol.

Initially there was no sign of wetting with different concentrations, but at higher Q_d and dispersed phase concentration exceeding 1% (w/w), an increased in $d_{3,2}$ was observed with RSF width exceeding 0.5 (Fig. 10.4b). The increase in $d_{3,2}$ was more prominent at dispersed phase concentration of 4% (w/w).

Moreover, the crystallization of β-sitosterol and γ-oryzanol (Fig. 10.5a) was observed in disperse phase having concentration >2% (w/w) after 30 min of emulsification. The formulated O/W emulsions with 0.5-1.0% (w/w) β-sitosterol and γ-oryzanol shows no signs of crystallization even after 24 h of emulsification. The droplet generation with 1% (w/w) concentration is depicted in Fig. 10.5b. The droplets detached smoothly from the asymmetric through-holes without any significant wetting or unstable emulsion droplets. Our results of this study correlates well with previous study of Neves, *et al.* [18], they encapsulated 2.5% (w/w) γ-oryzanol in O/W emulsions using straight-though MCE with average droplet diameter of 28.8 μm with coefficient of variation 3.8%.

(a)

(b)
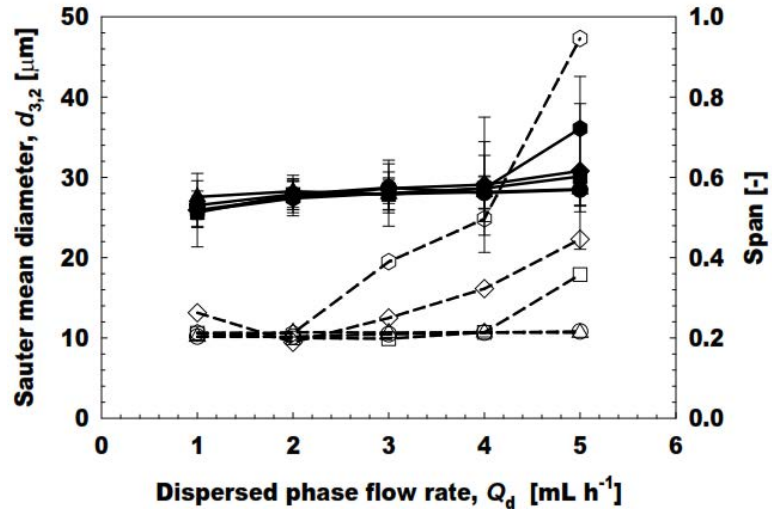
Figure 10.4: (a) Effect of concentration of β-sitosterol and γ-oryzanol on $d_{3,2}$ and RSF width of O/W emulsions. (—●—) denote $d_{3,2}$ and (-⊖-) denote RSF width of O/W emulsions. (b) Effect of concentration of β-sitosterol and γ-oryzanol on $d_{3,2}$ and RSF width of O/W emulsions under different dispersed phase flow rates. (—●—) denote 0.5%, (—▲—) 1%, (—■—) 2%, (—◆—) 3% and (—●—) denote 4% (w/w) β-sitosterol and γ-oryzanol, while same shape open keys denote RSFs of O/W emulsions.

(a)
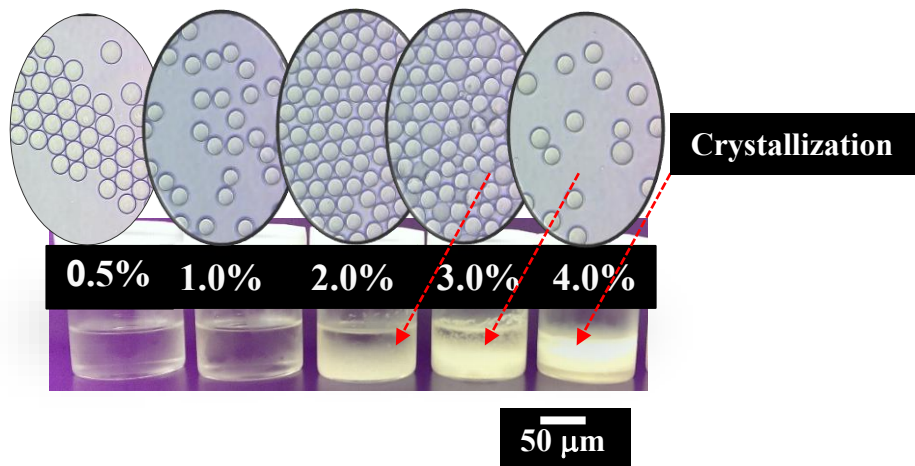
(b)
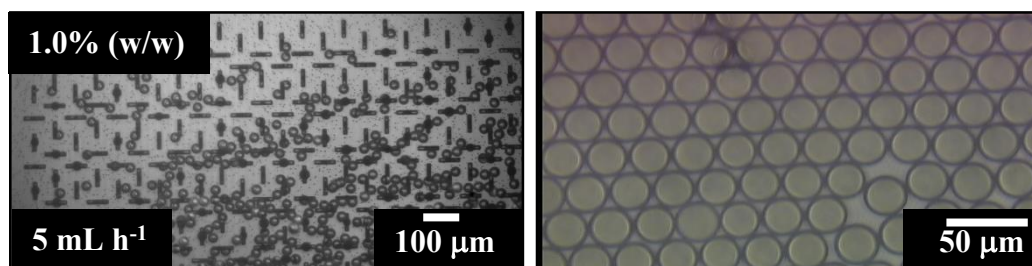
Figure 10.5: (a) Microscopic images of O/W emulsions with increasing concentration of β-sitosterol and γ-oryzanol (b) Droplet generation in MCE containing 1% (w/w) β-sitosterol and γ-oryzanol.

Effect of dispersed phase flow rate on preparation characteristics O/W emulsion droplets

A considerable challenge in microfluidic devices is in obtaining emulsions at high dispersed phase fluxes, sufficient to make the process suitable for industrial applications. Moreover, appropriate control of Q_d is needed to achieve monodisperse emulsions. The droplet production rate in MCE is proportional to Q_d and later depends upon capillary number (the balance between the viscous and interfacial forces) [39].

Fig. 10.6a depicts the effect of Q_d on the $d_{3,2}$ and RSF width of the generated droplets stabilized with 1% (w/w) Tween 20. The dispersed phase constitutes 1.0% (w/w) β-sitosterol and γ-oryzanol in MCT. The MCE was conducted by maintaining Q_d in between 0.5-14 mL h^{-1}, while the continuous phase flow rate was varied between 500-1000 mL h^{-1}. The $d_{3,2}$ increased from 25.14 to 30.05 μm with the increasing Q_d. The increase in $d_{3,2}$ have no impact on RSF width of O/W emulsions. The RSF width remain in range from 0.22 to 0.27 with increasing Q_d, only few channels produced polydispersed droplets (Fig. 10.6b) even at Q_d of 14 mL h^{-1}. There was no relative size stable zone as previously observed in many studies with MCE [40, 41]. The high stability of β-sitosterol and γ-oryzanol loaded emulsions at Q_d of 14 mL h^{-1} might attributed to surface activity of phytosterols that allow some of the β-sitosterol and γ-oryzanol to migrate to the oil-water interface of emulsion droplets [42]. Fig. 10.7a shows the effect of Q_c on $d_{3,2}$ and RSF of O/W emulsions. The monodisperse emulsions formulated at different Q_c shows no prominent difference in $d_{3,2}$ and RSF. The size of emulsion droplets was independent of Q_c in straight-through MCE and agreed well with previous findings [43].

We also investigated the influence of Q_d on the droplet generation frequency per MC array chip (f) and is presented in Fig. 10.7b. f can be estimated by:

$$f = \frac{Q_d}{V_{av}} = \frac{6Q_d}{\pi d_{3,2}^3} \qquad (10.5)$$

Where Q_d is the dispersed phase flow rate in mL h^{-1} and V_{av} is the average droplet volume. The monodisperse droplets produced at Q_d of 10 mL h^{-1} have maximum productivity of 7.19×10^{14} s^{-1}. During MCE, we observed more than 90% of MCs generated uniform sized droplets at Q_d of 10 mL h^{-1}. The droplet generation frequency from single MC (f_{MC}) increased linearly with Q_d and have f_{MC} of 27.16 s^{-1} at Q_d of 10 mL h^{-1} (Fig. 10.7b). The f in MCE greatly depends upon dispersed phase viscosity and can be increased to higher value using dispersed phases like alkanes or tetradecane [41].

(a)
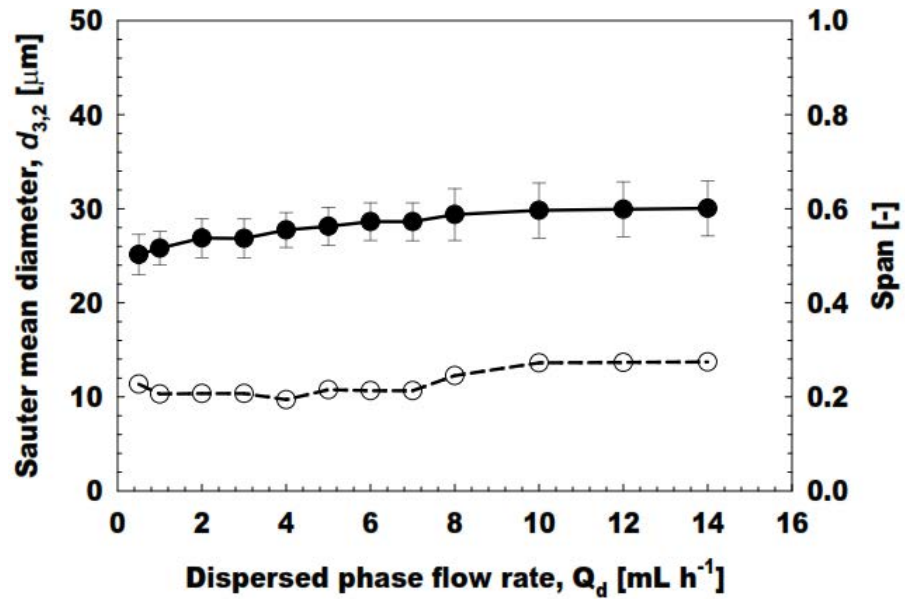
(b)

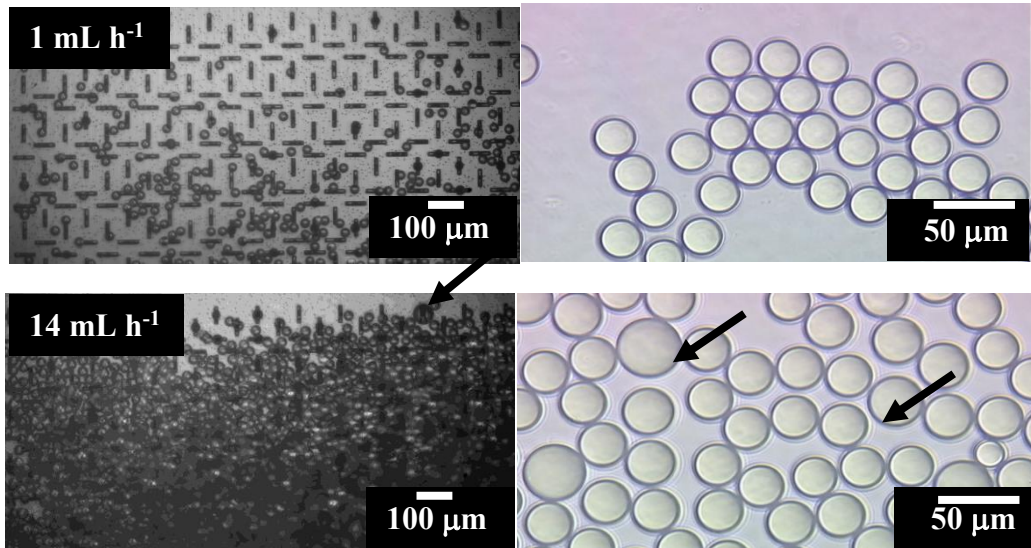**Figure 10.6: (a)** Effect of disperse phase flow rate on $d_{3,2}$ and RSF width of O/W emulsions encapsulating β-sitosterol and γ-oryzanol. (—●—) denote $d_{3,2}$ and (–⊖–) denote RSF width. **(b)** Droplet generation together with microscopic images at different dispersed phase flow rates. The arrow present polydisperse emulsion droplets.

(a)
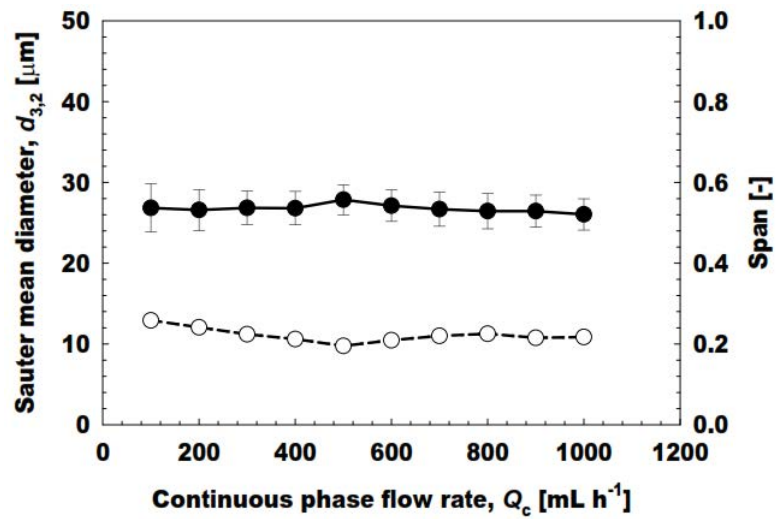
(b)
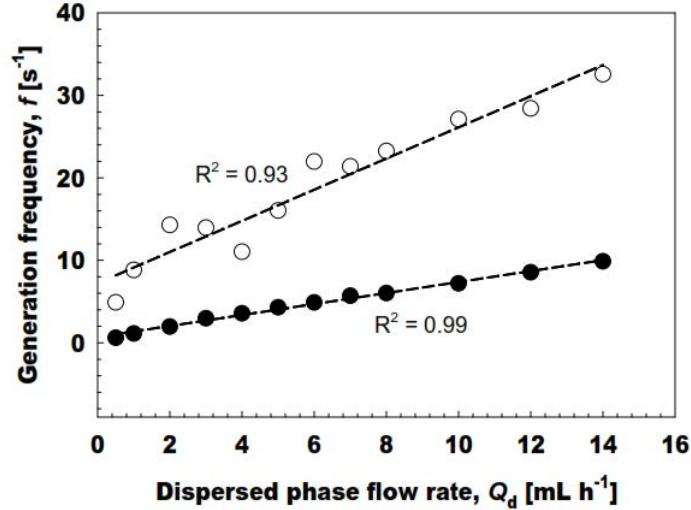
Figure 10.7: (a) Effect of continuous phase flow rate on $d_{3,2}$ and RSF width of O/W emulsions encapsulating β-sitosterol and γ-oryzanol. (━●━) denote $d_{3,2}$ and (-⊖-) denote RSF width. **(b)** The mean frequency of droplet generation, f as a function of the dispersed phase flow rate. (━●━) denote frequency per MC array chip (range 10^{14} s^{-1}) and (-⊖-) shows mean frequency from a single microchannel. Best-fit line for whole MC array chip ($R^2 = 0.99$): $f = 7 \times 10^{13}Q_d + 7 \times 10^{13}$; Best-fit line for each single microchannel ($R^2 = 0.93$): $f_{MC} = 1.89Q_d + 7.22$.

Storage stability of O/W emulsion droplets encapsulating β-sitosterol and γ-oryzanol

Storage stability of O/W emulsion droplets encapsulating 1% (w/w) β-sitosterol and γ-oryzanol was conducted at 4 and 25 ± 1°C for a period of 30 days. The storage stability was evaluated using either 1% (w/w) Tween 20 or 1% (w/w) ML-750 in Milli-Q water as continuous phase. The emulsion droplets were formulated by keeping Q_d at 2 mL h^{-1}. Immediately after the formulation all emulsions have light turbid appearance with good flow-ability. The physical appearance of O/W emulsions did not change during storage period. Fig. 10.8a shows the time changes in $d_{3,2}$ and RSF width of the formulated O/W emulsions stabilized with 1% (w/w) Tween 20. There was hardly any change in $d_{3,2}$ and RSF width of emulsions after 30 days of storage. The $d_{3,2}$ remain in ranged from 26.9 to 27.9 μm with RSF width <0.2 at 4 and 25 ± 1°C after 30 days of storage. Similarly, the emulsions stabilized with 1% (w/w) ML-750 (Fig. 10.8b) did not show any prominent change in droplet size distribution during stability evaluation, the $d_{3,2}$ ranged from 28.19 to 28.85 μm with RSF width <0.3 at 4 and 25 ± 1°C after 30 days of storage. Moreover, the

microscopic images (Fig. 10.8c) did not show any satellite droplets formation or coalescence during evaluated storage period.

The higher stability of emulsion droplets with Tween 20 and ML-750 were due to strong hydrophobic moiety that stabilized the O/W interfaces for longer period of time [44]. Moreover, the surface activity of β-sitosterol and γ-oryzanol might attribute towards stability of emulsions droplets [42]. Phytosterols have ability to influence the oxidative stability by themselves directly or indirectly through the alteration in the physical properties of the emulsion droplet due to their surface activity [45]. Niraula et al. [46] showed that the presence of surface active agent reduces the interfacial free energy at the interface and thus, renders some degree of stability to the resulting emulsion system. Izadi et al. [47], reported that the stability of phytosterol dispersion could be correlated with the decrease in surface tension and particle size by using oil and emulsifier as components of oil phase. The stability results of our study correlates well with the study of Izadi, et al. [47].

(a)
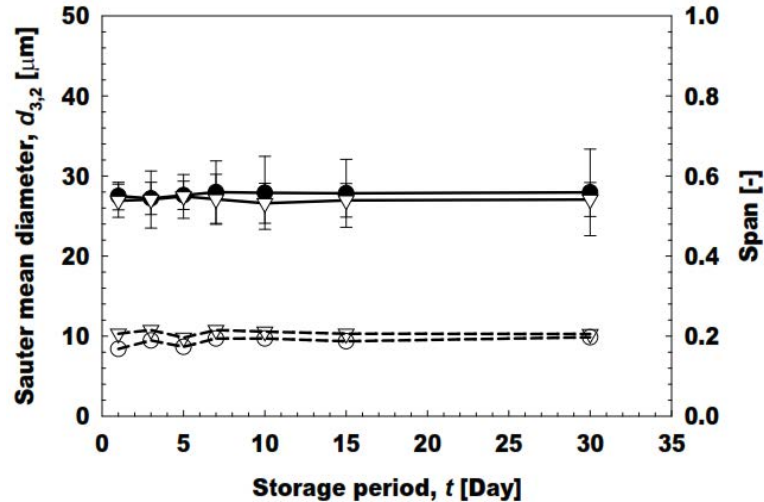
(b)
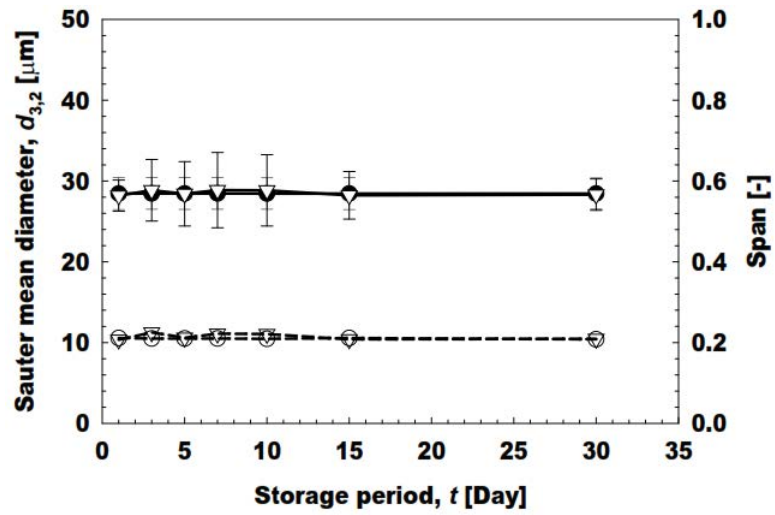
(c)
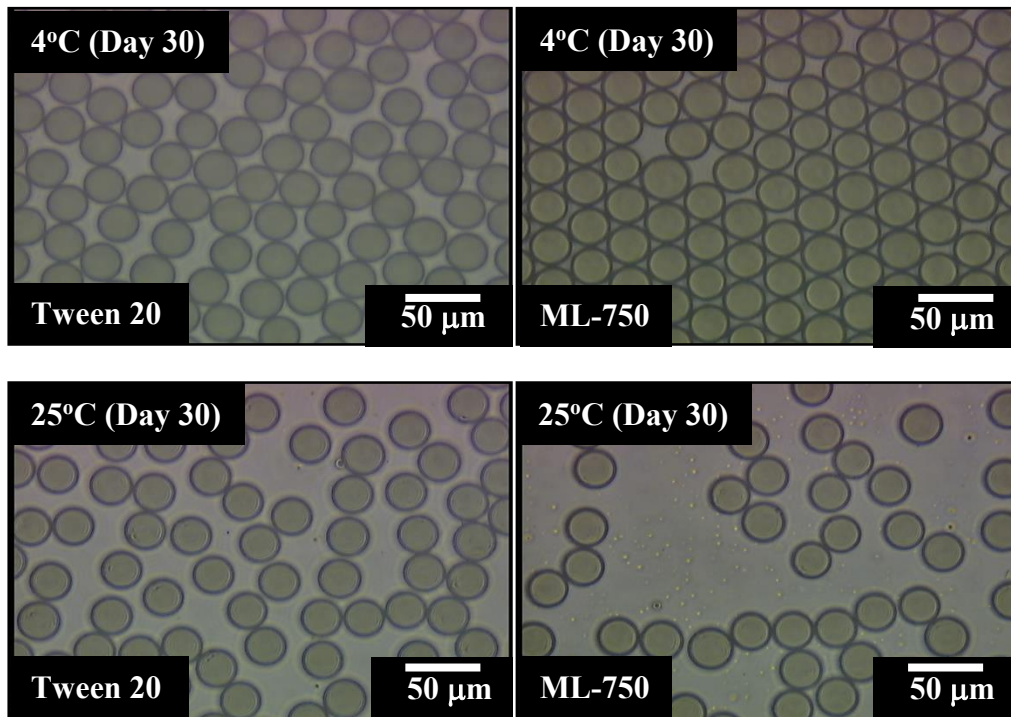
Figure 10.8: (a) Storage stability of O/W emulsions stabilized by 1% (w/w) Tween 20 encapsulating β-sitosterol and γ-oryzanol at 4 and 25 ± 1ºC. (b) Storage stability of O/W emulsions stabilized by 1% (w/w) ML-750 at 4 and 25 ± 1ºC. (─●─) denote $d_{3,2}$ and (-⊖-) denote RSF width at 4ºC. (─▽─) shows $d_{3,2}$ and (-▽-) shows RSF width at 25ºC. (c) Microscopic images of O/W emulsions stabilized by either 1% (w/w) Tween 20 or ML-750 after 30 days of storage at 4 and 25 ± 1ºC.

247

Encapsulation efficiencies of β-sitosterol and γ-oryzanol in O/W emulsion droplets

The freshly formulated O/W emulsions encapsulating β-sitosterol and γ-oryzanol had initial retention of 14.0 μg mL^{-1} γ-oryzanol and 53.5 μg mL^{-1} β-sitosterol in emulsion system stabilized by 1% (w/w) Tween 20. In comparison the emulsion system stabilized by 1% (w/w) ML-750 had almost similar initial retention of 13.8 μg mL^{-1} γ-oryzanol and 52.1 μg mL^{-1} β-sitosterol. These initial retentions were regarded as 100% encapsulated efficiencies (EEs). In MCE there was difficulties in maintaining volume fraction (φ_d) in comparison to conventional emulsification systems. The calculated φ_d during MCE corresponds to 0.40%.

Fig. 10.9 shows the EEs of β-sitosterol and γ-oryzanol in emulsions stabilized by 1% (w/w) Tween 20. There was slight decrease in EEs of β-sitosterol with storage time (Fig. 10.9a). The O/W emulsions have β-sitosterol EEs of more than 85% after 30 days of storage at 4 and 25 ± 1°C. Similarly, γ-oryzanol EEs of more than 80% was observed at 4°C and 86% at 25°C after 30 days of storage (Fig. 10.9b). In comparison slightly less EEs were observed in emulsions stabilized by 1% (w/w) ML-750. β-sitosterol EEs >80% was observed after 30 days of storage at 4 and 25 ± 1°C (Fig. 10.10a). More rapid decline in γ-oryzanol EEs were noticed in emulsions stabilized with ML-750. After 30 days of storage, these emulsions have γ-oryzanol EEs around 50% at 4 and 25 ± 1°C (Fig. 10.10b).

The decrease of γ-oryzanol EEs in emulsions stabilized by ML-750 can be attributed to the interaction of ML-750 with γ-oryzanol. The thinning of interfacial layer around emulsion droplets with storage time allows the partitioning of γ-oryzanol from oil phase to water phase. It is also possible that exchange phenomenan occur where γ-oryzanol is degraded in the water phase and re-partitions into the oil phase, especially at 25°C [48]. Good EEs > 60% of γ-oryzanol in solid lipid nanoparticles (SLNs) were reported by Ruktanonchai *et al.* [49], their study shows that %EE of γ-oryzanol was strongly dependent on the type of solid lipid used. Hassani *et al.* [50] Prepared lecithin stabilized nanoliposomes encapsulating γ-oryzanol and reported EE over 80% after 60 days of storage. The high EEs of β-sitosterol with different emulsifiers can be correlated with stronger surface activity of β-sitosterol [42]. This surface activity allow β-sitosterol to migrate at oil-water interface and restrict its partitioning between oil and water phase [42]. The EEs in present study correlates well with the previous EEs of bioactives in MCE. The EE of L-ascorbic

acid in different emulsions prepared through MCE was more 80% after 10 d of storage period at 4°C [21].

This high EE can be correlated with high degree of monodispersity in the emulsion system.

(a)
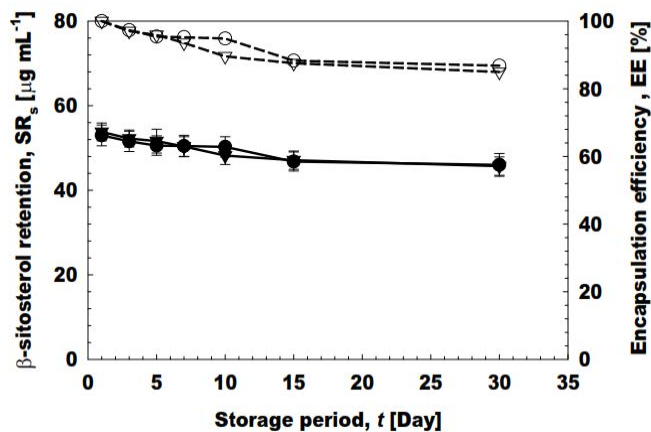
(b)

Figure 10.9: Retention and encapsulating efficiencies (EEs) of β-sitosterol and γ-oryzanol encapsulated O/W emulsions at 4 and 25 ± 1°C stabilized by 1% (w/w) Tween 20. (a) β-sitosterol, (b) γ-oryzanol. (—●—) denote β-sitosterol and γ-oryzanol retention at 4°C (-⊖-) denote β-sitosterol and γ-oryzanol (EEs) at 4°C. (—▽—) β-sitosterol and γ-oryzanol retention at and (⁻▽⁻) shows β-sitosterol and γ-oryzanol (EEs) at 25°C.

(a)

(b)

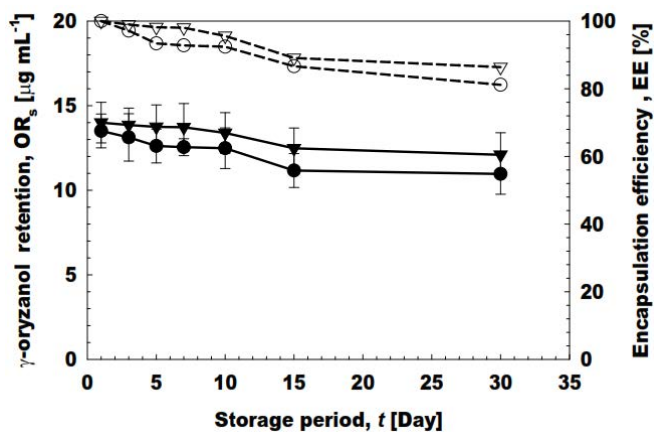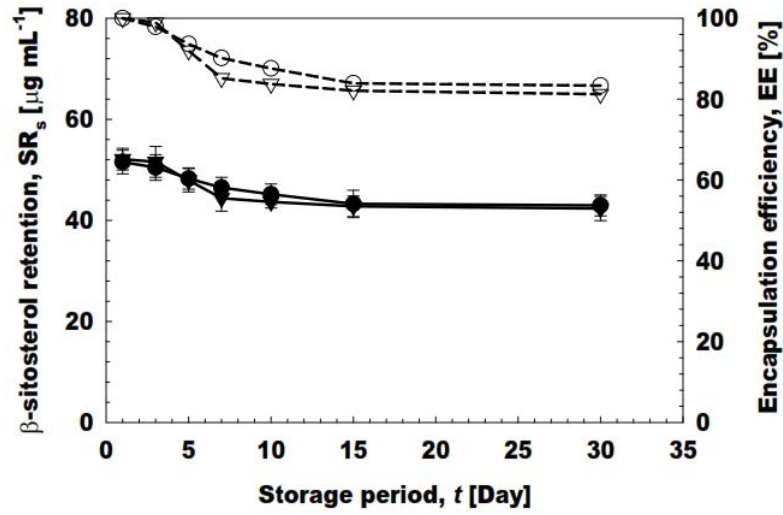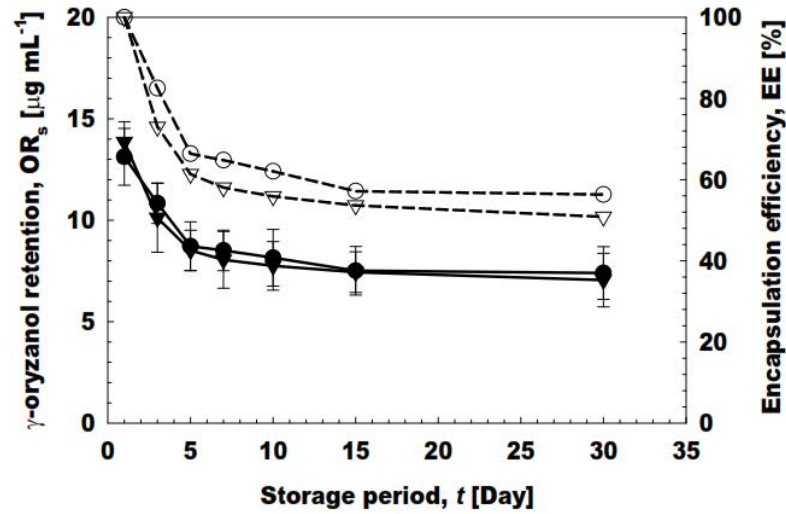Figure 10.10: Retention and encapsulating efficiencies (EEs) of β-sitosterol and γ-oryzanol encapsulated O/W emulsions at 4 and 25 ± 1ºC stabilized by 1% (w/w) ML-750. (a) β-sitosterol (b) γ-oryzanol. (—●—) denote β-sitosterol and γ-oryzanol retention at 4ºC (-⊝-) denote β-sitosterol and γ-oryzanol (EEs) at 4ºC. (—▽—) β-sitosterol and γ-oryzanol retention at and (⁻▽⁻) shows β-sitosterol and γ-oryzanol (EEs) at 25ºC.

References

[1] Leal-Calderon F, Schmitt V and Bibette J, Emulsion science: basic principles, Springer, New York, 2007.

[2] Schramm LL, Emulsions, foams, and suspensions: fundamentals and applications, John Wiley & Sons, Weinheim, 2006.

[3] Leal-Calderon F, Thivilliers F and Schmitt V, *Curr. Opin. Colloid Interface Sci.*, **12,** 206-212 (2007).

[4] Huang JS and Varadaraj R, *Curr. Opin. Colloid Interface Sci.*, **1,** 535-539 (1996).

[5] Ouyang Y, Mansell R and Rhue R, *Crit. Rev. Environ. Sci. Technol.*, **25,** 269-290 (1995).

[6] Nakano M, *Adv. Drug Deliv. Rev.*, **45,** 1-4 (2000).

[7] Santana R, Perrechil F and Cunha R, *Food Eng. Rev.*, **5,** 107-122 (2013).

[8] Gañán-Calvo AM, *Phys. Rev. Lett.*, **80,** 285 (1998).

[9] Perrin P, *Langmuir*, **14,** 5977-5979 (1998).

[10] Nakashima T, Shimizu M and Kukizaki M, *Adv. Drug Deliv. Rev.*, **45,** 47-56 (2000).

[11] Kawakatsu T, Kikuchi Y and Nakajima M, *J. Ame. Oil Chem. Soc.*, **74,** 317-321 (1997).

[12] Chu LY, Utada AS, Shah RK, Kim JW and Weitz DA, *Ange. Chem. Int. Ed.*, **46,** 8970-8974 (2007).

[13] Utada AS, Lorenceau E, Link DR, Kaplan PD, Stone HA and Weitz DA, *Science*, **308,** 537-541 (2005).

[14] Kobayashi I, Wada Y, Hori Y, Neves MA, Uemura K and Nakajima M, *Chem. Eng. Technol.*, **35,** 1865-1871 (2012).

[15] Kobayashi I, Nakajima M, Chun K, Kikuchi Y and Fukita H, *Aiche J.*, **48,** 1639-1644 (2002).

[16] Vladisavljevic GT, Khalid N, Neves MA, Kuroiwa T, Nakajima M, Uemura K, Ichikawa S and Kobayashi I, *Adv. Drug Deliv. Rev.*, **65,** 1626-1663 (2013).

[17] Vladisavljevic' GT, Kobayashi I and Nakajima M, *Microfluid Nanofluid.*, **13,** 151-178 (2012).

[18] Neves MA, Ribeiro HS, Kobayashi I and Nakajima M, *Food Biophys.*, **3,** 126-131 (2008).

[19] Souilem S, Kobayashi I, Neves M, Sayadi S, Ichikawa S and Nakajima M, *Food Bioprocess Technol*, **7,** 2014-2027 (2014).

[20] Neves MA, Ribeiro HS, Fujiu KB, Kobayashi I and Nakajima M, *Ind. Eng. Chem. Res.*, **47,** 6405-6411 (2008).

[21] Khalid N, Kobayashi I, Neves MA, Uemura K, Nakajima M and Nabetani H, *Colloid Surface A: Physicochemical and Engineering Aspects*, **458,** 69-77 (2014).

[22] Khalid N, Kobayashi I, Neves MA, Uemura K, Nakajima M and Nabetani H, *Colloid Surfaces A.*, **459,** 247-253 (2014).

[23] Patel M and Naik S, *J. Sci. Ind. Res*, **63,** 569-578 (2004).

[24] Kanno H, Usuki R and Kaneds T, *J. Jpn. Soc. Food Sci. Technol.*, **32,** 170 (1985).

[25] Wilson TA, Nicolosi RJ, Woolfrey B and Kritchevsky D, *J. Nutr. Biochem.*, **18,** 105-112 (2007).

[26] Murase Y and Iishima H, *Obstet Gynecol Prac*, **12,** 147-149 (1963).

[27] Phillips KM, Ruggio DM and Ashraf-Khorassani M, *J. Agric. Food Chem.*, **53,** 9436-9445 (2005).

[28] Scholle JM, Baker WL, Talati R and Coleman CI, *J. Am. Coll. Nutr.*, **28,** 517-524 (2009).

[29] Genser B, Silbernagel G, De Backer G, Bruckert E, Carmena R, Chapman MJ, Deanfield J, Descamps OS, Rietzschel ER, Dias KC and Marz W, *Eur. Heart J.*, **33,** 444-451 (2012).

[30] Berges RR, Kassen A and Senge T, *BJU Int.*, **85,** 842-846 (2000).

[31] Katan MB, Grundy SM, Jones P, Law M, Miettinen T and Paoletti R, *Mayo Clin. proceed*, **78,** 965-978 (2003).

[32] Hamedi A, Ghanbari A, Saeidi V, Razavipour R and Azari H, *J. Functional Food*, **8,** 252-258 (2014).

[33] Ghaderi S, Ghanbarzadeh S, Mohammadhassani Z and Hamishehkar H, *Adv Pharm Bull*, **4,** (2014).

[34] Khuwijitjaru P, Yuenyong T, Pongsawatmanit R and Adachi S, *J. Oleo Sci.*, **58,** 491-497 (2009).

[35] Delaney B, Stevens LA, Schmelzer W, Haworth J, McCurry S, Hilfinger JM, Kim JS, Tsume Y, Amidon GL and Kritchevsky D, *J. Nutr. Biochem.*, **15,** 289-295 (2004).

[36] Gawrysiak-Witulska M, Rudzinska M, Wawrzyniak J and Siger A, *J. Am. Oil Chem. Soc.*, **89,** 1673-1679 (2012).

[37] Daksha A, Jaywant P, Bhagyashree C and Subodh P, *Electronic J. Environ. Agric. Food Chem.*, **9,** 1593-1597 (2010).

[38] Engel R and Schubert H, *Innov. Food Sci. Emerg. Technol.*, **6,** 233-237 (2005).

[39] Sugiura S, Nakajima M, Kumazawa N, Iwamoto S and Seki M, *J. Phys. Chem. B*, **106,** 9405-9409 (2002).

[40] Vladisavljevic GT, Kobayashi I and Nakajima M, *Powder Technol.*, **183,** 37-45 (2008).

[41] Vladisavljevic GT, Kobayashi I and Nakajima M, *Microfluid. Nanofluid.*, **10,** 1199-1209 (2011).

[42] Cercaci L, Rodriguez-Estrada MT, Lercker G and Decker EA, *Food Chem.*, **102,** 161-167 (2007).

[43] Kobayashi I, Mukataka S and Nakajima M, *Ind. Eng. Chem. Res.*, **44,** 5852-5856 (2005).

[44] Carnero Ruiz C, Molina-Bolívar J, Aguiar J, MacIsaac G, Moroze S and Palepu R, *Colloid Polym Sci*, **281,** 531-541 (2003).

[45] Chen B, McClements DJ and Decker EA, *Crit. Rev. Food Sci. Nutr.*, **51,** 901-916 (2011).

[46] Niraula B, King TC, Chun TK and Misran M, *Colloid Surface A.*, **251,** 117-132 (2004).

[47] Izadi Z, Nasirpour A and Garousi G, *J. Dispersion Sci. Technol.*, **33,** 1715-1722 (2012).

[48] Müller RH, Petersen RD, Hommoss A and Pardeike J, *Adv. Drug Deliv. Rev.*, **59,** 522-530 (2007).

[49] Ruktanonchai U, Sakulkhu U, Bejrapha P, Opanasopit P, Bunyapraphatsara N, Junyaprasert V and Puttipipatkhachorn S, *J. Microencapsul.*, **26,** 614-626 (2009).

[50] Hassani ZM, Ghanbarzadeh B, Hamishehkar H, Mokarram RR and Hosseini M, *Iranian J. Polymer Sci. Technol. (In Persion)*, **26,** 425-413 (2014).

Chapter 11

Conclusions and future perspectives

Chapter 2 deals with the formulation of monodisperse food-grade W/O/W emulsions loaded with a high concentration of L-AA in inner aqueous droplets through rotor-stator homogenization and subsequent MCE. The key point of this chapter is stable generation of uniformly sized W/O droplets that encapsulate a high concentration of L-AA via an asymmetric straight-through MC array, without visible leakage and breakage of inner aqueous droplets during MCE. Successful MCE is achieved under appropriate concentrations of the hydrophobic emulsifier added in the oil phase and the hydrophilic emulsifier added in the outer aqueous phase. Slight increases in W/O droplet size during storage may be attributed to slight and slow swelling of inner aqueous droplets. The formulated W/O/W emulsions had longer physical stability with L-AA retention during storage.

Chapter 3 focuses on preparation of monodisperse aqueous microspheres loaded with L-AA using MCE. The methodology presented in this study enables producing encapsulated nutraceutical products containing high concentrations of L-AA. Appropriate control of Na-alginate and $MgSO_4$ concentrations, compositions of the disperse and continuous phases, and operating conditions are needed to prepare stable monodisperse aqueous microspheres containing high concentrations of L-AA via MC arrays. The successful composition includes 1% (w/w) $MgSO_4$, 2% (w/w) Na-alginate, and a maximum L-AA concentration of 30% (w/w). The results also indicated that partial linkage of Mg^{2+} ions with Na-alginate could develop a soft gel-like structure, resulting in smooth detachment and generation of microspheres from MC arrays. Uniformly sized aqueous microspheres generated under mild processing conditions with MCE could increase the encapsulation efficiency and storage stability of L-AA in different food and pharmaceutical products. The through-put studies with straight through MCE concludes optimized emulsification conditions at 20% (w/w) L-AA, 2% (w/w) Na-alginate and 1% (w/w) Mg_2SO_4 in the dispersed phase under J_d of 5 L m^{-2} h^{-1}, while 5% (w/w) TGCR in water-saturated decane as the continuous phase. The resultant microspheres have good physical and chemical stability for more than 10 d at 40 ^oC. Moreover, they exhibit high EE of more than 70% during 10 d of evaluated period at 40 ^oC.

Chapter 4 shows food-grade W/O emulsions containing L-AA up to 30% (w/v) in the dispersed aqueous phase using conventional approach. Adequate homogenization conditions enabled preparing W/O emulsions with an L-AA retention rate > 95%, regardless of L-AA concentration. The prepared W/O emulsions containing high concentration of L-AA were well stabilized at 4 and 25^oC for more than 30 d

with good organoleptic profile. All prepared W/O emulsions showed relatively higher retention of ~50% at 4°C and ~30% at 25°C after 30 d storage with first order kinetic fitting. These findings were not affected by the type of oil used in this study. The above retention time could be further improved by using mixed emulsifier system or addition of some bulking agents like gelatin that increase the viscosity of dispersed phase.

Chapter 5 deals with food-grade W/O/W emulsions containing a high concentration of L-AA using conventional emulsification system and selected compositions, including gelatin in the inner aqueous phase and glucose in both aqueous phases. In particular, the formulations containing gelatin contributed to better flowability and higher L-AA retention. The prepared W/O/W emulsions containing high concentrations of L-AA were physically stable with slight changes in droplet size and size distribution during 35 d of storage at 4 °C. The W/O/W emulsions also demonstrated relatively high retention of L-AA after 30 d of storage, and their retention kinetics followed a first-order kinetics equation.

Chapter 6 shows monodisperse food-grade O/W emulsions loaded with ergocalciferol using grooved and straight through MCE. The key point of this research is stable generation of uniformly sized O/W droplets that encapsulate ergocalciferol via an asymmetric straight-through MC array, without any coalescence or wetting of dispersed phase during MCE. Successful grooved type MCE is achieved with different food grade vegetable oils and emulsifiers, when used at 1% (w/w) in Milli-Q water. The high through put studies with straight through MCE indicates successful operating conditions under low dispersed phase flux at 5 L m^{-2} h^{-1} and under 1% (w/w) Tween 20 as optimum emulsifier in Milli-Q water. There was hardly any increase in mean droplet diameter during 15 d of storage period. The formulated emulsions containing erogcalciferol have encapsulating efficiency of more than 85% after 10 d of storage time. The better physical and chemical stability correlates well with the monodispersity of system.

Chapter 7 shows food grade monodisperse O/W emulsions containing both ergocalciferol and cholecalciferol using straight through MCE. In this study uniform sized emulsion droplets were stably generated via an asymmetric straight-through MC array, without any significant wetting or outflow of dispersed phase at optimum processing conditions. The optimum emulsification conditions evolves low dispersed phase flux at 10 L m^{-2} h^{-1} and under 1% (w/w) Tween 20 as potential hydrophilic emulsifier in Milli-Q water. The formulated emulsion droplets have good stability of more than 15 d at 4 and 25°C.

Moreover, they exhibit a good encapsulation efficiency of more than 65-75% at 4 and 25°C and during evaluated storage period.

Chapter 8 utilizes both rotor-stator homogenizer (RSH) and high pressure homogenization (HPH) to fabricate both ergocalciferol and cholecalciferol emulsions. Moreover, the effect of different food grade oils on vitamin D emulsions was thoroughly studied. Nevertheless, there are studies that predicted the release profile of vitamin D in different nanoparticles, but there were no reports that describe the release profile of both ergocalciferol and cholecalciferol in emulsions prepared with RSH and HPH. This study showed that O/W emulsions formulated from RSH or HPH offers an inexpensive means to encapsulate vitamin D. Moreover, the formulation of these simple emulsion techniques is easily adoptable at industrial level. The study showed that droplet size of O/W emulsions encapsulating vitamin D depends upon homogenization speed and homogenization type. HPH significant reduces the droplet size to sub-micron level, yet polydispersity is the major problem in both types of homogenization techniques. The HPH stabilize the O/W emulsions to longer period of time without any significant deformation, on the other hand RSH at low speed destabilized the emulsions due to Oswald ripening and flocculation. Moreover, the study concluded that homogenization techniques have no marked effect on encapsulation efficiencies of vitamin D loaded emulsions. The prepared emulsions either with rotor-stator or high pressure homogenization retains about 50% of ergocalciferol and cholecalciferol after 7 d of storage at 4°C, afterwards followed rapid decline in encapsulation efficiencies.

Chapter 9 deals with quercetin encapsulation. Quercetin has been claimed to have countless health benefits, but its poor solubility in aqeous solutions, low bioavailability, low permeability, cystallization and hydrophobic nature limits its applications in food products. The chapter demonstrated successful formulation of food grade O/W emulsions encapsulating quercetin through straight-through MCE. Quercetin at concentration of 0.4 mg mL^{-1} in different food grade oils does not influence the emulsion formation and monodispersity. The optimized production parameters includes dispersed phase flux of 20-40 L m^{-2} h^{-1} and continuous flow velocity ranging between 5.0 mm s^{-1} to 20.0 mm s^{-1}. The study also investigate the effect of different emulsifiers and conclude non-ionic emulsifiers as optimum emulsifiers that influence the storage stability. Protein based emulsifiers and ionic emulsifiers althrough produces monondisperse emulsion droplets but have impact on droplet size during storage at 4 and 25 °C. The

formulated O/W emulsions with 1% (w/w) Tween 20 have encapsulation efficiency of more than 80% and 70% at 4 and 25°C after 30 d of storage. The better physical and chemical stability points the monodispersity of emulsions generated from MCE. Moreover, these emulsions were generated under extreme mild conditions with energy efficiency corresponds to 27.5%.

Chapter 10 shows food grade monodisperse O/W emulsions encapsulating both β-sitosterol and γ-oryzanol using straight-through MCE. The optimized dispersed phase composition include 1% (w/w) β-sitosterol and γ-oryzanol in MCT, while 1% (w/w) Tween 20 in Milli-Q water as optimized continuous phase. The optimum MCE conditions evolves low dispersed phase flow rate of 2 mL h^{-1} with varying flow rate of continuous phase. These optimized conditions produces uniform sized emulsion droplets via an asymmetric straight-through MC array, without any outflow of dispersed phase. The formulated emulsion droplets have good stability of more than 30 d at 4 and 25 °C. Moreover, the formulated emulsions with β-sitosterol and γ-oryzanol have a good encapsulation efficiency of more than 80% at 4 and 25°C during 30 d of storage period.

The research indicate that MCE is a promising technique for encapsulating bioactive compounds, with superior control of processing parameters and various other physical conditions. The forthcoming scaling up of MCE devices is expected to further improve the quality of different emulsions and make practical their production on industrial scales.

List of Publications

Khalid N, Kobayashi I, Neves MA, Uemura K, Nakajima M. Preparation and characterization of water-in-oil emulsions loaded with high concentration of L-ascorbic acid. *LWT-Food Science and Technology*.2013, Vol. 51, no. 2, p. 448-454.

Khalid N, Kobayashi I, Neves M, Uemura K, Nakajima M. Preparation and Characterization of Water-in-Oil-in-Water Emulsions Containing a High Concentration of L-Ascorbic Acid. 2013. *Bioscience, Biotechnology, and Biochemistry*. Vol. 77, no. 6, p. 1171-1178.

Khalid N, Kobayashi I, Neves M, Uemura K, Nakajima M, Nabetani H. Monodisperse W/O/W emulsions encapsulating L-ascorbic acid: Insights in their formulation using Microchannel emulsification and stability studies. 2014. *Colloids and Surface A: Physicochemical and Engineering Aspects.* Vol. 458, no. 8, p. 69-77.

Khalid N, Kobayashi I, Neves M, Uemura K, Nakajima M, Nabetani H. Formulation of monodisperse water-in-oil emulsions encapsulating calcium ascorbate and ascorbic acid 2-glucoside by microchannel emulsification. 2014. *Colloids and Surface A: Physicochemical and Engineering Aspects*. Vol. 459, no. 9, p. 247-253.

Khalid N, Kobayashi I, Wang Z, Neves M, Uemura K, Nakajima M, Nabetani H. Formulation of monodisperse O/W emulsions loaded with ergocalciferol and cholecalciferol by microchannel emulsification: Insights of production characteristics and stability. 2015. *International Journal of Food Science and Technology*. In Press. DOI: 10.1111/ijfs.12832.

Khalid N, Kobayashi I, Neves M, Uemura K, Nakajima M, Nabetani H. Monodisperse Aqueous microspheres encapsulating high concentration of L-ascorbic acid: Insights of preparation and stability

evaluation from straight-through microchannel emulsification. 2015. *Bioscience, Biotechnology, and Biochemistry*. In Press.

Khalid N, Kobayashi I, Neves M, Uemura K, Nakajima M, Nabetani H. Preparation of monodisperse aqueous microspheres containing high concentration of L-ascorbic acid by microchannel emulsification. 2015. *Journal of Microencapsulation*. Revised version submitted to Journal.

Khalid N, Kobayashi I, Wang Z, Neves M, Uemura K, Nakajima M, Nabetani H. The Preparation characteristics and stability evaluation of oil-in-water emulsions loaded with ergocalciferol by microchannel emulsification. In Preparation.

Khalid N, Kobayashi I, Wang Z, Neves M, Uemura K, Nakajima M, Nabetani H. Formulation and characterization of food grade oil-in-water emulsions encapsulating mixture of cholcalciferol and ergocalciferol by different homogenization techniques. In Preparation.

Khalid N, Kobayashi I, Neves M, Uemura K, Nakajima M, Nabetani H. Oil-in-water emulsions encapsulating quercetin using microchannel emulsification: Effect of different emulsifiers on generation characteristics and stability. In Preparation.

Khalid N, Kobayashi I, Neves M, Uemura K, Nakajima M, Nabetani H. Encapsulation of γ-oryzanol plus β-sitosterol in oil-in-water emulsions: Insights of formulation characteristics with microchannel emulsification. In Preparation.

Proceedings

Khalid, N, Kobayashi I, Nakajima M, Neves AM, Uemura K. Preparation and Characterization of Water-in-Oil emulsions containing higher concentration of Ascorbic acid. 77th Annual meeting of chemical society of Japan. 11-13th March. Tokyo. 2012.

Khalid N, Kobayashi I, Neves AM, Uemura K, Nakajima M. Formulation characteristics of water-in-oil-in-water emulsions encapsulating L-ascorbic acid using microchannel emulsification. Japan Society of Food Engineering, 9-11th August, Sapporo.2012.

Khalid N, Kobayashi I, Neves AM, Uemura K, Nakajima M. Formulation and stability of water-in-oil emulsions encapsulating high concentration of L-ascorbic acid. Japan Society of Food Engineering, 9-11th August, Sapporo.2012.

Khalid N, Kobayashi I, Neves AM, Uemura K. Nakajima, M. Preparation characteristics of water-in-oil-water emulsions containing high concentration of L-ascorbic acid by microchannel emulsification. World Congress on Oleo Science & 29th ISF Congress. Nagasaki, Japan, 29th September, 2012.

Khalid N, Kobayashi I, Neves AM, Uemura K, Nakajima M. Formulation characteristics of water-in-oil-in-water emulsions encapsulating L-ascorbic acid by microchannel emulsfication. FORMULA VII. Mulhouse, 1st-4th July, France. 2013.

Khalid N, Neves AM, Kobayashi I, Uemura K, Nakajima M. Formulation and characterization of water-in-oil emulsions encapsulating L-ascorbic acid in high concentrations. The 60th Annual Meeting, The Japanese Society for Food Science and Technology. Jissen Women's Educational Institute, Tokyo, Japan. Proceedings, 2Fa12, p. 105. August 30th. 2013.

Khalid N, Neves AM, Kobayashi I, Uemura K, Nakajima M, Nabetani H. Preparation of monodisperse aqueous liquid microspheres containing high-concentration of L-ascorbic acid by microchannel emulsfication." The Annual Meeting of Japan Society for Bioscience, Biotechnology and Agrochemistry, 2014. Meiji University, Tokyo, Japan. Proceedings, 2B02p08, p. 534. March 28th. 2014.

Khalid N, Kobayashi I, Neves AM, Uemura K, Nakajima M, Nabetani H. Characterization of aqueous liquid microspheres encapsulating high concentration of L-ascorbic acid prepared by microchannel emulsfication. Japan Society of Food Engineering, 8th August, Tsukuba.2014.

Khalid N, Kobayashi I, Wang, Z, Neves AM, Uemura K, Nakajima M, Nabetani H. Preparation, characterization, stability and release profile of O/W emulsions loaded with vitamin D$_2$ by microchannel emulsification. Japan Society of Food Engineering, 8th August, Tsukuba. 2014.

Khalid N, Kobayashi I, Wang, Z, Neves AM, Uemura K, Nakajima M, Nabetani H. Effect of concentration of sodium cholate on production of O/W emulsions encapsulating vitamin D by microchannel emulsification. Japan Society of Food Engineering, 8th August, Tsukuba. 2014.

Khalid N, Kobayashi I, Neves AM, Uemura K, Nakajima M, Nabetani H. Formulation of monodisperse W/O emulsions encapsulating ascorbic acid derivatives by microchannel emulsification. Japan Society of Food Engineering, 8th Tsukuba. 2014.

Khalid N, Neves AM, Kobayashi I, Uemura K, Nakajima M, Nabetani H. Preparation, characterization, stability and release profile of O/W emulsions loaded with vitamin D$_2$ by microchannel emulsification. The 61st Annual Meeting, The Japanese Society for Food Science and Technology. Nakamura Gakuen University, Fukuoka, Japan. August 30th. 2014.

Khalid N, Kobayashi I, Neves AM, Uemura K, Nakajima M, Nabetani H. Preparation and characterization of submicron O/W emulsions encapsulating vitamin D. 46th Autumn meeting of chemical society of Japan. 17-19th September. Kyushu University, Fukuoka, Japan. 2014.

Khalid N, Kobayashi I, Wang, Z, Neves AM, Uemura K, Nakajima M, Nabetani H. Preparation of monodisperse O/W emulsions loaded with ergocalciferol using microchannel emulsification. 1st Congress on food structure design. 15-17th October. Porto, Portugal. 2014.

Khalid N, Kobayashi I, Neves AM, Uemura K, Nakajima M, Nabetani H. Practical application of monodisperse emulsions in innovative food products: Insights of ergocalciferol and cholecalciferol encapsulation by microchannel emulsification. 50th Volume celebration conference of International Journal of Food Science and Technology. 17-19th February, Lincoln University, New Zealand. 2015.

Khalid N, Kobayashi I, Neves AM, Uemura K, Nakajima M, Nabetani H. Preparation of quercetin-loaded O/W emulsions using microchannel emulsification. 80th Annual meeting of chemical society of Japan. 19-21st March. Shibaura Institute of Technology, Tokyo, Japan. 2015. (Accepted).

Khalid N, Kobayashi I, Neves AM, Uemura K, Nakajima M, Nabetani H. Microchannel emulsification a promising technique for generating monodisperse oil-in-water emulsions encapsulating quercetin. 12th Asian Congress of Nutrition. 14-18th May, Yokohama, Japan (Accepted).

Khalid N, Kobayashi I, Neves AM, Uemura K, Nakajima M, Nabetani H. Formulation characteristics of oil-in-water emulsions encapsulating beta-sitosterol and gamma-oryzanol by straight-through microchannel emulsification. 12th International Congress on Engineering and Food. 14-18th June, Québec, Canada. (Accepted).

Khalid N, Kobayashi I, Neves AM, Uemura K, Nakajima M, Nabetani H. Effect of emulsifiers on long term stability of oil-in-water emulsions encapsulating quercetin by straight-through microchannel emulsification. 12th International Congress on Engineering and Food. 14-18th June, Québec, Canada. (Accepted).